UNDERSTANDING PROSTATE CANCER PATHOGENESIS

A Dissertation

Presented to the Faculty of the Graduate School

of Cornell University

in Partial Fulfillment of the Requirements for the Degree of

Doctor of Philosophy

by

Chieh-Yang Cheng

August 2014

UNDERSTANDING PROSTATE CANCER PATHOGENESIS

Chieh-Yang Cheng, Ph. D.

Cornell University 2014

Prostate cancer is the most prevalent type of cancer in men. However, there is no cure for relapsed androgen withdrawal-refractory prostate cancer which is fatal due to metastasis. Many studies have demonstrated the existence of cancer cells with stem cell properties (aka cancer propagating cells (CPCs)) within the cancer cell population. CPCs may cause cancer recurrence due to resistence to conventional therapies. Understanding molecular and cellular mechanisms governing normal prostate stem cells and CPCs may improve our understanding and provide new opportunities for the design of therapeutics acting specifically on CPCs. Two of such mechanisms, p53/microRNA-34/Met network and neuroendocrine (NE) signaling are the topic of my dissertation.

microRNA-34 (miR-34) family has been proposed to play a tumor suppressor role in various cancers, including the prostate cancer. However, direct genetic evidence for the tumor suppressor functions of miR-34 under physiologically relevant settings has been lacking. By using newly generated mice carrying conditional alleles of *mir-34*, we have shown that miR-34 cooperates with p53 in suppression of prostate carcinogenesis by joint control of MET-dependent prostate stem/progenitor cells. Thus, therapeutic targeting of MET is likely to affect CPCs, particularly in p53 and miR-34 deficient patients.

NE signaling has been shown to be one of the features in advanced prostate cancer. However, the roles of NE cells in prostate carcinogenesis and development are insufficiently elucidated. By using bacterial artificial chromosome (BAC) we have generated a mouse model for conditional NE cell ablation, and shown that prostate epithelium-specific ablation of NE cells results in prostate hypotrophy, suggesting NE cells play an important role in prostate development. Moreover, we have studied effects of neuropeptide in *membrane metallo-endopeptidase* (*Mme)* null mice, and shown that *Mme* cooperates with *Pten* to suppress prostate carcinogenesis in the control of prostate stem/progenitor cells. Gastrin-releasing peptide (GRP), a substrate of MME, showed similar effects on mouse prostate stem/progenitor cells and human prostate CPCs. These effects were effectively abrogated by GRP receptor (GRPR) antagonist or knockdown of GRPR expression. Taken together, these findings show critical role of NE signaling in prostate development and carcinogenesis and GRPR is a potential therapeutics targeting prostate CPCs.

BIOGRAPHICAL SKETCH

Chieh-Yang Cheng was born on July 16th, 1981, in Taipei, Taiwan. Dedicated to a career in Chemistry and Biology, Chieh-Yang obtained his Bachelor's degree in Agricultural Chemistry and Master’s degree in Microbiology and Biochemistry from National Taiwan University. After the military service, Chieh-Yang worked in the field of Cancer Research in National Taiwan University Hospital as a research assistant. To achieve the long-term dream of curing cancer, Chieh-Yang decided to strengthen his expertise by pursuing an advanced degree. In the fall of 2008, Chieh-Yang started to study his Ph.D degree on modeling prostate cancer in the mouse under the guidance and supervision of Dr. Alexander Nikitin at Cornell University, Ithaca, NY.

ACKNOWLEDGMENTS

This is the most emotional section in the dissertation. I have so many people need to thank.

First, I would like to thank my advisor, Dr. Alexander Nikitin, for his guidance and training during my Ph.D degree, giving me the opportunity working on these exciting and changeling projects, and being the strongest “back-up” when I looked at him during my A-Exam. I also thank his patience on revising my all written stuff these years (which is not an easy job), as well as some lousy stuff I had done. I am also grateful for his mentorship, which makes me more independent and understand the reality of the real life. I sincerely respect his conscientious attitude on scientific research, which is a role model for my future career whatever I will do.

I also thank my Ph.D. committee members, Drs. John Schimenti, Tudorita Tumbar, and Mark Roberson, for their suggestions, comments and constructive criticisms throughout my studies, as well as the “kindness” during my A-Exam.

I thank Drs. Robert S. Weiss, Margaret McEntee, and the funding from Cornell Comparative Cancer Biology Training Program which supported my project. I thank my collaborators Drs. Heiko Hermeking and David Michael Nanus for providing the mouse models for my studies.

I acknowledge my former and present colleagues Chang-il Hwang, David Corney, Andrea Flesken-Nikitin, Jinhyang Choi, Le Cheng, Zongxiang Zhou, Urmi Chatterji, Meredith Stone, Elaina Wang, David Dupee, Ashley Odai-Afotey, Herman Yang, Connor Foster, and Dah-Jiun Fu. You guys helped me so much. I thank your countless

patience because I knew I bothered you a lot sometimes. Without your support by any means (technical skills, discussions, encouragements, taking care of mice, etc.), there is nothing I could fulfill in these years.

I thank Lavanya Sayam, Cornell Biomedical Sciences Flow Cytometry Core Lab, for excellent technical assistance with flow cytometry, and Dr. Ke-Yu Deng, Cornell Transgenic Facility, for making transgenic mice by DNA microinjection.

In addition, I would like to thank all my friends. There were too many precious and unforgettable memories with you guys. I am so lucky to know all of you. You enriched and cheered my life.

I also want to appreciate my family, for always supporting and caring about me spiritually and financially, which made me warm from the bottom of my heart and motivated me to keep fighting. Thank you, Skype, by the way.

Last but not least, I am grateful to my wife, Ya-Ting Liu, for her company, support, consideration, and sacrifice during this long and bittersweet journey. I appreciate she was always on my side and comforted me when I was upset and frustrated, and happy for me when I did anything successfully. Without her, I don’t think I can finish my Ph.D degree. I am so blessed to have her in my life. I love you.

TABLE OF CONTENTS

LIST OF FIGURES

LIST OF TABLES

LIST OF ABBREVIATIONS

AdCre	Adenovirus Cre recombinase
ALDH1	Aldehyde dehydrogenase 1
AMACR	Alpha-methylacyl-CoA racemase
BAC	Bacterial artificial chromosome
BrdU	5-bromo-2'-deoxyuridine
DAPI	4',6-diamidino-2-phenylindole
CDK	Cyclin dependent kinase
Chr	Chromosome
Cre	Cre-recombinase
CreERT2	Cre fused to a G400V/M543A/L544A triple mutation of the human estrogen receptor ligand binding domain
CPC	Cancer propagating cell
DNA	Deoxyribonucleic acid
DT	Diphtheria toxin
EGFP	Enhanced green fluorescent protein
EZH2	Enhancer of zeste homolog 2
FACS	Fluorescence activated cell sorting
GRP	Gastrin-releasing peptide
H&E	Hematoxylin&Eosin
IHC	Immunohistochemistry
MEF	Mouse embryonic fibroblast

MET	Hepatocyte growth factor receptor
mRNA	Messenger ribonucleic acid
miRNA	MicroRNA
MME	Membrane metallo-endopeptidase
NE	Neuroendocrine
NRSE	Neuro-restrictive suppressor element
p53	Tumor protein 53
PB	Probasin
PBS	Phosphate buffered saline
PCR	Polymerase chain reaction
PIN	Prostatic intraepithelial neoplasia
PSA	Prostate-specific antigen
PTEN	Phosphatase and tensin homolog
qRT	Quantitative reverse transcription
Sca-1	Stem cell antigen-1
s.c.	Subcutaneous
SYP	Synaptophysin
UGS	Urogenital sinus
UTR	Untranslated region

CHAPTER 1

INTRODUCTION

1.1 Prostate Cancer

Prostate cancer is the most frequently diagnosed cancer with an estimated annual incidence of 233,000 new cases and is only excelled by lung cancer as a leading cause of cancer-related death with an estimated incidence of 29,480 deaths in men for the United States in 2014 (Siegel et al., 2014). The clinical progression of prostate cancer is correlated with aging (Shen and Abate-Shen, 2010). Early in the course of the disease, prostate cancer grows slowly and is sensitive to androgens, proceeding after a long period of dormancy, from the normal prostate epithelium to prostatic intraepithelial neoplasia (PIN). This is followed by organ-confined prostate cancer and eventually metastatic prostate cancer (Abate-Shen and Shen, 2000). The major type of prostate cancer is adenocarcinoma. Other types of prostate cancer, such as small cell carcinoma and carcinoid tumors, are rare (di Sant'Agnese, 1992; Sun et al., 2009). The 5-year relative survival rate for men diagnosed in the United States from 2003 to 2009 with local or regional disease was 100%, and the rate for distant disease was 28%; a 99% survival rate was observed for all stages combined (American Cancer Society, 2014). Prostate cancer, like most other solid malignancies, can metastasize to distant organs, such as the liver, lung, brain, and bone with high propensity. Approximately 80% of the

men who had died from prostate cancer possessed bone metastases (Bubendorf et al., 2000; Li and Tang, 2011).

Generally, early localized disease can be cured by radical prostatectomy and radiation therapy with good prognosis (Cooperberg et al., 2005; Li and Tang, 2011). The androgen deprivation therapy is most commonly used against advanced disease, such as metastatic disease, recurrence after radical prostatectomy or radiotherapy and as neoadjuvant therapy. In general, prostate cancer has an initial response rate of 85-90%. However, most patients eventually relapse with castration-resistant prostate cancer after around 18 to 36 months, which turns into a more aggressive and ultimately fatal stage of disease (Cooperberg et al., 2005; Debes and Tindall, 2004; Harris et al., 2009; Li and Tang, 2011; Shen and Abate-Shen, 2010). Chemotherapy is another therapeutic option for treating castration-resistant prostate cancer. However, chemotherapy seems to have no benefit on survival even if it can significantly palliate pain (Buchler and Harland, 2007). No treatment has been proved effective on curing progressive hormone withdrawal-refractory prostate cancer. Moreover, the underlying mechanisms of prostate cancer carcinogenesis, recurrence, and metastasis are not well-understood (Bok and Small, 2002; Feldman and Feldman, 2001; Shen and Abate-Shen, 2010; Sun et al., 2009).

1.2 Stem Cells and Prostate Cancer

1.2.1 Prostate stem cells

The prostate epithelium consists of three differentiated cell types: luminal cells, basal cells, and a smaller number of NE cells (Abrahamsson, 1999; Isaacs, 2008). The adult mouse prostate regresses after castration and the prostate can be regenerated when androgen is restored. Such regression/regeneration manipulations can be cycled multiple times, suggesting the presence of prostate stem cells resistant to castration (English et al., 1987). Accumulating reports since this finding further indicate the existence of prostate stem cells. For example, stem cell antigen 1-positive (Sca-1^{+}) prostate basal cells are quiescent, are also positive for other stem cell markers, such as integrin α6 (CD49f) (Shinohara et al., 1999; Suzuki et al., 2000; Tani et al., 2000) and anti-apoptotic factor Bcl-2 (Domen et al., 2000; Potten et al., 1997; Tiberio et al., 2002), and are able to reconstitute the prostate gland by an in vivo renal capsule tissue regeneration assay, unlike the corresponding Sca-1^{-} cells (Burger et al., 2005; Xin et al., 2005). $Lin^{-}Sca\text{-}1^{+}CD49f^{hi}$ stem/basal cells (LSCs) can form prostate spheres and colonies in cell culture as well as reconstitute the prostate gland in vivo (Lawson et al., 2007). Tumor-associated calcium signal transducer 2 (Trop2) has been shown to be a marker to identify a subpopulation of mouse and human prostate basal cells with stem cell characteristics. Mouse prostate stem cells can be further enriched by sorting for $Trop2^{hi}$LSC cells (Goldstein et al., 2008). Moreover, CD117 is found to be expressed in mouse and human prostate basal cells, and generation of a prostate from a single adult mouse $Lin^{-}Sca\text{-}1^{+}CD133^{+}CD44^{+}CD117^{+}$ stem cell has been done after transplantation in vivo (Leong et al., 2008). Previous studies indicated that prostate stem cells are preferentially localized in the proximal regions of prostatic ducts (Leong et al., 2008; Salm et al., 2005; Tsujimura et al., 2002; Wang et al., 2007), and the relative

quiescence of the mouse prostate stem cells is likely maintained by a positive reciprocal regulatory loop formed from Notch and TGFβ signaling pathways (Salm et al., 2005; Valdez et al., 2012).

Using genetic lineage tracing experiments in mice with different promoters, several lines of evidence have indicated that the prostate stem/progenitor cells may also reside among the luminal cells. For example, luminal cells expressing Nkx3-1 (castration-resistant Nkx3-1-expressing cells, CARNs) are bipotential (give rise to both basal and luminal cells during regeneration), can self-renew in vivo in a regression/regeneration assay, and can reconstitute the intact prostate ducts (basal, luminal, and NE cells) in renal grafts by transplantation assay (Wang et al., 2009a). Lineage-restricted unipotent prostate progenitor cells have been shown to reside in both basal and luminal cell populations by using K14-CreER and K8-CreER^{T2} transgenic lines, respectively (Choi et al., 2012). Furthermore, by using the prostate-specific antigen PSA-CreER^{T2} mouse model prostate stem cells residing in luminal cells can survive, proliferate and regenerate in a regression/regeneration assay (Liu et al., 2011b). Last but not least, a recent study shows that prostate basal cells are a source of multipotent stem cells that can differentiate into all epithelial prostate cells (basal, luminal, and NE cells) as well as unipotent basal and luminal progenitors, which together contribute to the prostate postnatal development (Ousset et al., 2012; Wang et al., 2013).

As for the origin of human prostate stem cells, they seem to be localized in basal cell populations with expression of integrin α2β1 (Collins et al., 2001), CD133 (Richardson et al., 2004), breast cancer resistance protein (BCRP/ABCG2) (Huss et al., 2005), and Trop2 (Goldstein et al., 2008) based on findings so far.

1.2.2 Prostate cancer propagating cells

Cancer propagating cells (CPCs, aka cancer stem cells) are a subset of cancer cells which are capable of regenerating tumors, and may be involved in metastasis and therapy resistance (Clevers, 2011; Magee et al., 2012; Nguyen et al., 2012; Shackleton et al., 2009; Valent et al., 2012; Visvader and Lindeman, 2012). Various populations of human prostate CPCs have been reported. For example, CD44 expression was also shown to identify prostate cancer cells with CPC features. In prostate cancer cell lines (DU145) and xenograft models (LAPC9, LAPC4), the $CD44^+$ prostate cancer cells are relatively quiescent, more tumorigenic and metastatic than $CD44^-$ prostate cancer cells, express “stemness” genes, and are capable of undergoing asymmetric cell division. (Patrawala et al., 2007; Patrawala et al., 2006). In addition to $CD44^+$ prostate CPCs, $CD133^+$ (Miki et al., 2007; Vander Griend et al., 2008), $CXCR4^+$ (Dubrovska et al., 2012; Miki et al., 2007), TRA-1-60^+/$CD151^+$/ $CD166^+$ (Rajasekhar et al., 2011), $PSA^{-/lo}$ (Qin et al., 2012), HLA class I (HLAI) antigen-negative ($HLAI^-$) (Domingo-Domenech et al., 2012), side population (SP), (Patrawala et al., 2005), and aldehyde dehydrogenase-positive ($ALDH^+$) (Li et al., 2010b; van den Hoogen et al., 2010) prostate cancer cells have been uncovered as potential human prostate CPCs. Several reports point out the mechanisms in regulating prostate CPCs. Nanog (Jeter et al., 2009; Jeter et al., 2011), Pten/PI3K/ AKT pathway (Dubrovska et al., 2009), NFκB pathway (Rajasekhar et al., 2011), and miR-34a (Liu et al., 2011a) have been shown to be regulators of human prostate CPCs. Moreover, human prostate CPCs lacking differentiation markers

(CK18^{-}/ CK19^{-}) and HLA class I (HLAI^{-}) antigens show high activities for the Notch and Hedgehog signaling pathways and are resistant to docetaxel treatment (Domingo-Domenech et al., 2012).

As for the mouse CPCs, the Sca-1^{+} prostate cells initiate PIN formation upon lentiviral-mediated overexpression of AKT1, suggesting that Sca-1^{+} cells could be the potential CPCs (Xin et al., 2005). Lin^{-}Sca-1^{+}CD49f^{hi} cells show properties of CPCs such as high sphere forming and tumorigenic potential in Pten-deficient prostate cancer model (Mulholland et al., 2009). Likewise, some potential regulators, such as AKT and androgen receptor (AR) (Abou-Kheir et al., 2010), Bmi-1 (Lukacs et al., 2010b), and Trop2 (Stoyanova et al., 2012) have been addressed in regulating mouse prostate CPCs.

Finding the prostate CPCs in castration-resistant prostate cancer has drawn enormous attention. A previous report indicates that N-cadherin^{+} cells may be involved in castration-resistant prostate cancer development and prostate cancer metastasis (Tanaka et al., 2010). Another report shows that PSA$^{-/lo}$ prostate cancer cells are more clonogenic in androgen-deficient conditions in cell culture and more tumorigenic in castrated mice than the PSA^{+} prostate cancer cells, suggesting that the PSA$^{-/lo}$ cell population could be the prostate CPCs in castration-resistant prostate cancer and might become the therapeutic targets for castration-resistant prostate cancer (Qin et al., 2012).

In addition, it is noteworthy that NE cells are suggested to be a cell origin of prostate CPCs (Palapattu et al., 2009; Sotomayor et al., 2009). Expression of CD44 has been shown to be positively associated with cells of NE phenotype in human prostate cancer cell lines and is selectively displayed in NE tumor cells in vivo (Palapattu et al.,

2009). Furthermore, Oct4A, a stemness marker, is also expressed by a subpopulation of prostate chromogranin A (CgA) or synaptophysin (SYP) positive NE cells (Sotomayor et al., 2009). Thus, it is likely that prostate NE cells could transform into the CPCs while acquiring epigenetic modifications or genetic mutations.

1.2.3 Cell origin of prostate cancer

The major type of prostate cancer is adenocarcinoma, which is composed predominantly of luminal cells and sparsely of basal cells (Abate-Shen and Shen, 2000; Shen and Abate-Shen, 2010). Thus, prostate luminal cells are hypothesized to be the cell origin of prostate cancer after oncogenic transformation. This hypothesis has been supported by studies of lineage tracing in some mouse models. For example, targeted deletion of the *Pten* in CARNs of castrated male mice (*Nkx3-1*$^{CreERT2/+}$*; Pten*$^{flox/flox}$) results in carcinoma formation after androgen-mediated regeneration (Wang et al., 2009a). By using luminal cell-specific inducible Cre mice (*K8-CreERT2*$^{Tg/wt}$*; mTmG* $^{Tg/wt}$) and *K8-CreERT2*$^{Tg/wt}$*;Pten*$^{flox/flox}$ mice, luminal cells are shown to be more responsive to *Pten* null-induced prostate cancer formation. In contrast, basal cells are reluctant to be transformed directly upon *Pten* deleton, as evidenced by basal cell-specific inducible Cre mice (*K14-CreER*$^{Tg/Tg}$*;mTmG*$^{Tg/Tg}$) and *K14-CreER*$^{Tg/Tg}$*; Pten*$^{flox/flox}$ mice (Choi et al., 2012). Similar results was observed between *Nkx3.1*$^{CreERT2/+}$*; Pten*$^{flox/flox}$*; R26R-YFP/+* (luminal cells) and *CK5-CreER*^{T2}*; Pten*$^{flox/flox}$*; R26R-YFP/+* (basal cells) mice (Wang et al., 2013). Deletion of *Pten* in luminal cells by PSA-CreER^{T2} transgenic mice leads to prostate cancer, which also supports this notion (Ratnacaram et al., 2008).

On the other hand, some studies suggest that basal cells are the cell origin of prostate cancer by using tissue recombination/transplantation assay. For example, overexpression of AKT and AR in basal cells can lead to prostate cancer, whereas luminal cells fail to respond (Lawson et al., 2010). Similarly, co-expression of AKT, ETS-family transcription factor ERG, and AR in human prostate basal cells ($CD49f^{hi}Trop2^{hi}$) can cause these cells to undergo malignant transformation and initiate prostate cancer in immunodeficient mice, but co-expression of these genes in human luminal cells ($CD49f^{lo}Trop2^{hi}$) cannot (Goldstein et al., 2010). It is worth noting that the tissue recombination/transplantation assay does not exactly reflect physiological conditions. Therefore, whether functions of prostate stem cells or CPCs by using this method are obligate or facultative is still controversial.

1.3 p53/miR-34 Network

1.3.1 miR-34 in cancers

MicroRNAs (miRNAs) are about 20 to 24 nucleotides and are a non-coding subset of RNAs which control gene expression post-transcriptionally. In general, miRNAs bind to the 3' untranslated regions (UTRs) of messenger RNAs (mRNAs) and recruit the RNA-induced silencing complex (RISC), which causes the inhibition of translation and the degradation of the targeted mRNA (Hermeking, 2012; Winter et al., 2009). After the discovery of first and second miRNAs: lin-4 (Lee et al., 1993; Wightman et al., 1993) and let-7 (Reinhart et al., 2000), in *Caenorhabditis elegans*, significant advances and

explosive discovery of new miRNAs have been made in the past decade. Of which, miR-34 draws extensive attention because it is directly trans-activated by tumor suppressor p53 (Bommer et al., 2007; Chang et al., 2007; Corney et al., 2007; He et al., 2007; Raver-Shapira et al., 2007; Tarasov et al., 2007) and is considered to be an important component of the p53 network, being a surrogate of p53 in processes such as cell proliferation, survival, and senescence (Hermeking, 2010, 2012).

miR-34 comprises three family members: miR-34a (human: chr. 1, mouse: chr. 4), miR-34b (human: chr. 11, mouse: chr. 9), and miR-34c (human: chr. 11, mouse: chr. 9). miR-34a is encoded by its own transcript, whereas miR-34b and miR-34c come from a polycistronic transcript. Due to the high homology of the sequence, the miR-34 family may control an overlapping set of target genes and be functionally redundant (He et al., 2007). In human tissues, detectable levels of miR-34a are detected in the majority of organs, while, miR-34b/c expression levels are generally low except in lung, ovary, testes, and trachea (Hsu et al., 2008). In mouse tissues, miR-34a is detectable, albeit at lower levels, also in a variety of organs, whereas, miR-34b and miR-34c expression seems largely restricted to testis, brain, and lung (Concepcion et al., 2012).

mir-34a and *mir-34b/c* are located in the genomic sites that are frequently deleted in cancers (Calin et al., 2004; Cole et al., 2008). In addition, epigenetic modification such as hypermethylation in the promoter region of *mir-34* family often occurs in cancers (Lodygin et al., 2008; Lujambio et al., 2008; Vogt et al., 2011). Loss or down-regulation of miR-34 family in cancers suggests that miR-34 family is a potential tumor suppressor, such as in lung cancer (Bommer et al., 2007; Gallardo et al., 2009; Lodygin et al., 2008; Mudduluru et al., 2011; Wang et al., 2011; Wiggins et al., 2010), prostate

cancer (Fujita et al., 2008; Lodygin et al., 2008; Sethi et al., 2013), ovarian cancer (Corney et al., 2010; Kuo et al., 2009; Vogt et al., 2011), brain cancer (Cole et al., 2008; Feinberg-Gorenshtein et al., 2009; Li et al., 2009b; Wei et al., 2008; Welch et al., 2007; Yin et al., 2013), breast cancer (Lodygin et al., 2008; Mackiewicz et al., 2011; Mudduluru et al., 2011; Vogt et al., 2011), pancreas cancer (Chang et al., 2007; Lodygin et al., 2008; Vogt et al., 2011), colon cancer (Lodygin et al., 2008; Mudduluru et al., 2011; Roy et al., 2012; Tazawa et al., 2007; Toyota et al., 2008; Vogt et al., 2011), kidney cancer (Lodygin et al., 2008; Vogt et al., 2011), liver cancer (Li et al., 2009a; Tryndyak et al., 2009), bladder cancer (Lodygin et al., 2008), gastric cancer (Suzuki et al., 2010), pleural mesothelioma (Kubo et al., 2011), skin cancer (Lodygin et al., 2008), esophagus cancer (Chen et al., 2012), cervical cancer (Li et al., 2010a; Wang et al., 2009b), and leukemia and lymphoma (Chim et al., 2010; Mraz et al., 2009).

1.3.2 Tumor suppressor function of miR-34

Ectopic expression of miR-34 has been shown to inhibit different aspects of cancer-associated traits in various cancer cell types by regulating target genes, such as cell growth, metastasis, and cancer cell stemness (Hermeking, 2010, 2012; Siemens et al., 2013).

Ectopic expression of miR-34 may inhibit cell proliferation by leading to G1/G2 arrest, the decrease of cell doubling rates, and BrdU incorporation (Corney et al., 2007; He et al., 2007; Lodygin et al., 2008; Wiggins et al., 2010) and induce senescence (Christoffersen et al., 2010; He et al., 2007; Lodygin et al., 2008; Maes et al., 2009;

Tazawa et al., 2007) in cancer cells via repressing downstream targets, such as cyclin D1 (Sun et al., 2008), cyclin E2 (He et al., 2007), cyclin-dependent kinases 4 (He et al., 2007) and 6 (Sun et al., 2008), as well as mitogen-activated protein kinase kinase 1 (MEK1) (Ichimura et al., 2010), R-Ras (RRAS) (Kaller et al., 2011), platelet-derived growth factor receptor (PDGFRA) (Silber et al., 2012), hepatocyte growth factor receptor (MET) (Corney et al., 2010; He et al., 2007; Hwang et al., 2011), and MYC (Christoffersen et al., 2010). In addition, miR-34a has the pro-apoptotic function to repress BCL2 (Bommer et al., 2007; Cole et al., 2008) and survivin (Chen et al., 2010; Shen et al., 2012). Moreover, miR-34a can promote apoptosis by stimulating p53 activity in a positive feedback-loop by targeting SIRT1 (silent information regulator 1), a NAD-dependent deacetylase that deactivates p53 (Yamakuchi et al., 2008), and YY1 (Yin Yang 1), a transcriptional factor which interacts with p53 to promote p53 ubiquitination and degradation (Chen et al., 2011; Sui et al., 2004). Collectively, miR-34 is able to inhibit cell proliferation and induce apoptosis and senescence in cancer cells.

miR-34 downregulates the metastasis-associated genes, such as MET (Corney et al., 2010; He et al., 2007; Hwang et al., 2011), AXL (Kaller et al., 2011; Mudduluru et al., 2011), MTA2 (Kaller et al., 2011), and Notch1 (Du et al., 2012). Furthermore, miR-34 has been shown to regulate Wnt signaling pathway which is involved in metastasis (Malanchi et al., 2012; Nguyen et al., 2009; Oskarsson et al., 2011; Yook et al., 2005; Yook et al., 2006). miR-34 directly represses WNT1 and WNT3, as well as LRP6, a co-receptor of Frizzled that binds to Wnt ligands. miR-34 also represses downstream transcriptional mediators of Wnt signaling pathway, LEF1 and beta-catenin. Accordingly, miR-34 decreases Wnt-dependent, tissue-invasive activity of colorectal cancer cells

(Kim et al., 2011).

Another function ascribed to miR-34 is to regulate CPCs. miR-34a levels are lower in CD44-expressing prostate CPCs purified from xenograft and primary tumors. Ectopic expression of miR-34a in bulk or purified $CD44^+$ prostate cancer cells inhibited their abilities of clonogenic expansion, tumor regeneration, and metastasis in vivo (Liu et al., 2011a). miR-34 is suggested to be involved in suppressing pancreatic CPC self-renewal, potentially via the direct modulation of downstream targets Bcl-2 and Notch (Ji et al., 2009). miR-34a is also suggested to impair propagation properties of $CD15^+/CD133^+$ CPCs via targeting Notch ligand delta-like 1 and supports neural differentiation in medulloblastoma (de Antonellis et al., 2011). Moreover, Notch 1-targeting miR-34a is a cell-fate determinant of colon CPCs, helping to determine between self-renewal and differentiation (Bu et al., 2013). It is also worth noting that miR-34 may prevent induced pluripotent stem (iPS) cell reprogramming by directly inhibiting pluripotency genes, including NANOG, SOX2, and MYCN (Choi et al., 2011).

The tumor suppressor function of miR-34 was also tested in various animal models of cancer, such as xenografts of melanoma (Chen et al., 2010), non-small lung cancer (Trang et al., 2011; Wiggins et al., 2010), prostate cancer (Liu et al., 2011a), pancreatic cancer (Pramanik et al., 2011), and lymphoma (Craig et al., 2012). miR-34 leads to a significant reduction in cell proliferation and an increase in apoptosis for inhibiting the tumor burden, or enhances survival or substantial decrease in metastasis in mice. Thus, miR-34 has its therapeutic potential based on the studies above, and recently has become the first miRNA mimic to reach the clinic (Bouchie, 2013).

1.3.3 Function of miR-34 in vivo

The biological activities of miR-34 identified in cell cultures and animal models of cancer suggest that miR-34 is a promising tumor suppressor. However, contrary to expectations, no carcinogenesis except some minor developmental defects has been reported in studies of mice with targeted inactivating mutations of *mir-34* (Agostini et al., 2011; Boon et al., 2013; Concepcion et al., 2012; Wei et al., 2012). Such defects included reduction of proliferating cells in the dentate gyrus of the brain (Agostini et al., 2011), and mitigation of age-associated decline in cardiac function (Boon et al., 2013) in *mir-34a*$^{-/-}$ mice. Mice with osteoblast-specific inactivation of *mir-34b/c* have increase in osteoblast proliferation and differentiation (Wei et al., 2012). Furthermore, mice lacking all three *mir-34* genes have slight increase in the proliferation rate of early passage embryonic fibroblasts (Concepcion et al., 2012), but did not show impairment of the p53 response in a variety of ex vivo and in vivo assays (Concepcion et al., 2012). Most surprisingly, no increase in spontaneous or irradiation-induced carcinogenesis has been observed in mice lacking all *mir-34* genes by 18 month of age (Concepcion et al., 2012). Absence of all *mir-34* genes also did not facilitate B-cell lymphomagenesis in mice overexpressing c-Myc under the control of Eμ-promoter (Concepcion et al., 2012). Taken together, these observations are contradictory with previous reports showing tumor suppressive function of miR-34 based on experiments performed in settings that were not physiologically relevant. Consequently, dissecting the precise role of miR-34 in carcinogenesis in vivo is critical and essential for clinical therapeutics.

1.3.4 p53-independent regulation of miR-34

Although the canonical signaling pathway of miR-34 activation is p53-dependent (Bommer et al., 2007; Chang et al., 2007; Corney et al., 2007; He et al., 2007; Raver-Shapira et al., 2007; Tarasov et al., 2007), emerging evidence suggests that p53 is not an exclusive regulator for miR-34 activation. For example, miR-34a can be up-regulated to repress MYC during oncogene-induced senescence in human TIG3 fibroblasts (Christoffersen et al., 2010) and contributes to megakaryocytic differentiation of K562 cells (Navarro et al., 2009) in a p53-independent fashion. miR-34a repression upregulates expression of its target PDGFRA in proneural malignant gliomas, which is likely p53-independent (Silber et al., 2012). Within the samples of human glioblastoma, miR-34a levels are lower in mutant p53 tumors than in wild-type p53 tumors but the difference in miR-34a levels was smaller than the one measured between tumors and normal human brain. This also suggests that p53 mutations do not completely account for the decrease in miR-34a expression (Li et al., 2009b). SNAIL, ZEB1 (Siemens et al., 2011), and FoxO3a (Kress et al., 2011) might bypass p53 to regulate miR-34. It also suggests that p21 can be induced indirectly by miR-34 through repression of histone deacetylase 1 (HDAC1), irrespective of p53 status (Zhao et al., 2013). In wild-type p53 breast cancer samples, neither hypermethylation of the miR-34a promoter nor genetic variations of the p53-binding site were detected with downregulated miR-34a, providing evidence that miR-34a expression could be affected independent of p53 (Javeri et al., 2013).

Epigenetically, hypermethylation of miR-34 occurs in various cancers with p53-

deficient status (Corney et al., 2010; Lodygin et al., 2008; Lujambio et al., 2008; Vogt et al., 2011). For example, *p53*-null PC3 (Scott et al., 2003) and *p53*-mutated LAPC-4 (Klein et al., 1997) human prostate cancer cells both show downregulation of miR-34 by methylation (Fujita et al., 2008; Lodygin et al., 2008). These results suggest that existence of p53-independent regulation on tumor suppressive functions of miR-34. However, the evidence showing existence of p53-independent regulation of miR-34 in vivo has been lacking.

1.4 Prostate Neuroendocrine Regulation

1.4.1 Prostate neuroendocrine cells

Neuroendocrine (NE) cells are so named due to their dual endocrine and neural properties, acting in the autocrine/paracrine fashions. NE cells are scattered sparsely throughout the prostate epithelium. Although very little is known about the presence of NE cells in the developing prostate, recent studies have indicated that NE cells originate from the prostate epithelium stem/progenitor cells (Cheng et al., 2010; Huss et al., 2004a; Kurita et al., 2004; Leong et al., 2008; Liao et al., 2007; Litvinov et al., 2006; Nikitin et al., 2007; Ousset et al., 2012; Wang et al., 2009a; Wang et al., 2001; Wang et al., 2013; Zhou et al., 2007). An entire prostate gland with NE cells can be generated from prostate basal epithelium stem cells (Leong et al., 2008; Ousset et al., 2012; Wang et al., 2013) or luminal epithelium stem cells (Wang et al., 2009a). Other evidence, however, suggests that NE cells are of neurogenic origin (Aumuller et al., 1999). NE

cells were present in the surrounding mesenchyme and paraganglia, but not in UGS epithelium of 10-week-old human embryos. Proceeding to week 12, chromogranin A-positive cells (marker for NE cells) were present within the epithelial buds that ultimately develop into prostate glandular components. This suggests that NE cells are of neurogenic origin instead of prostate epithelium stem cells. However, this evidence could be circumstantial because the data were not based on lineage tracing experiments.

Prostatic NE cells contain dense-core cytoplasmic granules that store peptide hormones and pro-hormones. These granules contain either a single product or a mix of different products such as chromogranin A (CgA), neuron specific enolase (NSE), serotonin, neuropeptide Y, calcitonin gene family (calcitonin, katacalcin, and calcitonin gene-related peptide, CGRP), bombesin, gastrin-releasing peptide, somatostatin, vasoactive intestinal peptide, endothelin-1, human chorionic gonadotropin, thyroid-stimulating hormone, parathyroid hormone-related protein, neurotensin, and a number of other neuropeptides and proteins (Abrahamsson, 1999; Sun et al., 2009). Common markers for NE cells include CgA (Gazdar et al., 1988), NSE (Schmechel et al., 1978), neural cell adhesion molecules (NCAMs, so-called CD56) (Jin et al., 1991), CGRP (Cadieux et al., 1986), and SYP (Wiedenmann et al., 1986). NE cells do not proliferate ($Ki67^-$), and do not express p63 protein or PSA (Vashchenko and Abrahamsson, 2005) and lack AR expression (Krijnen et al., 1993), indicating that NE cells are androgen insensitive (Bang et al., 1994). Neuropeptides secreted by NE cells, acting as autocrine and paracrine growth factors, are suggested to be involved in facilitating the development and secretion of the prostate since receptors for some of the NE products

have been found to be expressed in the normal prostate (Abrahamsson, 1999; Vashchenko and Abrahamsson, 2005). However, the physiological role of prostatic NE cells is still not well understood.

1.4.2 Neuroendocrine cell differentiation in prostate cancer

NE cell differentiation is one of the features in prostate carcinogenesis (Bonkhoff and Berges, 2010; Debes and Tindall, 2004; Hansson and Abrahamsson, 2001, 2003; Sun et al., 2009). It is often identified by scattered clusters of differentiated NE cells among a predominant population of adenocarinoma, except for infrequent cases of small cell carcinoma or carcinoid (Komiya et al., 2009). NE cell differentiation and neuropeptides released by NE cells were suggested to be positively correlated with tumor progression, Gleason score, androgen deprivation therapy failure, and poor prognosis (Berruti et al., 2005; Grobholz et al., 2005; Kamiya et al., 2008; McWilliam et al., 1997; Sun et al., 2009; Taplin et al., 2005; Vashchenko and Abrahamsson, 2005).

Androgen ablation therapy is the main option for treating metastatic prostate cancer; however, patients who received a longer course of androgen ablation therapy have been found to have higher levels of NE cell differentiation (Hirano et al., 2004; Ismail et al., 2002; Ito et al., 2001). In addition to clinical specimens, androgen withdrawal-induced NE cell differentiation is also seen in prostate cancer cell culture and in vivo animal model studies. LNCaP cells (androgen dependent) without NE cell differentiation are able to be trans-differentiated into an NE-like phenotype in response to androgen deprivation and begin to express the NE cell markers (Shen et al., 1997; Yuan et al.,

2006; Zelivianski et al., 2001). The NE trans-differentiation induced by androgen deprivation can be reversed by the addition of dihydrotestosterone (DHT) and then can be restored by Casodex, an androgen antagonist. Moreover, androgen receptor (AR) knockdown in LNCaP cells also induces NE trans-differentiation (Wright et al., 2003). Collectively, it suggests that androgen-activated AR signaling suppresses NE differentiation. Similarly, in animal models, castration promotes NE differentiation of xenograft tumors formed by androgen dependent PC-295, PC-310 (Jongsma et al., 1999, 2000), LNCaP (Burchardt et al., 1999), or CWR22 cells (Huss et al., 2004b) cell lines. Taken together, cell culture, in vivo studies, as well as clinical observations, suggest that androgen ablation may enhance NE cell differentiation of prostate adenocarcinoma.

Several reports show that increased intracellular 3'-5'-cyclic adenosine monophosphate (cAMP) leads to NE cell differentiation of prostate cancer cells. Elevation of cAMP, by cAMP analogs and phosphodiesterase (which degrades cAMP by breaking the phosphodiester bond) inhibitors (Bang et al., 1994), forskolin (adenylate cyclase activator), or epinephrine (β-adrenergic receptor agonist) (Cox et al., 1999), induces NE cell differentiation of prostate cancer cells and NE cell differentiation of prostate cancer cells are reversible after removal of cAMP-elevating agents (Cox et al., 1999).

Interleukin-6 (IL-6) has been suggested to be positively correlated with prostate cancer progression (Adler et al., 1999; Drachenberg et al., 1999; Shariat et al., 2001). IL-6 is also able to induce NE cell differentiation of LNCaP cells (Deeble et al., 2001; Qiu et al., 1998; Wang et al., 2004). Moreover, elevated expression of gp130, the signal

transduction subunit of the IL-6 receptor, induces NE cell differentiation in LNCaP cells, also suggesting IL-6-induced NE cell differentiation of prostate cancer cells (Palmer et al., 2005). In addition to IL-6, other cytokines, such as IL-1β, are suggested to play a role in NE cell differentiation of prostate cancer (Chiao et al., 1999; Diaz et al., 1998).

NE cell differentiation of prostate cancer cells is suggested to be mediated by multiple signaling pathways in addition to the factors mentioned above. For example, heparin-binding epidermal growth factor *(*HB-EGF), an epidermal growth factor receptor (EGFR) ligand, can also promote NE cell differentiation (Adam et al., 2002; Humez et al., 2006; Kim et al., 2002). Vasoactive intestinal peptide (VIP) is a neuropeptide and can also promote NE cell differentiation of LNCaP cells (Gutierrez-Canas et al., 2005; Juarranz et al., 2001). Moreover, calcium chelator BAPTA/AM inhibits VIP-induced NE phenotype in LNCaP cells, whereas increased expression of calcium channel proteins promotes NE cell differentiation, suggesting an association between intracellular calcium level and NE cell differentiation of prostate cancer cells (Collado et al., 2005; Mariot et al., 2002; Vanoverberghe et al., 2004).

Although the roles of NE cells and their secreted neuropeptides in prostate cancer have been extensively studied in various cancer cell lines, mouse models of cancer, and human biopsies, the precise function and the mechanism of NE differentiation in prostate carcinogenesis in vivo are insufficiently elucidated so far.

1.4.3 The role of membrane metallo-endopeptidase in neuropeptide processing and prostate cancer

Membrane metallo-endopeptidase (MME), also known as CD10, neutral endopeptidase, enkephalinase, neprilysin, or common acute lymphoblastic leukemia antigen (CALLA), is a zinc-dependent cell surface peptidase which may metabolize neuropeptides (Roques et al., 1993; Turner and Tanzawa, 1997). MME cleaves peptide bonds on the amino side of hydrophobic amino acids and inactivates a variety of physiologically active neuropeptides, including neuropeptide Y, atrial natriuretic factor, substance P, bradykinin, oxytocin, Leu- and Met-enkephalins, cholecystokinin, vasoactive intestinal peptide, neurotensin, bombesin, endothelin-1, and gastrin-releasing peptide (Erdos and Skidgel, 1989; Medeiros Mdos and Turner, 1996; Shipp and Look, 1993; Sumitomo et al., 2005; Turner and Tanzawa, 1997).

Association of MME with various cancers has been observed (Maguer-Satta et al., 2011; Sumitomo et al., 2005), including prostate cancer. MME expression is lost or altered in over 50% of primary and metastatic prostate cancers, independently predicting a poor prognosis (Freedland et al., 2003; Osman et al., 2004; Papandreou et al., 1998). Therefore, it has been suggested that the loss or decrease in MME expression may promote peptide-mediated proliferation by allowing an accumulation of neuropeptides at the cell surface and facilitate neoplastic transformation or progression.

The tumor suppressive functions of MME have been extensively tested in various cell culture and ex vivo studies. The effects of MME on cell growth, cell motility, and cell survival are mediated through two major mechanisms: catalytic-dependent and catalytic-independent MME functions. The catalytic-dependent inactivation of MME substrates, such as neuropeptides which stimulate prostate cancer migration and invasion by bombesin-stimulated RhoA signaling (Zheng et al., 2006), and fibroblast

growth factor 2 which results in endothelial cell growth and angiogenesis by inducing Akt signaling (Goodman et al., 2006), has been reported. Catalytic-independent processes act via protein-protein interaction of MME's cytoplasmic domain with other important cellular proteins. For example, MME associates with p85, a PI3K subunit, and Lyn kinase indirectly via glycosylphosphatidylinositol (GPI)-microdomains to prevent focal adhesion kinase (FAK) activation by PI3K and thereby decrease cell motility (Ganju et al., 1996; Sumitomo et al., 2005; Sumitomo et al., 2000). Moreover, MME competes with CD44 and decreases its binding to ezrin/radixin/moesin (ERM) proteins, resulting in increased cell adhesion and decreased migration (Iwase et al., 2004). MME also recruits and interacts directly with endogenous Pten at the cell membrane, leading to prolonged Pten protein stability and increased Pten phosphatase activity, resulting in downregulation of Akt activity (Sumitomo et al., 2004). However, cooperative functions of MME and PTEN in prostate cancer suppression in vivo have not been studied.

Furthermore, the lentiviral and adenoviral delivery of MME has been shown to inhibit prostate cancer tumorigenicity in a xenograft model of human prostate cancer (Horiguchi et al., 2007; Iida et al., 2012). However, MME conventional knockout mice generated by Dr. Gerard's group show no cancer-related phenotype (Lu et al., 1995), indicating MME deficiency is insufficient to induce cancer formation in vivo, which is contradictory with previous reports showing tumor suppressive function of MME. Consequently, dissecting the precise role of MME in carcinogenesis in vivo is critical and essential for clinical therapeutics.

1.5 Concluding Remarks and Project Overview

miR-34 has been proposed to act as a tumor suppressor in various cell culture experiments and mouse models of cancer, which led to miR-34 becoming the first miRNA mimic to reach the clinic. However, no tumor phenotype was found in mouse models with conventional and conditional inactivation of *mir-34.* These findings placed the tumor suppressor function of miR-34 under suspicion, because previous finding of its functions were based on experiments performed in not physiologically relevant settings. Therefore, exploring the precise role of miR-34 in carcinogenesis will be vital to clinical therapy. In chapter 2, by using newly generated mice carrying conditional alleles of *mir-34a* and *mir-34b/c*, we have shown that miR-34 may cooperate with p53 in suppression of prostate carcinogenesis in addition to canonical activation of miR-34 by p53. Furthermore, we have shown that miR-34 and p53 jointly regulate MET-dependent growth, self-renewal, motility, and invasion of prostate epithelium stem cells, alterations of which may lead to cancer.

To address the role of NE signaling in prostate development, in Chapter 3, we identified upstream promoter regions sufficient for accurate expression of SYP, a marker of NE cells. By using this region, we generated Tg(*Syp-EGFP*^{loxP}*-DTA)147*^{Ayn} (*SypELDTA*) transgenic mice suitable for flexible organ-specific ablation of NE cells. By crossing this line with the *PB-Cre4* mouse line, which allows prostate epithelium-specific Cre-*loxP* mediated recombination, we showed a substantial decrease in the number of NE cells and associated prostate hypotrophy, suggesting that NE cells play an important role in prostate development. In Chapter 4, by using newly generated mice with prostate epithelium-specific inactivation of *Pten* and *Mme* null, we have shown that

unprocessed neuropeptides may enhance *Pten*-deficient prostate carcinogenesis by increase of stem cell activities, such as stem cell pool expansion, growth, and self-renewal. We also showed that these effects can be recapitulated by GRP, a major substrate of MME, in mouse prostate stem cells and human prostate CPCs. Our results demonstrate that MME suppresses prostate cancer by controlling GRP-dependent prostate stem/progenitor cells, and suggest that GRPR antagonists may be an effective therapeutics targeting prostate CPCs.

REFERENCES

American Cancer Society. Cancer Facts & Figures 2014. Atlanta: American Cancer Society; 2014.

Abate-Shen, C., and Shen, M.M. (2000). Molecular genetics of prostate cancer. Genes & development *14*, 2410-2434.

Abou-Kheir, W.G., Hynes, P.G., Martin, P.L., Pierce, R., and Kelly, K. (2010). Characterizing the contribution of stem/progenitor cells to tumorigenesis in the Pten-/- TP53-/- prostate cancer model. Stem cells *28*, 2129-2140.

Abrahamsson, P.A. (1999). Neuroendocrine differentiation in prostatic carcinoma. The Prostate *39*, 135-148.

Adam, R.M., Kim, J., Lin, J., Orsola, A., Zhuang, L., Rice, D.C., and Freeman, M.R. (2002). Heparin-binding epidermal growth factor-like growth factor stimulates androgen-independent prostate tumor growth and antagonizes androgen receptor function. Endocrinology *143*, 4599-4608.

Adler, H.L., McCurdy, M.A., Kattan, M.W., Timme, T.L., Scardino, P.T., and Thompson, T.C. (1999). Elevated levels of circulating interleukin-6 and transforming growth factor-beta1 in patients with metastatic prostatic carcinoma. The Journal of urology *161*, 182-187.

Agostini, M., Tucci, P., Steinert, J.R., Shalom-Feuerstein, R., Rouleau, M., Aberdam, D., Forsythe, I.D., Young, K.W., Ventura, A., Concepcion, C.P.*, et al.* (2011). microRNA-34a regulates neurite outgrowth, spinal morphology, and function. Proceedings of the National Academy of Sciences of the United States of America *108*, 21099-21104.

Aumuller, G., Leonhardt, M., Janssen, M., Konrad, L., Bjartell, A., and Abrahamsson, P.A. (1999). Neurogenic origin of human prostate endocrine cells. Urology *53*, 1041-1048.

Bang, Y.J., Pirnia, F., Fang, W.G., Kang, W.K., Sartor, O., Whitesell, L., Ha, M.J., Tsokos, M., Sheahan, M.D., Nguyen, P.*, et al.* (1994). Terminal neuroendocrine differentiation of human prostate carcinoma cells in response to increased intracellular

cyclic AMP. Proceedings of the National Academy of Sciences of the United States of America *91*, 5330-5334.

Berruti, A., Mosca, A., Tucci, M., Terrone, C., Torta, M., Tarabuzzi, R., Russo, L., Cracco, C., Bollito, E., Scarpa, R.M.*, et al.* (2005). Independent prognostic role of circulating chromogranin A in prostate cancer patients with hormone-refractory disease. Endocrine-related cancer *12*, 109-117.

Bok, R.A., and Small, E.J. (2002). Bloodborne biomolecular markers in prostate cancer development and progression. Nature reviews Cancer *2*, 918-926.

Bommer, G.T., Gerin, I., Feng, Y., Kaczorowski, A.J., Kuick, R., Love, R.E., Zhai, Y., Giordano, T.J., Qin, Z.S., Moore, B.B.*, et al.* (2007). p53-mediated activation of miRNA34 candidate tumor-suppressor genes. Current biology : CB *17*, 1298-1307.

Bonkhoff, H., and Berges, R. (2010). From pathogenesis to prevention of castration resistant prostate cancer. The Prostate *70*, 100-112.

Boon, R.A., Iekushi, K., Lechner, S., Seeger, T., Fischer, A., Heydt, S., Kaluza, D., Treguer, K., Carmona, G., Bonauer, A.*, et al.* (2013). MicroRNA-34a regulates cardiac ageing and function. Nature *495*, 107-110.

Bouchie, A. (2013). First microRNA mimic enters clinic. Nature biotechnology *31*, 577.

Bu, P., Chen, K.Y., Chen, J.H., Wang, L., Walters, J., Shin, Y.J., Goerger, J.P., Sun, J., Witherspoon, M., Rakhilin, N.*, et al.* (2013). A microRNA miR-34a-regulated bimodal switch targets notch in colon cancer stem cells. Cell stem cell *12*, 602-615.

Bubendorf, L., Schopfer, A., Wagner, U., Sauter, G., Moch, H., Willi, N., Gasser, T.C., and Mihatsch, M.J. (2000). Metastatic patterns of prostate cancer: an autopsy study of 1,589 patients. Human pathology *31*, 578-583.

Buchler, T., and Harland, S.J. (2007). Chemotherapy for hormone-resistant prostate cancer: Where are we today? Indian journal of urology : IJU : journal of the Urological Society of India *23*, 55-60.

Burchardt, T., Burchardt, M., Chen, M.W., Cao, Y., de la Taille, A., Shabsigh, A., Hayek, O., Dorai, T., and Buttyan, R. (1999). Transdifferentiation of prostate cancer cells to a

neuroendocrine cell phenotype in vitro and in vivo. The Journal of urology *162*, 1800-1805.

Burger, P.E., Xiong, X., Coetzee, S., Salm, S.N., Moscatelli, D., Goto, K., and Wilson, E.L. (2005). Sca-1 expression identifies stem cells in the proximal region of prostatic ducts with high capacity to reconstitute prostatic tissue. Proceedings of the National Academy of Sciences of the United States of America *102*, 7180-7185.

Cadieux, A., Springall, D.R., Mulderry, P.K., Rodrigo, J., Ghatei, M.A., Terenghi, G., Bloom, S.R., and Polak, J.M. (1986). Occurrence, distribution and ontogeny of CGRP immunoreactivity in the rat lower respiratory tract: effect of capsaicin treatment and surgical denervations. Neuroscience *19*, 605-627.

Calin, G.A., Sevignani, C., Dumitru, C.D., Hyslop, T., Noch, E., Yendamuri, S., Shimizu, M., Rattan, S., Bullrich, F., Negrini, M.*, et al.* (2004). Human microRNA genes are frequently located at fragile sites and genomic regions involved in cancers. Proceedings of the National Academy of Sciences of the United States of America *101*, 2999-3004.

Chang, T.C., Wentzel, E.A., Kent, O.A., Ramachandran, K., Mullendore, M., Lee, K.H., Feldmann, G., Yamakuchi, M., Ferlito, M., Lowenstein, C.J.*, et al.* (2007). Transactivation of miR-34a by p53 broadly influences gene expression and promotes apoptosis. Molecular cell *26*, 745-752.

Chen, Q.R., Yu, L.R., Tsang, P., Wei, J.S., Song, Y.K., Cheuk, A., Chung, J.Y., Hewitt, S.M., Veenstra, T.D., and Khan, J. (2011). Systematic proteome analysis identifies transcription factor YY1 as a direct target of miR-34a. Journal of proteome research *10*, 479-487.

Chen, X., Hu, H., Guan, X., Xiong, G., Wang, Y., Wang, K., Li, J., Xu, X., Yang, K., and Bai, Y. (2012). CpG island methylation status of miRNAs in esophageal squamous cell carcinoma. International journal of cancer Journal international du cancer *130*, 1607-1613.

Chen, Y., Zhu, X., Zhang, X., Liu, B., and Huang, L. (2010). Nanoparticles modified with tumor-targeting scFv deliver siRNA and miRNA for cancer therapy. Molecular therapy : the journal of the American Society of Gene Therapy *18*, 1650-1656.

Cheng, L., Ramesh, A.V., Flesken-Nikitin, A., Choi, J., and Nikitin, A.Y. (2010). Mouse models for cancer stem cell research. Toxicologic pathology *38*, 62-71.

Chiao, J.W., Hsieh, T.C., Xu, W., Sklarew, R.J., and Kancherla, R. (1999). Development of human prostate cancer cells to neuroendocrine-like cells by interleukin-1. International journal of oncology *15*, 1033-1037.

Chim, C.S., Wong, K.Y., Qi, Y., Loong, F., Lam, W.L., Wong, L.G., Jin, D.Y., Costello, J.F., and Liang, R. (2010). Epigenetic inactivation of the miR-34a in hematological malignancies. Carcinogenesis *31*, 745-750.

Choi, N., Zhang, B., Zhang, L., Ittmann, M., and Xin, L. (2012). Adult murine prostate basal and luminal cells are self-sustained lineages that can both serve as targets for prostate cancer initiation. Cancer cell *21*, 253-265.

Choi, Y.J., Lin, C.P., Ho, J.J., He, X., Okada, N., Bu, P., Zhong, Y., Kim, S.Y., Bennett, M.J., Chen, C.*, et al.* (2011). miR-34 miRNAs provide a barrier for somatic cell reprogramming. Nature cell biology *13*, 1353-1360.

Christoffersen, N.R., Shalgi, R., Frankel, L.B., Leucci, E., Lees, M., Klausen, M., Pilpel, Y., Nielsen, F.C., Oren, M., and Lund, A.H. (2010). p53-independent upregulation of miR-34a during oncogene-induced senescence represses MYC. Cell death and differentiation *17*, 236-245.

Clevers, H. (2011). The cancer stem cell: premises, promises and challenges. Nature medicine *17*, 313-319.

Cole, K.A., Attiyeh, E.F., Mosse, Y.P., Laquaglia, M.J., Diskin, S.J., Brodeur, G.M., and Maris, J.M. (2008). A functional screen identifies miR-34a as a candidate neuroblastoma tumor suppressor gene. Molecular cancer research : MCR *6*, 735-742.

Collado, B., Sanchez, M.G., Diaz-Laviada, I., Prieto, J.C., and Carmena, M.J. (2005). Vasoactive intestinal peptide (VIP) induces c-fos expression in LNCaP prostate cancer cells through a mechanism that involves Ca2+ signalling. Implications in angiogenesis and neuroendocrine differentiation. Biochimica et biophysica acta *1744*, 224-233.

Collins, A.T., Habib, F.K., Maitland, N.J., and Neal, D.E. (2001). Identification and isolation of human prostate epithelial stem cells based on alpha(2)beta(1)-integrin expression. Journal of cell science *114*, 3865-3872.

Concepcion, C.P., Han, Y.C., Mu, P., Bonetti, C., Yao, E., D'Andrea, A., Vidigal, J.A., Maughan, W.P., Ogrodowski, P., and Ventura, A. (2012). Intact p53-dependent responses in miR-34-deficient mice. PLoS genetics *8*, e1002797.

Cooperberg, M.R., Moul, J.W., and Carroll, P.R. (2005). The changing face of prostate cancer. Journal of clinical oncology : official journal of the American Society of Clinical Oncology *23*, 8146-8151.

Corney, D.C., Flesken-Nikitin, A., Godwin, A.K., Wang, W., and Nikitin, A.Y. (2007). MicroRNA-34b and MicroRNA-34c are targets of p53 and cooperate in control of cell proliferation and adhesion-independent growth. Cancer research *67*, 8433-8438.

Corney, D.C., Hwang, C.I., Matoso, A., Vogt, M., Flesken-Nikitin, A., Godwin, A.K., Kamat, A.A., Sood, A.K., Ellenson, L.H., Hermeking, H.*, et al.* (2010). Frequent downregulation of miR-34 family in human ovarian cancers. Clinical cancer research : an official journal of the American Association for Cancer Research *16*, 1119-1128.

Cox, M.E., Deeble, P.D., Lakhani, S., and Parsons, S.J. (1999). Acquisition of neuroendocrine characteristics by prostate tumor cells is reversible: implications for prostate cancer progression. Cancer research *59*, 3821-3830.

Craig, V.J., Tzankov, A., Flori, M., Schmid, C.A., Bader, A.G., and Muller, A. (2012). Systemic microRNA-34a delivery induces apoptosis and abrogates growth of diffuse large B-cell lymphoma in vivo. Leukemia *26*, 2421-2424.

de Antonellis, P., Medaglia, C., Cusanelli, E., Andolfo, I., Liguori, L., De Vita, G., Carotenuto, M., Bello, A., Formiggini, F., Galeone, A.*, et al.* (2011). MiR-34a targeting of Notch ligand delta-like 1 impairs CD15+/CD133+ tumor-propagating cells and supports neural differentiation in medulloblastoma. PloS one *6*, e24584.

Debes, J.D., and Tindall, D.J. (2004). Mechanisms of androgen-refractory prostate cancer. The New England journal of medicine *351*, 1488-1490.

Deeble, P.D., Murphy, D.J., Parsons, S.J., and Cox, M.E. (2001). Interleukin-6- and cyclic AMP-mediated signaling potentiates neuroendocrine differentiation of LNCaP prostate tumor cells. Molecular and cellular biology *21*, 8471-8482.

di Sant'Agnese, P.A. (1992). Neuroendocrine differentiation in human prostatic carcinoma. Human pathology *23*, 287-296.

Diaz, M., Abdul, M., and Hoosein, N. (1998). Modulation of neuroendocrine differentiation in prostate cancer by interleukin-1 and -2. The Prostate Supplement *8*, 32-36.

Domen, J., Cheshier, S.H., and Weissman, I.L. (2000). The role of apoptosis in the regulation of hematopoietic stem cells: Overexpression of Bcl-2 increases both their number and repopulation potential. The Journal of experimental medicine *191*, 253-264.

Domingo-Domenech, J., Vidal, S.J., Rodriguez-Bravo, V., Castillo-Martin, M., Quinn, S.A., Rodriguez-Barrueco, R., Bonal, D.M., Charytonowicz, E., Gladoun, N., de la Iglesia-Vicente, J.*, et al.* (2012). Suppression of acquired docetaxel resistance in prostate cancer through depletion of notch- and hedgehog-dependent tumor-initiating cells. Cancer cell *22*, 373-388.

Drachenberg, D.E., Elgamal, A.A., Rowbotham, R., Peterson, M., and Murphy, G.P. (1999). Circulating levels of interleukin-6 in patients with hormone refractory prostate cancer. The Prostate *41*, 127-133.

Du, R., Sun, W., Xia, L., Zhao, A., Yu, Y., Zhao, L., Wang, H., Huang, C., and Sun, S. (2012). Hypoxia-induced down-regulation of microRNA-34a promotes EMT by targeting the Notch signaling pathway in tubular epithelial cells. PloS one *7*, e30771.

Dubrovska, A., Elliott, J., Salamone, R.J., Telegeev, G.D., Stakhovsky, A.E., Schepotin, I.B., Yan, F., Wang, Y., Bouchez, L.C., Kularatne, S.A.*, et al.* (2012). CXCR4 expression in prostate cancer progenitor cells. PloS one *7*, e31226.

Dubrovska, A., Kim, S., Salamone, R.J., Walker, J.R., Maira, S.M., Garcia-Echeverria, C., Schultz, P.G., and Reddy, V.A. (2009). The role of PTEN/Akt/PI3K signaling in the maintenance and viability of prostate cancer stem-like cell populations. Proceedings of the National Academy of Sciences of the United States of America *106*, 268-273.

English, H.F., Santen, R.J., and Isaacs, J.T. (1987). Response of glandular versus basal rat ventral prostatic epithelial cells to androgen withdrawal and replacement. The Prostate *11*, 229-242.

Erdos, E.G., and Skidgel, R.A. (1989). Neutral endopeptidase 24.11 (enkephalinase) and related regulators of peptide hormones. FASEB journal : official publication of the Federation of American Societies for Experimental Biology *3*, 145-151.

Feinberg-Gorenshtein, G., Avigad, S., Jeison, M., Halevy-Berco, G., Mardoukh, J., Luria, D., Ash, S., Steinberg, R., Weizman, A., and Yaniv, I. (2009). Reduced levels of miR-34a in neuroblastoma are not caused by mutations in the TP53 binding site. Genes, chromosomes & cancer *48*, 539-543.

Feldman, B.J., and Feldman, D. (2001). The development of androgen-independent prostate cancer. Nature reviews Cancer *1*, 34-45.

Freedland, S.J., Seligson, D.B., Liu, A.Y., Pantuck, A.J., Paik, S.H., Horvath, S., Wieder, J.A., Zisman, A., Nguyen, D., Tso, C.L.*, et al.* (2003). Loss of CD10 (neutral endopeptidase) is a frequent and early event in human prostate cancer. The Prostate *55*, 71-80.

Fujita, Y., Kojima, K., Hamada, N., Ohhashi, R., Akao, Y., Nozawa, Y., Deguchi, T., and Ito, M. (2008). Effects of miR-34a on cell growth and chemoresistance in prostate cancer PC3 cells. Biochemical and biophysical research communications *377*, 114-119.

Gallardo, E., Navarro, A., Vinolas, N., Marrades, R.M., Diaz, T., Gel, B., Quera, A., Bandres, E., Garcia-Foncillas, J., Ramirez, J.*, et al.* (2009). miR-34a as a prognostic marker of relapse in surgically resected non-small-cell lung cancer. Carcinogenesis *30*, 1903-1909.

Ganju, R.K., Shpektor, R.G., Brenner, D.G., and Shipp, M.A. (1996). CD10/neutral endopeptidase 24.11 is phosphorylated by casein kinase II and coassociates with other phosphoproteins including the lyn src-related kinase. Blood *88*, 4159-4165.

Gazdar, A.F., Helman, L.J., Israel, M.A., Russell, E.K., Linnoila, R.I., Mulshine, J.L., Schuller, H.M., and Park, J.G. (1988). Expression of neuroendocrine cell markers L-dopa decarboxylase, chromogranin A, and dense core granules in human tumors of endocrine and nonendocrine origin. Cancer research *48*, 4078-4082.

Goldstein, A.S., Huang, J., Guo, C., Garraway, I.P., and Witte, O.N. (2010). Identification of a cell of origin for human prostate cancer. Science *329*, 568-571.

Goldstein, A.S., Lawson, D.A., Cheng, D., Sun, W., Garraway, I.P., and Witte, O.N. (2008). Trop2 identifies a subpopulation of murine and human prostate basal cells with stem cell characteristics. Proceedings of the National Academy of Sciences of the United States of America *105*, 20882-20887.

Goodman, O.B., Jr., Febbraio, M., Simantov, R., Zheng, R., Shen, R., Silverstein, R.L., and Nanus, D.M. (2006). Neprilysin inhibits angiogenesis via proteolysis of fibroblast growth factor-2. The Journal of biological chemistry *281*, 33597-33605.

Grobholz, R., Griebe, M., Sauer, C.G., Michel, M.S., Trojan, L., and Bleyl, U. (2005). Influence of neuroendocrine tumor cells on proliferation in prostatic carcinoma. Human pathology *36*, 562-570.

Gutierrez-Canas, I., Juarranz, M.G., Collado, B., Rodriguez-Henche, N., Chiloeches, A., Prieto, J.C., and Carmena, M.J. (2005). Vasoactive intestinal peptide induces neuroendocrine differentiation in the LNCaP prostate cancer cell line through PKA, ERK, and PI3K. The Prostate *63*, 44-55.

Hansson, J., and Abrahamsson, P.A. (2001). Neuroendocrine pathogenesis in adenocarcinoma of the prostate. Annals of oncology : official journal of the European Society for Medical Oncology / ESMO *12 Suppl 2*, S145-152.

Hansson, J., and Abrahamsson, P.A. (2003). Neuroendocrine differentiation in prostatic carcinoma. Scandinavian journal of urology and nephrology Supplementum, 28-36.

Harris, W.P., Mostaghel, E.A., Nelson, P.S., and Montgomery, B. (2009). Androgen deprivation therapy: progress in understanding mechanisms of resistance and optimizing androgen depletion. Nature clinical practice Urology *6*, 76-85.

He, L., He, X., Lim, L.P., de Stanchina, E., Xuan, Z., Liang, Y., Xue, W., Zender, L., Magnus, J., Ridzon, D.*, et al.* (2007). A microRNA component of the p53 tumour suppressor network. Nature *447*, 1130-1134.

Hermeking, H. (2010). The miR-34 family in cancer and apoptosis. Cell death and differentiation *17*, 193-199.

Hermeking, H. (2012). MicroRNAs in the p53 network: micromanagement of tumour suppression. Nature reviews Cancer *12*, 613-626.

Hirano, D., Okada, Y., Minei, S., Takimoto, Y., and Nemoto, N. (2004). Neuroendocrine differentiation in hormone refractory prostate cancer following androgen deprivation therapy. European urology *45*, 586-592; discussion 592.

Horiguchi, A., Zheng, R., Goodman, O.B., Jr., Shen, R., Guan, H., Hersh, L.B., and Nanus, D.M. (2007). Lentiviral vector neutral endopeptidase gene transfer suppresses prostate cancer tumor growth. Cancer gene therapy *14*, 583-589.

Hsu, S.D., Chu, C.H., Tsou, A.P., Chen, S.J., Chen, H.C., Hsu, P.W., Wong, Y.H., Chen, Y.H., Chen, G.H., and Huang, H.D. (2008). miRNAMap 2.0: genomic maps of microRNAs in metazoan genomes. Nucleic acids research *36*, D165-169.

Humez, S., Monet, M., Legrand, G., Lepage, G., Delcourt, P., and Prevarskaya, N. (2006). Epidermal growth factor-induced neuroendocrine differentiation and apoptotic resistance of androgen-independent human prostate cancer cells. Endocrine-related cancer *13*, 181-195.

Huss, W.J., Gray, D.R., Greenberg, N.M., Mohler, J.L., and Smith, G.J. (2005). Breast cancer resistance protein-mediated efflux of androgen in putative benign and malignant prostate stem cells. Cancer research *65*, 6640-6650.

Huss, W.J., Gray, D.R., Werdin, E.S., Funkhouser, W.K., Jr., and Smith, G.J. (2004a). Evidence of pluripotent human prostate stem cells in a human prostate primary xenograft model. The Prostate *60*, 77-90.

Huss, W.J., Gregory, C.W., and Smith, G.J. (2004b). Neuroendocrine cell differentiation in the CWR22 human prostate cancer xenograft: association with tumor cell proliferation prior to recurrence. The Prostate *60*, 91-97.

Hwang, C.I., Matoso, A., Corney, D.C., Flesken-Nikitin, A., Korner, S., Wang, W., Boccaccio, C., Thorgeirsson, S.S., Comoglio, P.M., Hermeking, H.*, et al.* (2011). Wild-type p53 controls cell motility and invasion by dual regulation of MET expression. Proceedings of the National Academy of Sciences of the United States of America *108*, 14240-14245.

Ichimura, A., Ruike, Y., Terasawa, K., Shimizu, K., and Tsujimoto, G. (2010). MicroRNA-34a inhibits cell proliferation by repressing mitogen-activated protein kinase kinase 1 during megakaryocytic differentiation of K562 cells. Molecular pharmacology *77*, 1016-1024.

Iida, K., Zheng, R., Shen, R., and Nanus, D.M. (2012). Adenoviral neutral endopeptidase gene delivery in combination with paclitaxel for the treatment of prostate cancer. International journal of oncology *41*, 1192-1198.

Isaacs, J.T. (2008). Prostate stem cells and benign prostatic hyperplasia. The Prostate *68*, 1025-1034.

Ismail, A.H., Landry, F., Aprikian, A.G., and Chevalier, S. (2002). Androgen ablation promotes neuroendocrine cell differentiation in dog and human prostate. The Prostate *51*, 117-125.

Ito, T., Yamamoto, S., Ohno, Y., Namiki, K., Aizawa, T., Akiyama, A., and Tachibana, M. (2001). Up-regulation of neuroendocrine differentiation in prostate cancer after androgen deprivation therapy, degree and androgen independence. Oncology reports *8*, 1221-1224.

Iwase, A., Shen, R., Navarro, D., and Nanus, D.M. (2004). Direct binding of neutral endopeptidase 24.11 to ezrin/radixin/moesin (ERM) proteins competes with the interaction of CD44 with ERM proteins. The Journal of biological chemistry *279*, 11898-11905.

Javeri, A., Ghaffarpour, M., Taha, M.F., and Houshmand, M. (2013). Downregulation of miR-34a in breast tumors is not associated with either p53 mutations or promoter hypermethylation while it correlates with metastasis. Medical oncology *30*, 413.

Jeter, C.R., Badeaux, M., Choy, G., Chandra, D., Patrawala, L., Liu, C., Calhoun-Davis, T., Zaehres, H., Daley, G.Q., and Tang, D.G. (2009). Functional evidence that the self-renewal gene NANOG regulates human tumor development. Stem cells *27*, 993-1005.

Jeter, C.R., Liu, B., Liu, X., Chen, X., Liu, C., Calhoun-Davis, T., Repass, J., Zaehres, H., Shen, J.J., and Tang, D.G. (2011). NANOG promotes cancer stem cell characteristics and prostate cancer resistance to androgen deprivation. Oncogene *30*, 3833-3845.

Ji, Q., Hao, X., Zhang, M., Tang, W., Yang, M., Li, L., Xiang, D., Desano, J.T., Bommer, G.T., Fan, D.*, et al.* (2009). MicroRNA miR-34 inhibits human pancreatic cancer tumor-initiating cells. PloS one *4*, e6816.

Jin, L., Hemperly, J.J., and Lloyd, R.V. (1991). Expression of neural cell adhesion molecule in normal and neoplastic human neuroendocrine tissues. The American journal of pathology *138*, 961-969.

Jongsma, J., Oomen, M.H., Noordzij, M.A., Van Weerden, W.M., Martens, G.J., van der Kwast, T.H., Schroder, F.H., and van Steenbrugge, G.J. (1999). Kinetics of neuroendocrine differentiation in an androgen-dependent human prostate xenograft model. The American journal of pathology *154*, 543-551.

Jongsma, J., Oomen, M.H., Noordzij, M.A., Van Weerden, W.M., Martens, G.J., van der Kwast, T.H., Schroder, F.H., and van Steenbrugge, G.J. (2000). Androgen deprivation of the PC-310 [correction of prohormone convertase-310] human prostate cancer model system induces neuroendocrine differentiation. Cancer research *60*, 741-748.

Juarranz, M.G., Bolanos, O., Gutierrez-Canas, I., Lerner, E.A., Robberecht, P., Carmena, M.J., Prieto, J.C., and Rodriguez-Henche, N. (2001). Neuroendocrine differentiation of the LNCaP prostate cancer cell line maintains the expression and function of VIP and PACAP receptors. Cellular signalling *13*, 887-894.

Kaller, M., Liffers, S.T., Oeljeklaus, S., Kuhlmann, K., Roh, S., Hoffmann, R., Warscheid, B., and Hermeking, H. (2011). Genome-wide characterization of miR-34a induced changes in protein and mRNA expression by a combined pulsed SILAC and microarray analysis. Molecular & cellular proteomics : MCP *10*, M111 010462.

Kamiya, N., Suzuki, H., Kawamura, K., Imamoto, T., Naya, Y., Tochigi, N., Kakuta, Y., Yamaguchi, K., Ishikura, H., and Ichikawa, T. (2008). Neuroendocrine differentiation in stage D2 prostate cancers. International journal of urology : official journal of the Japanese Urological Association *15*, 423-428.

Kim, J., Adam, R.M., and Freeman, M.R. (2002). Activation of the Erk mitogen-activated protein kinase pathway stimulates neuroendocrine differentiation in LNCaP cells independently of cell cycle withdrawal and STAT3 phosphorylation. Cancer research *62*, 1549-1554.

Kim, N.H., Kim, H.S., Kim, N.G., Lee, I., Choi, H.S., Li, X.Y., Kang, S.E., Cha, S.Y., Ryu, J.K., Na, J.M.*, et al.* (2011). p53 and microRNA-34 are suppressors of canonical Wnt signaling. Science signaling *4*, ra71.

Klein, K.A., Reiter, R.E., Redula, J., Moradi, H., Zhu, X.L., Brothman, A.R., Lamb, D.J., Marcelli, M., Belldegrun, A., Witte, O.N.*, et al.* (1997). Progression of metastatic human prostate cancer to androgen independence in immunodeficient SCID mice. Nature medicine *3*, 402-408.

Komiya, A., Suzuki, H., Imamoto, T., Kamiya, N., Nihei, N., Naya, Y., Ichikawa, T., and Fuse, H. (2009). Neuroendocrine differentiation in the progression of prostate cancer. International journal of urology : official journal of the Japanese Urological Association *16*, 37-44.

Kress, T.R., Cannell, I.G., Brenkman, A.B., Samans, B., Gaestel, M., Roepman, P., Burgering, B.M., Bushell, M., Rosenwald, A., and Eilers, M. (2011). The MK5/PRAK kinase and Myc form a negative feedback loop that is disrupted during colorectal tumorigenesis. Molecular cell *41*, 445-457.

Krijnen, J.L., Janssen, P.J., Ruizeveld de Winter, J.A., van Krimpen, H., Schroder, F.H., and van der Kwast, T.H. (1993). Do neuroendocrine cells in human prostate cancer express androgen receptor? Histochemistry *100*, 393-398.

Kubo, T., Toyooka, S., Tsukuda, K., Sakaguchi, M., Fukazawa, T., Soh, J., Asano, H., Ueno, T., Muraoka, T., Yamamoto, H*., et al.* (2011). Epigenetic silencing of microRNA-34b/c plays an important role in the pathogenesis of malignant pleural mesothelioma. Clinical cancer research : an official journal of the American Association for Cancer Research *17*, 4965-4974.

Kuo, K.T., Guan, B., Feng, Y., Mao, T.L., Chen, X., Jinawath, N., Wang, Y., Kurman, R.J., Shih Ie, M., and Wang, T.L. (2009). Analysis of DNA copy number alterations in ovarian serous tumors identifies new molecular genetic changes in low-grade and high-grade carcinomas. Cancer research *69*, 4036-4042.

Kurita, T., Medina, R.T., Mills, A.A., and Cunha, G.R. (2004). Role of p63 and basal cells in the prostate. Development *131*, 4955-4964.

Lawson, D.A., Xin, L., Lukacs, R.U., Cheng, D., and Witte, O.N. (2007). Isolation and functional characterization of murine prostate stem cells. Proceedings of the National Academy of Sciences of the United States of America *104*, 181-186.

Lawson, D.A., Zong, Y., Memarzadeh, S., Xin, L., Huang, J., and Witte, O.N. (2010). Basal epithelial stem cells are efficient targets for prostate cancer initiation. Proceedings of the National Academy of Sciences of the United States of America *107*, 2610-2615.

Lee, R.C., Feinbaum, R.L., and Ambros, V. (1993). The C. elegans heterochronic gene lin-4 encodes small RNAs with antisense complementarity to lin-14. Cell *75*, 843-854.

Leong, K.G., Wang, B.E., Johnson, L., and Gao, W.Q. (2008). Generation of a prostate from a single adult stem cell. Nature *456*, 804-808.

Li, B., Hu, Y., Ye, F., Li, Y., Lv, W., and Xie, X. (2010a). Reduced miR-34a expression in normal cervical tissues and cervical lesions with high-risk human papillomavirus

infection. International journal of gynecological cancer : official journal of the International Gynecological Cancer Society *20*, 597-604.

Li, H., and Tang, D.G. (2011). Prostate cancer stem cells and their potential roles in metastasis. Journal of surgical oncology *103*, 558-562.

Li, N., Fu, H., Tie, Y., Hu, Z., Kong, W., Wu, Y., and Zheng, X. (2009a). miR-34a inhibits migration and invasion by down-regulation of c-Met expression in human hepatocellular carcinoma cells. Cancer letters *275*, 44-53.

Li, T., Su, Y., Mei, Y., Leng, Q., Leng, B., Liu, Z., Stass, S.A., and Jiang, F. (2010b). ALDH1A1 is a marker for malignant prostate stem cells and predictor of prostate cancer patients' outcome. Laboratory investigation; a journal of technical methods and pathology *90*, 234-244.

Li, Y., Guessous, F., Zhang, Y., Dipierro, C., Kefas, B., Johnson, E., Marcinkiewicz, L., Jiang, J., Yang, Y., Schmittgen, T.D.*, et al.* (2009b). MicroRNA-34a inhibits glioblastoma growth by targeting multiple oncogenes. Cancer research *69*, 7569-7576.

Liao, C.P., Zhong, C., Saribekyan, G., Bading, J., Park, R., Conti, P.S., Moats, R., Berns, A., Shi, W., Zhou, Z.*, et al.* (2007). Mouse models of prostate adenocarcinoma with the capacity to monitor spontaneous carcinogenesis by bioluminescence or fluorescence. Cancer research *67*, 7525-7533.

Litvinov, I.V., Vander Griend, D.J., Xu, Y., Antony, L., Dalrymple, S.L., and Isaacs, J.T. (2006). Low-calcium serum-free defined medium selects for growth of normal prostatic epithelial stem cells. Cancer research *66*, 8598-8607.

Liu, C., Kelnar, K., Liu, B., Chen, X., Calhoun-Davis, T., Li, H., Patrawala, L., Yan, H., Jeter, C., Honorio, S.*, et al.* (2011a). The microRNA miR-34a inhibits prostate cancer stem cells and metastasis by directly repressing CD44. Nature medicine *17*, 211-215.

Liu, J., Pascal, L.E., Isharwal, S., Metzger, D., Ramos Garcia, R., Pilch, J., Kasper, S., Williams, K., Basse, P.H., Nelson, J.B.*, et al.* (2011b). Regenerated luminal epithelial cells are derived from preexisting luminal epithelial cells in adult mouse prostate. Molecular endocrinology *25*, 1849-1857.

Lodygin, D., Tarasov, V., Epanchintsev, A., Berking, C., Knyazeva, T., Korner, H., Knyazev, P., Diebold, J., and Hermeking, H. (2008). Inactivation of miR-34a by aberrant CpG methylation in multiple types of cancer. Cell cycle *7*, 2591-2600.

Lu, B., Gerard, N.P., Kolakowski, L.F., Jr., Bozza, M., Zurakowski, D., Finco, O., Carroll, M.C., and Gerard, C. (1995). Neutral endopeptidase modulation of septic shock. J Exp Med *181*, 2271-2275.

Lujambio, A., Calin, G.A., Villanueva, A., Ropero, S., Sanchez-Cespedes, M., Blanco, D., Montuenga, L.M., Rossi, S., Nicoloso, M.S., Faller, W.J.*, et al.* (2008). A microRNA DNA methylation signature for human cancer metastasis. Proceedings of the National Academy of Sciences of the United States of America *105*, 13556-13561.

Lukacs, R.U., Memarzadeh, S., Wu, H., and Witte, O.N. (2010). Bmi-1 is a crucial regulator of prostate stem cell self-renewal and malignant transformation. Cell stem cell *7*, 682-693.

Mackiewicz, M., Huppi, K., Pitt, J.J., Dorsey, T.H., Ambs, S., and Caplen, N.J. (2011). Identification of the receptor tyrosine kinase AXL in breast cancer as a target for the human miR-34a microRNA. Breast cancer research and treatment *130*, 663-679.

Maes, O.C., Sarojini, H., and Wang, E. (2009). Stepwise up-regulation of microRNA expression levels from replicating to reversible and irreversible growth arrest states in WI-38 human fibroblasts. Journal of cellular physiology *221*, 109-119.

Magee, J.A., Piskounova, E., and Morrison, S.J. (2012). Cancer stem cells: impact, heterogeneity, and uncertainty. Cancer cell *21*, 283-296.

Maguer-Satta, V., Besancon, R., and Bachelard-Cascales, E. (2011). Concise review: neutral endopeptidase (CD10): a multifaceted environment actor in stem cells, physiological mechanisms, and cancer. Stem cells *29*, 389-396.

Malanchi, I., Santamaria-Martinez, A., Susanto, E., Peng, H., Lehr, H.A., Delaloye, J.F., and Huelsken, J. (2012). Interactions between cancer stem cells and their niche govern metastatic colonization. Nature *481*, 85-89.

Mariot, P., Vanoverberghe, K., Lalevee, N., Rossier, M.F., and Prevarskaya, N. (2002). Overexpression of an alpha 1H (Cav3.2) T-type calcium channel during neuroendocrine differentiation of human prostate cancer cells. The Journal of biological chemistry *277*, 10824-10833.

McWilliam, L.J., Manson, C., and George, N.J. (1997). Neuroendocrine differentiation and prognosis in prostatic adenocarcinoma. British journal of urology *80*, 287-290.

Medeiros Mdos, S., and Turner, A.J. (1996). Metabolism and functions of neuropeptide Y. Neurochemical research *21*, 1125-1132.

Miki, J., Furusato, B., Li, H., Gu, Y., Takahashi, H., Egawa, S., Sesterhenn, I.A., McLeod, D.G., Srivastava, S., and Rhim, J.S. (2007). Identification of putative stem cell markers, CD133 and CXCR4, in hTERT-immortalized primary nonmalignant and malignant tumor-derived human prostate epithelial cell lines and in prostate cancer specimens. Cancer research *67*, 3153-3161.

Mraz, M., Malinova, K., Kotaskova, J., Pavlova, S., Tichy, B., Malcikova, J., Stano Kozubik, K., Smardova, J., Brychtova, Y., Doubek, M.*, et al.* (2009). miR-34a, miR-29c and miR-17-5p are downregulated in CLL patients with TP53 abnormalities. Leukemia *23*, 1159-1163.

Mudduluru, G., Ceppi, P., Kumarswamy, R., Scagliotti, G.V., Papotti, M., and Allgayer, H. (2011). Regulation of Axl receptor tyrosine kinase expression by miR-34a and miR-199a/b in solid cancer. Oncogene *30*, 2888-2899.

Mulholland, D.J., Xin, L., Morim, A., Lawson, D., Witte, O., and Wu, H. (2009). Lin-Sca-1+CD49fhigh stem/progenitors are tumor-initiating cells in the Pten-null prostate cancer model. Cancer research *69*, 8555-8562.

Navarro, F., Gutman, D., Meire, E., Caceres, M., Rigoutsos, I., Bentwich, Z., and Lieberman, J. (2009). miR-34a contributes to megakaryocytic differentiation of K562 cells independently of p53. Blood *114*, 2181-2192.

Nguyen, D.X., Chiang, A.C., Zhang, X.H., Kim, J.Y., Kris, M.G., Ladanyi, M., Gerald, W.L., and Massague, J. (2009). WNT/TCF signaling through LEF1 and HOXB9 mediates lung adenocarcinoma metastasis. Cell *138*, 51-62.

Nguyen, L.V., Vanner, R., Dirks, P., and Eaves, C.J. (2012). Cancer stem cells: an evolving concept. Nature reviews Cancer *12*, 133-143.

Nikitin, A.Y., Matoso, A., and Roy-Burman, P. (2007). Prostate stem cells and cancer. Histology and histopathology *22*, 1043-1049.

Oskarsson, T., Acharyya, S., Zhang, X.H., Vanharanta, S., Tavazoie, S.F., Morris, P.G., Downey, R.J., Manova-Todorova, K., Brogi, E., and Massague, J. (2011). Breast cancer cells produce tenascin C as a metastatic niche component to colonize the lungs. Nature medicine *17*, 867-874.

Osman, I., Yee, H., Taneja, S.S., Levinson, B., Zeleniuch-Jacquotte, A., Chang, C., Nobert, C., and Nanus, D.M. (2004). Neutral endopeptidase protein expression and prognosis in localized prostate cancer. Clin Cancer Res *10*, 4096-4100.

Ousset, M., Van Keymeulen, A., Bouvencourt, G., Sharma, N., Achouri, Y., Simons, B.D., and Blanpain, C. (2012). Multipotent and unipotent progenitors contribute to prostate postnatal development. Nature cell biology *14*, 1131-1138.

Palapattu, G.S., Wu, C., Silvers, C.R., Martin, H.B., Williams, K., Salamone, L., Bushnell, T., Huang, L.S., Yang, Q., and Huang, J. (2009). Selective expression of CD44, a putative prostate cancer stem cell marker, in neuroendocrine tumor cells of human prostate cancer. The Prostate *69*, 787-798.

Palmer, J., Ernst, M., Hammacher, A., and Hertzog, P.J. (2005). Constitutive activation of gp130 leads to neuroendocrine differentiation in vitro and in vivo. The Prostate *62*, 282-289.

Papandreou, C.N., Usmani, B., Geng, Y., Bogenrieder, T., Freeman, R., Wilk, S., Finstad, C.L., Reuter, V.E., Powell, C.T., Scheinberg, D.*, et al.* (1998). Neutral endopeptidase 24.11 loss in metastatic human prostate cancer contributes to androgen-independent progression. Nat Med *4*, 50-57.

Patrawala, L., Calhoun-Davis, T., Schneider-Broussard, R., and Tang, D.G. (2007). Hierarchical organization of prostate cancer cells in xenograft tumors: the CD44+alpha2beta1+ cell population is enriched in tumor-initiating cells. Cancer research *67*, 6796-6805.

Patrawala, L., Calhoun, T., Schneider-Broussard, R., Li, H., Bhatia, B., Tang, S., Reilly, J.G., Chandra, D., Zhou, J., Claypool, K.*, et al.* (2006). Highly purified CD44+ prostate cancer cells from xenograft human tumors are enriched in tumorigenic and metastatic progenitor cells. Oncogene *25*, 1696-1708.

Patrawala, L., Calhoun, T., Schneider-Broussard, R., Zhou, J., Claypool, K., and Tang, D.G. (2005). Side population is enriched in tumorigenic, stem-like cancer cells, whereas ABCG2+ and ABCG2- cancer cells are similarly tumorigenic. Cancer research *65*, 6207-6219.

Potten, C.S., Wilson, J.W., and Booth, C. (1997). Regulation and significance of apoptosis in the stem cells of the gastrointestinal epithelium. Stem cells *15*, 82-93.

Pramanik, D., Campbell, N.R., Karikari, C., Chivukula, R., Kent, O.A., Mendell, J.T., and Maitra, A. (2011). Restitution of tumor suppressor microRNAs using a systemic nanovector inhibits pancreatic cancer growth in mice. Molecular cancer therapeutics *10*, 1470-1480.

Qin, J., Liu, X., Laffin, B., Chen, X., Choy, G., Jeter, C.R., Calhoun-Davis, T., Li, H., Palapattu, G.S., Pang, S.*, et al.* (2012). The PSA(-/lo) prostate cancer cell population harbors self-renewing long-term tumor-propagating cells that resist castration. Cell stem cell *10*, 556-569.

Qiu, Y., Robinson, D., Pretlow, T.G., and Kung, H.J. (1998). Etk/Bmx, a tyrosine kinase with a pleckstrin-homology domain, is an effector of phosphatidylinositol 3'-kinase and is involved in interleukin 6-induced neuroendocrine differentiation of prostate cancer cells. Proceedings of the National Academy of Sciences of the United States of America *95*, 3644-3649.

Rajasekhar, V.K., Studer, L., Gerald, W., Socci, N.D., and Scher, H.I. (2011). Tumour-initiating stem-like cells in human prostate cancer exhibit increased NF-kappaB signalling. Nature communications *2*, 162.

Ratnacaram, C.K., Teletin, M., Jiang, M., Meng, X., Chambon, P., and Metzger, D. (2008). Temporally controlled ablation of PTEN in adult mouse prostate epithelium generates a model of invasive prostatic adenocarcinoma. Proceedings of the National Academy of Sciences of the United States of America *105*, 2521-2526.

Raver-Shapira, N., Marciano, E., Meiri, E., Spector, Y., Rosenfeld, N., Moskovits, N., Bentwich, Z., and Oren, M. (2007). Transcriptional activation of miR-34a contributes to p53-mediated apoptosis. Molecular cell *26*, 731-743.

Reinhart, B.J., Slack, F.J., Basson, M., Pasquinelli, A.E., Bettinger, J.C., Rougvie, A.E., Horvitz, H.R., and Ruvkun, G. (2000). The 21-nucleotide let-7 RNA regulates developmental timing in Caenorhabditis elegans. Nature *403*, 901-906.

Richardson, G.D., Robson, C.N., Lang, S.H., Neal, D.E., Maitland, N.J., and Collins, A.T. (2004). CD133, a novel marker for human prostatic epithelial stem cells. Journal of cell science *117*, 3539-3545.

Roques, B.P., Noble, F., Dauge, V., Fournie-Zaluski, M.C., and Beaumont, A. (1993). Neutral endopeptidase 24.11: structure, inhibition, and experimental and clinical pharmacology. Pharmacological reviews *45*, 87-146.

Roy, S., Levi, E., Majumdar, A.P., and Sarkar, F.H. (2012). Expression of miR-34 is lost in colon cancer which can be re-expressed by a novel agent CDF. Journal of hematology & oncology *5*, 58.

Salm, S.N., Burger, P.E., Coetzee, S., Goto, K., Moscatelli, D., and Wilson, E.L. (2005). TGF-{beta} maintains dormancy of prostatic stem cells in the proximal region of ducts. The Journal of cell biology *170*, 81-90.

Schmechel, D., Marangos, P.J., and Brightman, M. (1978). Neurone-specific enolase is a molecular marker for peripheral and central neuroendocrine cells. Nature *276*, 834-836.

Scott, S.L., Earle, J.D., and Gumerlock, P.H. (2003). Functional p53 increases prostate cancer cell survival after exposure to fractionated doses of ionizing radiation. Cancer research *63*, 7190-7196.

Sethi, S., Kong, D., Land, S., Dyson, G., Sakr, W.A., and Sarkar, F.H. (2013). Comprehensive molecular oncogenomic profiling and miRNA analysis of prostate cancer. American journal of translational research *5*, 200-211.

Shackleton, M., Quintana, E., Fearon, E.R., and Morrison, S.J. (2009). Heterogeneity in cancer: cancer stem cells versus clonal evolution. Cell *138*, 822-829.

Shariat, S.F., Andrews, B., Kattan, M.W., Kim, J., Wheeler, T.M., and Slawin, K.M. (2001). Plasma levels of interleukin-6 and its soluble receptor are associated with prostate cancer progression and metastasis. Urology *58*, 1008-1015.

Shen, M.M., and Abate-Shen, C. (2010). Molecular genetics of prostate cancer: new prospects for old challenges. Genes & development *24*, 1967-2000.

Shen, R., Dorai, T., Szaboles, M., Katz, A.E., Olsson, C.A., and Buttyan, R. (1997). Transdifferentiation of cultured human prostate cancer cells to a neuroendocrine cell phenotype in a hormone-depleted medium. Urologic oncology *3*, 67-75.

Shen, Z., Zhan, G., Ye, D., Ren, Y., Cheng, L., Wu, Z., and Guo, J. (2012). MicroRNA-34a affects the occurrence of laryngeal squamous cell carcinoma by targeting the antiapoptotic gene survivin. Medical oncology *29*, 2473-2480.

Shinohara, T., Avarbock, M.R., and Brinster, R.L. (1999). beta1- and alpha6-integrin are surface markers on mouse spermatogonial stem cells. Proceedings of the National Academy of Sciences of the United States of America *96*, 5504-5509.

Shipp, M.A., and Look, A.T. (1993). Hematopoietic differentiation antigens that are membrane-associated enzymes: cutting is the key! Blood *82*, 1052-1070.

Siegel, R., Ma, J., Zou, Z., and Jemal, A. (2014). Cancer statistics, 2014. CA: a cancer journal for clinicians *64*, 9-29.

Siemens, H., Jackstadt, R., Hunten, S., Kaller, M., Menssen, A., Gotz, U., and Hermeking, H. (2011). miR-34 and SNAIL form a double-negative feedback loop to regulate epithelial-mesenchymal transitions. Cell cycle *10*, 4256-4271.

Siemens, H., Jackstadt, R., Kaller, M., and Hermeking, H. (2013). Repression of c-Kit by p53 is mediated by miR-34 and is associated with reduced chemoresistance, migration and stemness. Oncotarget *4*, 1399-1415.

Silber, J., Jacobsen, A., Ozawa, T., Harinath, G., Pedraza, A., Sander, C., Holland, E.C., and Huse, J.T. (2012). miR-34a repression in proneural malignant gliomas upregulates expression of its target PDGFRA and promotes tumorigenesis. PloS one *7*, e33844.

Sotomayor, P., Godoy, A., Smith, G.J., and Huss, W.J. (2009). Oct4A is expressed by a subpopulation of prostate neuroendocrine cells. The Prostate *69*, 401-410.

Stoyanova, T., Goldstein, A.S., Cai, H., Drake, J.M., Huang, J., and Witte, O.N. (2012). Regulated proteolysis of Trop2 drives epithelial hyperplasia and stem cell self-renewal via beta-catenin signaling. Genes & development *26*, 2271-2285.

Sui, G., Affar el, B., Shi, Y., Brignone, C., Wall, N.R., Yin, P., Donohoe, M., Luke, M.P., Calvo, D., Grossman, S.R.*, et al.* (2004). Yin Yang 1 is a negative regulator of p53. Cell *117*, 859-872.

Sumitomo, M., Iwase, A., Zheng, R., Navarro, D., Kaminetzky, D., Shen, R., Georgescu, M.M., and Nanus, D.M. (2004). Synergy in tumor suppression by direct interaction of neutral endopeptidase with PTEN. Cancer cell *5*, 67-78.

Sumitomo, M., Shen, R., and Nanus, D.M. (2005). Involvement of neutral endopeptidase in neoplastic progression. Biochimica et biophysica acta *1751*, 52-59.

Sumitomo, M., Shen, R., Walburg, M., Dai, J., Geng, Y., Navarro, D., Boileau, G., Papandreou, C.N., Giancotti, F.G., Knudsen, B.*, et al.* (2000). Neutral endopeptidase inhibits prostate cancer cell migration by blocking focal adhesion kinase signaling. The Journal of clinical investigation *106*, 1399-1407.

Sun, F., Fu, H., Liu, Q., Tie, Y., Zhu, J., Xing, R., Sun, Z., and Zheng, X. (2008). Downregulation of CCND1 and CDK6 by miR-34a induces cell cycle arrest. FEBS letters *582*, 1564-1568.

Sun, Y., Niu, J., and Huang, J. (2009). Neuroendocrine differentiation in prostate cancer. American journal of translational research *1*, 148-162.

Suzuki, A., Zheng, Y., Kondo, R., Kusakabe, M., Takada, Y., Fukao, K., Nakauchi, H., and Taniguchi, H. (2000). Flow-cytometric separation and enrichment of hepatic progenitor cells in the developing mouse liver. Hepatology *32*, 1230-1239.

Suzuki, H., Yamamoto, E., Nojima, M., Kai, M., Yamano, H.O., Yoshikawa, K., Kimura, T., Kudo, T., Harada, E., Sugai, T.*, et al.* (2010). Methylation-associated silencing of microRNA-34b/c in gastric cancer and its involvement in an epigenetic field defect. Carcinogenesis *31*, 2066-2073.

Tanaka, H., Kono, E., Tran, C.P., Miyazaki, H., Yamashiro, J., Shimomura, T., Fazli, L., Wada, R., Huang, J., Vessella, R.L.*, et al.* (2010). Monoclonal antibody targeting of N-cadherin inhibits prostate cancer growth, metastasis and castration resistance. Nature medicine *16*, 1414-1420.

Tani, H., Morris, R.J., and Kaur, P. (2000). Enrichment for murine keratinocyte stem cells based on cell surface phenotype. Proceedings of the National Academy of Sciences of the United States of America *97*, 10960-10965.

Taplin, M.E., George, D.J., Halabi, S., Sanford, B., Febbo, P.G., Hennessy, K.T., Mihos, C.G., Vogelzang, N.J., Small, E.J., and Kantoff, P.W. (2005). Prognostic significance of plasma chromogranin a levels in patients with hormone-refractory prostate cancer treated in Cancer and Leukemia Group B 9480 study. Urology *66*, 386-391.

Tarasov, V., Jung, P., Verdoodt, B., Lodygin, D., Epanchintsev, A., Menssen, A., Meister, G., and Hermeking, H. (2007). Differential regulation of microRNAs by p53 revealed by massively parallel sequencing: miR-34a is a p53 target that induces apoptosis and G1-arrest. Cell cycle *6*, 1586-1593.

Tazawa, H., Tsuchiya, N., Izumiya, M., and Nakagama, H. (2007). Tumor-suppressive miR-34a induces senescence-like growth arrest through modulation of the E2F pathway in human colon cancer cells. Proceedings of the National Academy of Sciences of the United States of America *104*, 15472-15477.

Tiberio, R., Marconi, A., Fila, C., Fumelli, C., Pignatti, M., Krajewski, S., Giannetti, A., Reed, J.C., and Pincelli, C. (2002). Keratinocytes enriched for stem cells are protected from anoikis via an integrin signaling pathway in a Bcl-2 dependent manner. FEBS letters *524*, 139-144.

Toyota, M., Suzuki, H., Sasaki, Y., Maruyama, R., Imai, K., Shinomura, Y., and Tokino, T. (2008). Epigenetic silencing of microRNA-34b/c and B-cell translocation gene 4 is associated with CpG island methylation in colorectal cancer. Cancer research *68*, 4123-4132.

Trang, P., Wiggins, J.F., Daige, C.L., Cho, C., Omotola, M., Brown, D., Weidhaas, J.B., Bader, A.G., and Slack, F.J. (2011). Systemic delivery of tumor suppressor microRNA mimics using a neutral lipid emulsion inhibits lung tumors in mice. Molecular therapy : the journal of the American Society of Gene Therapy *19*, 1116-1122.

Tryndyak, V.P., Ross, S.A., Beland, F.A., and Pogribny, I.P. (2009). Down-regulation of the microRNAs miR-34a, miR-127, and miR-200b in rat liver during hepatocarcinogenesis induced by a methyl-deficient diet. Molecular carcinogenesis *48*, 479-487.

Tsujimura, A., Koikawa, Y., Salm, S., Takao, T., Coetzee, S., Moscatelli, D., Shapiro, E., Lepor, H., Sun, T.T., and Wilson, E.L. (2002). Proximal location of mouse prostate epithelial stem cells: a model of prostatic homeostasis. The Journal of cell biology *157*, 1257-1265.

Turner, A.J., and Tanzawa, K. (1997). Mammalian membrane metallopeptidases: NEP, ECE, KELL, and PEX. FASEB journal : official publication of the Federation of American Societies for Experimental Biology *11*, 355-364.

Valdez, J.M., Zhang, L., Su, Q., Dakhova, O., Zhang, Y., Shahi, P., Spencer, D.M., Creighton, C.J., Ittmann, M.M., and Xin, L. (2012). Notch and TGFbeta form a reciprocal positive regulatory loop that suppresses murine prostate basal stem/progenitor cell activity. Cell stem cell *11*, 676-688.

Valent, P., Bonnet, D., De Maria, R., Lapidot, T., Copland, M., Melo, J.V., Chomienne, C., Ishikawa, F., Schuringa, J.J., Stassi, G.*, et al.* (2012). Cancer stem cell definitions and terminology: the devil is in the details. Nature reviews Cancer *12*, 767-775.

van den Hoogen, C., van der Horst, G., Cheung, H., Buijs, J.T., Lippitt, J.M., Guzman-Ramirez, N., Hamdy, F.C., Eaton, C.L., Thalmann, G.N., Cecchini, M.G.*, et al.* (2010). High aldehyde dehydrogenase activity identifies tumor-initiating and metastasis-initiating cells in human prostate cancer. Cancer research *70*, 5163-5173.

Vander Griend, D.J., Karthaus, W.L., Dalrymple, S., Meeker, A., DeMarzo, A.M., and Isaacs, J.T. (2008). The role of CD133 in normal human prostate stem cells and malignant cancer-initiating cells. Cancer research *68*, 9703-9711.

Vanoverberghe, K., Vanden Abeele, F., Mariot, P., Lepage, G., Roudbaraki, M., Bonnal, J.L., Mauroy, B., Shuba, Y., Skryma, R., and Prevarskaya, N. (2004). Ca2+ homeostasis and apoptotic resistance of neuroendocrine-differentiated prostate cancer cells. Cell death and differentiation *11*, 321-330.

Vashchenko, N., and Abrahamsson, P.A. (2005). Neuroendocrine differentiation in prostate cancer: implications for new treatment modalities. European urology *47*, 147-155.

Visvader, J.E., and Lindeman, G.J. (2012). Cancer stem cells: current status and evolving complexities. Cell stem cell *10*, 717-728.

Vogt, M., Munding, J., Gruner, M., Liffers, S.T., Verdoodt, B., Hauk, J., Steinstraesser, L., Tannapfel, A., and Hermeking, H. (2011). Frequent concomitant inactivation of miR-34a and miR-34b/c by CpG methylation in colorectal, pancreatic, mammary, ovarian, urothelial, and renal cell carcinomas and soft tissue sarcomas. Virchows Archiv : an international journal of pathology *458*, 313-322.

Wang, G.M., Kovalenko, B., Wilson, E.L., and Moscatelli, D. (2007). Vascular density is highest in the proximal region of the mouse prostate. The Prostate *67*, 968-975.

Wang, Q., Horiatis, D., and Pinski, J. (2004). Inhibitory effect of IL-6-induced neuroendocrine cells on prostate cancer cell proliferation. The Prostate *61*, 253-259.

Wang, X., Kruithof-de Julio, M., Economides, K.D., Walker, D., Yu, H., Halili, M.V., Hu, Y.P., Price, S.M., Abate-Shen, C., and Shen, M.M. (2009a). A luminal epithelial stem cell that is a cell of origin for prostate cancer. Nature *461*, 495-500.

Wang, X., Wang, H.K., McCoy, J.P., Banerjee, N.S., Rader, J.S., Broker, T.R., Meyers, C., Chow, L.T., and Zheng, Z.M. (2009b). Oncogenic HPV infection interrupts the expression of tumor-suppressive miR-34a through viral oncoprotein E6. Rna *15*, 637-647.

Wang, Y., Hayward, S., Cao, M., Thayer, K., and Cunha, G. (2001). Cell differentiation lineage in the prostate. Differentiation; research in biological diversity *68*, 270-279.

Wang, Z., Chen, Z., Gao, Y., Li, N., Li, B., Tan, F., Tan, X., Lu, N., Sun, Y., Sun, J.*, et al.* (2011). DNA hypermethylation of microRNA-34b/c has prognostic value for stage non-small cell lung cancer. Cancer biology & therapy *11*, 490-496.

Wang, Z.A., Mitrofanova, A., Bergren, S.K., Abate-Shen, C., Cardiff, R.D., Califano, A., and Shen, M.M. (2013). Lineage analysis of basal epithelial cells reveals their unexpected plasticity and supports a cell-of-origin model for prostate cancer heterogeneity. Nature cell biology *15*, 274-283.

Wei, J., Shi, Y., Zheng, L., Zhou, B., Inose, H., Wang, J., Guo, X.E., Grosschedl, R., and Karsenty, G. (2012). miR-34s inhibit osteoblast proliferation and differentiation in the mouse by targeting SATB2. The Journal of cell biology *197*, 509-521.

Wei, J.S., Song, Y.K., Durinck, S., Chen, Q.R., Cheuk, A.T., Tsang, P., Zhang, Q., Thiele, C.J., Slack, A., Shohet, J.*, et al.* (2008). The MYCN oncogene is a direct target of miR-34a. Oncogene *27*, 5204-5213.

Welch, C., Chen, Y., and Stallings, R.L. (2007). MicroRNA-34a functions as a potential tumor suppressor by inducing apoptosis in neuroblastoma cells. Oncogene *26*, 5017-5022.

Wiedenmann, B., Franke, W.W., Kuhn, C., Moll, R., and Gould, V.E. (1986). Synaptophysin: a marker protein for neuroendocrine cells and neoplasms. Proceedings of the National Academy of Sciences of the United States of America *83*, 3500-3504.

Wiggins, J.F., Ruffino, L., Kelnar, K., Omotola, M., Patrawala, L., Brown, D., and Bader, A.G. (2010). Development of a lung cancer therapeutic based on the tumor suppressor microRNA-34. Cancer research *70*, 5923-5930.

Wightman, B., Ha, I., and Ruvkun, G. (1993). Posttranscriptional regulation of the heterochronic gene lin-14 by lin-4 mediates temporal pattern formation in C. elegans. Cell *75*, 855-862.

Winter, J., Jung, S., Keller, S., Gregory, R.I., and Diederichs, S. (2009). Many roads to maturity: microRNA biogenesis pathways and their regulation. Nature cell biology *11*, 228-234.

Wright, M.E., Tsai, M.J., and Aebersold, R. (2003). Androgen receptor represses the neuroendocrine transdifferentiation process in prostate cancer cells. Molecular endocrinology *17*, 1726-1737.

Xin, L., Lawson, D.A., and Witte, O.N. (2005). The Sca-1 cell surface marker enriches for a prostate-regenerating cell subpopulation that can initiate prostate tumorigenesis. Proceedings of the National Academy of Sciences of the United States of America *102*, 6942-6947.

Yamakuchi, M., Ferlito, M., and Lowenstein, C.J. (2008). miR-34a repression of SIRT1 regulates apoptosis. Proceedings of the National Academy of Sciences of the United States of America *105*, 13421-13426.

Yin, D., Ogawa, S., Kawamata, N., Leiter, A., Ham, M., Li, D., Doan, N.B., Said, J.W., Black, K.L., and Phillip Koeffler, H. (2013). miR-34a functions as a tumor suppressor modulating EGFR in glioblastoma multiforme. Oncogene *32*, 1155-1163.

Yook, J.I., Li, X.Y., Ota, I., Fearon, E.R., and Weiss, S.J. (2005). Wnt-dependent regulation of the E-cadherin repressor snail. The Journal of biological chemistry *280*, 11740-11748.

Yook, J.I., Li, X.Y., Ota, I., Hu, C., Kim, H.S., Kim, N.H., Cha, S.Y., Ryu, J.K., Choi, Y.J., Kim, J.*, et al.* (2006). A Wnt-Axin2-GSK3beta cascade regulates Snail1 activity in breast cancer cells. Nature cell biology *8*, 1398-1406.

Yuan, T.C., Veeramani, S., Lin, F.F., Kondrikou, D., Zelivianski, S., Igawa, T., Karan, D., Batra, S.K., and Lin, M.F. (2006). Androgen deprivation induces human prostate epithelial neuroendocrine differentiation of androgen-sensitive LNCaP cells. Endocrine-related cancer *13*, 151-167.

Zelivianski, S., Verni, M., Moore, C., Kondrikov, D., Taylor, R., and Lin, M.F. (2001). Multipathways for transdifferentiation of human prostate cancer cells into neuroendocrine-like phenotype. Biochimica et biophysica acta *1539*, 28-43.

Zhao, J., Lammers, P., Torrance, C.J., and Bader, A.G. (2013). TP53-independent Function of miR-34a via HDAC1 and p21(CIP1/WAF1.). Molecular therapy : the journal of the American Society of Gene Therapy *21*, 1678-1686.

Zheng, R., Iwase, A., Shen, R., Goodman, O.B., Jr., Sugimoto, N., Takuwa, Y., Lerner, D.J., and Nanus, D.M. (2006). Neuropeptide-stimulated cell migration in prostate cancer cells is mediated by RhoA kinase signaling and inhibited by neutral endopeptidase. Oncogene *25*, 5942-5952.

Zhou, Z., Flesken-Nikitin, A., and Nikitin, A.Y. (2007). Prostate cancer associated with p53 and Rb deficiency arises from the stem/progenitor cell-enriched proximal region of prostatic ducts. Cancer research *67*, 5683-5690.

CHAPTER 2

MIR-34 COOPERATES WITH P53 IN SUPPRESSION OF PROSTATE CANCER BY JOINT REGULATION OF STEM CELL COMPARTMENT

Chieh-Yang Cheng, Chang-Il Hwang, David C. Corney, Andrea Flesken-Nikitin, Longchang Jiang, Gülfem Meryem Öner, Robert J. Munroe, John C. Schimenti, Heiko Hermeking, and Alexander Yu. Nikitin, (2014). Cell Rep., S2211-1247 (14): 00123-00125. PMID: 24630988

Author contributions: Chieh-Yang Cheng and Alexander Yu. Nikitin designed the study, interpreted data and wrote the manuscript. Chieh-Yang Cheng, Chang-Il Hwang, David C. Corney, and Andrea Flesken-Nikitin performed experiments and analysed data. Jiang Long-Chang, Gülfem Meryem Öner, Robert J. Munroe, John C. Schimenti, and Heiko Hermeking contributed new reagents/analytic tools/*mir-34a*$^{-/-}$ and *mir-34a*$^{loxP/loxP}$ mice. Alexander Yu. Nikitin supervised the project and gave final approval.

2.1 Abstract

The miR-34 family was originally found to be a direct target of p53 and is a group of putative tumor suppressors. Surprisingly, mice lacking all *mir-34* genes show no increase in cancer formation by 18 months of age, hence placing the physiological relevance of previous studies in doubt. Here, we report that mice with prostate epithelium-specific inactivation of *mir-34* and *p53* show expansion of the prostate stem cell compartment and develop early invasive adenocarcinomas and high-grade prostatic intraepithelial neoplasia, whereas no such lesions are observed after inactivation of either the *mir-34* or *p53* genes alone by 15 months of age. Consistently, combined deficiency of p53 and miR-34 leads to acceleration of MET-dependent growth, self-renewal, and motility of prostate stem/progenitor cells. Our study provides direct genetic evidence that *mir-34* genes are bona fide tumor suppressors and identifies joint control of MET expression by p53 and miR-34 as a key component of prostate stem cell compartment regulation, aberrations in which may lead to cancer.

2.2 Introduction

The microRNA-34 (miR-34) is highly evolutionary conserved (Corney et al., 2007; He et al., 2007). In mammals, the miR-34 family is composed of three processed miRNAs that are encoded by two different genes: miR-34a is encoded by its own transcript, whereas miR-34b and miR-34c share a common primary transcript as a cluster. Due to the high homology among these three members, they have many similar targets and may be functionally redundant (He et al., 2007). miR-34 was the first miRNA reported to be

directly transactivated by tumor suppressor p53 (a.k.a Trp53/TP53), and is considered to be an important component of the p53 network (Hermeking, 2012).

In addition to transactivation-dependent decrease in expression levels in p53 deficient tumors, *mir-34* is also deleted or epigenetically down-regulated in multiple cancer cell lines and human malignancies (Bader, 2012; Hermeking, 2012). Ectopic expression of miR-34 has been shown to counteract various oncogenic processes by regulating target genes that function in cell cycle, apoptosis, senescence, cell migration, and invasion (Hermeking, 2012). Furthermore, treatment with miR-34 mimics inhibits cancer formation in transplantation experiments (Bader, 2012; Liu et al., 2011a).

Contrary to the expectations raised from experiments based on nonphysiological approaches, such as exogenous miR-34 introduction and miR-34 knockdown, only minor defects have been reported in studies of mice with targeted inactivating mutations of *mir-34* (Concepcion et al., 2012; Park et al., 2002; Wei et al., 2012). Moreover, complete genetic inactivation of miR-34 did not impair the p53 response in a variety of ex vivo and in vivo assays (Concepcion et al., 2012). Most surprisingly, no increase in spontaneous or irradiation-induced carcinogenesis has been observed in mice lacking all *mir-34* genes by 18 month of age (Concepcion et al., 2012). The absence of all *mir-34* genes also did not accelerate B-cell lymphomagenesis in mice overexpressing c-Myc under the control of *Eμ* promoter (Concepcion et al., 2012). These data question the native tumor-suppressive function of miR-34. Clarification of miR-34 role as a tumor suppressor is of particular importance because reintroduction of this miRNA into cancer cells has already reached phase 1 clinical trials (Bouchie, 2013).

A number of recent studies have provided evidence of p53-independent expression of miR-34. For example, miR-34a can be up-regulated to repress MYC during oncogene-induced senescence in human TIG3 fibroblasts (Christoffersen et al., 2010), and contributes to megakaryocytic differentiation of K562 cells (Navarro et al., 2009) in a p53-independent fashion. Consistent with these observations, levels of all miR-34 family members remain high in the brains, testes, and lungs of mice lacking p53 (Concepcion et al., 2012).

Methylation of *mir-34a* and *mir-34b/c* has been found in prostate cancers carrying mutant p53 (Fujita et al., 2008; Kojima et al., 2010; Liu et al., 2011a; Lodygin et al., 2008). Furthermore, frequent hypermethylation of *mir-34* in cancers with high occurrence of p53 mutations, such as ovarian and mammary carcinomas and soft tissue sarcomas (Corney et al., 2010; Lodygin et al., 2008; Vogt et al., 2011), suggests the coexistence of both alterations in the same neoplasms. These findings, together with reports of p53-independent regulation of miR-34, suggest that p53 and miR-34 may cooperate in cancer suppression. This possibility is also supported by our observation that p53 and miR-34 may jointly regulate MET receptor tyrosine kinase as a part of coherent feedforward loop in primary ovarian surface epithelium cells (Hwang et al., 2011). However, there is no direct experimental evidence for p53 and miR-34 cooperation in MET regulation in animal models. By using newly generated mice carrying conditional alleles of *mir-34a* and *mir-34b/c*, we show that miR-34 cooperates with p53 in suppression of prostate carcinogenesis by joint MET-mediated control of stem cell compartment.

2.3 Materials and Methods

Generation of mice with mir-34 conventional and conditional targeted mutations. All animal experiments were carried out in strict accordance with the recommendations of the Guide for the Care and Use of Laboratory Animals of the National Institutes of Health. The protocol was approved by the Institutional Laboratory Animal Use and Care Committee at Cornell University. *mir-34a* and *mir-34b/c* gene-targeting vectors were introduced into embryonic stem cells and homologous recombinants were identified by positive/negative selection and by a quantitative approach, respectively. After germ line transmission of the targeted allele, a *FRT*-flanked *Neo* cassette was excised by crosses with FLPeR transgenic mice. The resulting mice carrying conditional (floxed) alleles were crossed to *EIIa-Cre* mice to obtain conventional null alleles (Figures 2.1A and 2.1B). The lack of individual miR-34 family members was confirmed by qRT-PCR of the brain and the prostate of *mir-34*$^{-/-}$ mice (Figure 2.1C).

Targeting mir-34a and mir-34b/c genes. The conditional gene-targeting vector was constructed using a recombineering approach as described elsewhere (Liu et al., 2003). BAC clones RP23-410P10 and RP23-318E9 (C57Bl/6 genomic DNA; BACPAC Resource Center at Children's Hospital Oakland Research Institute, California) containing *mir-34a* and *mir-34b/c* locus, respectively, were used to generate the *mir-34a* and *mir-34b/c* conditional (floxed) allele. We engineered the *mir-34a* targeting construct with a 5 kb and 4.6 kb homologous arm on both the 5’ and 3’ ends, which flanked one *loxP* site and a neomycin resistance cassette (*Neo*) flanked by *FRT* sites with a *loxP*

site in upstream and downstream of *mir-34a*, respectively. Linearized *mir-34a* targeting vector was electroporated into E14 mouse embryonic stem cells (ES) cells, and cultured on the top of feeder cells with G418 (200 µg/ml) and Ganciclovir (0.2 µM) for positive and negative selection, respectively. ES clones (n=293) were picked up, and screened for correct homologous recombination by Southern blotting. The *mir-34b/c* targeting construct contained a 114 kb and 83 kb homologous arm on both the 5' and 3' ends, which flanked two *loxP* sites and *Neo* flanked by *FRT* sites downstream of *mir-34b/c*. Linearized *mir-34b/c* targeting vector was electroporated into v6.5 ES cells, and cultured on the top of feeder cells with G418 (200 µg/ml). ES clones (n=333) were picked up, and screened for correct homologous recombination by a quantitative PCR assay due to extremely long arms of homology. Correctly targeted clones undergoing correct homologous recombination were injected into C57Bl/6 blastocysts, to generate chimeric mice. After germ-line transmission of the targeted allele, *FRT* flanked *Neo* was removed by crosses with FLPeR mice (129S4/SvJaeSor-Gt(ROSA)26Sortm1(FLP1)Dym/J, The Jackson Laboratory. Bar Harbor, ME, stock number #00396; Farley et al., 2000). Following *Neo* removal null *mir-34a* and *mir-34b/c* alleles were obtained by crossing to *EIIa-Cre* mice (FVB/N-Tg(EIIa-cre)C5379Lmgd/J; The Jackson Laboratory, stock number #003314; Lakso et al., 1996). In some experiments we have also used *mir-34a*$^{-/-}$ and *mir-34a*$^{loxP/loxP}$ mice generated by Hermeking group (Nelson et al., 2006). Those mice were on SV/C57Bl6 background. The outcomes of experiments with all mouse strains have been very similar and are reported together. Compound mice carrying conventional (*mir-34a*$^{-/-}$*mir-34b/c*$^{-/-}$, *mir-34*$^{-/-}$) and conditional (*mir-34a*$^{loxP/loxP}$*mir-34b/c*$^{loxP/loxP}$, *mir-34*$^{L/L}$) targeted alleles of all *mir-34* genes were generated by crossing

mice with individual targeted alleles. To minimize the confounding effects of genetic background all mice were backcrossed to FVB/N for at least 10 generations, and all control experiments were performed on age and sex-matched mice of the same background.

Generation of mice with prostate epithelium-specific inactivation of p53, mir-34 and/or Met. ARR2PB-Cre transgenic mice (*PB-Cre4*; Wu et al., 2001) and *p53*$^{loxP/loxP}$ mice (p53L/L`: Marino et al., 2000) were backcrossed to FVB/N background for 20 generations. *PB-Cre4* male mice were crossed to *mir-34*$^{L/L}$, *p53*$^{L/L}$, and *p53*$^{L/L}$*mir-34*$^{L/L}$ female mice. Resulting *PB-Cre4mir-34*$^{L/L}$, *PB-Cre4p53*$^{L/L}$, and *PB-Cre4p53*$^{L/L}$*mir-34*$^{L/L}$ male mice were designated as mice with prostate epithelium (PE)-specific gene inactivation, *mir-34*$^{PE-/-}$, *p53*$^{PE-/-}$, and *p53*$^{PE-/-}$*mir-34*$^{PE-/-}$ mice, respectively. Mice with floxed *Met* (Huh et al., 2004) were crossed in a similar fashion to obtain *p53*$^{PE-/-}$*mir-34*$^{PE-/-}$*Met*$^{PE-/-}$ mice.

Pathologic assessment. Moribund mice, as well as those sacrificed according to schedule, were anesthetized with avertin and, if necessary, subjected to cardiac perfusion at 90 mm Hg with phosphate-buffered saline (PBS). After macroscopic evaluation during necropsy, brain, pituitary gland, Thyroid gland, lung, thymus, stomach, small and large intestine, liver, kidney, adrenal gland, gonads, spleen, pancreas, salivary gland, prostate or uterus, mammary gland, trigeminal nerve, thigh and cardiac muscle, humerus, tibia, femur, and lymph nodes were fixed in phosphate-buffered 4% paraformaldehyde tissues, embedded in paraffin and 4-µm-thick sections were stained

with Hematoxylin (Mayer's haemalum) and eosin. Mouse prostatic intraepithelial neoplasia (PIN) were defined according to earlier publications (Flesken-Nikitin et al., 2013; Park et al., 2002; Shappell et al., 2004; Zhou et al., 2006). Briefly, distal PIN1 has 1 or 2 layers of atypical cells; PIN2 has 3 or more layers of atypical cells, PIN3 occupies the near entire glandular lumen; and PIN4 fills and distorts the glandular profile, and is frequently marked by pronounced desmoplastic reaction. In agreement with the recent consensus report (Flesken-Nikitin et al., 2013), PIN1 and PIN2 represent low-grade PIN, and PIN3 and PIN4 represent high-grade PIN. Due to different architecture of the proximal regions of prostatic ducts, current PIN classification cannot be carefully applied to atypical proliferative lesions found in those structures. Thus we named those lesions as proximal duct dysplasia to stress their dissimilarity to PIN of distal regions of prostatic ducts. Given the complexity of the interpretation of mouse prostatic neoplastic lesions, we used term adenocarcinoma only for neoplasms with invasive growth confirmed by serial sections followed by 3D reconstruction.

Immunohistochemistry and quantitative image analysis. Immunoperoxidase staining of paraffin sections of paraformaldehyde-fixed tissue was performed by a modified Elite avidin-biotin-peroxidase (ABC) technique (Nikitin and Lee, 1996). Antigen retrieval was done by boiling the slides in 10 mM citric buffer (pH 6.0) for 10 min. The primary antibodies to Ki67 (Leica Microsystems; Bannockburn, IL; NCL-Ki67p, 1:1000), MET (Santa Cruz; Dallas, TX, sc-162, 1:200), keratin 5 (CK5, Covance: Dallas, TX, #PRB-160P, 1:1000), p63 (Santa Cruz, #sc-8431, 1:1000), EZH2 (Cell Signaling Technology; Danvers, MA; #5246, 1:200), and AMACR (Santa Cruz, #sc-107916, 1:100) were

incubated with deparaffinized sections at 4ºC overnight (Ki67, CK5, p63, EZH2, AMACR) or at room temperature (RT, MET) for 1 hour followed by incubation with secondary biotinylated antibody (1 hour, RT) and modified avidin-biotin-peroxidase (ABC) technique. Methyl green (Ki67, p63, EZH2) and hematoxylin (MET, CK5, AMACR) were used as the counterstain in immunoperoxidase stainings. Slides were scanned by ScanScope CS (Leica Biosystems, Vista, CA) with 40X objective followed by lossless compression. Quantitative analysis of IHC was performed with the ImageJ software (W. Rasband, National Institutes of Health, Bethesda, MD).

MicroRNA in situ hybridization. In situ hybridization was performed as previously described (Corney et al., 2010; Krizhanovsky and Lowe, 2009). Briefly, 6 µm-thick paraffin sections of 13.5-day-old FVB/N mouse embryos were deparaffinized and dehydrated, followed by 1-ethyl-3-(3-dimethylaminopropyl) carbodiimide (EDC) fixation (Meletis et al., 2006). Following pre-hybridization blocking, sections were incubated overnight at 55-56ºC with digoxigenin-labeled locked nucleic acid (LNA) modified miR-34a or miR-34b oligo probe (Exiqon, Woburn, MA). After stringency washes, sections were incubated with anti-digoxigenin alkaline phosphatase-labeled secondary antibody (Roche, Indianapolis, IN) overnight at 4ºC followed by development of stain with NBT/BCIP (Promega, Fitchburg, WI). Sections were counterstained with methyl green or nuclear fast red, dehydrated, cleared in xylene, coverslipped and scanned by ScanScope CS.

Cell culture. Embryonic stem cells were cultured in undifferentiating conditions on mitotically inactivated feeder cells and in the presence of leukemia inhibitory factor (LIF) at 37ºC in 5% CO_2. Briefly, medium used was Dulbecco's Modified Eagle Medium (high glucose) containing 15% heat-inactivated ES cell qualified fetal bovine serum, 6 mM L-glutamine, 1 mM sodium pyruvate, 1X Dulbecco's non-essential amino acids (all purchased from Invitrogen, Carlsbad, CA) plus 10^{-4} M 2-mercaptoethanol (Sigma, St. Louis, MO), and 103 units/ml LIF (Millipore, Billerica, MA). For positive neomycin selection, cells were cultured in medium containing 200 µg/ml G418. Mouse embryonic fibroblast (MEF) cells were prepared from gestational day (GD) 13.5-15.5 embryos carrying *Neo* under the control of *PGK* promoter (C57BL/6J-Tg(pPGKneobpA)3Ems/J, The Jackson Laboratory, stock number 002356; Aubrecht et al., 2011). Prior to use as feeder MEF cells were mitotically inactivated by exposure to 10 µg/ml mitomycin C for one hour at 37ºC followed by three washes with PBS. ES cells were routinely passaged using 0.25% trypsin/EDTA prior to reaching confluence. Feeder cells were separated from ES cells by differential attachment to gelatinized plates for one hour at 37ºC.

Primary prostate epithelial cell, stem/basal cell, and luminal cell populations were isolated following described procedures (Lawson et al., 2010; Lukacs et al., 2010a). Lipofectamin 2000 reagent (Invitrogen, Carlsbad, CA) was used for the transfection following manufacturer's recommendations. Control siRNA (Santa Cruz, #sc-37007) and two independent *Met* siRNAs (Santa Cruz, #sc-35924 and Life Technologies, #155340) were used for all knockdown experiments. Migration and invasion assays were performed as previously described (Corney et al., 2010). In experiments with

conditional gene inactivation, the efficiency of adenoviral infection followed by Cre-mediated gene excision was over 90% according to PCR genotyping (Figure 2.4C).

For hypoxia experiments CD49f^{hi}/Sca-1^{+} prostate stem cells were exposed for 24 hours to either normoxic (20% O_2) or hypoxic (0.2% O_2) conditions immediately after *fluorescence activated cell sorting*. For mithramycin A experiments prostate stem cells were treated with 100 nM mithramycin A (Sigma, #M6891) for one hour. MET expression was detected by Western blot after 24-hour culture.

Prostate sphere assay. Prostate sphere assays were performed as described previously (Lawson et al., 2010; Lukacs et al., 2010a). Briefly, 10^4 prostate stem cells or prostate luminal cells were resuspended in 120 µl of a 1:1 mixture of Matrigel (BD Biosciences, San Jose, CA, #354234) and PrEGM (Lonza, Allendale, NJ, #CC-3166), and plated around the rim of a well of a 12-well tissue culture plate. Matrigel mix was allowed to solidify at 37ºC for 15 min, and 1 ml of PrEGM was added per well. Media was changed every 3 days. To recover the spheres, each well was treated with enzyme mixture: 750 µl Collagenase/Dispase 4 mg/ml (Roche, #10269638001), 30 mg BSA (Sigma, #A3311), 1 µl DNase1 10 mg/ml (Sigma, #D4513), followed by Trypsin 0.25% EDTA (Cellgro, Manassas, VA, 25-052-Cl) to make cell suspensions, which were ready for passaging.

Quantitative reverse transcription - PCR. qRT-PCR was performed as previously described (Corney et al., 2007; Corney et al., 2010) using *Rnu6b* and *GAPDH* amplification as housekeeping control for miR-34 and *Met*, respectively.

Western blot and coimmunoprecipitation analysis. For western blot cell lysates were prepared using RIPA buffer (50 mM Tris-HCl, (pH 7.4), 1% Nonidet P-40, 0.25% Na-deoxicholate, 150 mM NaCl, 1 mM EDTA, 1 mM PMSF, Aprotinin, leupeptin, pepstatin: 1 µg/ml each, 1 mM Na_3VO_4, 1 mM NaF), followed by sonication for 10 seconds 5 times on ice. Lysates were then separated by 12% SDS-PAGE and transferred to PVDF membrane (Millipore #IPVH00010). The membrane was incubated overnight at 4ºC with antibodies to detect MET (Santa Cruz, #sc-162, 1:500), p53 (Santa Cruz, #sc-6243, 1:2000), SP1 (Millipore, #07-645, 1:2000), HIF1A (Santa Cruz, #sc-10790, 1:500), and GAPDH (Advanced Immunohistochemical Inc.; Long Beach, CA; #2-RGM2,1:5000), followed by incubation for 1 hour at room temperature with corresponding horseradish peroxidase-conjugated anti-rabbit secondary antibodies (Santa Cruz, #sc-2004, 1:2000) or anti-mouse secondary antibodies (Santa Cruz, #sc-2005, 1:2000) and developed using chemiluminescent substrate (Thermo Scientific, Rockford, IL, #34077).

For coimmunoprecipitation lysates were prepared in modified Lysis 250 buffer (50 mM Tris-HCl (pH 7.4), 100 mM NaCl, 5 mM EDTA, 0.1% NP-40 100 mM). The antibodies used for immunoprecipitation were SP1 (Millipore, #07-645, 1:2000) and p53 (Cell Signaling Technology, Danvers, MA, #2524, 1:2000). Cell extracts were incubated at 4ºC overnight with 2 µg of corresponding antibodies, followed by incubation with 20 µl of Protein A/G Plus UltraLink Resin (Thermo Scientific, #53135) for 2 hours at 4ºC. Immunoprecipitates were isolated by centrifugation and followed by 3 times washing with lysis buffer. Samples were resuspended in the 5X sample buffer, subjected to 10% SDS-polyacrylamide gel electrophoresis, transferred onto a PVDF membrane and the immunoprecipitated proteins were detected by Western blotting.

Met 3'UTR verification. Total RNA was isolated using mirVana miRNA Isolation kit (Ambion, Life Technologies; Grand Island, NY; #AM1560) according to the manufacturer's protocol, and RNA concentration and purity were determined by NanoDrop analysis. cDNA was prepared from 100 ng total RNA using SuperScript III (Invitrogen, Life Technologies; #18080-400). Primers designed to detect the 3'UTR of intact and truncated *Met* are as follows: F1: 5' CTG AAC TCG GTT AGC CTC CCA 3', F2: 5' CTC TGG GAG CTC ATG ACG AGA 3', R1: 5' AGT TGG ACT TAC ACT TCG GGC 3', R2: 5' TCA CAG TAT ACA AGA TGT TAC GTC A 3', R3: 5' AGG AAG GGG GTC TTA AAT GCT TCA 3'. PCR fragments were cloned using pGEM-T Vector System (Promega; Madison, WI; #A3600) according to the manufacturer's protocol. DNA sequencing was done by Cornell Genomics Facility, Biotechnology Resource Center.

Statistical analysis. Statistical analyses were performed with InStat 3.10 and Prism 6 software (GraphPad). A Two-tailed unpaired t-test, direct Fisher's tests, and a log-rank Mantel-Haenszel test were used as appropriate.

2.4 Results

2.4.1 Mice with *mir-34* conventional knockout have only minor developmental alterations

By using gene targeting of *mir-34a* and *mir-34b/c* loci and subsequent crosses of mice we prepared mice with conventional triple knockout (*mir-34a*$^{-/-}$*mir-34b/c*$^{-/-}$) and conditional (floxed, *mir-34a*$^{loxP/loxP}$*mir-34b/c*$^{loxP/loxP}$) triple alleles (Figure 2.1), and designated them as *mir-34*$^{-/-}$ and *mir-34*$^{L/L}$, respectively.

Consistent with a previous report (Concepcion et al., 2012), our findings indicate that germ line genetic inactivation of *mir-34* has only a minor effect on normal development (Figure 2.2). *mir-34*$^{-/-}$ mice are viable and fertile. There was no difference in body size, growth pattern, and life span compared to age- and sex-matched wild-type mice up to 18 months of age (data not shown). After extensive histological evaluation of all major organs and systems the only consistent observation was focal irregular arrangement and increased cell number of Purkinje neurons in the cerebellum. This phenotype was particularly pronounced in males, where the distance between Purkinje neurons was significantly shorter than that of wild-type controls matched by age, sex, and genetic background (Figures 2.2A-2.2D). Consistent with this observation, miR-34a, miR-34b, and miR-34c are highly expressed in Purkinje neurons of wild-type mice according to in situ hybridization (Figures 2.2E and 2.2F). This raises the possibility that miR-34 plays a role in cerebellar development. Increased number of Purkinje neurons has been reported in *Bcl-2* transgenic mice (Zanjani et al., 1996) and BCL-2 is one of the miR-34 targets (Ji et al., 2009). Thus it is tempting to speculate that miR-34 deficiency results in increased BCL-2 expression, and subsequently causes increased number of Purkinje neurons. According to several tests, such as hanging wire test, rotarod, and foot print analysis there were no prominent locomotor abnormalities (data not shown). However, more in depths study of Purkinje neuron-related phenotype in

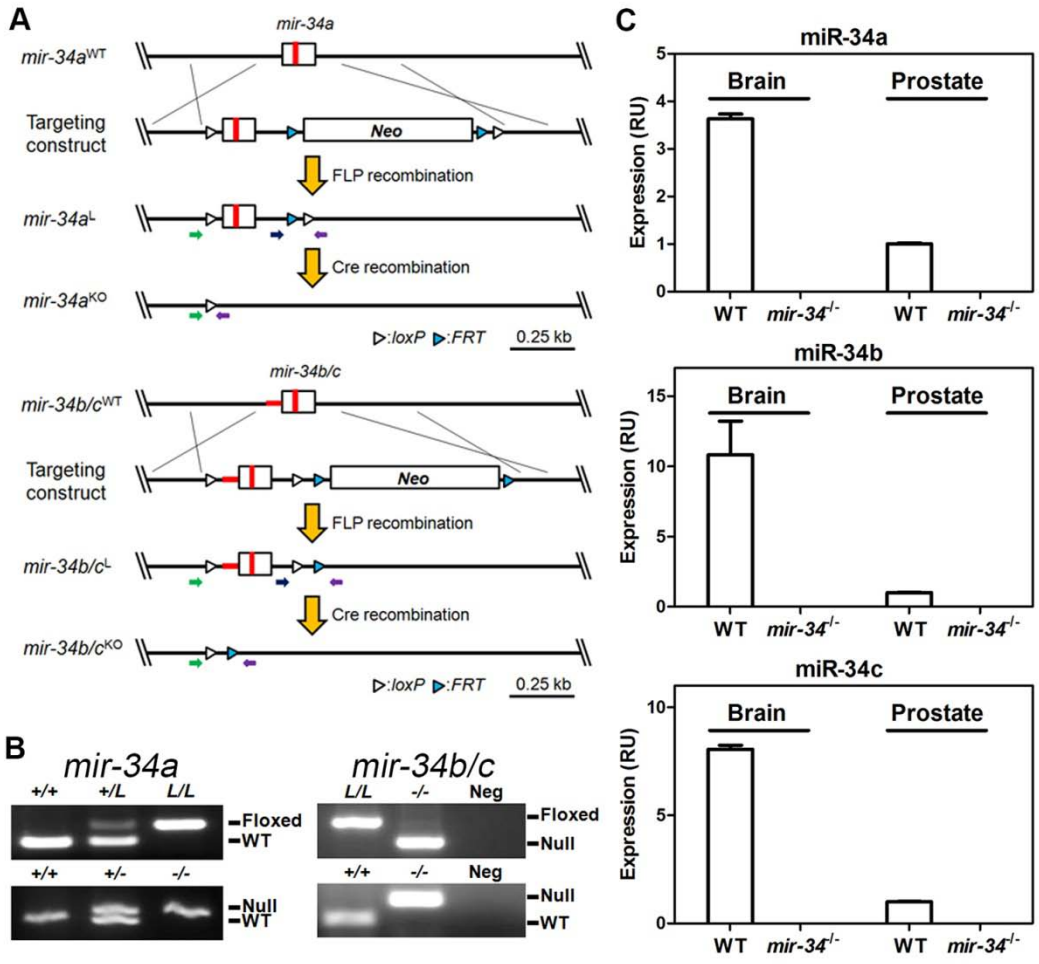

Figure 2.1 Generation and characterization of conditional (floxed) and conventional targeted mutations of *mir-34* genes. (A) The schematic drawings of floxed and conventional knockout alleles of *mir-34a* and *mir-34b/c* prepared by homologous recombination. Neomycin resistance cassette (*Neo*) is flanked by *FRT* sites and is excised by flippase (FLP). *mir-34* (red box) is flanked by two *loxP* sites (white triangles) and is excised by Cre recombinase. Colored arrows indicate PCR primers used for genotyping. (B) PCR genotyping of mice carrying conditional (floxed, L) and conventional knockout (null) alleles. Neg, negative control; WT, wild-type. (C) Levels of miR-34a, miR-34b, and miR-34c from the brain and the prostate of age-matched WT and *mir-34*$^{-/-}$ mice (n=3). RU, relative units. Error bars denote SD.

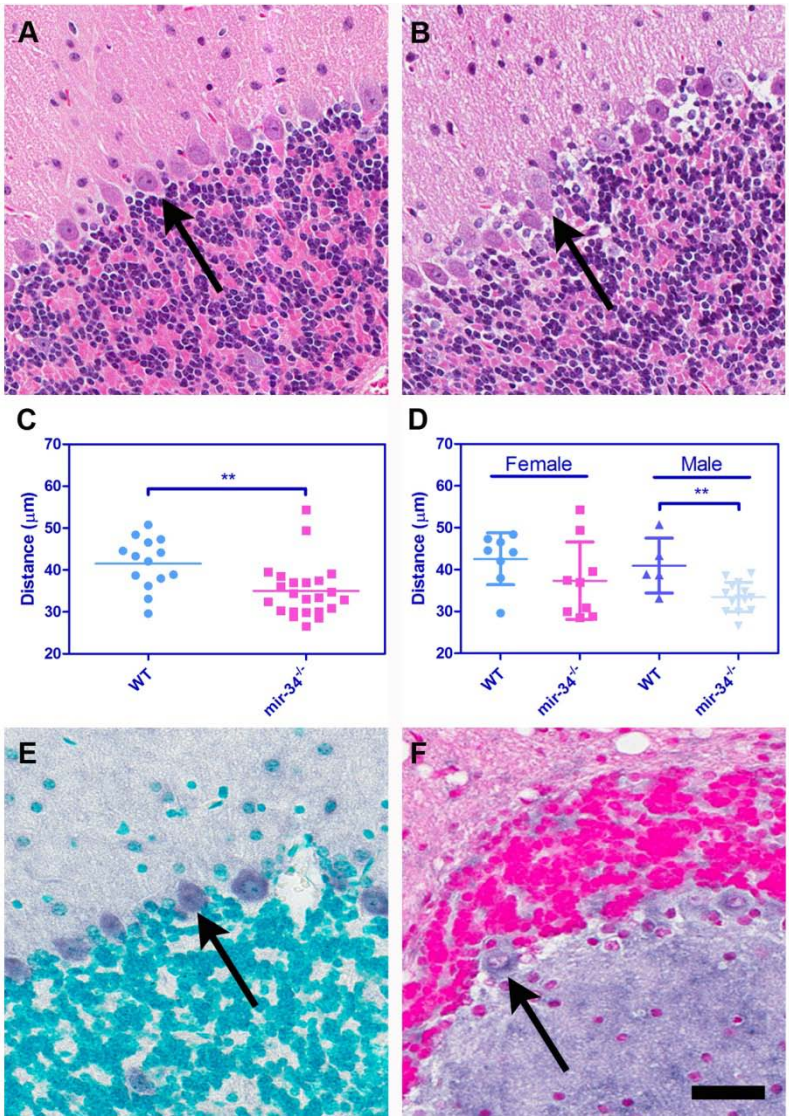

Figure 2.2 *mir-34*$^{-/-}$ mice display increase in number and irregular arrangement of Purkinje neurons. (A, B) Purkinje neurons in the cerebellum of wild-type (WT; A) and *mir-34*$^{-/-}$ (B) mice. The arrows indicate normal (A) and irregular (B) arrangement of Purkinje neurons, respectively (C, D). Distance between Purkinje neurons in mixed (C) and separate (D) gender WT (male, n=6; female, n=8) and *mir-34*$^{-/-}$ (male, n=14; female, n=9) mice. (E, F) Expression (dark blue/purple) of miR-34a (E, arrow) and miR-34b and miR-34c (F, arrow) in Purkinje neurons of the cerebellum of WT mice. (A, B) Hematoxylin and eosin. (E, F) In situ hybridization, digoxigenin method. Methyl green (E) and nuclear fast red (F) counterstain. Scale bar, 25 µm for all histological images. **P<0.01. Error bars denote SD.

mice lacking all *mir-34* genes could be merited. On the other hand, we also have not observed any significant pathological phenotypes, including cancers, in *mir-34*$^{-/-}$ mice (n=19) between 15 and 18 months of age.

2.4.2 miR-34 cooperates with p53 in suppression of prostate carcinogenesis

To rule out the possibility that mice somehow physiologically compensate for germline *mir-34* deficiency, we performed prostate epithelium-specific *mir-34* deletion. This was accomplished by using a *PB-Cre4* transgene, in which a modified probasin promoter drives postnatal expression of Cre recombinase in the prostate epithelium (Chen et al., 2005; Zhou et al., 2006). Consistent with previous reports and our findings in *mir-34*$^{-/-}$ mice, mice lacking all *mir-34* genes in the prostate epithelium cells (*mir-34*$^{PE-/-}$ mice) did not show any atypical lesions by 15 months of age (Figures 2.3A, 2.3B, and 2.4A; Table 2.1).

To test if miR-34 may have p53-independent function, we determined the expression levels of miR-34 family after *p53* deletion in FACS-purified *p53*$^{L/L}$ prostate epithelium cells exposed to Ad-*Cre*. Significant levels of miR-34 expression were still detected after *p53* inactivation (Figures 2.4B and 2.4C).

To test if p53 and miR-34 may cooperate in suppressing prostate carcinogenesis we generated *p53*$^{PE-/-}$ and *p53*$^{PE-/-}$*mir-34*$^{PE-/-}$ mice by crossing *p53*$^{L/L}$ mice with *mir-34*$^{L/L}$ and *PB-Cre4* mice. Consistent with previous reports on lack or low frequency of neoplastic lesions in mice with prostate epithelium-specific *p53* inactivation (Chen et al., 2005; Zhou et al., 2006), only 1 out of 11 *p53*$^{PE-/-}$ mice (9%) showed PIN1 by 9 months

of age in the distal regions of prostatic ducts. By 15 months of age more of *p53*$^{PE-/-}$ mice developed PINs. However, all of them were of low-grade (PIN1 or PIN2; Figures 2.3A, 2.3B, and 2.4A; Table 2.1). No significant changes were observed in the proximal regions of prostatic ducts, where are known to encompass a prostate epithelium stem cell compartment (Leong et al., 2008; Tsujimura et al., 2002).

In contrast, beginning at 3 months of age *p53*$^{PE-/-}$*mir-34*$^{PE-/-}$ mice showed dysplastic lesions characterized by varying degree of nuclear atypia and loss of normal cellular arrangement in the proximal regions of prostatic ducts (Figures 2.3A and 2.4A; Table 2.1). From 9 months of age mice majority of mice had advanced dysplastic lesions which frequently filled up expanded ducts and 15% and 36% of mice developed early invasive adenocarcinomas at 9 and 15 months, respectively (Figures 2.3A and 2.4A; Table 2.1). In the distal regions of prostatic ducts, the first PIN1 lesions were detected already by 3 months of age (Figures 2.3B and 2.4A; Table 2.1). High-grade PIN lesions (PIN3 and 4) have been observed by 9 months of age and 64% (9 out of 14) of mice had such lesions at 15 months of age. Consistent with these findings, adenocarcinomas and high-grade PIN lesions of the proximal and distal regions of prostatic ducts, respectively, characterized by elevated expression of such markers of early prostate cancer as AMACR and EZH2, and increased number of K5 and p63 positive cells (Figure 2.3C). Similarly, higher proliferative activity has been observed in both proximal and distal regions of prostatic ducts of *p53*$^{PE-/-}$*mir-34*$^{PE-/-}$ mice (Figures 2.3D and 2.3E). In summary, these results show that miR-34 and p53 cooperate in suppression of prostate carcinogenesis.

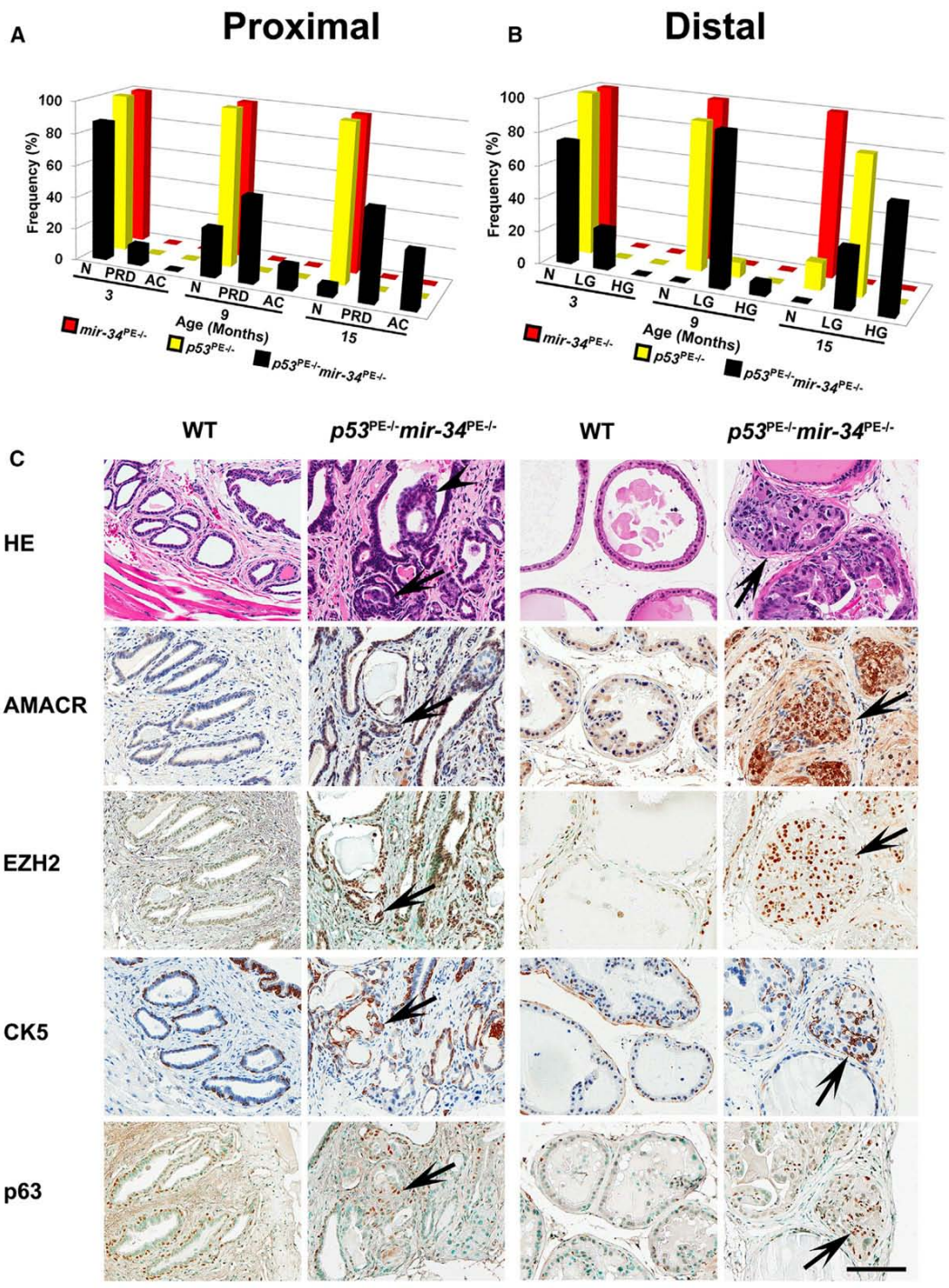
A
Proximal
B
Distal
Frequency (%)
100
80
60
40
20
0
N PRD AC
N PRD AC
N PRD AC
3
9
15
Age (Months)
mir-34PE-/-
p53PE-/-
p53PE-/-mir-34PE-/-
N LG HG
N LG HG
N LG HG
WT
p53PE-/-mir-34PE-/-
C
HE
AMACR
EZH2
CK5
p63
D
Ki67-positive cells (%)
E
Ki67-positive cells (%)

Figure 2.3 miR-34 and p53 cooperate in suppression of prostate carcinogenesis. (A and B) A quantitative analysis of the frequency of neoplastic lesions in proximal (A) and distal (B) regions of prostatic ducts. N, normal; PRD, proximal dysplastic lesions; AC, adenocarcinoma; LG, low-grade PIN; HG, high-grade PIN. (C) Proximal (left two columns) and distal (right two columns) regions of prostatic ducts in 15-month-old WT and *p53*$^{PE-/-}$*mir-34*$^{PE-/-}$ mice. Adenocarcinomas invading the surrounding stroma (arrows) and filling up the lumen (arrowheads) in the proximal regions of the prostatic ducts of *p53*$^{PE-/-}$*mir-34*$^{PE-/-}$ mice are shown. PIN4 (arrows) in the distal regions of the prostatic ducts of *p53*$^{PE-/-}$*mir-34*$^{PE-/-}$ mice is shown. As compared to the prostate epithelium of WT mice, both adenocarcinomas and PIN4 (arrows) show higher expression levels of AMACR and EZH2 and an increased number of CK5 and p63-positive cells. HE, hematoxylin and eosin staining. The ABC Elite method with hematoxylin (AMACR, CK5) or methyl green (EZH2, and p63) counterstaining was performed. Scale bar, 100 mm for all images. (D and E) A quantitative analysis of the proliferation rate in proximal (D) and distal (E) regions of prostatic ducts. *P<0.05; **P<0.01. Error bars denote SD.

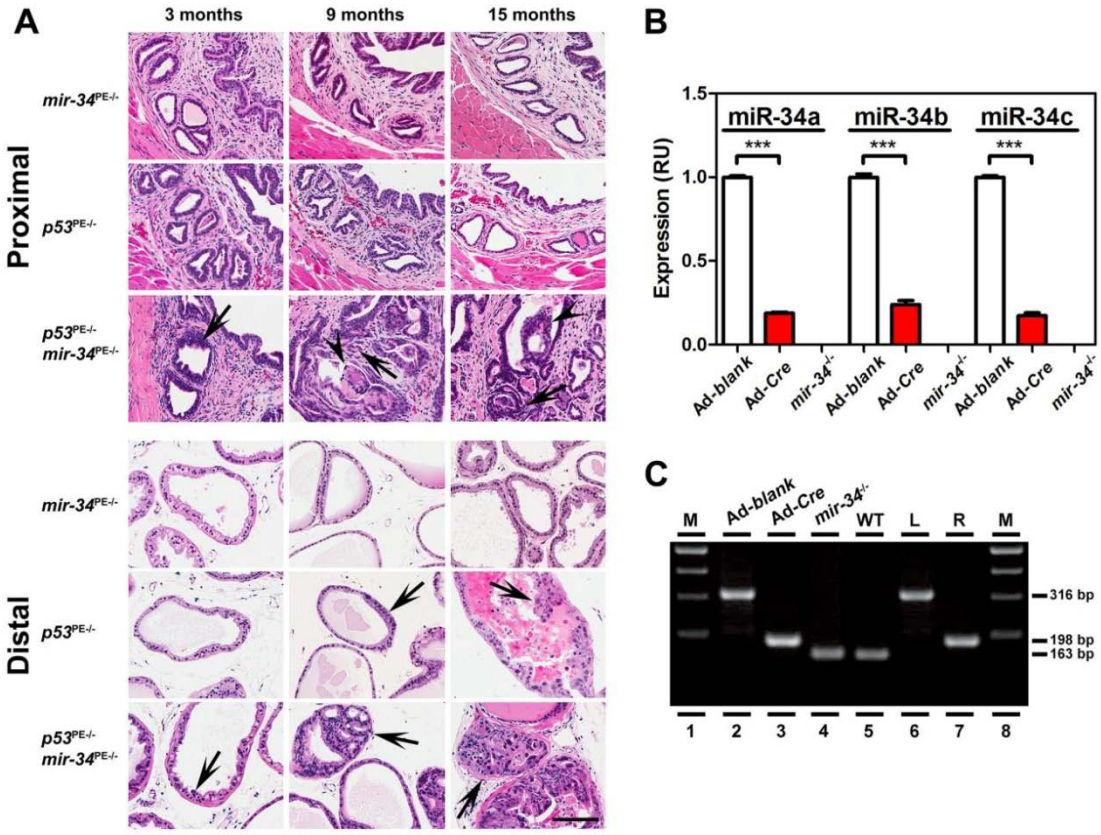

Figure 2.4 miR-34 has p53-independent function in suppression of prostate carcinogenesis. (A) Proximal and distal regions of prostatic ducts in 3, 9, and 15-month-old *mir-34*$^{PE-/-}$, *p53*$^{PE-/-}$ and *p53*$^{PE-/-}$*mir-34*$^{PE-/-}$ mice. Dysplastic lesions (3 months, arrow) and adenocarcinomas (9 and 15 months) invading surrounding stroma (arrows) and filling up the lumen (arrowheads) in the proximal regions of prostatic ducts of *p53*$^{PE-/-}$*mir-34*$^{PE-/-}$ mice. Low-grade prostatic intraepithelial neoplasia (PIN1, 9 months; PIN2, 15 months, arrows) in the distal regions of prostatic ducts of *p53*$^{PE-/-}$ mice. PIN1 (3 months, arrow) and high-grade PINs (PIN3, 9 months; PIN4, 15 months, arrows) in the distal regions of prostatic ducts of *p53*$^{PE-/-}$*mir-34*$^{PE-/-}$ mice. Note densely fibrotic stroma surrounding PIN4. Hematoxylin and eosin. Scale bar, 100 µm for all images. (B) qRT-PCR of miR-34 expression in Ad-*blank* or Ad-*Cre*-infected *p53*$^{L/L}$ and *mir-34*$^{-/-}$ prostate epithelium cells. ***P<0.001. Error bars denote SD. (C) PCR analysis of *p53* gene structure in *p53*$^{L/L}$ prostate epithelium cells infected with Ad-*blank* (lane 2) or Ad-*Cre* (lane 3), and in *mir-34*$^{-/-}$ prostate epithelium cells (lane 4). Control samples include WT (lane 5), floxed (L, lane 6); and homozygous recombinant (R, lane 7) *p53*. 316, 198, and 163 bp fragments are diagnostic for floxed, excised, and WT alleles of the *p53* gene, respectively. M (lanes 1 and 8), DNA marker.

Table 2.1 Prostatic Lesions in Mice with Prostate Epithelium Specific Inactivation of *mir-34a, b/c* (*mir-34*$^{PE-/-}$), *p53* (*p53*$^{PE-/-}$) and Their Combination (*p53*$^{PE-/-}$*mir-34*$^{PE-/-}$).

Strain	Prostatic region	Lesion*	Age (months)		
			3	9	15
mir-34$^{PE-/-}$	Proximal	None	100 (9/9)[#]	100 (7/7)	100 (4/4)
		Dysplasia	0 (0/9)	0 (0/7)	0 (0/4)
		Adenocarcinoma			
	Distal	None	100 (0/9)	100 (7/7)	0 (0/4)
		PIN1	0 (0/9)	0 (0/7)	0 (0/4)
		PIN2	0 (0/9)	0 (0/7)	0 (0/4)
		PIN3	0 (0/9)	0 (0/7)	0 (0/4)
		PIN4	0 (0/9)	0 (0/7)	0 (0/4)
p53$^{PE-/-}$	Proximal	None	100 (9/9)	100 (11/11)	100 (12/12)
		Dysplasia	0 (0/9)	0 (0/11)	0 (0/12)
		Adenocarcinoma	0 (0/9)	0 (0/11)	0 (0/12)
	Distal	None	100 (9/9)	91 (10/11)	17 (2/12)
		PIN1	0 (0/9)	9 (1/11)	66 (8/12)
		PIN2	0 (0/9)	0 (0/11)	17 (2/12)
		PIN3	0 (0/9)	0 (0/11)	0 (0/12)
		PIN4	0 (0/9)	0 (0/11)	0 (0/12)
p53$^{PE-/-}$ *mir-34*$^{PE-/-}$	Proximal	None	87 (7/8)	31 (4/13)	7 (1/14)
		Dysplasia	13 (1/8)	54 (7/13)	57 (8/14)
		Adenocarcinoma	0 (0/8)	15 (2/13)	36 (5/14)
	Distal	None	75 (6/8)	0 (0/13)	0 (0/14)
		PIN1	25 (2/8)	31 (4/13)	0 (0/14)
		PIN2	0 (0/8)	61 (8/13)	36 (5/14)
		PIN3	0 (0/8)	8 (1/13)	43 (6/14)
		PIN4	0 (0/8)	0 (0/13)	21 (3/14)

[*]Lesions of the distal region of prostatic duct can be additionally classified as low-grade (PIN1 and PIN2) and high-grade (PIN3 and PIN4).

[#]% (number of mice with lesion out of total number of mice).

2.4.3 p53 and miR-34 cooperate in control of prostate stem/progenitor cell activity

According to our pathological evaluation, stem/progenitor cell-enriched proximal regions of prostatic ducts were specifically affected in *p53*$^{PE-/-}$*mir-34*$^{PE-/-}$ mice. To test if combined p53 and miR-34 deficiency affects functional properties of prostate stem/progenitor cells, we isolated such cells by fluorescence-activated cell sorting (FACS) based on their CD49f^{hi}/Sca-1^{+} profile. Mice with prostate-specific deletions of either *mir-34* or *p53* had slightly more stem/progenitor cells than background-matched wild-type (WT) mice (Figure 2.5A). However, the pool of CD49f^{hi}/Sca-1^{+} cells deficient for both miR-34 and p53 increased by 39% and constituted 7.1% of the prostate epithelium versus 5.1% in WT. Notably, the CD49f^{hi}/Sca-1^{+} fraction isolated from prostates of *p53*$^{PE-/-}$*mir-34*$^{PE-/-}$ mice formed prostaspheres far more efficiently and of larger size (Figures 2.5B and 2.5C). Both higher frequency and size of spheres formed by p53 and miR-34-deficient CD49f^{hi}/Sca-1^{+} stem cells were maintained over multiple passages (dissociation and clonal formation), suggesting a role for these genes in the control of self-renewal. At the same time, no difference among genotypes was observed in CD49f^{lo}/Sca-1^{-} luminal cells (Figure 2.5D). These cells formed very few spheres after first plating and no spheres were observed after first passage. Thus, miR-34 and/or p53 deficiency are unlikely to reprogram differentiated cells towards stem cell state.

To test whether observed properties represent direct effects of p53 and/or miR-34 on prostate stem/progenitor cells, we have isolated CD49f^{hi}/Sca-1^{+} stem/progenitor cells and CD49f^{lo}/Sca-1^{-} luminal cells from prostates of WT, *mir-34*$^{L/L}$, *p53*$^{L/L}$, and *p53*$^{L/L}$ *mir-34*$^{L/L}$ mice and, followed by infection with Ad-*Cre* or Ad-*blank*, subjected them to the

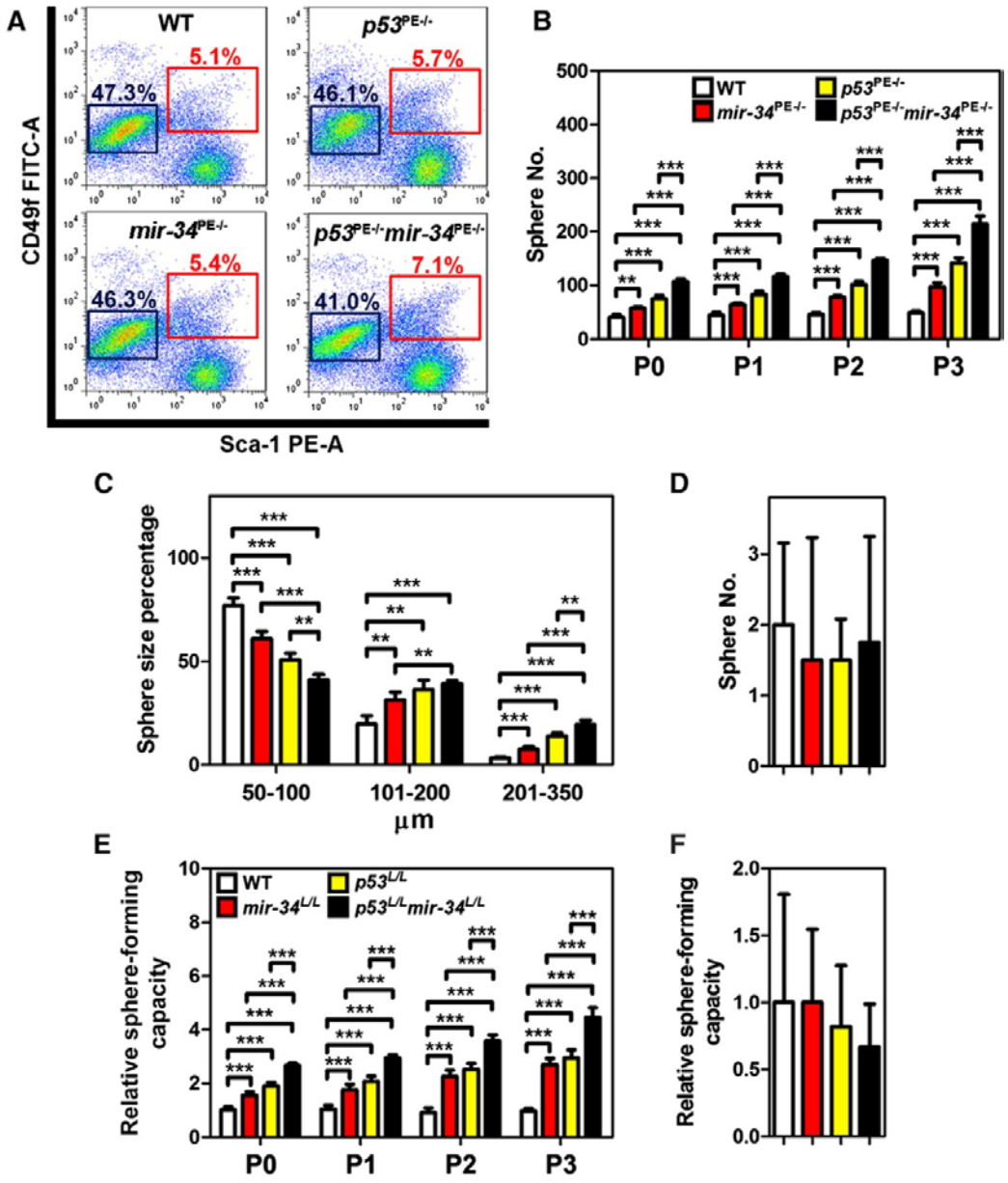

Figure 2.5 Deletions of both *p53* and *mir-34* promote prostate stem/progenitor cell expansion and sphere-forming capacity. (A) A quantitative analysis of distribution of CD49f^{hi}/Sca-1^{+} stem/progenitor cells and CD49f^{lo}/Sca-1^{-} luminal cells from 3-month-old WT, *mir-34*$^{PE-/-}$, *p53*$^{PE-/-}$, and *p53*$^{PE-/-}$*mir-34*$^{PE-/-}$ mice (n=3). Red and blue frames represent stem/progenitor cell and luminal cell populations, respectively. (B-D) The frequency (B and D) and size (C) of spheres formed by CD49f^{hi}/Sca-1^{+} stem/progenitor cells (B and C) and CD49f^{lo}/Sca-1^{-} (D) luminal cells from 3-month-old WT, *mir-34*$^{PE-/-}$, *p53*$^{PE-/-}$, and *p53*$^{PE-/-}$*mir-34*$^{PE-/-}$ mice (n=3). P0-P3, passages 0–3. (E and F) The relative frequency of sphere formation by CD49f^{hi}/Sca-1^{+} stem/progenitor cells (E) and CD49f^{lo}/Sca-1^{-} luminal cells (F) isolated from WT, *mir-34*$^{L/L}$, *p53*$^{L/L}$, and *p53*$^{L/L}$*mir-34*$^{L/L}$ mice followed by Ad-*Cre* infection (n=3). Sphere counts were normalized to the Ad-*blank*-infected spheres of each passage. **P < 0.01; ***P < 0.001. Error bars denote SD.

prostasphere formation experiments (Figures 2.5E and 2.5F). Consistently, the lack of both p53 and miR-34 had the most pronounced effect on frequency of stem/progenitor cells in consecutive passages.

2.4.4 p53 and miR-34 regulation of stem/progenitor cells depends on MET

In addition to invasive growth of cells in the prostate stem cell compartment of *p53*$^{PE-/-}$ *mir-34*$^{PE-/-}$ mice, we have noted that some of the cells from the p53 and miR-34-deficient prostaspheres were spreading into surrounding matrix (Figure 2.6A). Because MET plays a crucial role in regulation of cell motility and invasion (Trusolino et al., 2010) and is a known target of p53 (Hwang et al., 2011) and miR-34 (Corney et al., 2010; He et al., 2007; Hwang et al., 2011), we have tested its expression in FACS-isolated populations of the prostate epithelium. CD49f^{hi}/Sca-1^{+} prostate stem/progenitor cells had far higher levels of expression as compared to CD49f^{lo}/Sca-1^{-}luminal cells (Figure 2.6B). Deficiency for either miR-34 or p53 slightly increased MET levels in stem/progenitor cells, whereas such cells from *p53*$^{PE-/-}$*mir-34*$^{PE-/-}$ showed the highest MET expression (Figures 2.6B and 2.6C). Consistently, CD49f^{hi}/Sca-1^{+} prostate stem/progenitor cells deficient for both miR-34 and p53 had the highest motility in migration assay (Figure 2.6D) and some trend, albeit not statistically significant, towards increased invasive activity (Figure 2.6E). To the contrary, CD49f^{lo}/Sca-1^{-} luminal cells deficient for p53 and/or miR-34 had no significant differences in their motility (Figure 2.6F) and invasion (Figure 2.6G). Consistent with ex vivo results, we also observed elevated levels of MET expression in cells of the proximal regions of prostatic ducts of *p53*$^{PE-/-}$*mir-34*$^{PE-/-}$ mice,

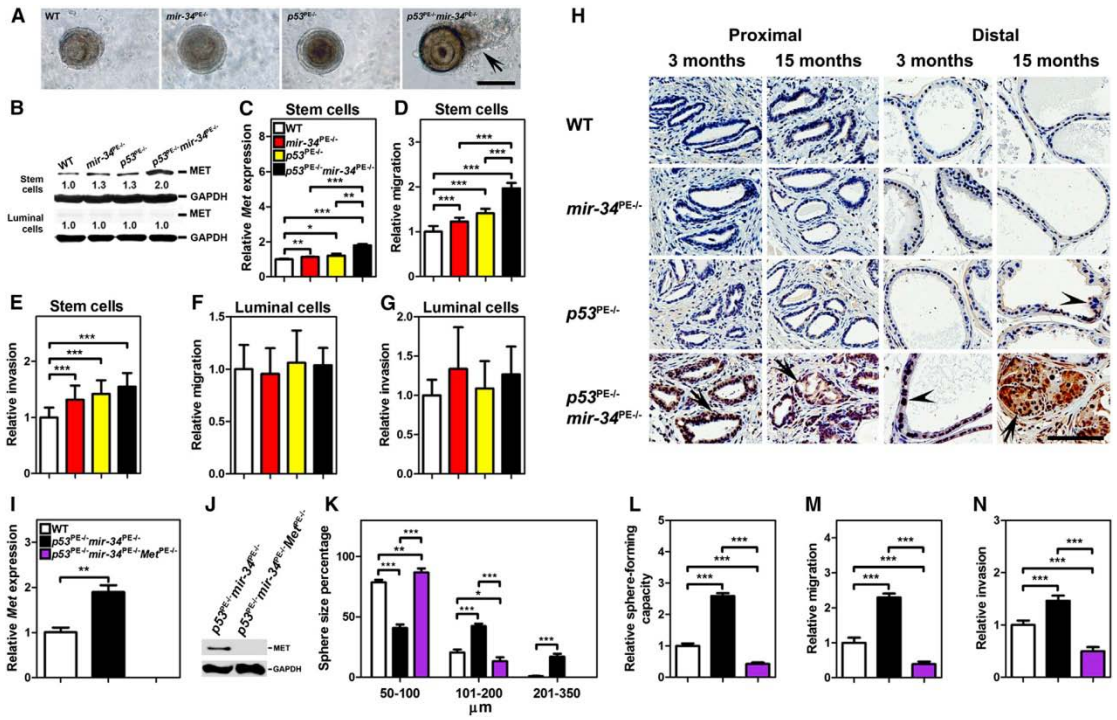

Figure 2.6 MET expression is essential for the increased growth, sphere-forming capacity, motility, and invasion of p53 and miR-34-deficient prostate stem/progenitor cells. (A-H) Prostasphere formation (A), western blot (B), and qRT-PCR (C) of *Met* expression, migration (D and F), and invasion (E and G) by CD49f^{hi}/Sca-1^{+} stem/progenitor cells (A-E) and CD49f^{lo}/Sca-1^{-} luminal cells (B, F, and G) of 3-month-old WT, *mir-34*$^{PE-/-}$, *p53*$^{PE-/-}$, and *p53*$^{PE-/-}$*mir-34*$^{PE-/-}$ mice (n=3). (A) Note the outgrowth of cells from prostaspheres prepared from *p53*$^{PE-/-}$*mir-34*$^{PE-/-}$ mice (arrow). (H) MET expression in the cells of proximal and distal regions of prostatic ducts of 3- and 15-month-old WT, *mir-34*$^{PE-/-}$, *p53*$^{PE-/-}$, and *p53*$^{PE-/-}$*mir-34*$^{PE-/-}$ mice is shown. MET expression (arrows) is detected in the proximal regions of the prostatic ducts of 3- and 15-month-old *p53*$^{PE-/-}$*mir-34*$^{PE-/-}$ mice and in the PIN4 of the distal region in 15-month-old *p53*$^{PE-/-}$*mir-34*$^{PE-/-}$ mice. PIN1 (arrowheads) in the distal regions of prostatic ducts lacks MET expression in both *p53*$^{PE-/-}$ and *p53*$^{PE-/-}$*mir-34*$^{PE-/-}$ mice. The ABC Elite method with hematoxylin counterstaining was performed. Scale bars, 100 mm. (I–N) qRT-PCR (I) and western blot (J) of *Met* expression, prostasphere size (K), sphere-forming capacity (L), migration (M), and invasion (N) of CD49f^{hi}/Sca-1^{+} stem/progenitor cells isolated from 3-month-old WT, *p53*$^{PE-/-}$*mir-34*$^{PE-/-}$, and *p53*$^{PE-/-}$*mir-34*$^{PE-/-}$*Met*$^{PE-/-}$ mice (n=3). *P < 0.05; **P < 0.01; ***P < 0.001. Error bars denote SD.

as compared to WT mice and mice with inactivation of either *mir-34* or *p53* (Figure 2.6H). MET expression was below detectable levels in the epithelium of the distal regions of prostatic ducts in all strains. The only exception was elevated MET expression in high-grade PINs in $p53^{PE-/-}mir\text{-}34^{PE-/-}$ mice, suggesting a possible increase in the number of stem cell-like cells in such lesions.

To test if MET overexpression is essential for the observed phenotypes, *Met* was inactivated using a conditional $Met^{L/L}$ allele. *Met* inactivation abrogated growth, sphere-forming capacity, cell motility, and invasion of p53 and miR-34-deficient $CD49f^{hi}/Sca\text{-}1^{+}$ prostate stem/progenitor cells (Figures 2.6I-2.6N). Effects of MET downregulation on growth, sphere-forming capacity, cell motility, and invasion of WT prostate stem/ progenitor cells were less prominent (Figures 2.7A–2.7G), consistent with the lower levels of MET expression in such cells. However, 2-fold induction of MET expression by hypoxia resulted in a comparable increase of all the above parameters (Figures 2.7A–2.7G). Similar to *p53*/*mir-34*-inactivation experiments, this phenotype was reversed after MET knockdown, indicating a critical role for MET in prostate stem/progenitor cell regulation.

Previously it has been shown that p53 may negatively regulate MET expression by the miR-34-mediated targeting of MET (Corney et al., 2007; He et al., 2007; Hwang et al., 2011). Supporting these observations, we have observed the preserved 3'UTR carrying two binding sites for miR-34 in prostate stem/progenitor cells (Figure 2.8). We have also reported that p53 also represses MET expression by miR-34-independent inhibition of SP1 binding to *Met* promoter in the ovarian surface epithelium cells (Hwang et al., 2011). Consistent with this mechanism, MET reciprocal coimmunoprecipitation

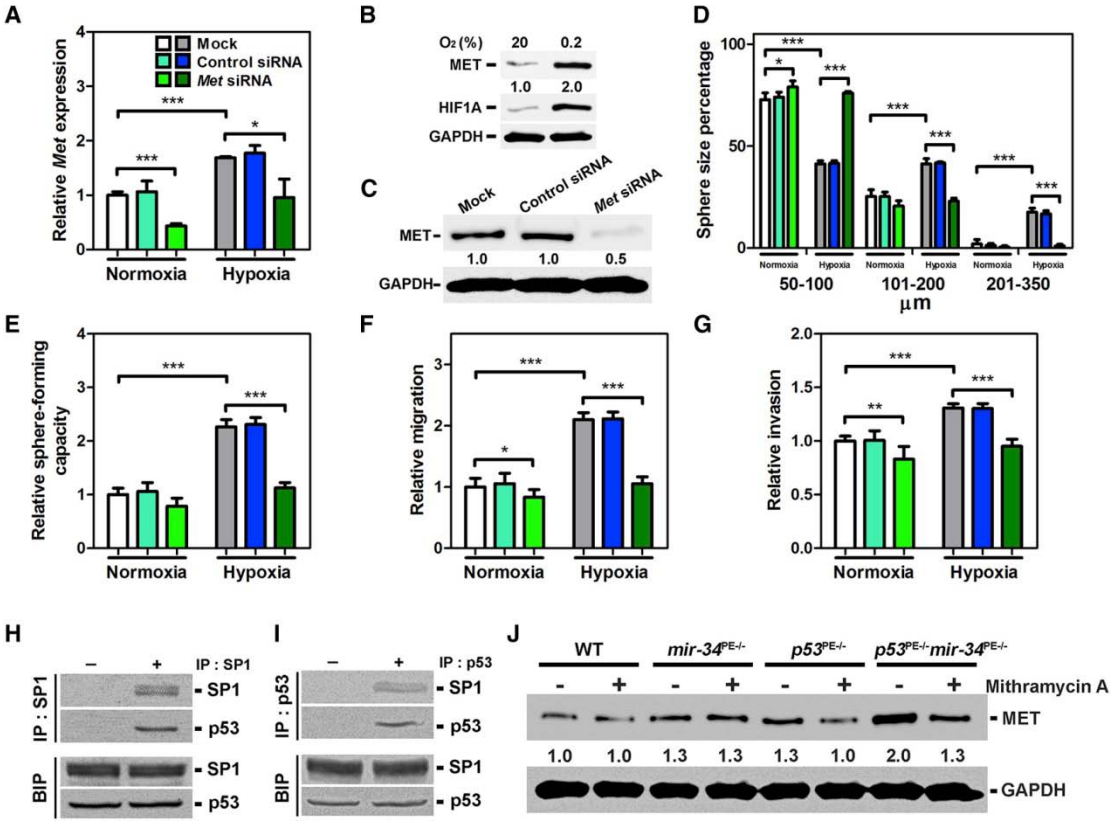

Figure 2.7 MET is essential for the growth, sphere-forming capacity, motility, and invasion of WT prostate stem/progenitor cells and is partially regulated by SP1 interacting with p53. (A-G) qRT-PCR (A) and western blot (B and C) of *Met* expression, prostasphere size (D), sphere-forming capacity (E), migration (F), and invasion (G) of CD49f^{hi}/Sca-1^{+} stem/progenitor cells isolated from 3-month-old WT mice (n = 3) and cultured under normoxic (20% O_2, A, B, and D-G) and hypoxic (0.2% O_2, A-G) conditions. *P < 0.05; **P < 0.01; ***P < 0.001. Error bars denote SD. Very similar results were obtained in separate experiments with two different *Met* small interfering RNAs (siRNAs). (H and I) Coimmunoprecipitation of cell lysates with SP1 (H) or p53 (I) antibodies followed by western blot with p53 or SP1 antibodies, respectively (upper panels). Samples of the same lysates were used for western blot with p53 or SP1 antibodies before immunoprecipitation (lower panels). CD49f^{hi}/Sca-1^{+} stem/progenitor cells isolated from 3-month-old WT mice (n = 3) were used. IP, immunoprecipitation. BIP, before immunoprecipitation. (J) The effect of mithramycin A (100 nM) on MET expression of CD49f^{hi}/Sca-1^{+} stem/progenitor cells isolated from 3-month-old WT, *p53*$^{PE-/-}$*mir-34*$^{PE-/-}$, and *p53*$^{PE-/-}$*mir-34*$^{PE-/-}$*Met*$^{PE-/-}$ mice (n=3).

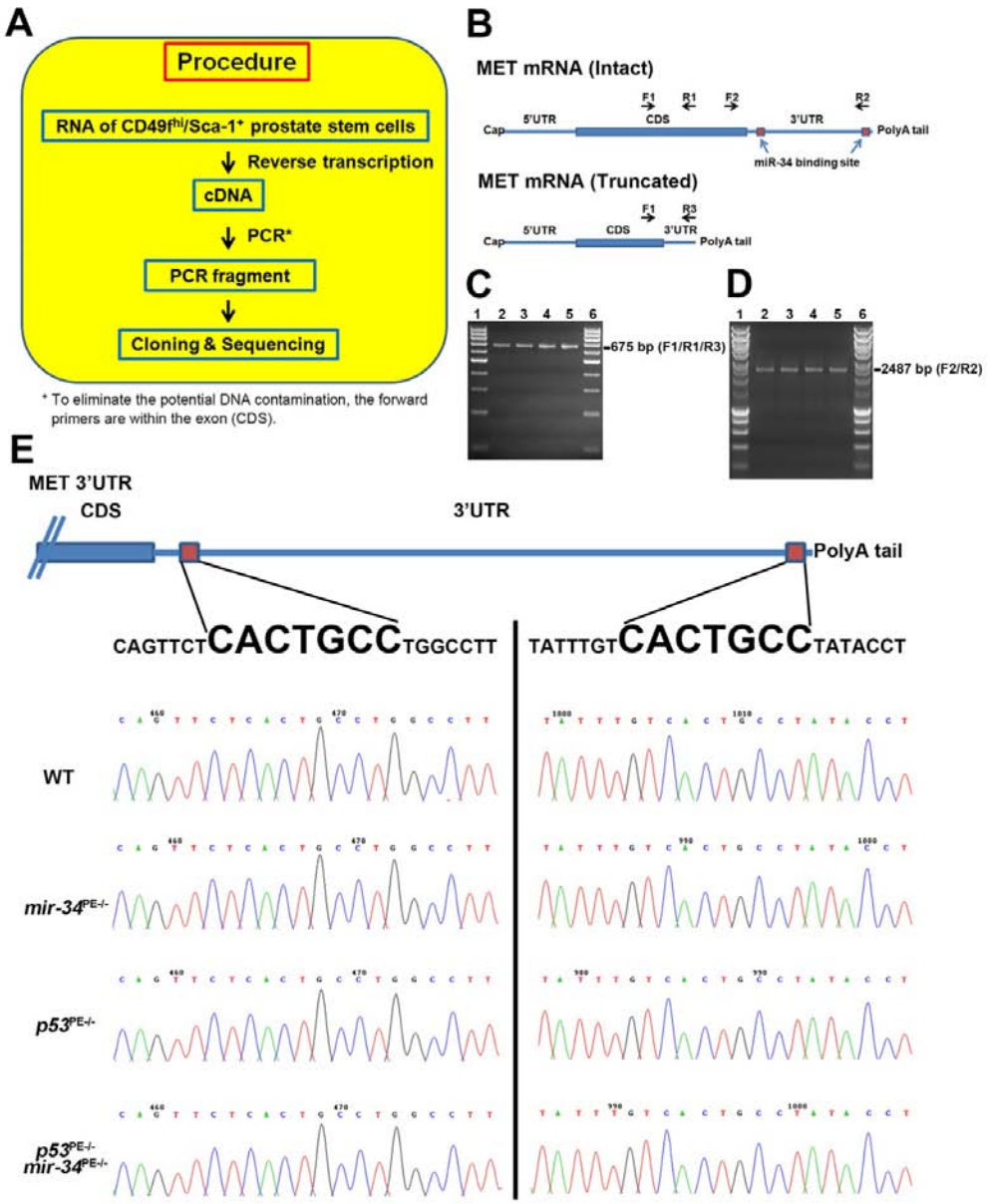

Figure 2.8 Two miR-34 binding sites of *Met* 3'UTR are intact in *p53*- and/or *mir-34*-deficient prostate stem/progenitor cells. (A) Experimental design. (B) Schematic diagrams of the intact *Met* mRNA containing miR-34 binding sites (upper) and truncated *Met* mRNA (lower). Primers (F1, F2, R1, R2, R3) are used for detecting the *Met* 3' UTR. CDS, coding sequence. (C) Detection of 3'UTR of the truncated *Met* gene (494 bp) and internal fragment of the intact *Met* gene (675 bp) by F1/R1/R3 primer set. Only 675 bp is detected in all samples. (D) Detection of 3'UTR of the intact *Met* gene (2487 bp) by F2/R2 primer set. (C, D) WT (lane 2), *mir-34*$^{PE-/-}$(lane 3), *p53*$^{PE-/-}$ (lane 4), and *p53*$^{PE-/-}$ *mir-34*$^{PE-/-}$ (lane 5) prostate stem/progenitor cells. DNA marker (lanes 1 and 6). (E) Sequencing results of two miR-34 binding sites of *Met* 3'UTR in WT, *p53*- and/or *mir-34*-deficient prostate stem/progenitor cells.

experiments have shown that p53 physically interacts with endogenous SP1 in the prostate stem/progenitor cells (Figures 2.7H and 2.7I). Furthermore, SP1 inhibition results in reduction of MET expression in prostate stem/progenitor cells deficient for either p53 or both miR-34 and p53, but not for miR-34 alone (Figure 2.7J).

2.5 Discussion

Our study provides a direct genetic proof that miRNAs of the miR-34 family may act as tumor suppressors in concert with other genes, such as *p53*. These findings offer a solid physiological basis for rational design of diagnostic and therapeutic approaches. Because the lack of *mir-34* genes alone is insufficient for cancer initiation, their downregulation is likely to occur at some point during tumor progression. However, the preexistence of *mir-34* methylation in some normal cells cannot be excluded. Further genomic studies in conjunction with animal modeling should be able to address this question. Although our current studies have been focused on prostate cancer, tissue-specific inactivation of *mir-34* and *p53* in other tissues will address likely interactions of these genes in other cell lineages.

Our observations confirm the earlier findings that p53 may negatively regulate MET expression by miR-34-mediated targeting of MET and by miR-34-independent inhibition of SP1 binding to the MET promoter. Notably, according to our previous ex vivo studies, inactivation of both mechanisms is required to achieve the highest MET overexpression, cell motility, and invasion (Hwang et al., 2011). Our present study supports this possibility in an autochthonous model of cancer. Our findings also show that miR-34

effects on MET regulation occur both in a p53-dependent and -independent manner. Specific mechanisms for p53-independent miR-34 regulation remain to be determined.

Previous studies have shown that p53 and miR-34 affect induced pluripotent stem cell reprogramming (Choi et al., 2011; Krizhanovsky and Lowe, 2009). p53 mediates the onset of senescence of endothelial progenitor cells (Rosso et al., 2006) and negatively regulates proliferation and survival of neural stem cells (Meletis et al., 2006). Constitutive p53 activation results in depletion of adult stem cells in bone marrow, brain and testes (Liu et al., 2010). It has been reported that ectopic expression of miR-34a may inhibit prostate cancer-propagating cells (also known as cancer stem cells or cancer-initiating cells) and metastasis by directly repressing CD44 (Liu et al., 2011a). However, the role of miR-34 in regulation of normal adult stem cell has been unclear. Our study fills this gap by showing that miR-34 regulates prostate stem/progenitor cells in cooperation with p53. It will be of interest to see if similar cooperation of miR-34 and p53 may play role in stem cell compartments of other cell lineages.

It has been previously reported that prostate cancer-propagating cells express MET, and depletion of MET results in a decrease in prostasphere formation (Rajasekhar et al., 2011). However, the direct role of MET in regulation of normal prostate stem/progenitor cells and mechanisms controlling its expression have been uncertain. Our studies on prostate cells collected either in the early stages of carcinogenesis or immediately after *mir-34* and *p53* inactivation provide a missing link between normal biological functions of MET and promotion of aberrant expansion of the stem/progenitor cell pool, which may eventually lead to cancer. Considering that MET is particularly

overexpressed in stem/progenitor cells lacking both p53 and miR-34, its therapeutic targeting may be especially effective in p53 and miR-34-deficient cancer cases.

Some cancers arise from stem/progenitor cells (Flesken-Nikitin et al., 2013; Schepers et al., 2012), while others may originate from more differentiated cells (Friedmann-Morvinski et al., 2012). In our study, we have observed that neoplastic lesions in the distal regions of prostatic ducts, which are mainly populated by transit-amplifying and differentiated cells, never progress to frank invasive adenocarcinomas. These findings support observations in other models that cancers arising from stem cell compartments are more aggressive (Flesken-Nikitin et al., 2013). Our autochthonous mouse model of prostate cancer based on prostate epithelium-specific inactivation of *p53* and *mir-34* should provide a valuable tool for further elucidation of the role of individual cell subpopulations in prostate cancer pathogenesis.

REFERENCES

Aubrecht, J., Goad, M.E., Czopik, A.K., Lerner, C.P., Johnson, K.A., Simpson, E.M., and Schiestl, R.H. (2011). A high G418-resistant neo(R) transgenic mouse and mouse embryonic fibroblast (MEF) feeder layers for cytotoxicity and gene targeting in vivo and in vitro. Drug and chemical toxicology *34*, 433-439.

Bader, A.G. (2012). miR-34 - a microRNA replacement therapy is headed to the clinic. Front Genet *3*, 120.

Bouchie, A. (2013). First microRNA mimic enters clinic. Nat Biotechnol *31*, 577.

Chen, Z., Trotman, L.C., Shaffer, D., Lin, H.K., Dotan, Z.A., Niki, M., Koutcher, J.A., Scher, H.I., Ludwig, T., Gerald, W.*, et al.* (2005). Crucial role of p53-dependent cellular senescence in suppression of Pten-deficient tumorigenesis. Nature *436*, 725-730.

Choi, Y.J., Lin, C.P., Ho, J.J., He, X., Okada, N., Bu, P., Zhong, Y., Kim, S.Y., Bennett, M.J., Chen, C.*, et al.* (2011). miR-34 miRNAs provide a barrier for somatic cell reprogramming. Nat Cell Biol *13*, 1353-1360.

Christoffersen, N.R., Shalgi, R., Frankel, L.B., Leucci, E., Lees, M., Klausen, M., Pilpel, Y., Nielsen, F.C., Oren, M., and Lund, A.H. (2010). p53-independent upregulation of miR-34a during oncogene-induced senescence represses MYC. Cell Death Differ *17*, 236-245.

Concepcion, C.P., Han, Y.C., Mu, P., Bonetti, C., Yao, E., D'Andrea, A., Vidigal, J.A., Maughan, W.P., Ogrodowski, P., and Ventura, A. (2012). Intact p53-dependent responses in miR-34-deficient mice. PLoS Genet *8*, e1002797.

Corney, D.C., Flesken-Nikitin, A., Godwin, A.K., Wang, W., and Nikitin, A.Y. (2007). MicroRNA-34b and MicroRNA-34c are targets of p53 and cooperate in control of cell proliferation and adhesion-independent growth. Cancer research *67*, 8433-8438.

Corney, D.C., Hwang, C.I., Matoso, A., Vogt, M., Flesken-Nikitin, A., Godwin, A.K., Kamat, A.A., Sood, A.K., Ellenson, L.H., Hermeking, H.*, et al.* (2010). Frequent downregulation of miR-34 family in human ovarian cancers. Clin Cancer Res *16*, 1119-1128.

Farley, F.W., Soriano, P., Steffen, L.S., and Dymecki, S.M. (2000). Widespread recombinase expression using FLPeR (flipper) mice. Genesis *28*, 106-110.

Flesken-Nikitin, A., Hwang, C.I., Cheng, C.Y., Michurina, T.V., Enikolopov, G., and Nikitin, A.Y. (2013). Ovarian surface epithelium at the junction area contains a cancer-prone stem cell niche. Nature *495*, 241-245.

Friedmann-Morvinski, D., Bushong, E.A., Ke, E., Soda, Y., Marumoto, T., Singer, O., Ellisman, M.H., and Verma, I.M. (2012). Dedifferentiation of neurons and astrocytes by oncogenes can induce gliomas in mice. Science *338*, 1080-1084.

Fujita, Y., Kojima, K., Hamada, N., Ohhashi, R., Akao, Y., Nozawa, Y., Deguchi, T., and Ito, M. (2008). Effects of miR-34a on cell growth and chemoresistance in prostate cancer PC3 cells. Biochem Biophys Res Commun *377*, 114-119.

He, L., He, X., Lim, L.P., de Stanchina, E., Xuan, Z., Liang, Y., Xue, W., Zender, L., Magnus, J., Ridzon, D.*, et al.* (2007). A microRNA component of the p53 tumour suppressor network. Nature *447*, 1130-1134.

Hermeking, H. (2012). MicroRNAs in the p53 network: micromanagement of tumour suppression. Nat Rev Cancer *12*, 613-626.

Huh, C.G., Factor, V.M., Sanchez, A., Uchida, K., Conner, E.A., and Thorgeirsson, S.S. (2004). Hepatocyte growth factor/c-met signaling pathway is required for efficient liver regeneration and repair. Proceedings of the National Academy of Sciences of the United States of America *101*, 4477-4482.

Hwang, C.I., Matoso, A., Corney, D.C., Flesken-Nikitin, A., Korner, S., Wang, W., Boccaccio, C., Thorgeirsson, S.S., Comoglio, P.M., Hermeking, H.*, et al.* (2011). Wild-type p53 controls cell motility and invasion by dual regulation of MET expression. Proceedings of the National Academy of Sciences of the United States of America *108*, 14240-14245.

Ji, Q., Hao, X., Zhang, M., Tang, W., Yang, M., Li, L., Xiang, D., Desano, J.T., Bommer, G.T., Fan, D.*, et al.* (2009). MicroRNA miR-34 inhibits human pancreatic cancer tumor-initiating cells. PLoS One *4*, e6816.

Kojima, K., Fujita, Y., Nozawa, Y., Deguchi, T., and Ito, M. (2010). MiR-34a attenuates paclitaxel-resistance of hormone-refractory prostate cancer PC3 cells through direct and indirect mechanisms. Prostate *70*, 1501-1512.

Krizhanovsky, V., and Lowe, S.W. (2009). Stem cells: The promises and perils of p53. Nature *460*, 1085-1086.

Lakso, M., Pichel, J.G., Gorman, J.R., Sauer, B., Okamoto, Y., Lee, E., Alt, F.W., and Westphal, H. (1996). Efficient in vivo manipulation of mouse genomic sequences at the zygote stage. Proceedings of the National Academy of Sciences of the United States of America *93*, 5860-5865.

Lawson, D.A., Zong, Y., Memarzadeh, S., Xin, L., Huang, J., and Witte, O.N. (2010). Basal epithelial stem cells are efficient targets for prostate cancer initiation. Proceedings of the National Academy of Sciences of the United States of America *107*, 2610-2615.

Leong, K.G., Wang, B.E., Johnson, L., and Gao, W.Q. (2008). Generation of a prostate from a single adult stem cell. Nature *456*, 804-808.

Liu, C., Kelnar, K., Liu, B., Chen, X., Calhoun-Davis, T., Li, H., Patrawala, L., Yan, H., Jeter, C., Honorio, S*., et al.* (2011). The microRNA miR-34a inhibits prostate cancer stem cells and metastasis by directly repressing CD44. Nat Med *17*, 211-215.

Liu, D., Ou, L., Clemenson, G.D., Jr., Chao, C., Lutske, M.E., Zambetti, G.P., Gage, F.H., and Xu, Y. (2010). Puma is required for p53-induced depletion of adult stem cells. Nat Cell Biol *12*, 993-998.

Liu, P., Jenkins, N.A., and Copeland, N.G. (2003). A highly efficient recombineering-based method for generating conditional knockout mutations. Genome Res *13*, 476-484.

Lodygin, D., Tarasov, V., Epanchintsev, A., Berking, C., Knyazeva, T., Korner, H., Knyazev, P., Diebold, J., and Hermeking, H. (2008). Inactivation of miR-34a by aberrant CpG methylation in multiple types of cancer. Cell Cycle *7*, 2591-2600.

Lukacs, R.U., Goldstein, A.S., Lawson, D.A., Cheng, D., and Witte, O.N. (2010). Isolation, cultivation and characterization of adult murine prostate stem cells. Nat Protoc *5*, 702-713.

Marino, S., Vooijs, M., van Der Gulden, H., Jonkers, J., and Berns, A. (2000). Induction of medulloblastomas in p53-null mutant mice by somatic inactivation of Rb in the external granular layer cells of the cerebellum. Genes & development *14*, 994-1004.

Meletis, K., Wirta, V., Hede, S.M., Nister, M., Lundeberg, J., and Frisen, J. (2006). p53 suppresses the self-renewal of adult neural stem cells. Development *133*, 363-369.

Navarro, F., Gutman, D., Meire, E., Caceres, M., Rigoutsos, I., Bentwich, Z., and Lieberman, J. (2009). miR-34a contributes to megakaryocytic differentiation of K562 cells independently of p53. Blood *114*, 2181-2192.

Nelson, P.T., Baldwin, D.A., Kloosterman, W.P., Kauppinen, S., Plasterk, R.H., and Mourelatos, Z. (2006). RAKE and LNA-ISH reveal microRNA expression and localization in archival human brain. Rna *12*, 187-191.

Nikitin, A., and Lee, W.H. (1996). Early loss of the retinoblastoma gene is associated with impaired growth inhibitory innervation during melanotroph carcinogenesis in Rb+/- mice. Genes & development *10*, 1870-1879.

Park, J.H., Walls, J.E., Galvez, J.J., Kim, M., Abate-Shen, C., Shen, M.M., and Cardiff, R.D. (2002). Prostatic intraepithelial neoplasia in genetically engineered mice. The American journal of pathology *161*, 727-735.

Rajasekhar, V.K., Studer, L., Gerald, W., Socci, N.D., and Scher, H.I. (2011). Tumour-initiating stem-like cells in human prostate cancer exhibit increased NF-kappaB signalling. Nat Commun *2*, 162.

Rosso, A., Balsamo, A., Gambino, R., Dentelli, P., Falcioni, R., Cassader, M., Pegoraro, L., Pagano, G., and Brizzi, M.F. (2006). p53 Mediates the accelerated onset of senescence of endothelial progenitor cells in diabetes. The Journal of biological chemistry *281*, 4339-4347.

Schepers, A.G., Snippert, H.J., Stange, D.E., van den Born, M., van Es, J.H., van de Wetering, M., and Clevers, H. (2012). Lineage tracing reveals Lgr5+ stem cell activity in mouse intestinal adenomas. Science *337*, 730-735.

Shappell, S.B., Thomas, G.V., Roberts, R.L., Herbert, R., Ittmann, M.M., Rubin, M.A., Humphrey, P.A., Sundberg, J.P., Rozengurt, N., Barrios, R.*, et al.* (2004). Prostate pathology of genetically engineered mice: definitions and classification. The consensus report from the Bar Harbor meeting of the Mouse Models of Human Cancer Consortium Prostate Pathology Committee. Cancer research *64*, 2270-2305.

Trusolino, L., Bertotti, A., and Comoglio, P.M. (2010). MET signalling: principles and functions in development, organ regeneration and cancer. Nat Rev Mol Cell Biol *11*, 834-848.

Tsujimura, A., Koikawa, Y., Salm, S., Takao, T., Coetzee, S., Moscatelli, D., Shapiro, E., Lepor, H., Sun, T.T., and Wilson, E.L. (2002). Proximal location of mouse prostate epithelial stem cells: a model of prostatic homeostasis. The Journal of cell biology *157*, 1257-1265.

Vogt, M., Munding, J., Gruner, M., Liffers, S.T., Verdoodt, B., Hauk, J., Steinstraesser, L., Tannapfel, A., and Hermeking, H. (2011). Frequent concomitant inactivation of miR-34a and miR-34b/c by CpG methylation in colorectal, pancreatic, mammary, ovarian, urothelial, and renal cell carcinomas and soft tissue sarcomas. Virchows Arch *458*, 313-322.

Wei, J., Shi, Y., Zheng, L., Zhou, B., Inose, H., Wang, J., Guo, X.E., Grosschedl, R., and Karsenty, G. (2012). miR-34s inhibit osteoblast proliferation and differentiation in the mouse by targeting SATB2. The Journal of cell biology *197*, 509-521.

Wu, X., Wu, J., Huang, J., Powell, W.C., Zhang, J., Matusik, R.J., Sangiorgi, F.O., Maxson, R.E., Sucov, H.M., and Roy-Burman, P. (2001). Generation of a prostate epithelial cell-specific Cre transgenic mouse model for tissue-specific gene ablation. Mech Dev *101*, 61-69.

Zanjani, H.S., Vogel, M.W., Delhaye-Bouchaud, N., Martinou, J.C., and Mariani, J. (1996). Increased cerebellar Purkinje cell numbers in mice overexpressing a human bcl-2 transgene. J Comp Neurol *374*, 332-341.

Zhou, Z., Flesken-Nikitin, A., Corney, D.C., Wang, W., Goodrich, D.W., Roy-Burman, P., and Nikitin, A.Y. (2006). Synergy of p53 and Rb deficiency in a conditional mouse model for metastatic prostate cancer. Cancer research *66*, 7889-7898.

CHAPTER 3

DETECTION AND ORGAN-SPECIFIC ABLATION OF NEUROENDOCRINE CELLS BY *SYNAPTOPHYSIN* LOCUS-BASED BAC CASSETTE IN TRANSGENIC MICE

Chieh-Yang Cheng, Zongxiang Zhou, Alexander Yu. Nikitin, (2013). PLoS One. 22; 8(4): e60905. PMID: 23630575.

Author contributions: Chieh-Yang Cheng and Alexander Yu. Nikitin designed the study, interpreted data and wrote the manuscript. Chieh-Yang Cheng and Zongxiang Zhou performed experiments and analysed data. Alexander Yu. Nikitin supervised the project and gave final approval.

3.1 Abstract

The role of cells of the diffuse neuroendocrine system in development and maintenance of individual organs and tissues remains poorly understood. Here we identify a regulatory region sufficient for accurate *in vivo* expression of synaptophysin (SYP), a common marker of neuroendocrine differentiation, and report generation of Tg(*Syp-EGFP*^{loxP}*-DTA)147*^{Ayn} (*SypELDTA*) mice suitable for flexible organ-specific ablation of neuroendocrine cells. These mice express EGFP and diphtheria toxin fragment A (DTA) in SYP positive cells before and after Cre-*loxP* mediated recombination, respectively. As a proof of principle, we have crossed *SypELDTA* mice with *EIIA-Cre* and *PB-Cre4* mice. *EIIA-Cre* mice express Cre recombinase in a broad range of tissues, while *PB-Cre4* mice specifically express Cre recombinase in the prostate epithelium. Double transgenic *EIIA-Cre; SypELDTA* embryos exhibited massive cell death in SYP positive cells. At the same time, *PB-Cre4; SypELDTA* mice showed a substantial decrease in the number of neuroendocrine cells and associated prostate hypotrophy. As no increase in cell death and/or Cre-*loxP* mediated recombination was observed in non-neuroendocrine epithelium cells, these results suggest that neuroendocrine cells play an important role in prostate development. High cell type specificity of *Syp* locus-based cassette and versatility of generated mouse model should assure applicability of these resources to studies of neuroendocrine cell functions in various tissues and organs.

3.2 Introduction

Neuroendocrine (NE) cells have both neuronal and endocrine phenotypes (Montuenga et al., 2003). The diffuse neuroendocrine system (DNES) is composed of NE cells scattered throughout the entire body either as single cells or clusters, such as solitary pulmonary NE cells (PNECs) and neuroepithelial bodies (NEBs) (Linnoila, 2006), the islets of Langerhans in the pancreas (Ahren, 2000; Koh et al., 2012), gastrointestinal NE cells (Dockray, 2003; Kuliczkowska-Plaksej et al., 2012), dermal NE cells (so-called Merkel cells) (Tachibana, 1995), adrenal medullary NE cell (de Diego et al., 2008; Douglas et al., 2010; Mravec, 2005), and prostate NE cells (Abrahamsson, 1999). PNECs are implicated in regulation of lung maturation and growth, function as oxygen-sensing chemoreceptors and are likely important for lung stem cell niches (Linnoila, 2006). Gastrointestinal NE cells are known to control gastrointestinal secretion, motility, growth, immune cell function and food intake (Dockray, 2003). Though there has been progress in understanding the function of NE cells, the physiological role of NE cells in most other organs is not well understood.

Cells with NE differentiation are also present in many cancer types, with their representation ranging from being the major component in small cell carcinomas of the lung (Linnoila, 2006) and prostate (Sun et al., 2009), as well as NE tumors of gastrointestinal tract (Gustafsson et al., 2008), to more limited quantity in other cancers, such as adenocarcinomas of the lung (Linnoila, 2006) and prostate (Sun et al., 2009). Unfortunately, the cell of origin of neoplastic NE cells and their contribution to cancer progression remain insufficiently elucidated (Cheng and Nikitin, 2011; Linnoila, 2006; Montuenga et al., 2003; Sun et al., 2009).

NE cells are detected by a number of markers, such as chromogranin A (CgA) (Gazdar et al., 1988), neuron-specific enolase (NSE) (Schmechel et al., 1978), neural cell adhesion molecules (NCAMs, so-called CD56) (Jin et al., 1991), calcitonin gene-related peptide (CGRP) (Cadieux et al., 1986) and SYP (Wiedenmann et al., 1986). However, the use of NSE (Haimoto et al., 1985; Schmechel, 1985; Seshi et al., 1988) or CD56 (Kaufmann et al., 1997; Lantuejoul et al., 1998) is limited because of their poor specificity and/or sensitivity. CgA reactivity is strongly dependent on the number of neurosecretory vesicles per cell and is frequently lost in neoplastic NE cells (Jensen et al., 1990), while only subset of NE cells expresses CGRP (Weichselbaum et al., 2005). In contrast, SYP is expressed in a broad-spectrum of normal and neoplastic NE and neural cells (Gould et al., 1987; Wiedenmann et al., 1986).

SYP is a major integral membrane protein of small synaptic vesicles and belongs to a family of proteins that includes synaptogyrin (SYG) and synaptoporin (Sudhof et al., 1987). It has been reported that in cell culture transfection experiments the 1.2 kb upstream region of rat *Syp* promoter is insufficient to confer cell type specific expression (Bargou and Leube, 1991). It has also been suggested that NE cell specific silencer elements lay within the 2.6 kb upstream fragment of *Syp* (Bargou and Leube, 1991). At the same time, other cell culture studies have reported that neuron-restrictive silencer element *(NRSE),* a binding site for RE-1 silencing transcription factor (REST), a.k.a. neuron-restrictive silencer factor (NRSF), is located within the first intron of *Syp* gene (Lietz et al., 2003). However, the regulatory region sufficient for accurate *in vivo* expression of SYP remains unknown, thereby preventing development of genetic constructs allowing *Syp*-specific gene expression.

Since SYP is among the most reliable markers for NE cells, we generated mice with *Syp* locus-based Bacterial Artificial Chromosome (BAC) cassettes. We show that in combination with the preserved *NRSE* in the first intron, only the 121 kb upstream and 36 kb downstream regions, but not the 3 kb upstream region, allow for accurate expression of reporter gene in SYP expressing cells in the mouse. We also show that SYP positive cells can be accurately ablated in either the embryo or in the postnatal adult prostate after induction of DTA expression (Ivanova et al., 2005) by Cre-*loxP* mediated recombination in crosses of *SypELDTA* mice with *EIIA-Cre* (Lakso et al., 1996) or *PB-Cre4* (Wu et al., 2001) mice, respectively. The *Syp* containing BAC cassette and generated mice should provide useful tools for studies of NE cell biological roles in development and maintenance of various tissues and organs.

3.3 Materials and Methods

Ethics statement. This study was carried out in strict accordance with the recommendations of the Guide for the Care and Use of Laboratory Animals of the National Institutes of Health. The protocol was approved by the Institutional Laboratory Animal Use and Care Committee at Cornell University (Permit Number: 2000-0116). All efforts were made to minimize animal suffering.

Bioinformatics analyses. Analysis of sequence and species comparisons were performed by using the University of California Santa Cruz Genome Browser (UCSC, http://genome.ucsc.edu/).

Generation of SypELDTA mice. A BAC clone containing approximately 121 kb and 36 kb of 5' and 3' DNA flanking the *Syp* locus was modified by insertion of a *loxP-EGFP-Neo cassette-Stop-loxP-DTA-bpA* cassette to replace the sequence spanning intron 1 downstream of *NRSE* to exon 7 of *Syp* locus by homologous recombination. The BAC constructs were microinjected into male pronuclei of fertilized oocytes from FVB/N mice to generate the *SypELDTA* mice. *EIIA-Cre* (FVB/N-Tg(EIIa-cre)C5379Lmgd/J) transgenic mice (The Jackson Laboratory, Bar Harbor, ME, stock number #003314) (Lakso et al., 1996), *Rosa26Stop^{loxP}LacZ* (B6;129S4-*Gt(ROSA)26Sor^{tm1Sor}*/J) reporter mice (The Jackson Laboratory, stock number #003309) (Soriano, 1999), and *ARR$_2$PB-Cre* transgenic male mice on FVB/N (*PB-Cre4*) (Wu et al., 2001) were described previously. Details about generation of the targeting construct and BAC recombineering are described in the Generation of the targeting construct and BAC recombineering.

Generation of the targeting construct and BAC recombineering. The components of the BAC targeting vector were as follows: *pBS302* ((Sauer, 1993), plasmid 11925), *pcDNA3-EGFP* (D. Golenbock, plasmid 13031), and *PGKDTAbpA* ((Soriano, 1997), plasmid 13440), all from Addgene (Cambridge, MA), and *PL452* (Liu et al., 2003), National Cancer Institute - Frederick, Bethesda, MD). The ApaI-NotI DNA fragment of *loxP-EGFP-Neocassette-Stop-loxP-DTA-bpA* was made by cloning from DNA fragments of *loxP-Stop-loxP* (*pBS302*), *EGFP* (*pcDNA3-EGFP*), *Neo cassette* (*PL452*), and *DTA-bpA* (*PGKDTAbpA*), and inserted into the backbone of *PGKDTAbpA* to generate the final BAC targeting vector *pBS-loxP-EGFP-Neo cassette-Stop-loxP-DTA-bpA*. BAC clone (*RP23-267C15*), which contains *Syp* locus, was purchased from

"BACPAC Resource Center" (BPRC, Oakland, CA). *Syp* homologous arms were amplified and inserted upstream and downstream of *loxP-EGFP-Neo cassette-Stop-loxP-DTA-bpA* sequence in plasmid *pBS-loxP-EGFP-Neo cassette-Stop-loxP-DTA-bpA*. 5' arm was a 510 bp fragment, containing exon 1 and *NRSE* of intron 1 within *Syp* locus, upstream of the middle of intron 1. It was generated by PCR that used forward primer (KpnI-F1) 5'-CCG TTG GGT ACC TTG CTG GCA CTG CTG CTG GCA GAC A-3' and reverse primer (ApaI-R1) 5'-CCG TTG GGG CCC GCT CCG GGG GTG AAA GGG TCG TC-3'. To avoid possible interference of transgene expression by start codon ATG in exon 1 of *Syp* locus, we changed ATG to GCA (alanine) in forward primer of 5' arm fragment. 3' arm was a 500 bp PCR product downstream of exon 7 of *Syp* locus that was generated by the forward primer (NotI-F1) 5'-TGC CGT TGG CGG CCG CGT CCC GGC TCT TTT TCT CAG TGC GC-3', and the reverse primer (SacII-R2) 5'-CCG TTG CCG CGG AGA CAG GCC TTT CAT CTT GGG CGC C-3'. The homology arms were inserted after KpnI/ApaI (5' arm) and NotI/SacII (3' arm) digestion and the targeting cassette was released from the plasmid by KpnI/SacII. EL350 bacteria carrying *RP23-267C15* were electroporated with the targeting cassette DNA and selected with kanamycin and chloramphenicol. Homologous recombination was verified by sequencing of PCR products obtained using primers flanking the homology arms and *loxP-EGFP-Neo cassette-Stop-loxP-DTA-bpA* fragment. The primer sets were BAC upstream: forward primer 5'-ACT GAG CGG TCC TCT TAC CAC CC-3' and reverse primer 5'-CCT GCA CGA CGC GAG CTG C-3'; and BAC downstream: forward primer 5'-CTC CAC ACA GGC ATA GAG TGT CTG C-3' and reverse primer 5'-CCC ACT GCA CCT CTG CCC AAA GA-3' (Figure S1A).

The *RP23-267C15* was cloned into *pBACe3.6* vector, which has a wild type *loxP* site. In order to eliminate potential mis-recombination between the transgene cassette and an endogenous *loxP* site in the *pBACe3.6* vector, we replaced the vector-derived *loxP* site with a *β-lactamase* sequence from *pGEM-T* vector (Promega, Madison, WI, #A3600) using homologous recombination (Figure S1B). The modified BAC construct was named *SypELDTA* (Figure 3A). Furthermore, to evaluate applicability of the shorter upstream sequence of *Syp* for cell type specific expression, we used the same homologous recombination strategy and retrieved the sequence *SypP-loxP-EGFP-Neo cassette-Stop-loxP-DTA-bpA* from *SypELDTA* into *pGEM-T* vector. The modified BAC construct used in cell culture study was named *sSypELDTA* (Figure 3B). *SypELDTA* and *sSypELDTA* constructs were purified (QIAGEN Plasmid Midi Kit, Valencia, CA, #12143) and microinjected into pronuclei of fertilized oocytes of FVB/N mice in the Cornell Transgenic Mouse Core facility.

Genotyping. PB-Cre4 transgenic mice were identified by primers Cre5' (5'-GGA CAT GTT CAG GGA TCG CCA GGC G-3') and Cre3' (5'-GCA TAA CCA GTG AAA CAG CAT TGC TG-3'). PCR amplification of *Cre* resulted in 296 bp DNA fragment. Endogenous *Rb* was identified by primers Rb5' (5'-CGG AAG AAG AAC GTT TGT CCA TTC A-3') and Rb3' (5'-CGC TGC TAT ACG TAG CCA TTA CAA C-3'). PCR amplification of *Rb* resulted in 196 bp DNA fragment. *EGFP* was identified by primers EGFP5' (5'-CCT CGT GAC CAC CCT GAC CTA CGG C-3') and EGFP3' (5'-GCC GTC CTC GAT GTT GTG GCG GAT C-3'). PCR amplification of *EGFP* resulted in 346 bp DNA fragment. *Neomycin* was identified by primers Neo5' (5'-GCC GCC GTG TTC

CGG CTG TCA GCG C-3') and Neo3' (5'-CCG AGT ACG TGC TCG CTC GAT GCG A-3'). PCR amplification of *Neomycin* resulted in 342 bp DNA fragment. *DTA* was identified by primers DTA5' (5'-AGC TTG GGC TGC AGG TCG AGG GAC C-3') and DTA3' (5'-ACG TCA CTT TGA CCA CGC CTC CAG C-3'). PCR amplification of *DTA* resulted in 348 bp DNA fragment. The PCR temperature profile was 35 cycles for 94°C for 30 seconds, 60°C for 1 minute, and 72°C for 2 minutes with extension of the last cycle for 10 minutes at 72°C (Nikitin and Lee, 1996).

Cell culture experiments. Mouse *p53* and *Rb* double deficient prostate adenocarcinoma cell lines PCN1 and PCN3 were established from prostate carcinomas of *PB-Cre4; $p53^{loxP/loxP}Rb^{loxP/loxP}$* mice (Zhou et al., 2006). They were maintained in the Dulbecco's Modification of Eagle's Medium (DMEM, Cellgrow, Manassas, VA, #15-018-CV), supplementary with fetal bovine serum (FBS, Invitrogen, Carlsbad, CA, #16000-044), L-Glutamine (Cellgrow, #25-005-Cl), Na-Pyruvate (Cellgrow, #25-000-Cl), and Penicillin-Streptomycin (Cellgrow, #30-002-Cl).

For EGFP detection experiment, PCN1 and PCN3 cells were seeded in triplicate in 12-well plates and transfected the next day with *sSypELDTA* using Lipofectamine 2000 (Invitrogen, #11668019). 48 hours after transfection, EGFP signal was observed via fluorescent microscopy.

For DTA detection, cells were transfected with plasmids *PGKDTAbpA*, *sSypELDTA*, and *SypDTA*. *sSypELDTA* transfected cells were infected by Adenovirus-*Cre* (Ad-*Cre*) 48 hours post-transfection. 24 hours after infection, RT-PCR was carried out for all groups. RNA was isolated using mirVana miRNA Isolation Kit (Ambion, Austin,

TX, #AM1561) according to the manufacturer's protocol. RNA concentration and purity were determined by NanoDrop. cDNA was prepared from 100 ng total RNA using SuperScript III (Invitrogen, Carlsbad, CA, #18080-051) and amplified with DTA forward primer 5'-ATG GAT CCT GAT GAT GTT GTT GAT TCT TCT AAA TC-3' and a reverse primer 5'-TTA GAG CTT TAA ATC TCT GTA GGT AGT TTG TCC AA-3', yielding a 657 bp PCR product. The PCR temperature profile was 30 cycles for 95ºC for 45 seconds, 60ºC for 45 seconds, and 72ºC for 1 minute with the extension of last cycle for 1 minute at 72ºC.

For detection of Cre-*loxP* mediated recombination, EL350 cells were cultured in 10 ml of LB broth at *32*°C overnight. 10 ml EL350 was divided into two 5 ml EL350 vials. One EL350 vial was treated with 100 µl 10% arabinose and other EL350 vial served as a control without arabinose induction. After one hour culture at 32°C, EL350 cells were electroporated with *sSypELDTA* and selected with ampicillin on LB plate. After 16 hours incubation at 32°C, colonies were picked, and Cre-*loxP* mediated recombination was verified by sequencing of PCR products obtained using forward primer (F1) 5'-CTC ACT GCC GCA GAG GGG GCC TCC A-3', forward primer (F2) 5'-ATG GAT CCT GAT GAT GTT GTT GAT TCT TCT AAA TC-3' and a reverse primer (R1) 5'-ACG TCA CTT TGA CCA CGC CTC CAG C-3'. Combination of F1 and R1 primers and that of F2 and R1 yielded 617 bp and 256 bp PCR products, respectively.

Transgene copy number quantification. Transgene copy number was carried out by Southern blotting and qPCR. Genomic DNA was isolated with a Gentra Puregene Tissue Kit (Qiagen, #158667). Genomic DNA from the *sSypELDTA* mouse (line 141)

was digested by restriction enzymes AflII, AscI, and PacI (New England Biolabs, Ipswich, MA), and detected by Southern blotting with ^{32}P-labeled *EGFP* probe. 1117 bp *EGFP* probe was prepared by PCR using primers 5'EGFP (5'-ATG GTG AGC AAG GGC GAG GAG C-3') and 3'EGFP (5'-CCT GCA CGA CGC GAG CTG C-3'). The copy number of *sSypELDTA* transgene was estimated by densitometric analysis with Image J software (NIH, Bethesda, MD). To perform qPCR, 60 ng DNA was amplified with custom TaqMan real time *EGFP* probe (forward primer: 5'-CAC ATG AAG CAG CAC GAC TT-3'; reverse primer: 5'-GTG CGC TCC TGG ACG TA-3'), followed by normalization to the endogenous *β-actin*. All PCR reactions were performed in triplicate on AB 7500 Real Time PCR system (Applied Biosystems Inc, Foster City, CA). After getting relative quantification among each line, copy number was estimated by normalizing to copy number of *sSypELDTA* transgene in line 141.

Microdissection-polymerase chain reaction. For laser microdissection, 4-µm-thick paraffin sections were prepared on PET (polyethylene terephthalate)-membrane slides for laser microdissection (Leica microsystems, Buffalo Grove, IL, #11505151) and stained with hematoxylin and eosin. Prostate cells from different areas (proximal region, ventral lobe, dorsolateral lobe, anterior lobe, muscular layer) were microdissected using a blue laser (Laser Microdissection System, Leica AS, Heidelberg, Germany), collected into caps of 0.6 ml Eppendorf tubes filled with lysis buffer, digested in proteinase K, divided equally among tubes for detection of recombination and used for subsequent PCR amplification following previously described protocol (Nikitin and Lee, 1996). *EGFP* was identified by primers EGFP5' (5'-CCT CGT GAC CAC CCT GAC CTA CGG C-3')

and EGFP3’ (5'-GCC GTC CTC GAT GTT GTG GCG GATC-3'). PCR amplification of *EGFP* resulted in 346 bp DNA fragment.

Histotechnology. Mice euthanized according to schedule were subjected to cardiac perfusion by phosphate-buffered 4% paraformaldehyde. After digital camera photography during necropsy, collected tissues were processed for embedding in paraffin. Histological evaluations were done on 4-µm-thick sections stained with hematoxylin (Mayer's haemalum) and eosin. Transverse sections of the whole prostate were scanned by ScanScope (Aperio Technologies, Vista, CA) with 40X objective followed by lossless compression and assessment of all alterations in identical anatomic regions.

Immunohistochemical analyses. Immunoperoxidase staining of paraffin sections of paraformaldehyde-fixed tissue was performed by a modified avidin-biotin-peroxidase (ABC) technique (Nikitin and Lee, 1996). Antigen retrieval was done by boiling the slides in 10 mM citric buffer (pH 6.0) for 10 minutes. The primary antibodies to cytokeratin-8 (CK8), cytokeratin-5 (CK5), SYP and cleaved Caspase-3 were incubated with deparaffinized sections at 4°C overnight. After incubation with methanol (Fisher Scientific, Bohemia, NY, #A454-4) containing 0.3% hydrogen peroxide (Sigma, St. Louis, MO, #H1009), sections were subsequently incubated with biotinylated secondary antibody for 30 minutes at room temperature and subsequently detected with the ABC Elite kit (Vector Laboratories, Burlingame, CA, #PK-6100) and 3,3-diaminobenzidine (DAB; Sigma, #D4418) as substrate. Hematoxylin was used as the counterstain in

immunoperoxidase stainings. Double immunofluorescence staining was performed by incubation of SYP and EGFP, or β-galactosidase primary antibody at 4°C overnight, followed by Alexa-Fluor 594-conjugated and Alexa-Fluor 488- conjugated secondary antibodies. To stain cell nuclei, sections were incubated with a 10 µg/ml solution of 4',6-diamidino-2-phenylindole (DAPI; Sigma, #D9542) for 3 min. Antibody sources and dilutions are listed in the Immunohistochemical analyses - antibody sources and dilutions.

Immunohistochemical analyses - antibody sources and dilutions. Primary antibody: rat anti-CK8 (Develop-mental Studies Hybridoma Bank, University of Iowa, IA, #TROMA-I, 1:10), rabbit anti-CK5 (Covance, NJ, # PRB-160P, 1:1000), mouse anti-SYP (BD Biosciences, San Jose, CA, #611880, 1:200), rabbit anti-cleaved Caspase-3 (Cell Signaling, Danvers, MA, #9661, 1:200), rabbit anti-GFP (NOVUS biological, Littleton, CO, #NB600-303, 1:1000), rabbit anti-β-galactosidase (abcam, Cambridge, MA, #ab616-1, 1:200). Secondary antibody: biotinylated goat anti-mouse (Vector Laboratories, Burlingame, CA, # BA-9200, 1:200), biotinylated goat anti-rabbit (Vector Laboratories, #BA-1000, 1:200), biotinylated goat anti-rat (Vector Laboratories, # BA-9400, 1:200), donkey Alexa-Fluor 594-conjugated anti-mouse (Invitrogen, Carlsbad, CA, #A21203, 1:200), donkey Alexa-Fluor 488-conjugated anti-rabbit (Invitrogen, #A21206, 1:200), donkey Alexa-Fluor 594-conjugated anti-rabbit (Invitrogen, #404239, 1:200), donkey Alexa-Fluor 488-conjugated anti-mouse (Invitrogen, #A21202, 1:200).

Morphometric quantitative analyses. Five digital images of serial sections scanned by ScanScope with 40X objective were captured for each slide and transferred to Image J for manual counting of all epithelial cells (at least 1,000 cells) and SYP positive cells among them. The sizes of prostate lobes were determined by measuring the distance from the edge of each lobe to the urethra. The size of each prostatic duct was determined by measuring its diameter.

Western blot analyses. PCN1, PCN2, and PCN3 cell lysates were prepared using RIPA buffer (Tris-HCl 50 mM, pH 7.4; Nonidet P-40 1%; Na-deoxicholate 0.25%; NaCl 150 mM; EDTA 1 mM; PMSF 1 mM; Aprotinin, leupeptin, pepstatin: 1 µg/mL each; Na_3VO_4 1 mM; NaF 1 mM), separated by 12% SDS-PAGE and transferred to PVDF membrane (Millipore). The membrane was incubated overnight at 4°C with antibodies to detect SYP (Dako, CA, #A0010, 1:100), followed by incubation for 1 hour at room temperature with horseradish peroxidase-conjugated secondary antibodies (Santa Cruz Biotechnology, CA, #sc-2301, 1:2000) and developed using chemiluminescent substrate (Thermo scientific, Rockford, IL, #34077).

*Statistical analyses. S*tatistical analyses were performed with InStat 3.10 and Prism 5.01 software. (GraphPad, Inc., San Diego, CA). Two-tailed unpaired *t*-test was used in all calculations.

3.4 Results

3.4.1 Genomic structure of *Syp* locus and BAC engineering for the generation of *SypELDTA* constructs

To identify the region containing all transcriptional *cis*-elements sufficient for accurate SYP expression *in vivo*, we have analyzed the genomic *Syp* locus by using the UCSC Genome Browser. The *Syp* locus is located on mouse chromosome X and contains 7 exons and 6 introns. Locations of *Syp* locus and other surrounding genes are preserved among different species, such as rat and human (Figure 3.1A). Notably, *NRSE* within the first intron of *Syp* is highly conserved among closely related mammalian species (Figure 3.1B). Furthermore, comparison of the *Syp* upstream region also displays high conservation in proximal (approximate 0 to -600 bp) and distal (approximate -2000 to -3000 bp) regions relative to transcription start site (Figure 3.2). It may imply that not only *NRSE* but also the sequences of those conserved regions are involved in conferring the cell type specific expression of SYP. Therefore, for molecular engineering we have decided to use mouse BAC clone *RP23-267C15* because it encompasses the entire *Syp* locus and, thus, is likely to contain all transcriptional *cis*-elements required for recapitulation of the endogenous cell specific gene expression.

First, *loxP-EGFP-Neo cassette-Stop-loxP-DTA-bpA* sequence was constructed to replace the sequence between 3' *NRSE* and exon 7 of *Syp* locus in BAC (Figure 3.3A). As a result, the *Syp* promoter specifically drives EGFP expression to label the SYP expressing cells. Following Cre-*loxP* mediated recombination, DTA can be expressed to ablate the SYP expressing cells. Second, the *loxP* site in the backbone of *RP23-267C15* was also replaced with *β-lactamase* sequence to avoid unintended Cre-

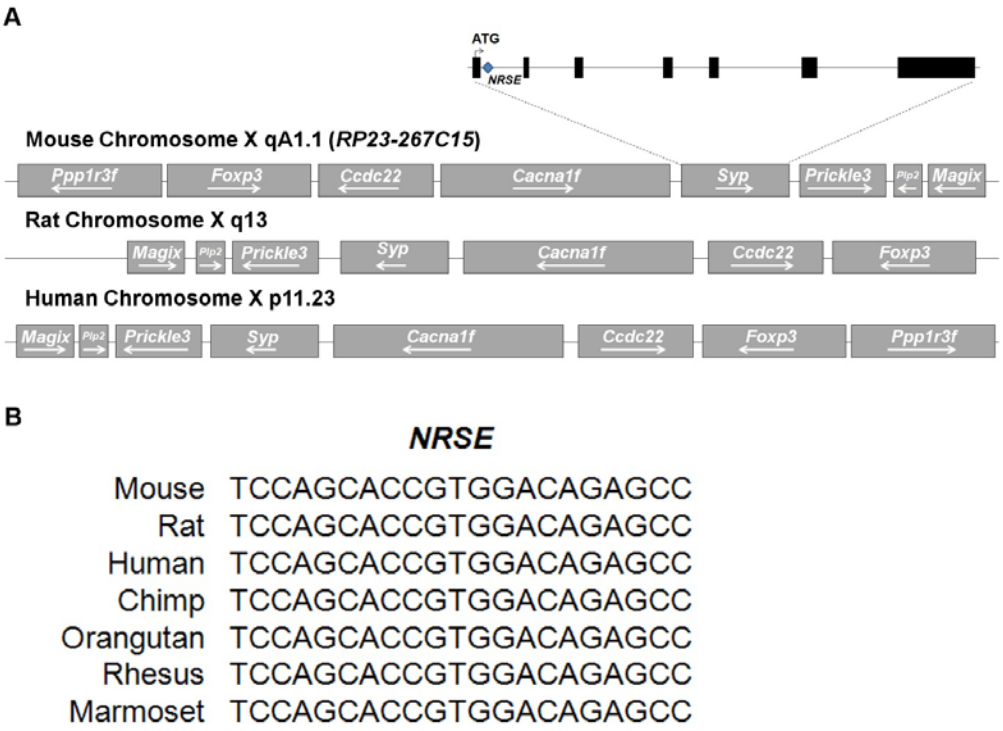

Figure 3.1 Genomic structure of the *Syp* gene. (A) Location of the *Syp* locus on mouse, rat, and human chromosome X. Mouse *Syp* contains 7 exons (black boxes). The translation initiation codon, ATG, is located in the first exon. The *NRSE* is located within the first intron of *Syp*. (B) Sequence comparison of the *NRSE* derived from *Syp* across species.

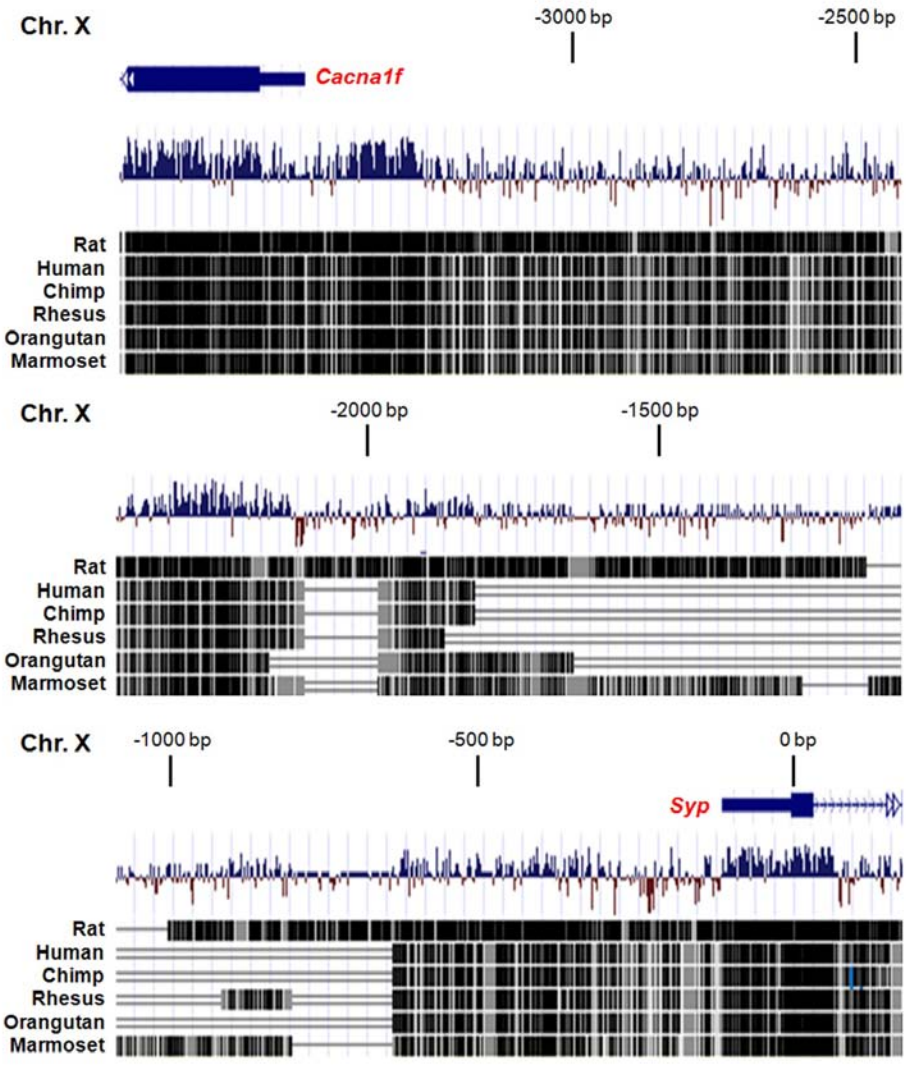

Figure 3.2 Sequence comparison of upstream region of *Syp* across species. Black lines and boxes represent highly conserved areas of the *Syp* upstream region. The position of upstream sequence is relative to the *Syp* transcription start site (0 bp). The assembly dates of the upstream regions are July 2007 (*Mus musculus*), November 2004 (*Rattus norvegicus*), February 2009 (*Homo sapiens*), October 2010 (*Pan troglodytes*), January 2006 (*Macaca mulatta*), July 2007 (*Pongo pygmaeus abelii*), and March 2009 (*Callithrix jacchus*).

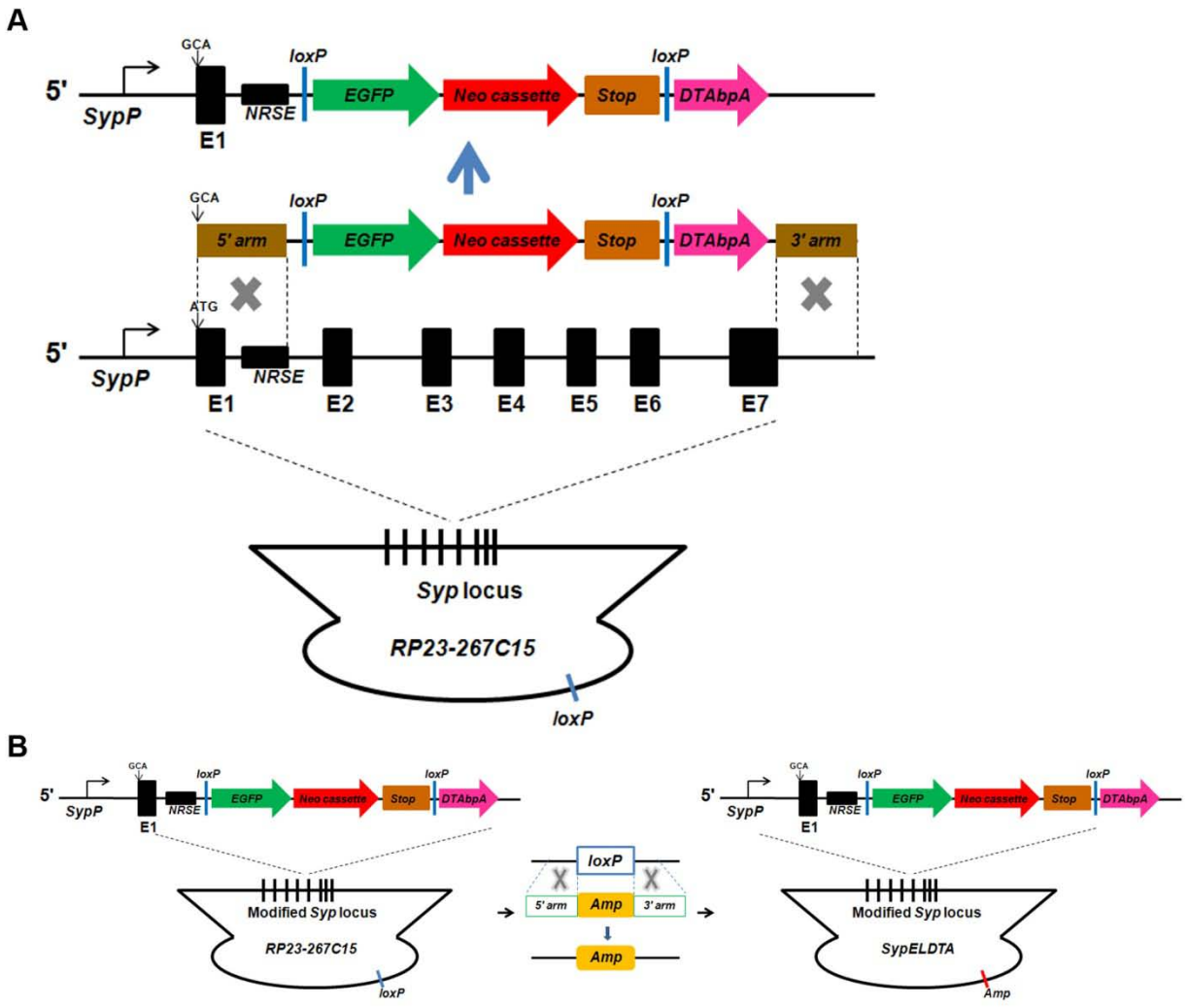

Figure 3.3 Generation of the BAC targeting construct. (A) The targeting strategy was to replace exon region of the *Syp* locus with *loxP-EGFP-Neo cassette-Stop-loxP-DTA-bpA* by homologous recombination. Exon 1 and intron 1 have been preserved because of the *NRSE* sequence, which is essential for silencing activity in non-neuronal cells. Start codon ATG in exon 1 was mutated to alanine codon GCA. *SypP*: *synaptophysin* promoter. *NRSE*: neuro-restrictive suppressor element. (B) The backbone of *RP23-267C15* (*pBACe3.6* vector) contains a *loxP* site which has been replaced with *β-lactamase* sequence by homologous recombination. The modified BAC construct was named *SypELDTA.*

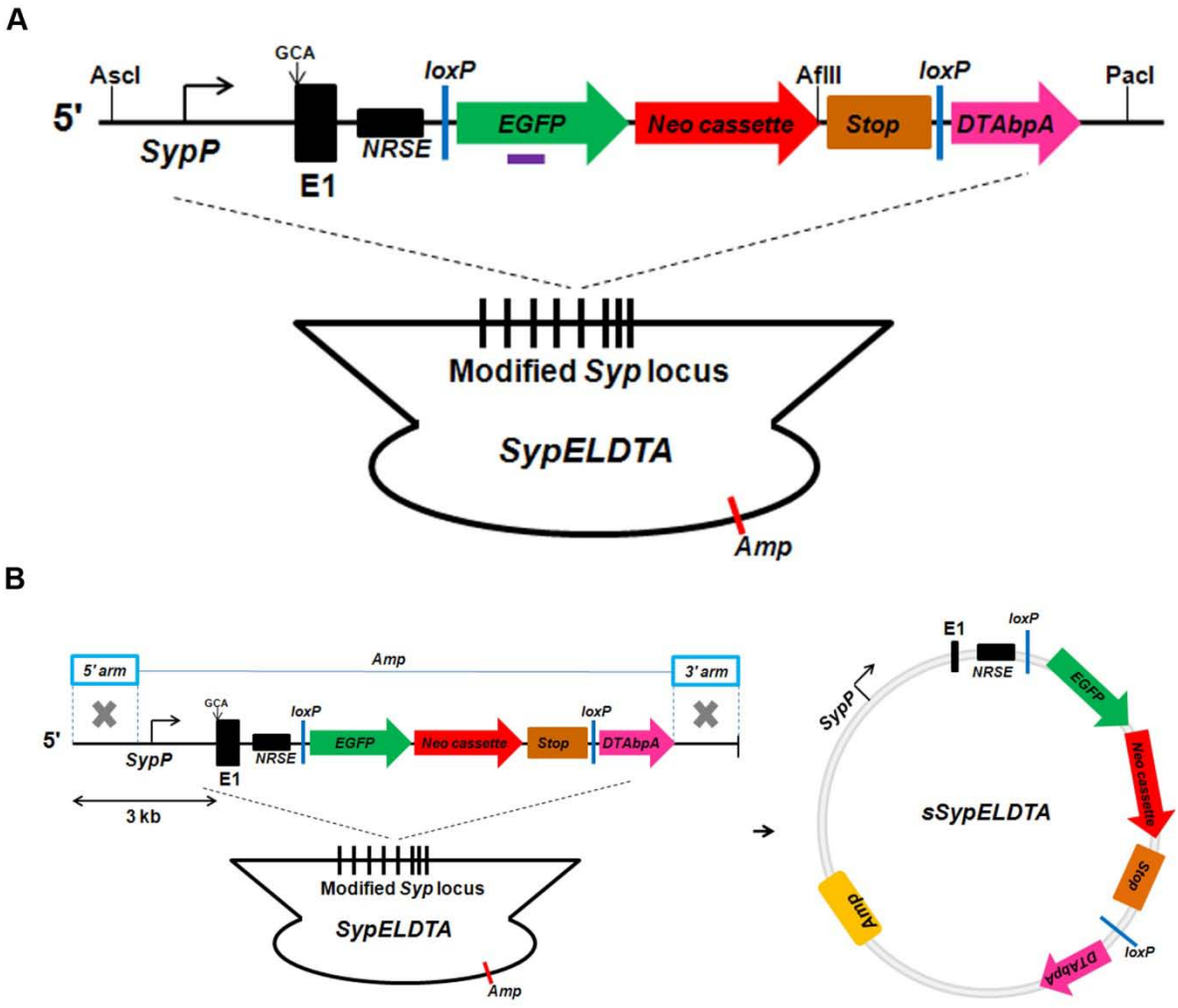

Figure 3.4 BAC transgenic constructs. (A) *SypELDTA* construct. The purple bar represents the *EGFP* probe. Restriction enzyme sites for Southern blot are indicated. (B) *sSypELDTA* construct. The fragment *SypP-loxP-EGFP-Neo cassette-Stop-loxP-DTA-bpA* from *SypELDTA* was cloned into *pGEM-T* vector. 3 kb upstream fragment of *Syp* was used to drive downstream gene expression.

mediated recombination due to multiple *loxP* sites (Figure 3.3B). The modified BAC construct is named *SypELDTA* (173 kb) (Figure 3.4A). It contains 121 kb and 36 kb upstream and downstream DNA sequences flanking the *Syp* gene, respectively. To evaluate applicability of shorter upstream sequence of *Syp* for cell type specific expression, the sequence *SypP-loxP-EGFP-Neo cassette-Stop-loxP-DTA-bpA* from *SypELDTA* was retrieved into *pGEM-T* vector. The retrieving BAC construct is named *sSypELDTA* (12 kb; Figure 3.4B). It contains a 3 kb upstream fragment of the *Syp* promoter region.

3.4.2 BAC transgene function in mammalian and bacterial cell culture

Functionality of BAC construct was tested in cultured prostate cells and bacteria. *sSypELDTA* was transfected into the mouse *p53* and *Rb* deficient prostate adenocarcinoma cell lines PCN1 and PCN3, which were established from prostate carcinomas of *PB-Cre4; p53*$^{loxP/loxP}$*Rb*$^{loxP/loxP}$ mice (Zhou et al., 2006). Consistent with our observation that PCN3 cells but not PCN1 cells express SYP (Figure 3.5A), EGFP positive cells have been observed only in PCN3 cells (Figures 3.5B-G) after transfection of *sSypELDTA*. Thus, 3 kb upstream fragment of *Syp* promoter region was sufficient to drive the transgene expression specifically in NE cells.

To test for Cre-*loxP* mediated recombination, *sSypELDTA* was electroporated into the *Escherichia coli* (*E. coli*) EL350 system, which contains a tightly controlled arabinose-inducible *Cre* gene. As shown by PCR, successful Cre-*loxP* mediated recombination of *sSypELDTA* in bacterial system was observed after arabinose

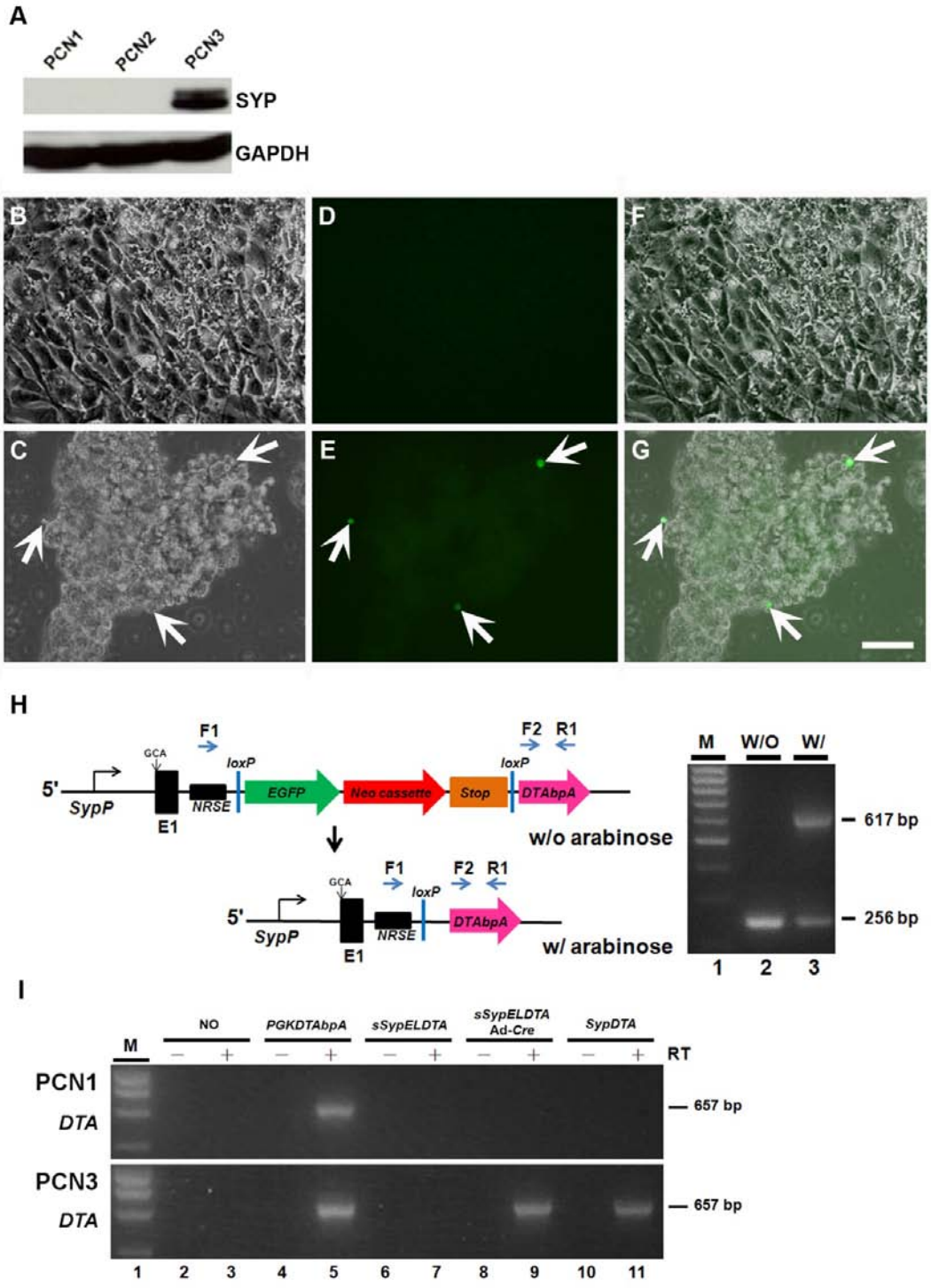
A
PCN1
PCN2
PCN3
SYP
GAPDH
B
D
F
C
E
G
H
F1
F2
R1
GCA
loxP
5'
SypP
E1
NRSE
EGFP
Neo cassette
Stop
DTAbpA
w/o arabinose
w/ arabinose
M
W/O
W/
617 bp
256 bp
1
2
3
I
NO
PGKDTAbpA
sSypELDTA
sSypELDTA
Ad-Cre
SypDTA
RT
PCN1
DTA
PCN3
DTA
657 bp
657 bp
1
2
3
4
5
6
7
8
9
10
11

Figure 3.5 Functional testing of *sSypELDTA* in cultured prostate NE cells and *E. coli.* (A) SYP expression in PCN1-PCN3 cells by western blotting. GAPDH, internal control. (B-G) Detection of EGFP expression by BAC transgene in prostate cancer cell line with NE differentiation (PCN3, C, E, G, arrows), but not in line without NE differentiation (PCN1, B, D, F). (B, C) Light microscopy, (D, E) green fluorescence, (F, G) merged images. Calibration bar: 200 μm (B-G). (H) Detection of Cre-*loxP* mediated recombination in *sSypELDTA* transgenic construct in the bacterial system EL350. EL350 bacteria, which contain endogenous arabinose-inducible *Cre*, were transformed with *sSypELDTA* transgenic construct and induced with arabinose. PCR genotyping was performed with F1/F2/R1 primers without (lane 2) and with (lane 3) arabinose induction. 256 bp and 617 bp fragments are diagnostic for internal control (primer F2/R1) and Cre-mediated recombination (primer F1/R1), respectively. Lane 1: marker (M). (I) Detection of DTA expression by *sSypELDTA* transgenic construct in the prostate cancer cell lines by RT-PCR. Lane 1: marker (M); Lane 2 (without RT) and Lane 3 (with RT): no transfection; Lane 4 (without RT) and Lane 5 (with RT): *PGKDTAbpA* transfection; Lane 6 (without RT) and Lane 7 (with RT): *sSypELDTA* transfection; Lane 8 (without RT) and Lane 9 (with RT): *sSypELDTA* transfection followed by Ad-*Cre* infection; Lane 10 (without RT) and Lane 11 (with RT): *SypDTA* transfection. 657 bp fragment is diagnostic for DTA mRNA; RT, reverse transcriptase.

induction (Figure 3.5H). The construct resulting from Cre-*loxP* mediated recombination was named *SypDTA*. To confirm that DTA expression driven by *Syp* promoter could be detected after Cre-*loxP* mediated recombination in mouse cells, reverse transcriptase PCR (RT-PCR) was performed with different constructs transfected into PCN1 and PCN3 after Adenovirus-*Cre* (Ad-*Cre*) infection. DTA expression could be detected in *SypDTA*-infected PCN3 cells and *sSypELDTA*-infected PCN3 cells followed by Ad-*Cre* infection. Conversely, no DTA expression could be detected in PCN1 cells. Thus, DTA was expressed specifically in NE cells after Cre-*loxP* mediated recombination (Figure 3.5I).

3.4.3 BAC transgene expression in *SypELDTA* transgenic mice

To test transgene expression *in vivo*, *sSypELDTA* and *SypELDTA* DNA were used to generate transgenic lines 141-143 and 144-148, respectively (Table 3.1). Based on Southern blotting and quantitative PCR (qPCR), all mice of lines 144-148 carried a single copy of transgene, while copy number of *sSypELDTA* transgene was variable among lines 141-143 (Figure 3.6, Table 3.1).

To confirm the specificity of transgene expression in transgenic mice, co-localization of transgene-derived EGFP and endogenous SYP has been determined by double immunofluorescence staining in prostate NE cells (Figure 3.7A). *sSypELDTA* transgenic mice had expression of transgene in non-NE epithelium cells of the prostate (Figure 3.8, Table 3.1). In contrast, no EGFP expression was detected in SYP negative cells (Figure 3.9, Table 3.2) of *SypELDTA* mice. Among 5 tested transgenic lines, the

Table 3.1 Characterization of Transgenic Lines 141-148

Transgene	Line	Male germ line transmission	Copy number	Transgene expression in prostate NE cells (%)*	Transgene expression in prostate non-NE cells
sSypELDTA	141	Yes	11	72	Yes
	142	Yes	2	81	Yes
	143	Yes	ND#	ND	Yes
SypELDTA	144	No	1	ND	ND
	145	Yes	1	88	No
	146	No	ND	ND	ND
	147	Yes	1	90	No
	148	Yes	1	83	No

*Percentage of EGFP; SYP double positive cells within total number of SYP positive cells was determined by double immunofluorescence staining.
#Not done

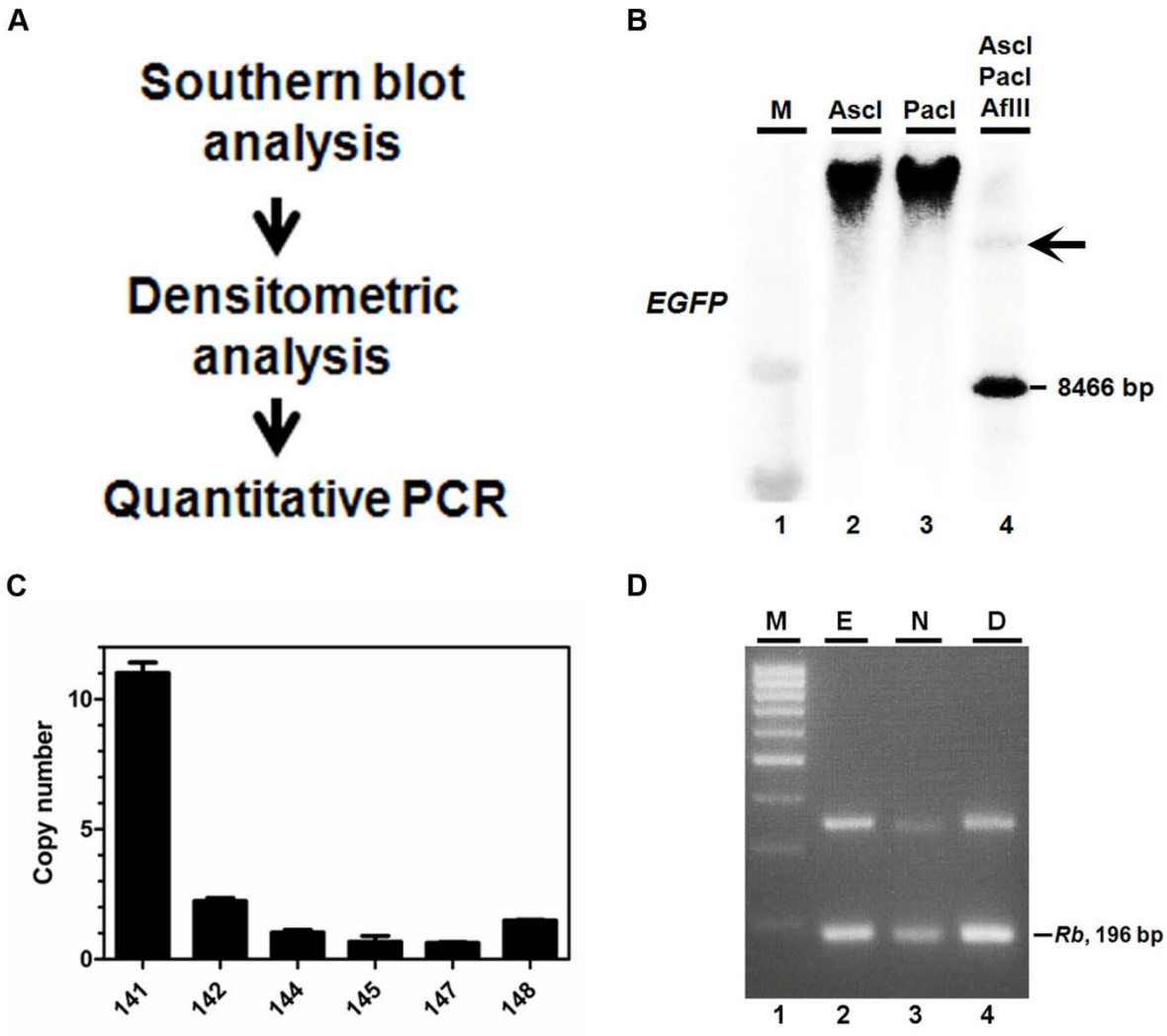

Figure 3.6 The transgene copy number in mice of *sSypELDTA* lines 141-143 and *SypELDTA* lines 144-148. (A) Experimental design. (B) Southern blot analysis of transgenic line 141. Genomic DNA digested with restriction enzymes AscI (Lane 2), PacI (Lane 3), and AscI, PacI and AflII (Lane 4). Lane 1: DNA marker (M). AflII but not AscI and PacI restriction sites are present within the transgene. 8,466 bp band in lane 4 is diagnostic for multiple transgene copies integrated into a single genomic site, whereas top band (arrow) is diagnostic for single copy of transgene. *EGFP*, DNA probe. (C) Quantification of transgene copy number in transgenic lines by quantitative PCR. Transgenic line 141 carrying 11 copies of transgene was used as a reference to estimate copy number of other lines. (D) Genotyping analysis of transgenic line 147. The upper bands are diagnostic for *EGFP* (lane 2, E, 346 bp), *Neomycin* (lane 3, N, 342 bp), and *DTA* (lane 4, D, 348 bp) fragments of transgene. 196 bp band in lanes 2-4 is internal control (endogenous *Rb*). Lane 1: DNA marker (M).

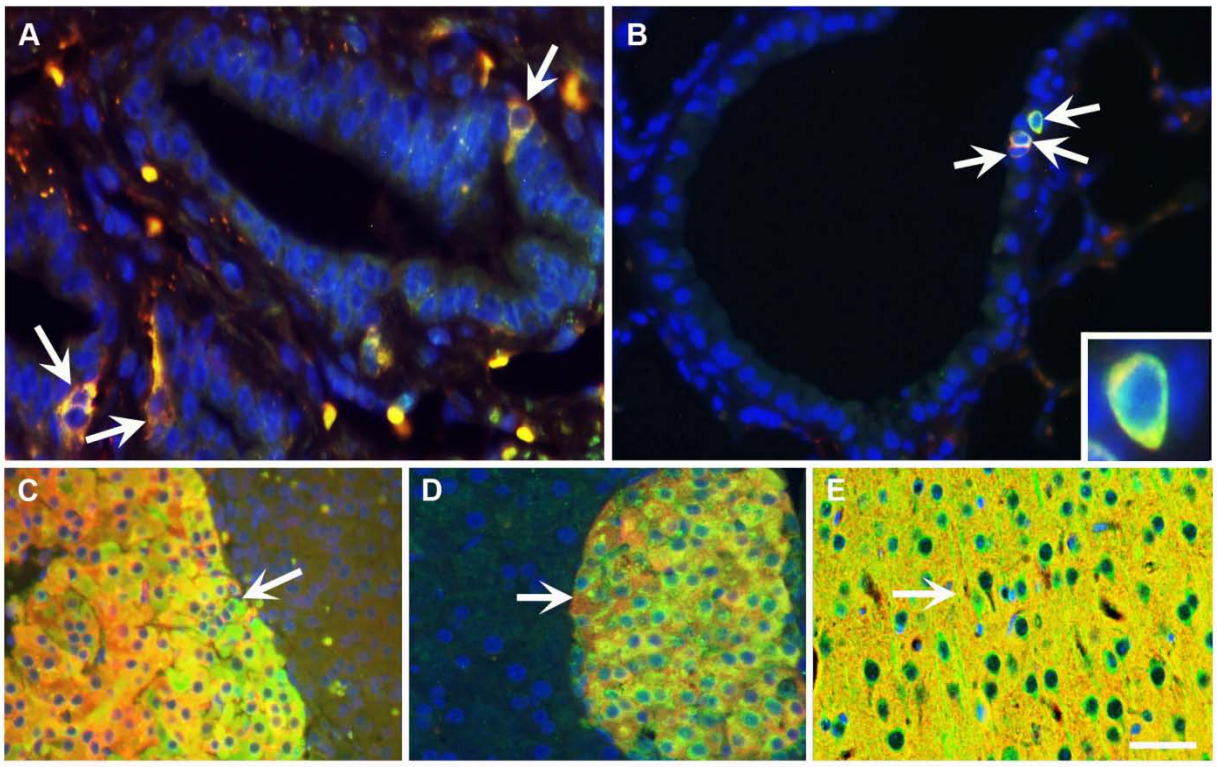

Figure 3.7 *SypELDTA* transgene expression is highly specific for SYP expressing cells. (A-E) Co-expression of EGFP (green) and SYP (red) in prostate NE cells (A), lung NE cells (B; inset: high magnification), medulla of adrenal gland (C), pancreatic islets of Langerhans (D), and brain (E) of *SypELDTA* transgenic mice. Yellow color (arrows) indicates co-localization of EGFP and SYP fluorescent signals. Counterstaining with DAPI, blue. Calibration bar: 18 µm (A), 37 µm (B), 50 µm (C-E), 8 µm (inset).

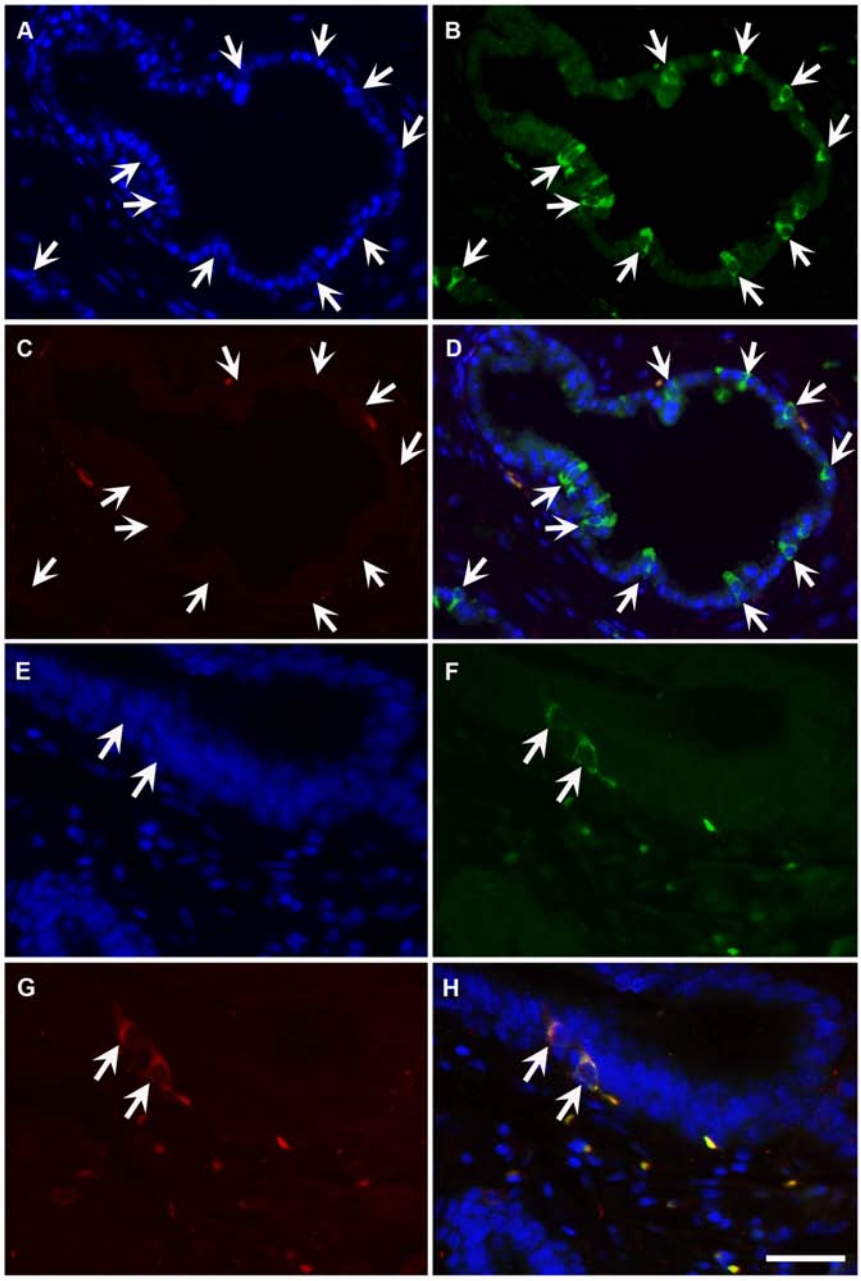

Figure 3.8 Transgene expression in *sSypELDTA* lines 141-143. (A-H) Detection of EGFP (B, D, F, H, green) and SYP (C, D, G, H, red) expression (arrows) in non-NE (A-D) and NE cells (E-H) of the prostate epithelium. Yellow color in overlay (D, H) indicates co-localization of EGFP and SYP fluorescent signals. Counterstaining with DAPI (A, D, E, H, blue). Calibration bar: 50 µm (A-D), 18 µm (E-H).

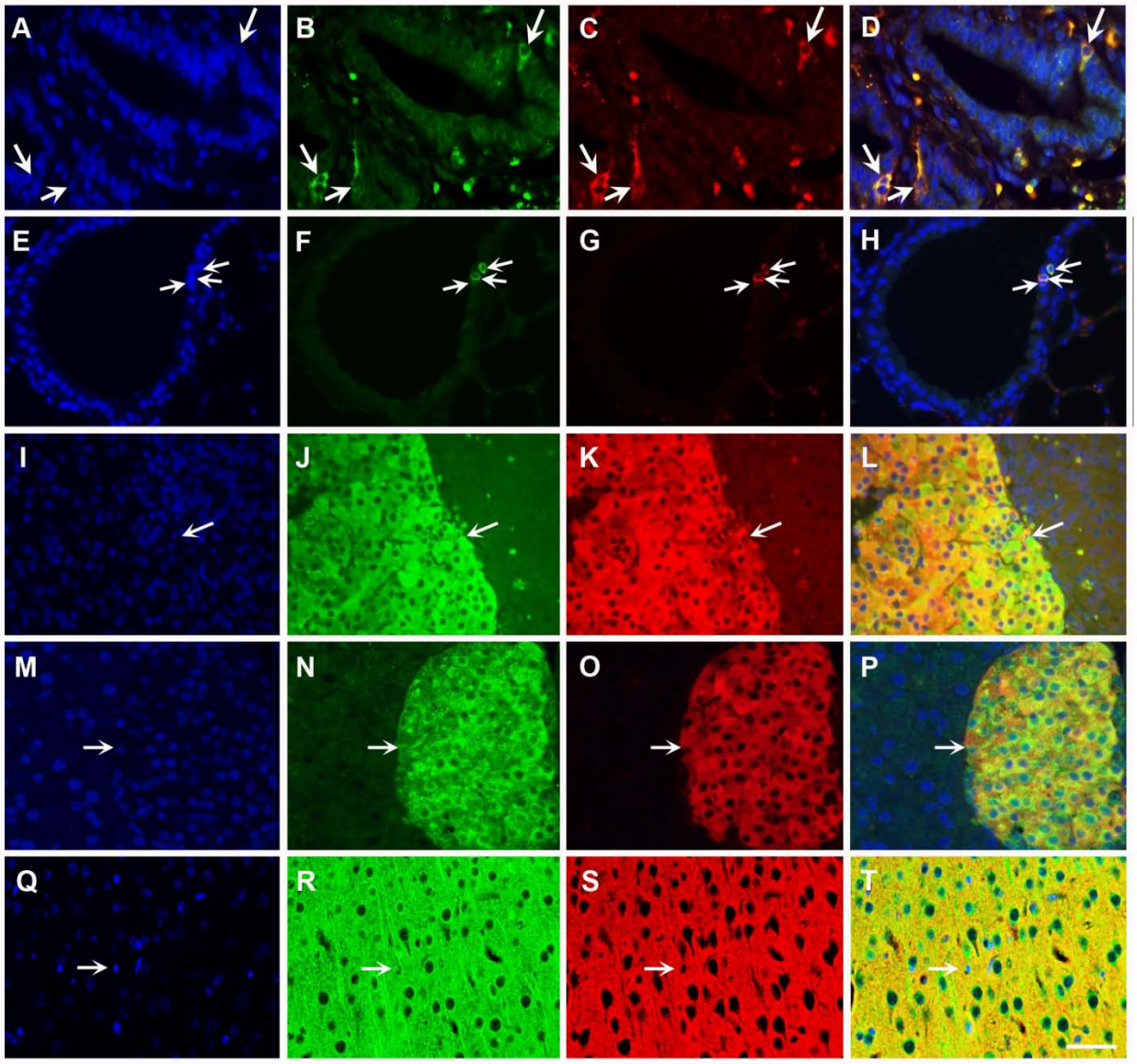

Figure 3.9 *SypELDTA* transgene expression has high specificity in SYP expressing cells. (A-T) Detection of EGFP (B, D, F, H, J, L, N, P, R, T, green) and SYP (C, D, G, H, K, L, O, P, S, T, red) expression (arrows) in prostate NE cells (A-D), lung NE cells (E-H), medulla of adrenal gland (I-L), islets of Langerhans in pancreas (M-P), and brain (Q-T) of *SypELDTA* line 147 transgenic mice. Yellow color in overlay (D, H, L, P, T) indicates co-localization of EGFP and SYP fluorescent signals. Counterstaining with DAPI (A, D, E, H, I, L, M, P, Q, T, blue). Calibration bar: 25 μm (A-D), 50 μm (E-T).

Table 3.2 Transgene Expression in *SypELDTA* Line 147

Tissue	Transgene expression in SYP expressing cells (%)*	Transgene expression in non-SYP expressing cells
Brain	100	0
Lung	92	0
Medulla of adrenal gland	98	0
Islets of Langerhans	100	0

*Percentage of EGFP; SYP double positive cells within total number of SYP positive cells was determined by double immunofluorescence staining.

line 147 had the highest frequency (90%) of SYP positive NE cells co-expressing EGFP (Table 3.1). Furthermore, co-expression of EGFP and SYP in line 147 has also been observed in the lung NE cells (Figure 3.7B), medulla of adrenal gland (Figure 3.7C), islets of Langerhans in pancreas (Figure 3.7D), and brain (Figure 3.7E).

3.4.4 DTA expression in *EIIA-Cre; SypELDTA* embryo

To confirm that DTA expression driven by *Syp* promoter is able to ablate SYP positive cell lineage, DTA expression was examined by crossing the male *SypELDTA* mice of line 147 with female *EIIA-Cre* transgenic mice, following collection of embryos on gestational day (GD) 10.5 (Figure 3.10A). Adenoviral *EIIA* promoter targets expression of Cre recombinase to the early mouse embryo and Cre-mediated recombination occurs in a wide range of tissues, thereby allowing assessing effects of transgene expression in multiple organs and tissues (Lakso et al., 1996). *EIIA-Cre; SypELDTA* embryos had rare SYP positive cells in the brain and dorsal root ganglia (Figures 3.10B, D, F). Consistent with induction of apoptosis pathway by DTA (Chang et al., 1989a; Chang et al., 1989b), a significant number of cleaved Caspase-3 positive cells were detected in the same structures (Figures 3.10C, E, G). The brain and dorsal root ganglia of *EIIA-Cre* littermates had abundant SYP positive cells (Figures 3.10H, J, L), but almost no cleaved Caspase-3 positive cells (Figures 3.10I, K, M). Thus, our construct was effective in conditional ablation of SYP expressing cells by DTA *in vivo*.

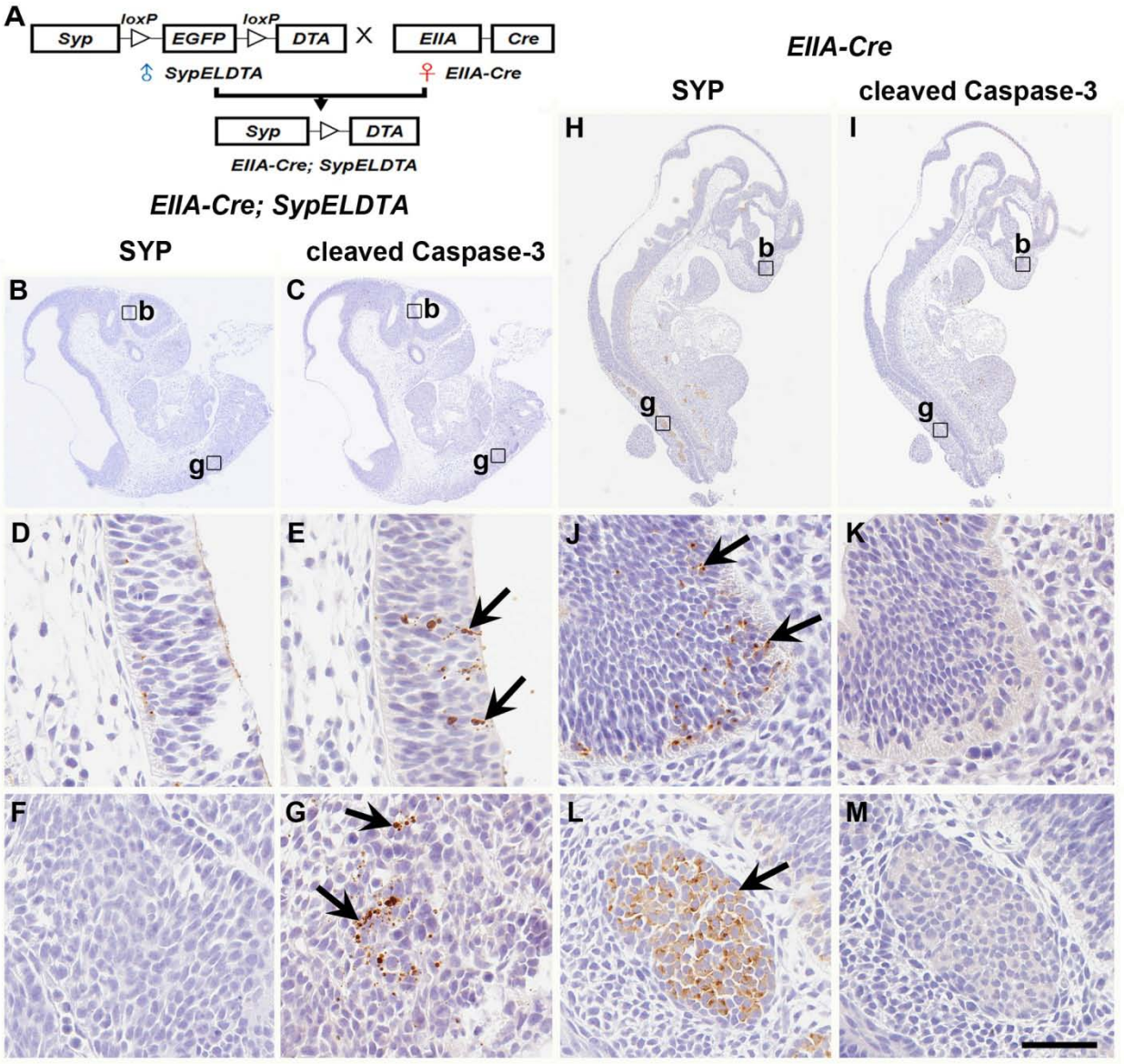

Figure 3.10 *EIIA-Cre; SypELDTA* embyros exhibit massive cell death in SYP positive cells. (A) Design of crosses between male *SypELDTA* and female *EIIA-Cre* transgenic mice. (B-M) SYP (B, D, F, H, J, L) and cleaved Caspase-3 (C, E, G, I, K, M) expression (arrows) in serial sections of *EIIA-Cre; SypELDTA* (B-G) and *EIIA-Cre* (H-M) embryos collected on gestational day 10.5. High (D-G, J-M) magnification images of brain (D, E, J, K) and dorsal root ganglion (F, G ,L, M) regions shown as rectangles in low magnification images (B, C, H, I). b, brain, g, dorsal root ganglia. ABC Elite method. Hematoxylin counterstaining. Calibration bar: 950 μm (B, C, H, I), 50 μm (D-G, J-M).

3.4.5 Effect of prostate epithelium-specific NE cell ablation

Modified *probasin* promoter drives expression of Cre recombinase in the prostate epithelium of postnatal mouse prostate of *PB-Cre4* transgenic mice (Chen et al., 2005; Wu et al., 2001). By using *PB-Cre4* mice we have previously determined that deletion of tumor suppressor genes *p53* and *Rb* results in prostate carcinomas with NE differentiation (Zhou et al., 2006; Zhou et al., 2007). We have also reported that expansion of NE cells is observed in prostate adenocarcinomas in *PB-Cre4; Pten*$^{loxP/loxP}$ mice, particularly after castration (Liao et al., 2007). To verify that Cre recombinase under the control of *probasin* promoter is expressed in NE cells, which are concentrated in the prostate proximal region (Figure 3.11), Cre-mediated recombination in prostate NE cells was examined by crossing *PB-Cre4* transgenic mice (Wu et al., 2001) with R26R reporter mice (Soriano, 1999). The expression of β-galactosidase is possible only after Cre-mediated deletion of a stop codon flanked by *loxP* sites. Double immunofluorescence staining showed co-localized expression of β-galactosidase and SYP in the proximal region of prostatic ducts of *PB-Cre4; R26R* mice. Thus, Cre-*loxP* mediated recombination occurs in NE cell lineage after Cre expression directed by *probasin* promoter (Figure 3.12).

To evaluate whether prostate epithelium-specific NE cell ablation impacts prostate development and function, male *PB-Cre4* transgenic mice have been crossed with female *SypELDTA* (lines 147 and 148) mice to get *PB-Cre4; SypELDTA* male offspring (Figure 3.13A). Both lines shown similar phenotypes and line 147 has been characterized to the fullest extent. As compared to wild-type (FVB/N) and *SypELDTA*

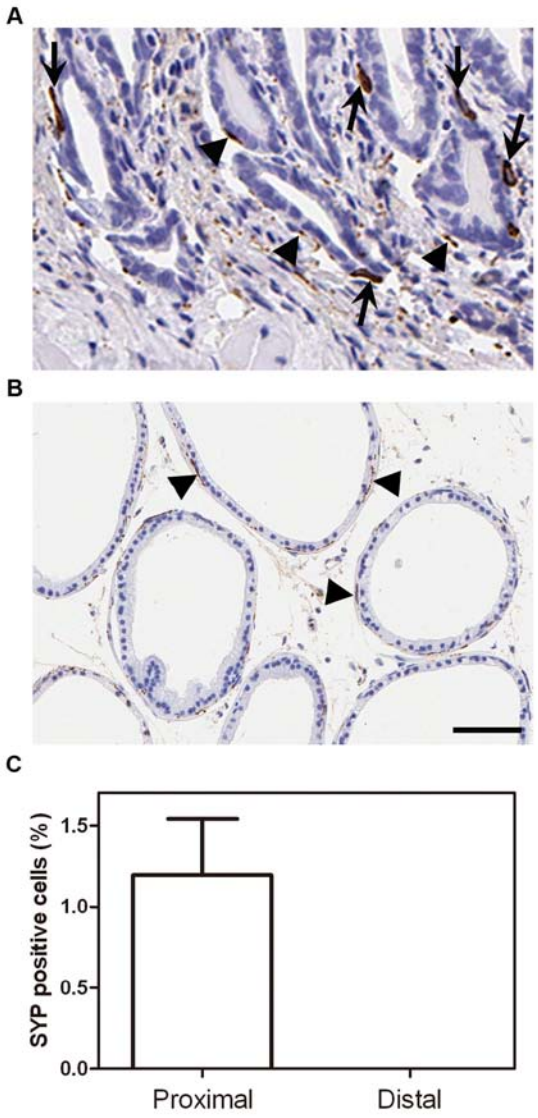

Figure 3.11 NE cells are mostly located in the proximal region of prostatic ducts. (A, B) SYP expression in NE cells in proximal (A) and distal (B) regions of prostatic ducts of the prostate (n=6). NE cells and nerve terminals are indicated by arrows and arrowheads, respectively. Calibration bar: 50 μm (A), 100 μm (B). (C) Quantification of SYP positive NE cells. Distal regions of prostatic ducts contain no NE cells. Error bar denotes SD.

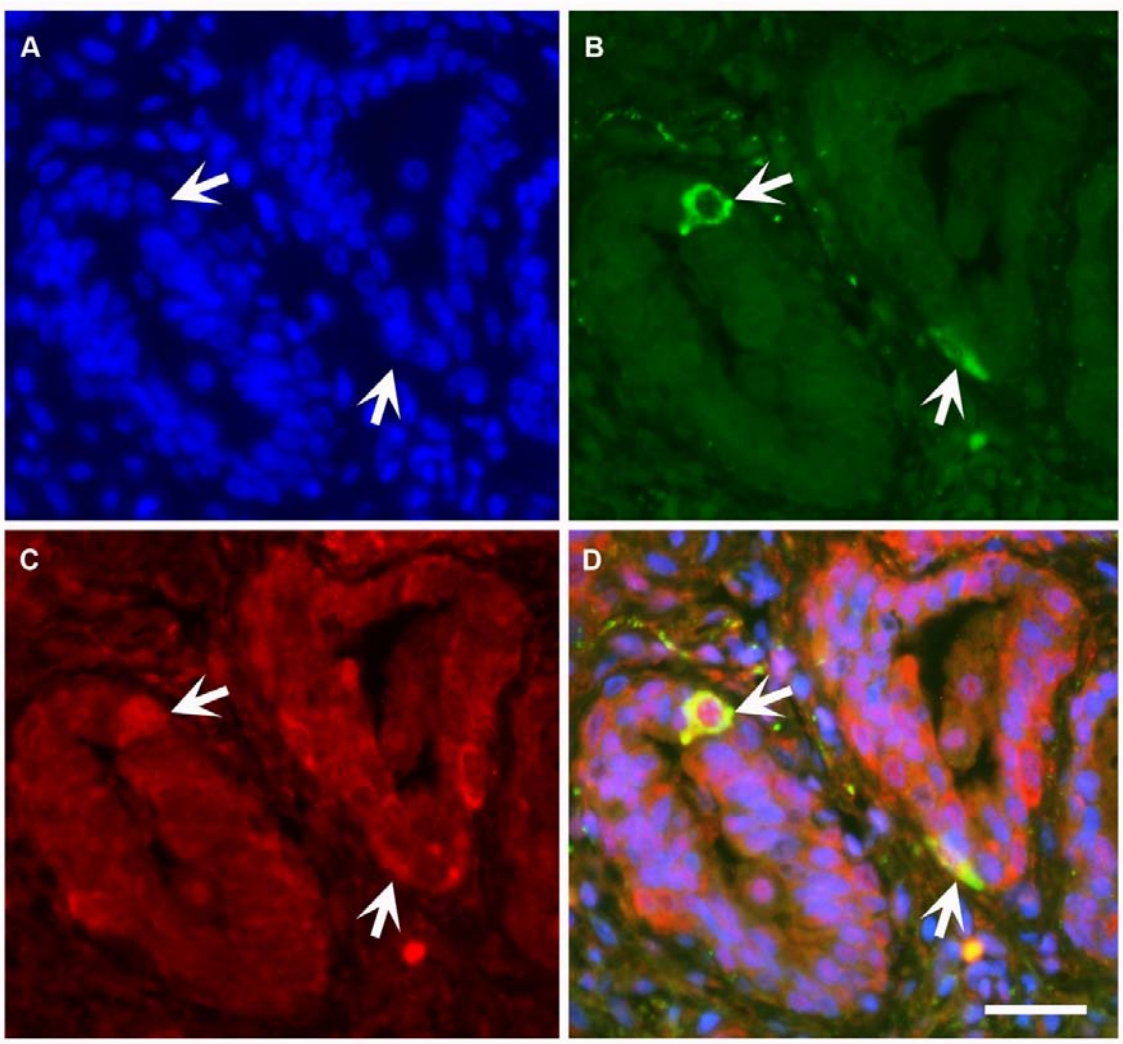

Figure 3.12 Cre recombinase under the control of *probasin* promoter is expressed in prostate NE cells. (A-D) Detection of SYP (B, D, green) and β-galactosidase (C, D, red, indicative of Cre-*loxP* mediated recombination) expression (arrows) in the prostate NE cells in *PB-Cre4; R26R* mice harboring *Probasin-Cre* and *lacZ* reporter gene. Yellow color in overlay (D) indicates co-localization of SYP and β-galactosidase fluorescent signals. Counterstaining with DAPI (A, D, blue). Calibration bar: 50 μm (A-D).

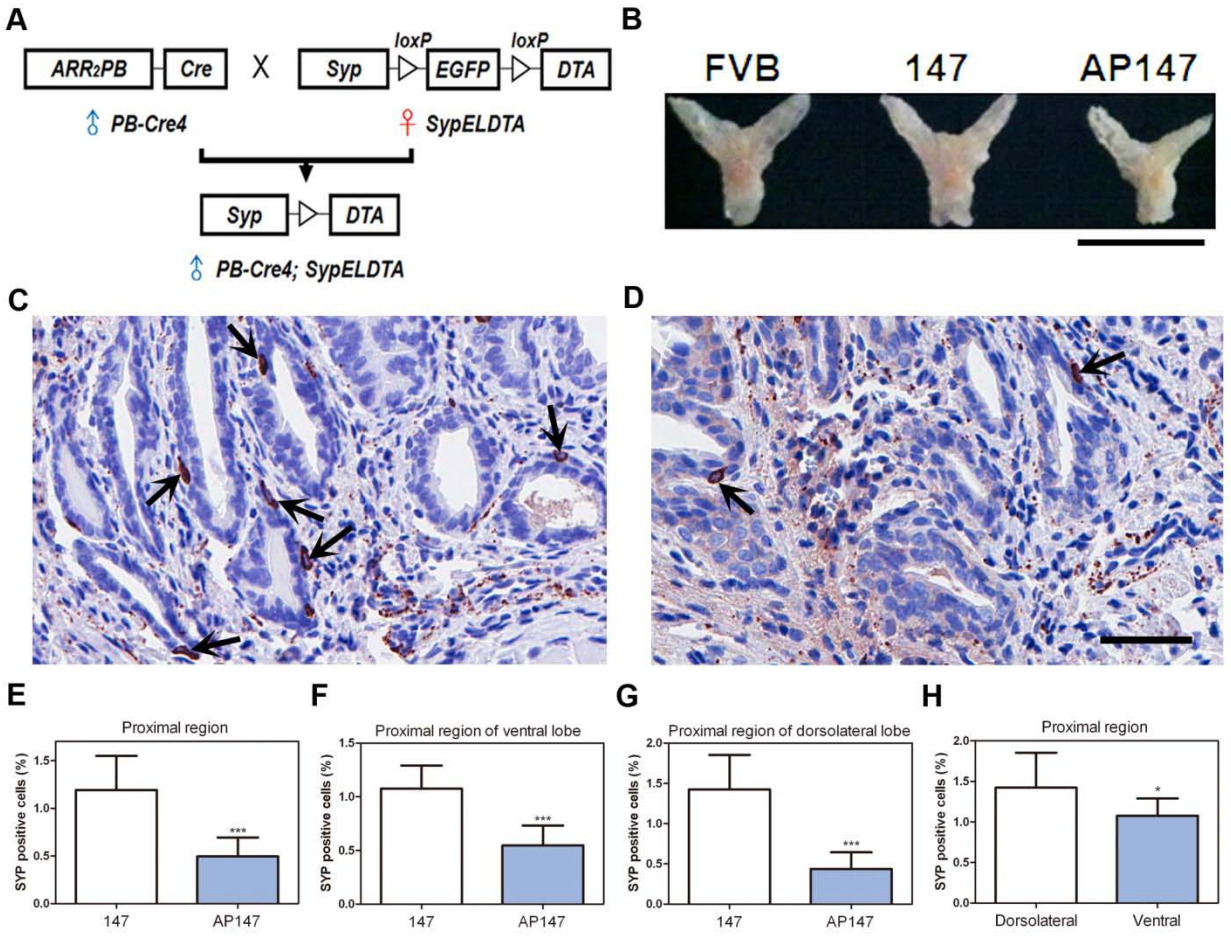

Figure 3.13 *PB-Cre4; SypELDTA* line 147 mice show decreased number of NE cells and prostate hypotrophy. (A) Design of crosses between male *PB-Cre4* and female *SypELDTA* transgenic mice resulting in male *PB-Cre4; SypELDTA* offspring with prostate epithelium-specific NE cell ablation. (B) Gross images of the prostate from wild-type FVB/N (FVB), *SypELDTA* (147), *PB-Cre4; SypELDTA* (AP147) mice. Calibration bar: 0.5 cm. (C, D) Detection of SYP positive NE cells (arrows) in the prostate proximal region of age-matched *SypELDTA* (C; n=4) and *PB-Cre4; SypELDTA* (D; n=4) mice. ABC Elite method. Hematoxylin counterstaining. Calibration bar: 50 µm. (E-G) Quantification of NE cells in the proximal regions of whole prostate (E), and in the proximal regions of ventral (F) and dorsolateral (G) lobes of prostates from age-matched *SypELDTA* (147; n=4) and *PB-Cre4; SypELDTA* (AP147; n=4) mice. (H) Quantification of NE cells in proximal regions of dorsolateral and ventral lobes of the prostates from *SypELDTA* mice (n=4). *P<0.05. ***P<0.001. All error bars denote SD.

(147) age-matched controls and littermates, the size of prostate of *PB-Cre4; SypELDTA* (AP147) was smaller (Figures 3.13B and 3.14). In agreement with earlier reports of broad *PB-Cre4* transgene expression in the prostate epithelium (Wu et al., 2001), loss of floxed *EGFP* was reproducibly observed in all prostate lobes according to microdissection-PCR genotyping of AP147 (Figure 3.15). However, only the NE cell population was diminished by 60% in AP147 mice as compared to controls according to immunostaining for SYP in the proximal regions of prostatic ducts (147 vs. AP147: 1.19±0.34% vs. 0.5±0.19%, P<0.0001; Figures 3.13C-E). The decrease was observed consistently in various areas of the proximal region, such as ventral (1.07±0.22% vs. 0.55±0.18%, P<0.0001; Figure 3.13F) and dorsolateral (1.42±0.39% vs. 0.44±0.19%, P<0.0001; Figure 3.13G) lobes. In addition, the average diameter of prostatic ducts in distal regions was decreased, especially in the dorsolateral lobe (Figure 3.16). Interestingly, more NE cells were observed (1.42±0.39% vs. 1.07±0.22%, P=0.0252; Figure 3.13H) and higher percentage of NE cells was ablated (70% vs. 49%; Figures 3.13F, G) in the proximal regions of prostatic ducts of dorsolateral lobes, as compared to those of ventral lobes, which could be associated with the smaller diameter of prostatic ducts in dorsolateral lobes.

Except for the size of lumens, there were no significant changes in overall morphology of prostatic ducts in the ventral and dorsolateral lobes of AP147 mice, or in either the proximal or distal regions of prostatic ducts (Figure 3.16). NE cell ablation did not result in any detectable changes to the extent of luminal (CK8) and basal (CK5) differentiation in the proximal and distal regions of ducts (Figure 3.17). No significant cell death was observed in luminal and basal cells in any of the regions (Figure 3.18),

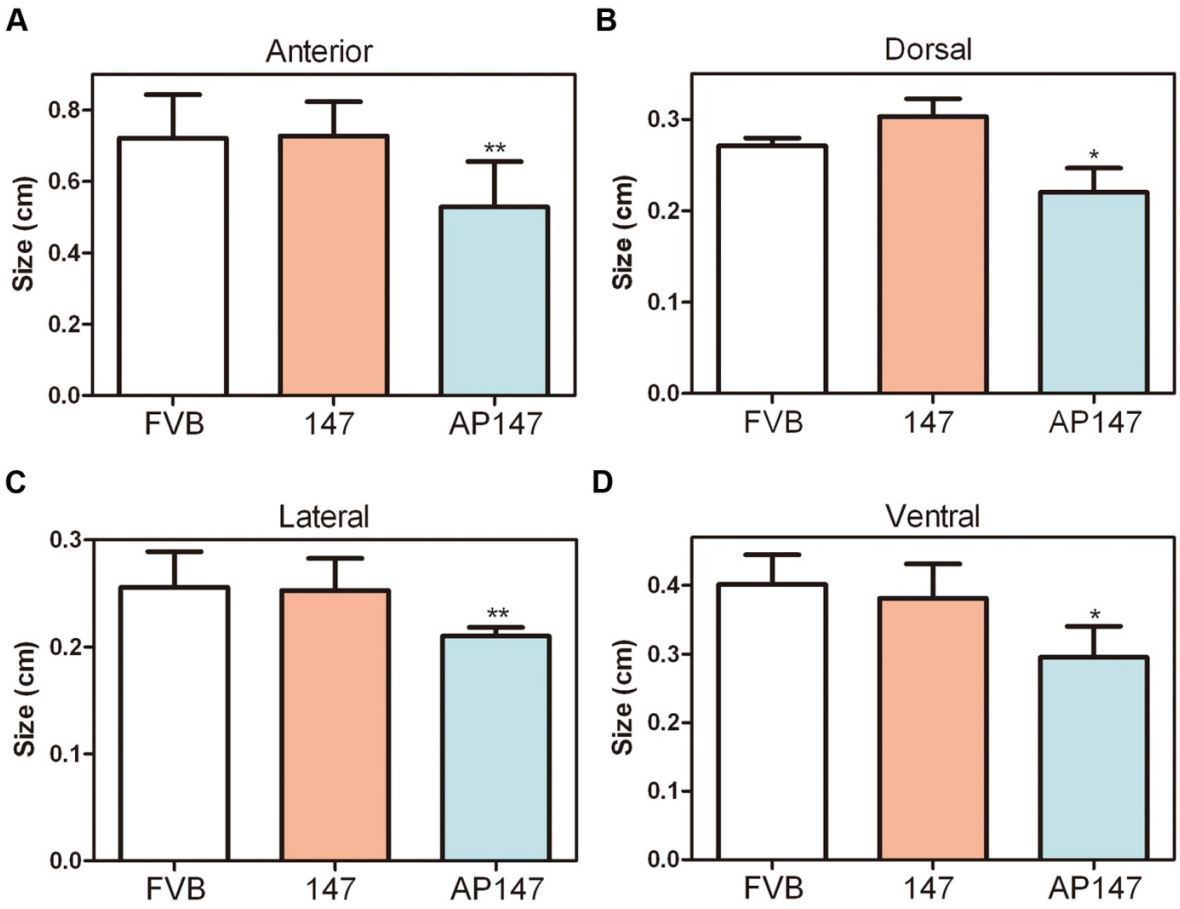

Figure 3.14 Reduced sizes of prostate lobes in *PB-Cre4; SypELDTA* mice. (A-D) Quantification of size of anterior (A), dorsal(B), lateral (C), and ventral (D) lobes among age-matched FVB/N (FVB, n=4), *SypELDTA* (147; n=4), and *PB-Cre4; SypELDTA* (AP147; n=4) mice. *P<0.05. **P<0.01. Error bar denotes SD.

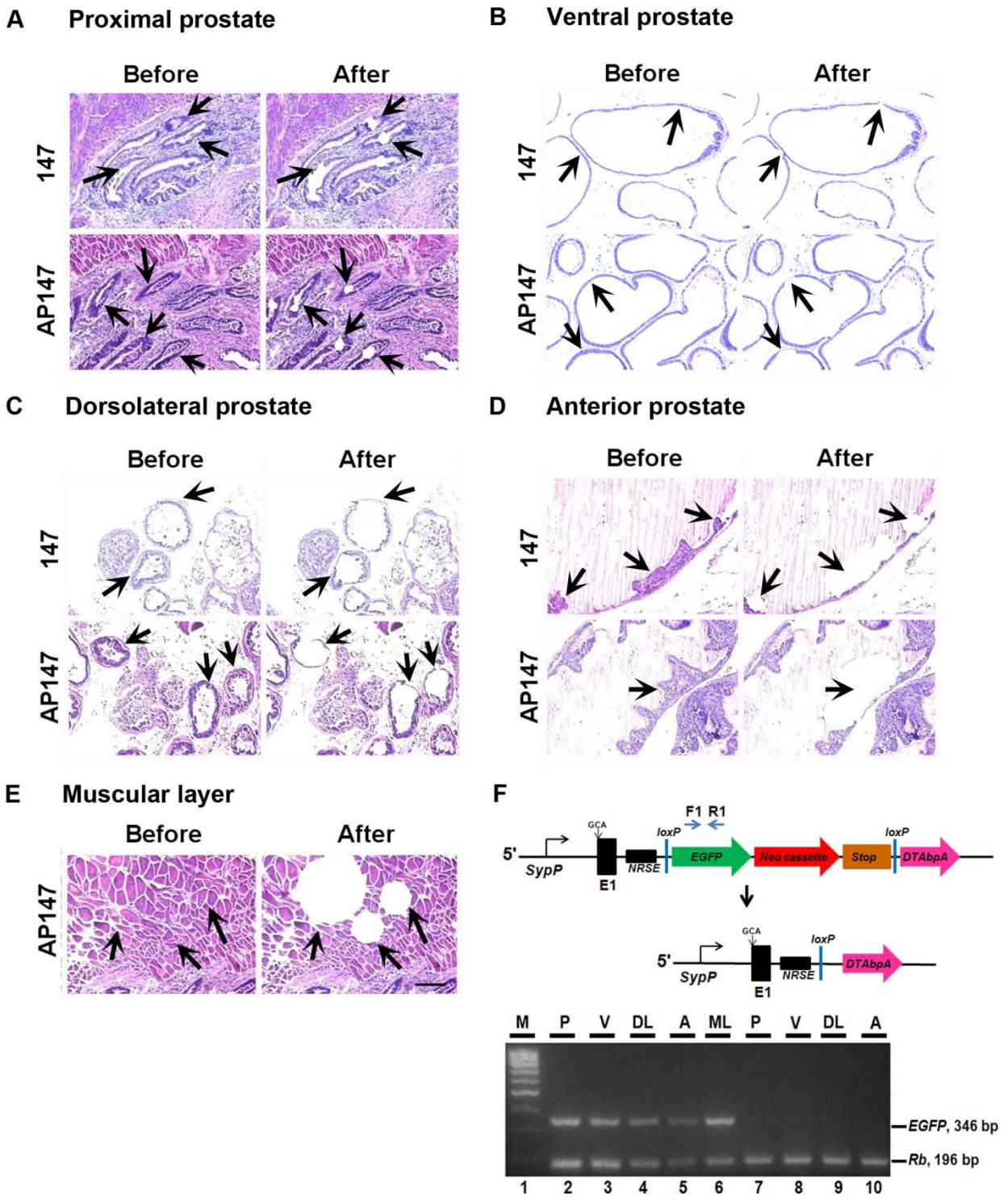
A
Proximal prostate
Before
After
147
AP147
B
Ventral prostate
Before
After
147
AP147
C
Dorsolateral prostate
Before
After
147
AP147
D
Anterior prostate
Before
After
147
AP147
E
Muscular layer
Before
After
AP147
F
F1 R1
GCA
loxP
loxP
5'
SypP
E1
NRSE
EGFP
Neo cassette
Stop
DTAbpA
GCA
loxP
5'
SypP
E1
NRSE
DTAbpA
M P V DL A ML P V DL A
EGFP, 346 bp
Rb, 196 bp
1 2 3 4 5 6 7 8 9 10

Figure 3.15 *PB-Cre* drives Cre-*loxP* recombination in the prostate of *PB-Cre4; SypELDTA* mice. (A-F) Microdissection-PCR. Proximal (A) and distal (ventral, B, dorsolateral, C, and anterior, D) regions of prostatic ducts and the muscular layer of the prostate (E) of age-matched *SypELDTA* (147) and *PB-Cre4; SypELDTA* (AP147) mice before and after microdissection. Hematoxylin and eosin. Calibration bar: 50 µm (A-E). (F) PCR design and detection of Cre-*loxP* mediated recombination in microdissected proximal region (P, lane 2 and 7), and ventral (V, lane 3 and 8), dorsolateral (DL, lane 4 and 9), anterior (A, lane 5 and 10) distal regions, and muscular layer (ML, lane 6) of prostates from *SypELDTA*(lanes 2-5) and *PB-Cre4; SypELDTA* (lanes 6-10) mice. 346 bp fragment is generated with primers F1and R1and is diagnostic for *EGFP* (present before Cre-loxP mediated recombination). 196 bp fragment (endogenous *Rb*) is internal control. Lane 1: marker (M).

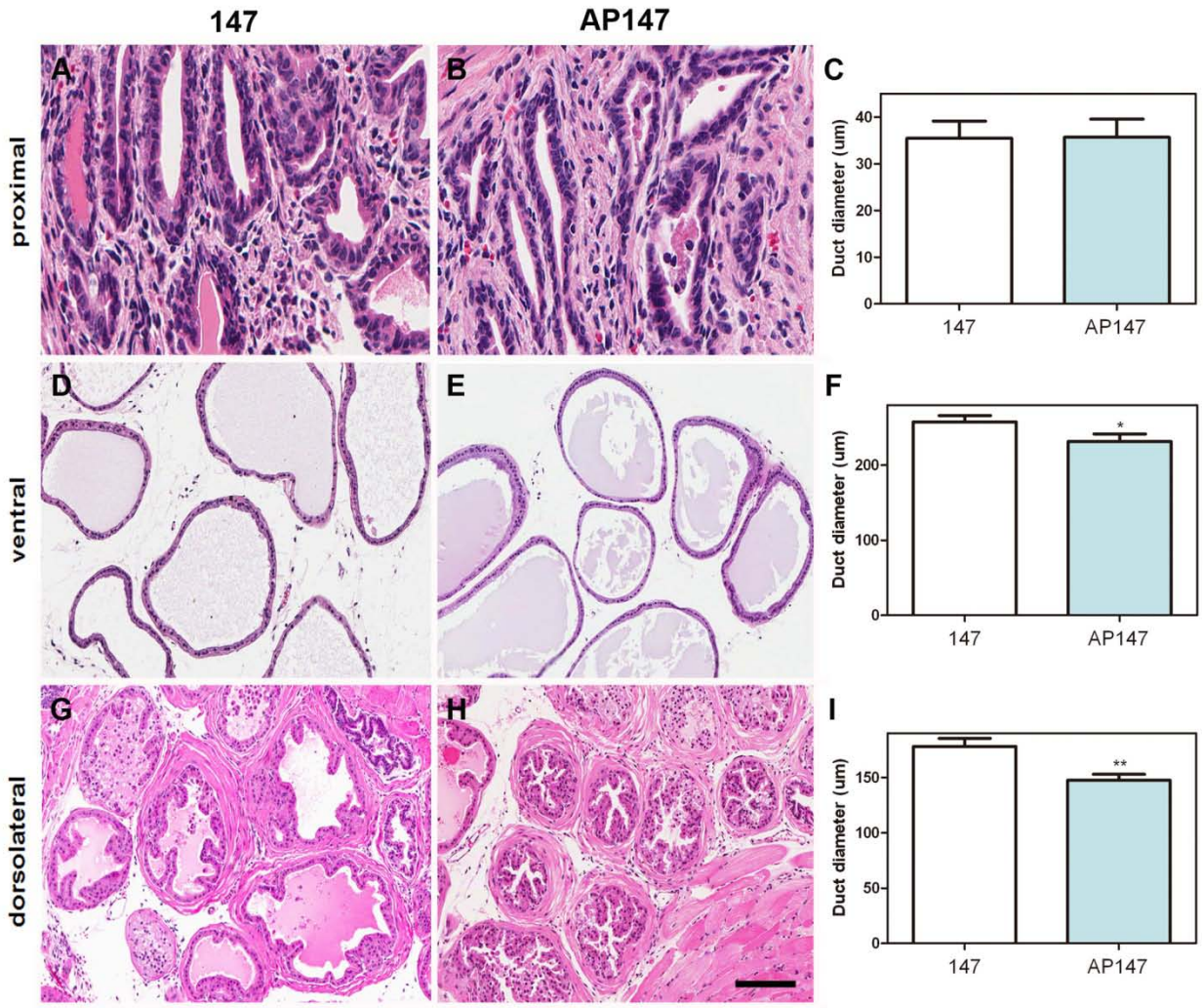

Figure 3.16 NE cell ablation results in proportional reduction of prostatic duct diameters in distal regions. (A-I) Histology (A, B, D, E, G, H) and quantification of diameters (C, F, I) of proximal (A, B, C) and distal (ventral, D, E, F, and dorsolateral, G, H, I) regions of prostatic ducts of age-matched *SypELDTA* (147; n=6; A, D, G) and *PB-Cre4; SypELDTA* (AP147, n=6; B, E, H) mice. Hematoxylin and eosin. Calibration bar: 50 μm (A, B), 100 μm (D, E, G, H). *P<0.05. **P<0.01. All error bars denote SD.

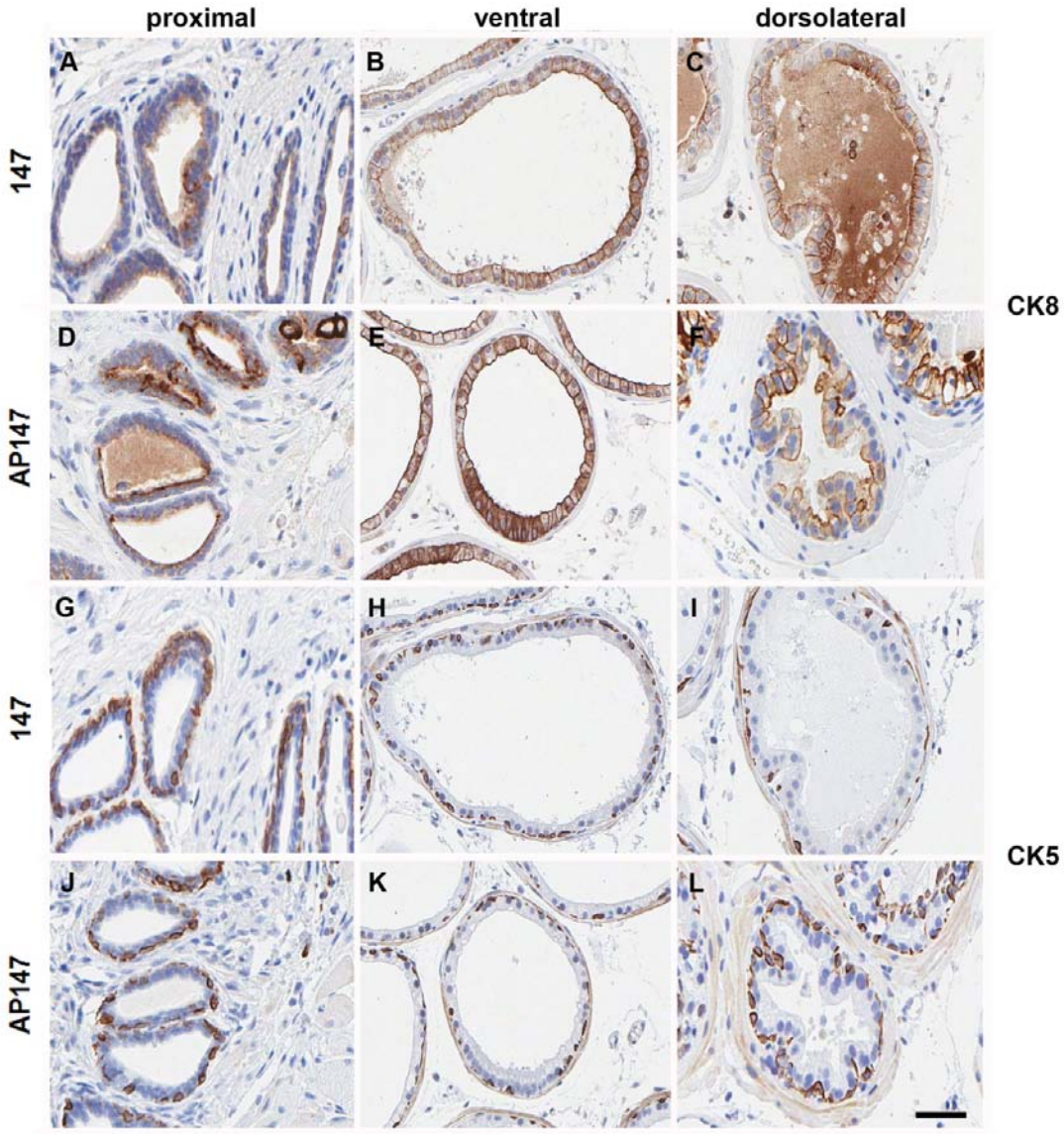

Figure 3.17 NE cell ablation does not affect luminal (CK8+) or basal (CK5+) cell differentiation. (A-L) Detection of CK8 (A-F) and CK5 (G-L) expression (brown) in epithelial cells of proximal (A, D, G, J) and distal (ventral, B, E, H, K, and dorsolateral, C, F, I, L) regions of prostatic ducts in age-matched *SypELDTA* (147, A-C, G-I) and *PB-Cre4; SypELDTA* (AP147, D-F, J-L) mice. ABC Elite method. Hematoxylin counterstaining. Calibration bar: 50 μm (A-L).

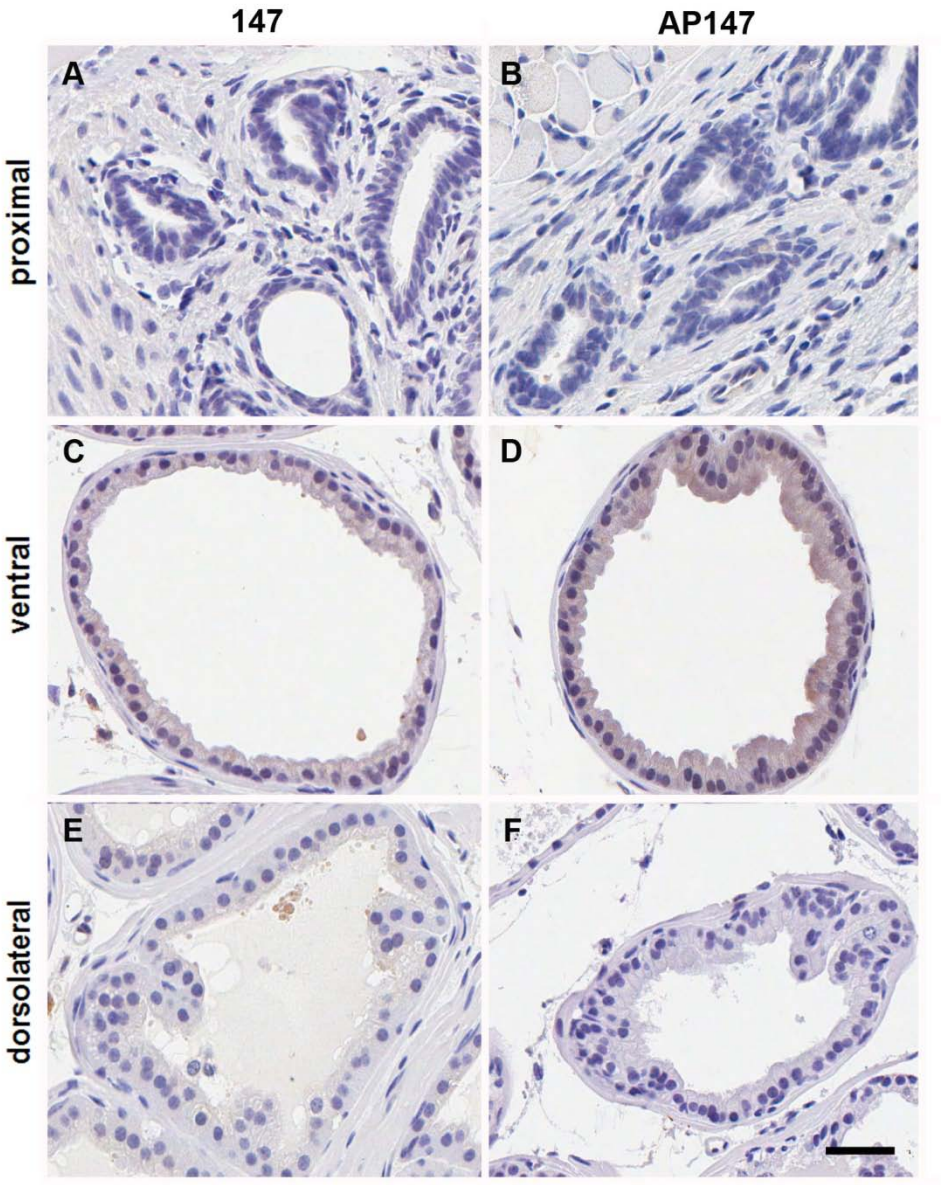

Figure 3.18 No significant cell death is observed in prostate epithelium non-NE cells in *PB-Cre4; SypELDTA* mice. (A-F) cleaved Caspase-3 expression in proximal (A, B), and distal (ventral, C, D, and dorsolateral, E, F) regions of prostatic ducts in age-matched *SypELDTA* (147, A, C, E) and *PB-Cre4; SypELDTA* (AP147, B, D, F) mice. The staining of embryonic dorsal root ganglia (Figure 5) served as a positive control for cleaved Caspase-3 immunostaining. ABC Elite method. Hematoxylin counterstaining. Calibration bar: 50 μm (A-F).

which implies a tight regulation of *Syp* promoter in prostate non-NE epithelium cells. Taken together, these results support the notion that NE cells play an important role in prostate development.

3.5 Discussion

Previous report indicated that 2.6 kb but not 1.2 kb upstream fragment of *Syp* was sufficient to confer cell type specific expression (Bargou and Leube, 1991). Consistent with this observation, we have found high evolutionary conservation not only in the proximal (0 to -600 bp) but also distal (-2000 to -3000 bp) regions of the *Syp* gene. Based on this information, we have designed transgenic constructs preserving *NRSE* in the first intron of *Syp* gene and containing either 3 kb or 121 kb upstream regulatory sequence. While 3 kb sequence was sufficient for NE specific expression of transgene in cultured cells, it did not assure specificity of gene expression in the transgenic mice. At the same time, a longer promoter has been highly specific for NE cells. These results suggest that other *cis*-elements, farther than 3 kb upstream fragment, provide the cell type specific expression in the context of the whole organism. It is also possible that the 36 kb 3' flanking region of *Syp* might play a role in regulating cell specificity as well, similarly to other genes, such as human *tyrosine hydroxylase* (Wong et al., 1995). Also, longer upstream and downstream regions of *Syp* locus may better insulate the *Syp* promoter from position effects by other genes at the site of transgene integration (Yang and Gong, 2005). However, given NE cell specific expression of 3 kb construct after its multi-copy integration in cell culture, the latter possibility is less likely. Identification of

environment driven mechanisms responsible for accurate gene expression should allow much better understanding of *Syp* regulation.

It should be noted that in addition to NE cells, SYP is also expressed in neurons of the nervous system (Gould et al., 1987; Wiedenmann et al., 1986). Unlike other REST regulated genes, such as *BDNF* and *GluR2* genes, *Syp* is similarly regulated in neuronal and NE cells (Hohl and Thiel, 2005). Consistently, we have observed broad expression of *Syp* driven EGFP and DTA in mouse neurons of the brain and spinal ganglia. Thus, our model can be used for targeted ablation of NE and/or neuronal cells depending on a particular *Cre* driving promoter.

Some neuropeptides, such as calcitonin gene-related peptide (CGRP) and gastrin-releasing peptide (GRP) are expressed only in subsets of NE cells (di Sant'Agnese et al., 1989; Sunday et al., 1988; Weichselbaum et al., 2005). Therefore, theoretically it is possible that some NE cells do not express SYP. Although we were unable to find any literature supporting this possibility, our *SypELDTA* mice should allow detection of such cells by using double immunofluorescence for various NE markers before and after *Syp*-driven ablation in future.

As a proof of the utility of our model, we performed prostate epithelium-specific ablation of NE cells. The mouse prostate is composed of a series of branching ducts, each containing distal, intermediate and proximal regions relative to the urethra (Sugimura et al., 1986). Each duct contains three differentiated cell types: luminal, basal and NE cells, with stem cells preferentially concentrated in the proximal region (Leong et al., 2008; Salm et al., 2005; Tsujimura et al., 2002; Wang et al., 2007)**.** NE cells secrete a large number of neuropeptides which can be mitogenic and growth-promoting.

Receptors for some of the NE products have been found to be expressed in benign prostate and/or prostate cancer. It has been proposed that the NE cells may regulate the growth, differentiation and secretory activity of the prostatic epithelium, possibly through a paracrine mechanism (Abrahamsson, 1999). However, studies directly addressing role of NE cells in prostate development have been lacking.

Based on co-detection of SYP and EGFP double immunofluorescence, as well as lack of Cre-mediated recombination and cell death in prostate non-NE epithelium cells of *PB-Cre4; SypELDTA* mice, expression of *SypELDTA* has been highly specific to SYP positive prostate NE cells. Consistent with the important role of NE cells in prostate biology, prostates with decreased number of NE cells were hypotrophic, with decreased sizes of prostate lobes and reduced average diameters of prostatic ducts. Notably, the most pronounced effect of NE ablation on prostate hypotrophy was in the dorsolateral prostate, where NE cells were ablated to the greatest extent. Our study also indicates that NE cells are located in the proximal regions of the prostatic ducts, the area of preferential stem cell location. Future in-depths studies should address the kinetics of NE cell ablation effects and explore if the effect of NE cells on prostate size can be explained by their proximity to prostate stem cells.

It should be noted that in spite of 90% gene expression specificity in prostate NE cells of *SypELDTA* line 147 mice, we observed only 60% decrease in number of prostate NE cells in *PB-Cre4; SypELDTA* mice. Consistent with previous study describing compartmentalization of gene expression between prostate lobes (Abbott et al., 2003), our results support a possibility that efficiency of Cre-mediated homologous recombination is different in NE cells of a particular region. We also cannot exclude that

there are intrinsic differences in regulation of gene expression in individual NE cells, which may lead to the reduction of DTA expression in some of them. Thus, further improvements in design of constructs for highly efficient NE cell ablation may yield even more dramatic effect on prostate hypotrophy.

NE cell differentiation is positively correlated with prostate cancer progression, castrate-resistance and poor prognosis (Debes and Tindall, 2004; Sun et al., 2009). Previous reports have indicated that NE cells can stimulate cell proliferation, invasion, and apoptosis resistance of cultured prostate cancer cells (Sun et al., 2009). However, specific mechanisms involved in the pathogenesis of NE differentiation are not well known. Crossing *PB-Cre4; SypELDTA* transgenic mice with *Pten* knockout mice (Liao et al., 2007; Wang et al., 2003) or other established mouse prostate cancer models with preferential NE differentiation, such as TRAMP or LADY (Kaplan-Lefko et al., 2003; Masumori et al., 2001), should decisively determine the role of NE cells in prostate carcinogenesis. More generally, *SypELDTA* mice should be useful for studying other NE neoplasms, such as small cell lung carcinoma and NE tumors in the gastrointestinal tract (Linnoila, 2006; Montuenga et al., 2003; Sun et al., 2009).

Taken together, we have identified a region of *Syp* gene sufficient for faithful expression of genetic constructs. We have also successfully generated the *SypELDTA* mouse model suitable for flexible organ-specific detection and ablation of NE cells. This model system should provide an important tool for studies of NE cell functions in development and carcinogenesis in various tissues.

REFERENCES

Abbott, D.E., Pritchard, C., Clegg, N.J., Ferguson, C., Dumpit, R., Sikes, R.A., and Nelson, P.S. (2003). Expressed sequence tag profiling identifies developmental and anatomic partitioning of gene expression in the mouse prostate. Genome Biol *4*, R79.

Abrahamsson, P.A. (1999). Neuroendocrine differentiation in prostatic carcinoma. The Prostate *39*, 135-148.

Ahren, B. (2000). Autonomic regulation of islet hormone secretion--implications for health and disease. Diabetologia *43*, 393-410.

Bargou, R.C., and Leube, R.E. (1991). The synaptophysin-encoding gene in rat and man is specifically transcribed in neuroendocrine cells. Gene *99*, 197-204.

Cadieux, A., Springall, D.R., Mulderry, P.K., Rodrigo, J., Ghatei, M.A., Terenghi, G., Bloom, S.R., and Polak, J.M. (1986). Occurrence, distribution and ontogeny of CGRP immunoreactivity in the rat lower respiratory tract: effect of capsaicin treatment and surgical denervations. Neuroscience *19*, 605-627.

Chang, M.P., Baldwin, R.L., Bruce, C., and Wisnieski, B.J. (1989a). Second cytotoxic pathway of diphtheria toxin suggested by nuclease activity. Science *246*, 1165-1168.

Chang, M.P., Bramhall, J., Graves, S., Bonavida, B., and Wisnieski, B.J. (1989b). Internucleosomal DNA cleavage precedes diphtheria toxin-induced cytolysis. Evidence that cell lysis is not a simple consequence of translation inhibition. The Journal of biological chemistry *264*, 15261-15267.

Chen, Z., Trotman, L.C., Shaffer, D., Lin, H.K., Dotan, Z.A., Niki, M., Koutcher, J.A., Scher, H.I., Ludwig, T., Gerald, W.*, et al.* (2005). Crucial role of p53-dependent cellular senescence in suppression of Pten-deficient tumorigenesis. Nature *436*, 725-730.

Cheng, C.Y., and Nikitin, A.Y. (2011). Neuroendocrine cells: potential cells of origin for small cell lung carcinoma. Cell cycle *10*, 3629-3630.

de Diego, A.M., Gandia, L., and Garcia, A.G. (2008). A physiological view of the central and peripheral mechanisms that regulate the release of catecholamines at the adrenal medulla. Acta Physiol (Oxf) *192*, 287-301.

Debes, J.D., and Tindall, D.J. (2004). Mechanisms of androgen-refractory prostate cancer. The New England journal of medicine *351*, 1488-1490.

di Sant'Agnese, P.A., de Mesy Jensen, K.L., and Ackroyd, R.K. (1989). Calcitonin, katacalcin, and calcitonin gene-related peptide in the human prostate. An immunocytochemical and immunoelectron microscopic study. Arch Pathol Lab Med *113*, 790-796.

Dockray, G. (2003). Making sense of gut contents. Scand J Gastroenterol *38*, 451-455.

Douglas, S.A., Sreenivasan, D., Carman, F.H., and Bunn, S.J. (2010). Cytokine interactions with adrenal medullary chromaffin cells. Cell Mol Neurobiol *30*, 1467-1475.

Gazdar, A.F., Helman, L.J., Israel, M.A., Russell, E.K., Linnoila, R.I., Mulshine, J.L., Schuller, H.M., and Park, J.G. (1988). Expression of neuroendocrine cell markers L-dopa decarboxylase, chromogranin A, and dense core granules in human tumors of endocrine and nonendocrine origin. Cancer research *48*, 4078-4082.

Gould, V.E., Wiedenmann, B., Lee, I., Schwechheimer, K., Dockhorn-Dworniczak, B., Radosevich, J.A., Moll, R., and Franke, W.W. (1987). Synaptophysin expression in neuroendocrine neoplasms as determined by immunocytochemistry. The American journal of pathology *126*, 243-257.

Gustafsson, B.I., Kidd, M., and Modlin, I.M. (2008). Neuroendocrine tumors of the diffuse neuroendocrine system. Curr Opin Oncol *20*, 1-12.

Haimoto, H., Takahashi, Y., Koshikawa, T., Nagura, H., and Kato, K. (1985). Immunohistochemical localization of gamma-enolase in normal human tissues other than nervous and neuroendocrine tissues. Laboratory investigation; a journal of technical methods and pathology *52*, 257-263.

Hohl, M., and Thiel, G. (2005). Cell type-specific regulation of RE-1 silencing transcription factor (REST) target genes. Eur J Neurosci *22*, 2216-2230.

Ivanova, A., Signore, M., Caro, N., Greene, N.D., Copp, A.J., and Martinez-Barbera, J.P. (2005). In vivo genetic ablation by Cre-mediated expression of diphtheria toxin fragment A. Genesis *43*, 129-135.

Jensen, S.M., Gazdar, A.F., Cuttitta, F., Russell, E.K., and Linnoila, R.I. (1990). A comparison of synaptophysin, chromogranin, and L-dopa decarboxylase as markers for neuroendocrine differentiation in lung cancer cell lines. Cancer research *50*, 6068-6074.

Jin, L., Hemperly, J.J., and Lloyd, R.V. (1991). Expression of neural cell adhesion molecule in normal and neoplastic human neuroendocrine tissues. Am J Pathol *138*, 961-969.

Kaplan-Lefko, P.J., Chen, T.M., Ittmann, M.M., Barrios, R.J., Ayala, G.E., Huss, W.J., Maddison, L.A., Foster, B.A., and Greenberg, N.M. (2003). Pathobiology of autochthonous prostate cancer in a pre-clinical transgenic mouse model. Prostate *55*, 219-237.

Kaufmann, O., Georgi, T., and Dietel, M. (1997). Utility of 123C3 monoclonal antibody against CD56 (NCAM) for the diagnosis of small cell carcinomas on paraffin sections. Human pathology *28*, 1373-1378.

Koh, D.S., Cho, J.H., and Chen, L. (2012). Paracrine Interactions Within Islets of Langerhans. J Mol Neurosci.

Kuliczkowska-Plaksej, J., Milewicz, A., and Jakubowska, J. (2012). Neuroendocrine control of metabolism. Gynecol Endocrinol *28 Suppl 1*, 27-32.

Lakso, M., Pichel, J.G., Gorman, J.R., Sauer, B., Okamoto, Y., Lee, E., Alt, F.W., and Westphal, H. (1996). Efficient in vivo manipulation of mouse genomic sequences at the zygote stage. Proc Natl Acad Sci U S A *93*, 5860-5865.

Lantuejoul, S., Moro, D., Michalides, R.J., Brambilla, C., and Brambilla, E. (1998). Neural cell adhesion molecules (NCAM) and NCAM-PSA expression in neuroendocrine lung tumors. Am J Surg Pathol *22*, 1267-1276.

Leong, K.G., Wang, B.E., Johnson, L., and Gao, W.Q. (2008). Generation of a prostate from a single adult stem cell. Nature *456*, 804-808.

Liao, C.P., Zhong, C., Saribekyan, G., Bading, J., Park, R., Conti, P.S., Moats, R., Berns, A., Shi, W., Zhou, Z.*, et al.* (2007). Mouse models of prostate adenocarcinoma with the capacity to monitor spontaneous carcinogenesis by bioluminescence or fluorescence. Cancer Res *67*, 7525-7533.

Lietz, M., Hohl, M., and Thiel, G. (2003). RE-1 silencing transcription factor (REST) regulates human synaptophysin gene transcription through an intronic sequence-specific DNA-binding site. European journal of biochemistry / FEBS *270*, 2-9.

Linnoila, R.I. (2006). Functional facets of the pulmonary neuroendocrine system. Lab Invest *86*, 425-444.

Liu, P., Jenkins, N.A., and Copeland, N.G. (2003). A highly efficient recombineering-based method for generating conditional knockout mutations. Genome Res *13*, 476-484.

Masumori, N., Thomas, T.Z., Chaurand, P., Case, T., Paul, M., Kasper, S., Caprioli, R.M., Tsukamoto, T., Shappell, S.B., and Matusik, R.J. (2001). A probasin-large T antigen transgenic mouse line develops prostate adenocarcinoma and neuroendocrine carcinoma with metastatic potential. Cancer Res *61*, 2239-2249.

Montuenga, L.M., Guembe, L., Burrell, M.A., Bodegas, M.E., Calvo, A., Sola, J.J., Sesma, P., and Villaro, A.C. (2003). The diffuse endocrine system: from embryogenesis to carcinogenesis. Prog Histochem Cytochem *38*, 155-272.

Mravec, B. (2005). A new focus on interoceptive properties of adrenal medulla. Auton Neurosci *120*, 10-17.

Nikitin, A., and Lee, W.H. (1996). Early loss of the retinoblastoma gene is associated with impaired growth inhibitory innervation during melanotroph carcinogenesis in Rb+/- mice. Genes Dev *10*, 1870-1879.

Salm, S.N., Burger, P.E., Coetzee, S., Goto, K., Moscatelli, D., and Wilson, E.L. (2005). TGF-{beta} maintains dormancy of prostatic stem cells in the proximal region of ducts. The Journal of cell biology *170*, 81-90.

Sauer, B. (1993). Manipulation of transgenes by site-specific recombination: use of Cre recombinase. Methods Enzymol *225*, 890-900.

Schmechel, D., Marangos, P.J., and Brightman, M. (1978). Neurone-specific enolase is a molecular marker for peripheral and central neuroendocrine cells. Nature *276*, 834-836.

Schmechel, D.E. (1985). Gamma-subunit of the glycolytic enzyme enolase: nonspecific or neuron specific? Laboratory investigation; a journal of technical methods and pathology *52*, 239-242.

Seshi, B., True, L., Carter, D., and Rosai, J. (1988). Immunohistochemical characterization of a set of monoclonal antibodies to human neuron-specific enolase. The American journal of pathology *131*, 258-269.

Soriano, P. (1997). The PDGF alpha receptor is required for neural crest cell development and for normal patterning of the somites. Development *124*, 2691-2700.

Soriano, P. (1999). Generalized lacZ expression with the ROSA26 Cre reporter strain. Nature genetics *21*, 70-71.

Sudhof, T.C., Lottspeich, F., Greengard, P., Mehl, E., and Jahn, R. (1987). A synaptic vesicle protein with a novel cytoplasmic domain and four transmembrane regions. Science *238*, 1142-1144.

Sugimura, Y., Cunha, G.R., and Donjacour, A.A. (1986). Morphogenesis of ductal networks in the mouse prostate. Biol Reprod *34*, 961-971.

Sun, Y., Niu, J., and Huang, J. (2009). Neuroendocrine differentiation in prostate cancer. American journal of translational research *1*, 148-162.

Sunday, M.E., Kaplan, L.M., Motoyama, E., Chin, W.W., and Spindel, E.R. (1988). Gastrin-releasing peptide (mammalian bombesin) gene expression in health and disease. Lab Invest *59*, 5-24.

Tachibana, T. (1995). The Merkel cell: recent findings and unresolved problems. Arch Histol Cytol *58*, 379-396.

Tsujimura, A., Koikawa, Y., Salm, S., Takao, T., Coetzee, S., Moscatelli, D., Shapiro, E., Lepor, H., Sun, T.T., and Wilson, E.L. (2002). Proximal location of mouse prostate epithelial stem cells: a model of prostatic homeostasis. The Journal of cell biology *157*, 1257-1265.

Wang, G.M., Kovalenko, B., Wilson, E.L., and Moscatelli, D. (2007). Vascular density is highest in the proximal region of the mouse prostate. The Prostate *67*, 968-975.

Wang, S., Gao, J., Lei, Q., Rozengurt, N., Pritchard, C., Jiao, J., Thomas, G.V., Li, G., Roy-Burman, P., Nelson, P.S.*, et al.* (2003). Prostate-specific deletion of the murine Pten tumor suppressor gene leads to metastatic prostate cancer. Cancer cell *4*, 209-221.

Weichselbaum, M., Sparrow, M.P., Hamilton, E.J., Thompson, P.J., and Knight, D.A. (2005). A confocal microscopic study of solitary pulmonary neuroendocrine cells in human airway epithelium. Respir Res *6*, 115.

Wiedenmann, B., Franke, W.W., Kuhn, C., Moll, R., and Gould, V.E. (1986). Synaptophysin: a marker protein for neuroendocrine cells and neoplasms. Proc Natl Acad Sci U S A *83*, 3500-3504.

Wong, S.C., Moffat, M.A., Coker, G.T., Merlie, J.P., and O'Malley, K.L. (1995). The 3' flanking region of the human tyrosine hydroxylase gene directs reporter gene expression in peripheral neuroendocrine tissues. J Neurochem *65*, 23-31.

Wu, X., Wu, J., Huang, J., Powell, W.C., Zhang, J., Matusik, R.J., Sangiorgi, F.O., Maxson, R.E., Sucov, H.M., and Roy-Burman, P. (2001). Generation of a prostate epithelial cell-specific Cre transgenic mouse model for tissue-specific gene ablation. Mech Dev *101*, 61-69.

Yang, X.W., and Gong, S. (2005). An overview on the generation of BAC transgenic mice for neuroscience research. Curr Protoc Neurosci *Chapter 5*, Unit 5 20.

Zhou, Z., Flesken-Nikitin, A., Corney, D.C., Wang, W., Goodrich, D.W., Roy-Burman, P., and Nikitin, A.Y. (2006). Synergy of p53 and Rb deficiency in a conditional mouse model for metastatic prostate cancer. Cancer research *66*, 7889-7898.

Zhou, Z., Flesken-Nikitin, A., and Nikitin, A.Y. (2007). Prostate cancer associated with p53 and Rb deficiency arises from the stem/progenitor cell-enriched proximal region of prostatic ducts. Cancer research *67*, 5683-5690.

CHAPTER 4

MME SUPPRESSES PROSTATE CANCER BY CONTROLLING GRP-DEPENDENT STEM/PROGENITOR CELL POOL

Chieh-Yang Cheng, Zongxiang Zhou, David Dupee, Meredith Stone, Elaina Wang, David M. Nanus, and Alexander Yu. Nikitin

Author contributions: Chieh-Yang Cheng and Alexander Yu. Nikitin designed the study, interpreted data and wrote the manuscript. Chieh-Yang Cheng, Zongxiang Zhou, David Dupee, Meredith Stone, and Elaina Wang performed experiments and analysed data. David M. Nanus contributed new reagents/comments/*Mme*$^{-/-}$ mice. Alexander Yu. Nikitin supervised the project.

4.1 Abstract

Membrane metallo-endopeptidase (MME) is responsible for the catalytic inactivation of neuropeptide substrates and is downregulated in a significant fraction of prostate cancers. Re-introduction of *MME* into *MME*-deficient neoplastic cells results in cancer suppression. However, mice lacking *Mme* do not develop prostatic neoplastic lesions, thereby placing in doubt MME's role as an authentic tumor suppressor. Here we report that MME cooperates with PTEN in the regulation of normal and neoplastic prostate stem/progenitor cells. In the mouse model of prostate carcinogenesis associated with PTEN deficiency, lack of MME results in expansion of prostate stem/progenitor cell pool and development of advanced adenocarcinomas with extensive vascular invasion. Effects of MME deficiency on prostate stem/progenitor cells and cancer propagating (aka stem) cells are recapitulated by addition of the main MME substrate, gastrin-releasing peptide (GRP). Importantly, GRP receptor antagonist [Tyr^4, D-Phe^{12}]-Bombesin abrogates those effects and delays tumor growth by reducing the pool of cancer propagating cells. Our study provides a definitive proof of tumor suppressive role of MME and uncovers an important function of the MME/GRP pathway in the control of prostate stem/progenitor cells. Furthermore, it identifies GRP receptor as a valuable target for therapies aimed at eradication of prostate cancer propagating cells.

4.2 Introduction

Prostate cancer is the most frequently diagnosed cancer and is expected to remain the second leading cause of cancer-related death in men in 2014 (Siegel et al., 2014). Aberrations in neuroendocrine signaling frequently present in prostate cancer, and neuropeptides, such as gastrin-releasing peptide (GRP), have been reported to be associated with accelerated prostate cancer progression and poor prognosis (Amorino and Parsons, 2004; Gkonos et al., 1995; Sun et al., 2009; Uchida et al., 2006). GRP can promote cell proliferation and accelerate migration and invasion of PC-3, DU-145, TSU-pr1 and LNCaP prostate cancer cells (Aprikian et al., 1997; Hoosein et al., 1993; Nagakawa et al., 1998; Nagakawa et al., 2001; Sumitomo et al., 2000). Consistently, targeting of the GRP receptor has been reported to suppress the growth of human prostate cancer cells in cell culture and in xenografts (Hohla and Schally, 2010; Mansi et al., 2013; Stangelberger et al., 2008). However, specific mechanisms by which neuropeptide dysregulation may be involved in the pathogenesis of prostate cancer remain insufficiently elucidated.

Membrane metallo-endopeptidase (MME, aka Neutral endopeptidase, Neprilysin, Enkephalinase, CALLA, CD10, EC 3.4.24.11) is a cell-surface peptidase, which cleaves peptide bonds on the amino side of hydrophobic amino acids. MME is the key enzyme in the processing of a variety of physiologically active peptides including GRP (Erdos and Skidgel, 1989; Shipp and Look, 1993; Zheng et al., 2006). MME is downregulated in a large fraction of primary and metastatic prostate cancers, independently predicting an inferior prognosis (Freedland et al., 2003; Osman et al., 2004; Papandreou et al., 1998). MME expression reduces growth, motility (Sumitomo et al., 2000), and survival (Sumitomo et al., 2001) of cancer cells in cell culture. Consistent with these

observations, both lentiviral and adenoviral replacements of MME inhibit prostate cancer tumorigenicity in xenograft experiments. (Horiguchi et al., 2007; Iida et al., 2012). However, mice lacking *Mme* show no cancer-related phenotype (Lu et al., 1995), raising a question about physiological relevance of MME's tumor suppressive effects.

To establish the role of *MME* in prostate carcinogenesis we used an autochthonous mouse model of prostate neoplasia associated with deficiency of the *Pten* tumor suppressor gene. In this model, prostate carcinogenesis is initiated by the prostate epithelium-specific inactivation of *Pten* driven by PB-*Cre4* transgene (*Pten*$^{PE-/-}$ mice; Adisetiyo et al., 2013; Chen et al., 2005; Cheng et al., 2014; Liao et al., 2007; Trotman et al., 2003; Wang et al., 2003; Wu et al., 2001; Zhou et al., 2006). The majority of *Pten*$^{PE-/-}$ mice develop high-grade prostatic intraepithelial neoplasms (HG-PINs) and a few animals show early adenocarcinomas characterized by stromal invasion. This model is particularly relevant to human disease because PTEN is frequently absent or downregulated in human prostate cancer (Cairns et al., 1997; Li et al., 1997). Previous cell culture studies have shown a potential cooperation between MME and PTEN (Sumitomo et al., 2004). Consistent with this possibility, the bioinformatics analysis of alterations via the cBioPortal for Cancer Genomics (Cerami et al., 2012; Gao et al., 2013) shows that downregulation of MME is observed in 42% and 63% of PTEN-deficient cases of human primary and metastatic prostate cancers, respectively (Taylor et al., 2010).

It has been reported that *Pten* conditional deletion in the prostate epithelium leads to basal cell proliferation with concomitant expansion of the prostate stem/progenitor-like Sca-1^{+} and BCL-2^{+} subpopulation (Wang et al., 2006). CD49f^{hi}/Sca-

1^+ *Pten*-deficient neoplastic cells exhibits cancer propagating cell properties, such as high sphere-forming capacity, sustained self-renewal, increased proliferation, and tumorigenic potential, as compared with other isogenic subpopulations (Mulholland et al., 2009). Prostate cancer propagating cells have also been shown to be regulated by the PTEN/PI3K/AKT pathway (Dubrovska et al., 2009).

In the current study we show that additional deficiency for MME facilitates expansion of the prostate/stem cell pool associated with *Pten* loss and leads to morphologically detectable neoplastic lesions of the prostate stem/progenitor cell compartment followed by the formation of aggressive prostate cancers manifesting frequent vascular invasion. We also show that effects of MME on normal prostate stem/progenitor cells and cancer propagating cells depend on its substrate, GRP, and can be abrogated by either GRP receptor (GRPR) antagonist or *GRPR* siRNA knockdown. These findings offer a new mechanism by which neuropeptide-mediated dysregulation may facilitate cancer progression.

4.3 Materials and Methods

Mice. ARR$_2$PB-Cre transgenic male mice on FVB/N background (*PB-Cre4*) (Wu et al., 2001) were crossed with *Pten$^{loxP/loxP}$* (Lesche et al., 2002) female mice on the 129/BALB/c background. Resulting *PB-Cre4Pten$^{loxP/loxP}$* male mice were designated as *Pten*$^{PE-/-}$ mice. *Pten*$^{PE-/-}$ male mice were crossed with *Mme* null female mice on a C57BL6 background (*Mme$^{-/-}$*) (Lu et al., 1995). Offspring with *PB-Cre4 Mme$^{-/-}$ Pten$^{loxP/loxP}$* genotype were designated as *Mme$^{-/-}$Pten$^{PE-/-}$* mice. To minimize the

confounding effects of genetic background, *Pten*$^{PE-/-}$ and *Mme*$^{-/-}$*Pten*$^{PE-/-}$ mice were backcrossed to FVB/N for at least 10 crosses and all control experiments were performed on age and sex-matched mice of the same background. All animal experiments were carried out in strict accordance with the recommendations of the Guide for the Care and Use of Laboratory Animals of the National Institutes of Health. The protocol was approved by the Institutional Laboratory Animal Use and Care Committee at Cornell University. All efforts were made to minimize animal suffering.

Immunohistochemistry and quantitative image analysis. Immunoperoxidase staining of paraffin sections of paraformaldehyde-fixed tissue was performed by a modified Elite avidin-biotin-peroxidase (ABC) technique (Nikitin and Lee, 1996). Antigen retrieval was done by boiling the slides in 10 mM citric buffer (pH 6.0) for 10 min. The primary antibodies to MME (Santa Cruz; Dallas, TX; #sc-80021, 1:100), Ki67 (Leica Microsystems; Bannockburn, IL; #NCLKi67p, 1:1000), EZH2 (Cell Signaling Technology; Danvers, MA; #5246, 1:200), keratin 5 (CK5, Covance; Dallas, TX, #PRB-160P, 1:2500), keratin 8 (CK8, Developmental Studies Hybridoma Bank; Iowa City, IA; #TROMA-I, 1:10), p63 (Santa Cruz, #sc-8431, 1:1000), PTEN (Cell Signaling Technology, #9559S, 1:800), pAKT (Cell Signaling Technology, # 3787S, 1:50), SYP (BD Biosciences; #611880, 1:500), GRP (Santa Cruz, #sc-7788, 1:100), NT (Santa Cruz, #sc-20806, 1:1000), and VIP (Abcam; Cambridge, MA; #ab8556, 1:200) were incubated with deparaffinized sections at 4ºC overnight, followed by incubation with secondary biotinylated antibody (1 hour, room temperature) and modified avidin-biotin-peroxidase (ABC) technique. Methyl green was used as the counterstain in immunoperoxidase

stainings. Slides were scanned by ScanScope CS (Leica Biosystems, Vista, CA) with a 40X objective followed by lossless compression. Quantitative analysis of immunohistochemistry (IHC) was performed with the ImageJ software (W. Rasband, National Institutes of Health, Bethesda, MD).

Tumorigenicity experiments. Human prostate cancer PC3 cells (5 x 10^6 cells) were suspended in the mixture of 200 µl PBS and 200 µl Matrigel (BD Biosciences, #356237) and injected subcutaneously into 5-week-old NSG (NOD.Cg-*Prkdc*^{scid}*Il2rg*^{tm1Wjl}/SzJ4; The Jackson Laboratory, stock number #005557) male mice (Fridman et al., 2012; Shultz et al., 2005). Intra-peritoneal injection of GRPR antagonist (0.8 µg/g body weight/day in PBS) was started when the tumor size reached 10 mm^3 (Chanda et al., 2010; Pinski et al., 1993). After 26 days of treatment with GRPR antagonist, mice were euthanized and subjected to necropsy. Tumor xenografts were collected for pathological evaluation and ALDEFLUOR assay followed by FACS analysis

Pathologic assessment. Moribund mice, as well as those sacrificed according to schedule, were anesthetized with avertin and, if necessary, subjected to cardiac perfusion at 90 mm Hg with PBS. After macroscopic evaluation during necropsy, lung, liver, prostate, and lymph nodes were fixed in phosphate-buffered 4% paraformaldehyde and embedded in paraffin. 4-µm-thick sections were stained with Hematoxylin (Mayer's haemalum) and eosin. Mouse prostatic intraepithelial neoplasia (PIN) and adenocarcinoma were defined according to earlier publications (Ittmann et al., 2013; Park et al., 2002; Shappell et al., 2004; Zhou et al., 2006). Briefly, distal PIN 1

has 1 or 2 layers of atypical cells; PIN 2 has 3 or more layers of atypical cells, PIN 3 occupies the near entire glandular lumen; and PIN 4 fills and distorts the glandular profile, and is frequently marked by pronounced desmoplastic reaction. In agreement with the recent consensus report (Ittmann et al., 2013), PIN1 and PIN2 represent low-grade PIN (LG PIN) and PIN3 and 4 represent high-grade PIN (HG PIN). Due to different architecture of the proximal regions of prostatic ducts, current PIN classification cannot be carefully applied to atypical proliferative lesions found in those structures. Thus we named those lesions as proximal duct dysplasia to stress their dissimilarity to PIN of distal regions of prostatic ducts. Given the complexity and controversial nature of the interpretation of stromal microinvasion we used the term “early adenocarcinoma” only for neoplasms with invasive stromal growth confirmed by serial sections followed by 3D reconstruction. We used the term “advanced adenocarcinoma” for neoplasms invading blood and lymphatic vessels.

Cell culture. DU145 and PC3 cell lines were obtained from the American Type Culture Collection (ATCC) and cultured in minimum essential medium (Cellgrow, #10-010-CV) and F-12K (Cellgrow, #10-025-CV), respectively, supplemented with 10% heat-inactivated fetal bovine serum (FBS, GIBCO, #16141-079) and Penicillin-Streptomycin (Cellgrow, #30-002-Cl). The cultures were maintained at 37ºC in a 5 % CO_2 incubator.

Primary mouse prostate cells were isolated following described procedures (Lawson et al., 2010; Lukacs et al., 2010a). Lipofectamin 2000 reagent (Invitrogen; Carlsbad, CA, #11668-030) was used for the transfection following manufacturer’s recommendations. Control siRNA (Santa Cruz, #sc-37007) and two independent human

GRPR siRNAs (Santa Cruz, # sc-106924 and Life Technologies, #145216) and mouse *Grpr* siRNAs (Life Technologies, #157912 and #157914) were used for all knockdown experiments.

5-bromo-2'deoxyuridine (BrdU) staining (Flesken-Nikitin et al., 2013), migration and invasion assays (Corney et al., 2010) were performed as previously described.

ALDEFLUOR assay and Fluorescence Activated Cell Sorting. For detection of aldehyde dehydrogenase (ALDH) enzymatic activity, 10^6 cells were placed in ALDEFLUOR buffer and processed for staining with the ALDEFLUOR Kit (STEM CELL, #01700) according to the manufacturer's protocol. Unstained and ALDH inhibitor (diethylaminobenzaldehyde, DEAB)-treated cells served as controls. For detection of CD44-expressing cancer cells, prostate cancer cells were stained for CD44 (BD Bioscience, #553134) to sort CD44-positive and CD44-negative cells. Cell sorting and data analysis were performed on a FACS Aria II sorter equipped with the FACS DiVa software (BD Bioscience).

Prostate sphere assay. The preparation of prostate epithelial cell suspensions, stem/basal cells, and luminal cells from male mice and the prostate sphere assay were performed as described previously (Cheng et al., 2014; Lawson et al., 2010; Lukacs et al., 2010a). Briefly, 10^4 mouse prostate stem/basal cells, mouse prostate luminal cells, human prostate cancer cells, and human prostate cancer propagating cells were resuspended in 120 µl of a 1:1 mixture of Matrigel (BD Biosciences, #354234) and PrEGM (Lonza, #CC-3166), and plated around the rim of a well of a 12-well tissue

culture plate. Matrigel mix was allowed to solidify at 37°C for 15 min, and 1 ml of PrEGM was added to each well. Media were changed every 3 days. To recover the spheres, each well was treated with enzyme mixture: 750 µl Collegenase/Dispase 4 mg/ml (Roche, #10269638001), 30 mg BSA (Sigma, #A3311), and 1 µl DNase1 10mg/ml (Sigma, D4513). This was followed by treatment with Trypsin 0.25% EDTA (Cellgrow, 25-052-Cl) to make cell suspensions, which were ready for passage.

GRP and GRPR antagonist treatment. 5 nM GRP (Gastrin-releasing peptide human, Sigma, #G8022) (Dai et al., 2002) and 4 µM GRPR antagonist ([Tyr^4, D-Phe^{12}]-Bombesin, Sigma, #B0650) (Heinz-Erian et al., 1987) were used for cell culture experiments. Media were changed every 3 days.

Western blot. For western blot, cell lysates were prepared using RIPA buffer (50 mM Tris-HCl, (pH 7.4), 1% Nonidet P-40, 0.25% Na-deoxicholate, 150 mM NaCl, 1 mM EDTA, 1 mM PMSF, Aprotinin, leupeptin, pepstatin: 1 µg/ml each, 1 mM Na3VO4, 1 mM NaF), and 10 seconds of sonication on ice 5 times. Lysates were then separated by 12% SDS-PAGE and transferred to PVDF membrane (Millipore #IPVH00010). The membrane was incubated overnight at 4ºC with antibodies to detect GRPR (Santa Cruz, #sc-32903, 1:1000) and GAPDH (Advanced Immunohistochemical Inc.; Long Beach, CA; #2-RGM2,1:5000), followed by incubation for 1 hour at room temperature with corresponding horseradish peroxidase-conjugated anti-rabbit secondary antibodies (Santa Cruz, #sc-2004, 1:2000) or anti-mouse secondary antibodies (Santa Cruz, #sc-

2005, 1:2000), and developed using chemiluminescent substrate (Thermo Scientific, Rockford, IL, #34077).

Statistical analysis. Statistical analyses were performed with InStat 3.10 and Prism 6 software. (GraphPad, Inc., San Diego, CA). A two-tailed unpaired t-test, direct Fisher's tests, and a log-rank Mantel-Haenszel test were used as appropriate.

4.4 Results

4.4.1 MME cooperates with PTEN in suppression of prostate cancer in autochthones mouse model

To test potential cooperation of *Mme* and *Pten* genes in suppression of prostate cancer, we evaluated MME expression in HG-PINs and early invasive adenocarcinomas typical for *Pten*$^{PE-/-}$ mice. While irregular MME expression was observed in the majority of neoplastic lesions, MME was absent in the areas of stromal invasion (Figure 4.1). No significant alterations in MME expression were detected in the proximal regions of prostatic ducts, consistent with the lack of neoplastic lesions in that part of the prostate in *Pten*$^{PE-/-}$ mice (Figures 4.1 and 4.2A, Table 4.1).

Next we crossed *Mme*$^{-/-}$ and *Pten*$^{PE-/-}$ mice, and evaluated prostates of age-matched wild-type (WT), *Mme*$^{-/-}$, and *Pten*$^{PE-/-}$ and *Mme*$^{-/-}$*Pten*$^{PE-/-}$ strains (Figures 4.2 and 4.3, Table 4.1). Consistent with previous observations, *Mme*$^{-/-}$ mice did not develop any neoplastic lesions by 16 months of age, while *Pten*$^{PE-/-}$ mice showed low- and high-

grade PINs at 3 months and onwards. At 16 months, 33% of *Pten*$^{PE-/-}$ mice developed early invasive adenocarcinomas, characterized by separate nests of neoplastic cells in the desmoplastic stroma (Figure 4.3A). All neoplastic lesions were in the distal regions of prostatic ducts. Unlike *Pten*$^{PE-/-}$ mice, *Mme*$^{-/-}$*Pten*$^{PE-/-}$ mice developed dysplastic lesions followed by adenocarcinomas in the proximal regions of the prostatic ducts (Figure 4.2A). Furthermore, some adenocarcinomas have shown distinct vascular invasion, a feature not characteristic of prostatic lesions in *Pten*$^{PE-/-}$ mice (Figures 4.2A and 4.3A). Consistent with these histological observations, the prostatic epithelium of *Mme*$^{-/-}$*Pten*$^{PE-/-}$ mice was characterized by a significantly higher proliferative rate according to Ki67 staining (Figures 4.2A, 4.2B, 4.3A, and 4.3B), expressed higher amounts of a marker of early prostate cancer, EZH2, and showed an increased number of CK5 and p63 positive cells as compared to prostatic lesions in *Pten*$^{PE-/-}$ mice. Prostatic epithelium lesions of *Mme*$^{-/-}$*Pten*$^{PE-/-}$ mice also showed higher levels of pAKT, suggesting the existence of additional MME-dependent mechanisms of regulation of this downstream target of PTEN. Also, consistent with our previous observation (Liao et al., 2007), prostatic neoplastic lesions of *Pten*$^{PE-/-}$ mice had an increased number of synaptophysin-positive neuroendocrine cells in the distal regions of prostatic ducts (Figures 4.3A and 4.3C). However, this number was not additionally elevated in *Mme*$^{-/-}$ *Pten*$^{PE-/-}$ mice. In sum, lack of both MME and PTEN not only promoted lesions typically observed in the prostates of *Pten*$^{PE-/-}$ mice but also resulted in distinct, additional neoplasms located in the proximal regions of prostatic ducts.

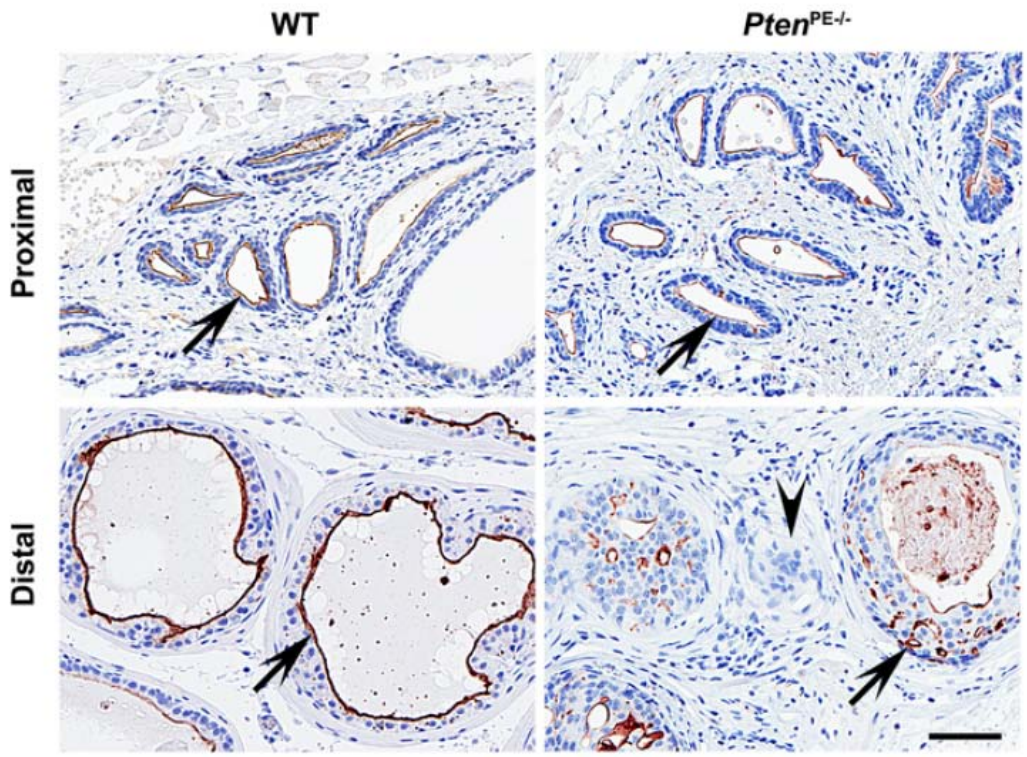

Figure 4.1 Alterations of *MME* expression in prostate adenocarcinoma of *Pten*$^{PE-/-}$ mice. MME expression (arrows) in the proximal and distal regions of prostatic ducts of wild-type (WT) and *Pten*$^{PE-/-}$ mice. Note that area of stromal invasion (arrowhead) by early adenocarcinoma lacks MME expression in *Pten*$^{PE-/-}$ mice. The ABC Elite method with hematoxylin counterstaining was performed. Scale bar, 60 μm. Immunostainings are representative of four WT and two *Pten*$^{PE-/-}$ mice, respectively.

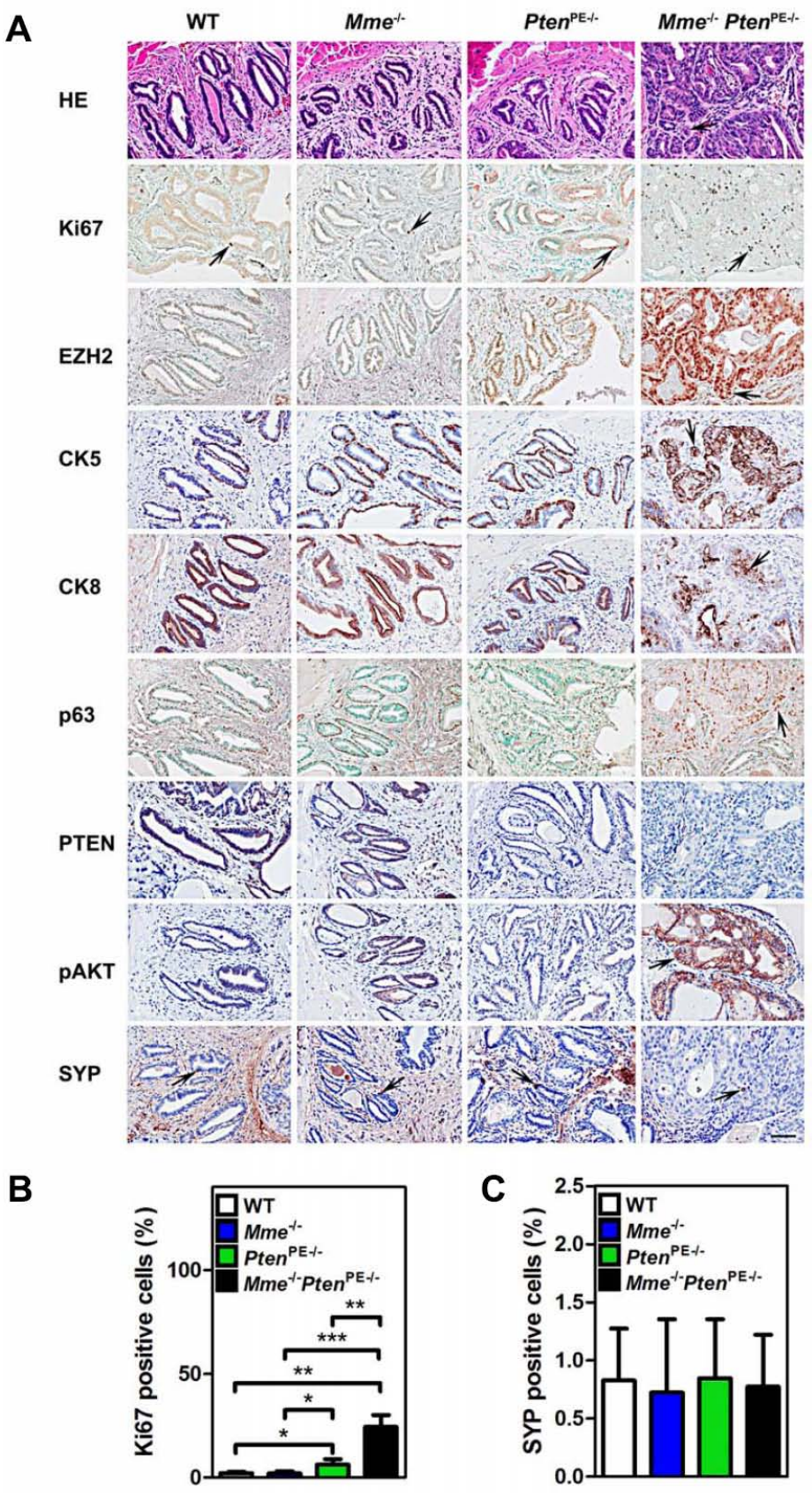
A
WT
Mme-/-
PtenPE-/-
Mme-/- PtenPE-/-
HE
Ki67
EZH2
CK5
CK8
p63
PTEN
pAKT
SYP
B
Ki67 positive cells (%)
WT
Mme-/-
PtenPE-/-
Mme-/-PtenPE-/-
100
50
0
*
*
**
**
***
**
C
SYP positive cells (%)
2.5
2.0
1.5
1.0
0.5
0.0

Figure 4.2 *Mme* and *Pten* cooperate in suppression of prostate carcinogenesis in the proximal regions of prostatic ducts of the mouse. (A) Proximal regions of prostatic ducts in 16-month-old WT (n=5), *Mme*$^{-/-}$ (n=15), *Pten*$^{PE-/-}$ (n=9) and *Mme*$^{-/-}$ *Pten*$^{PE-/-}$ (n=12) mice. The arrows indicate adenocarcinoma (HE) in *Mme*$^{-/-}$*Pten*$^{PE-/-}$ mice or positive immunostained cells. As compared to the prostate epithelium of WT, *Mme*$^{-/-}$, and *Pten*$^{PE-/-}$ mice, adenocarcinomas of *Mme*$^{-/-}$*Pten*$^{PE-/-}$ mice show higher expression levels of EZH2 and pAKT, and an increased number of Ki67, CK5, and p63 positive cells, but no differences in number of synaptophysin (SYP) positive cells. HE, hematoxylin and eosin staining. The ABC Elite method with hematoxylin (CK5, CK8, PTEN, pAKT, and SYP) or methyl green (Ki67, EZH2, and p63) counterstaining was performed. Scale bar, 60 µm for all images. (B and C) A quantitative analysis of the proliferation rate (B) and frequency of SYP positive cells (C) in proximal regions of prostatic ducts. *P<0.05; **P<0.01; ***P<0.001. Error bars denote SD. (A-C) All results are representative of at least three mice per genotype.

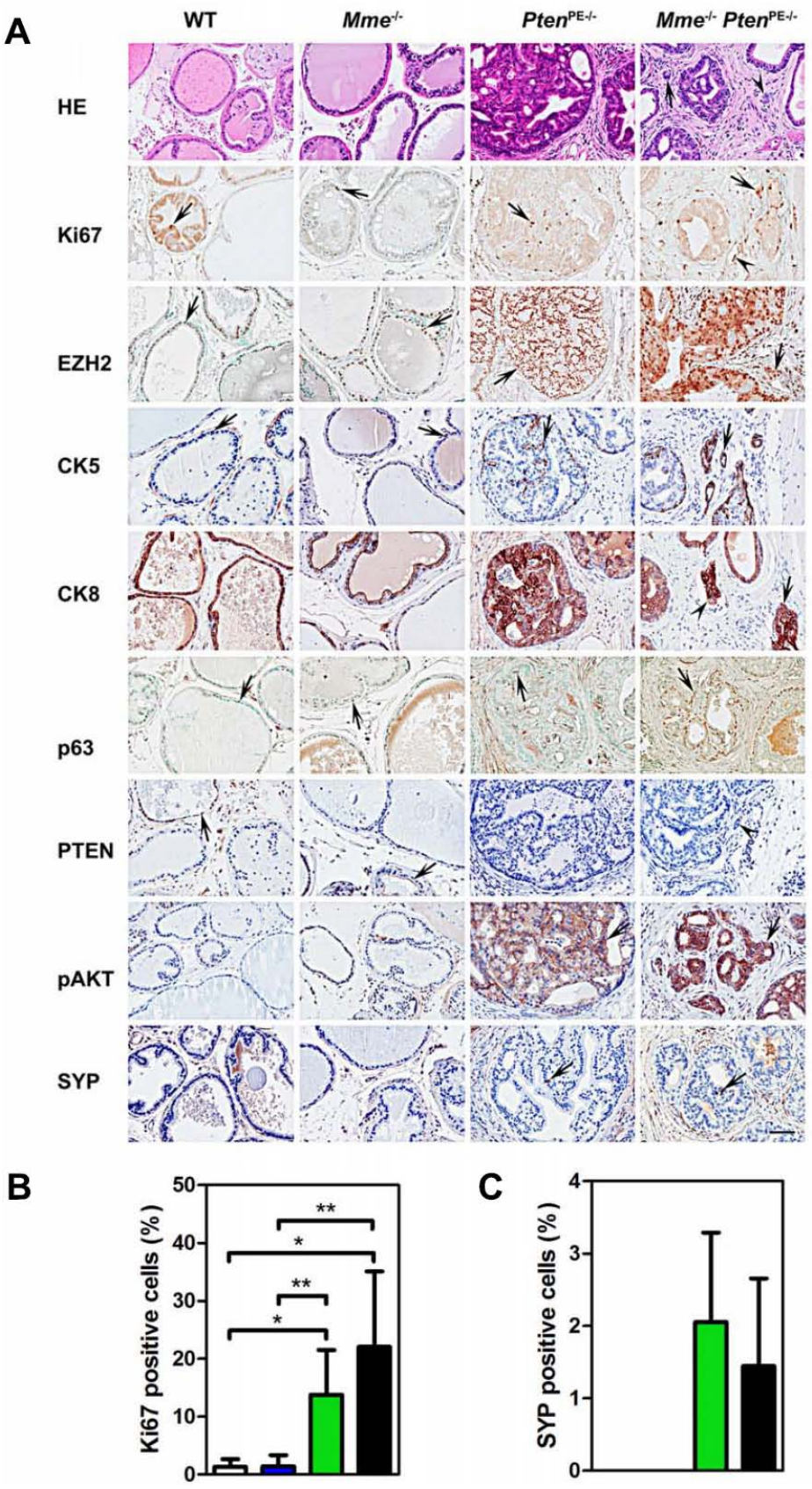
A
WT
Mme-/-
PtenPE-/-
Mme-/- PtenPE-/-
HE
Ki67
EZH2
CK5
CK8
p63
PTEN
pAKT
SYP
B
Ki67 positive cells (%)
50
40
30
20
10
0
**
*
**
*
C
SYP positive cells (%)
4
3
2
1
0

Figure 4.3 Lack of MME promotes carcinogenesis associated with PTEN deficiency in the distal regions of prostatic ducts. (A) Distal regions of prostatic ducts in 16-month-old WT (n=5), *Mme*$^{-/-}$ (n=15), *Pten*$^{PE-/-}$ (n=9), and *Mme*$^{-/-}$*Pten*$^{PE-/-}$ (n=12) mice. The arrows indicate invasive adenocarcinomas in *Mme*$^{-/-}$*Pten*$^{PE-/-}$ mice (HE, PTEN) or positive immunostained cells, and the arrowheads indicate vascular invasion in *Mme*$^{-/-}$*Pten*$^{PE-/-}$ mice. As compared to the prostate epithelium of *Pten*$^{PE-/-}$ mice, adenocarcinomas of *Mme*$^{-/-}$*Pten*$^{PE-/-}$ mice show higher expression levels of EZH2 and pAKT and a trend in increased number of Ki67 positive cells, but no difference in number of SYP positive cells. HE, hematoxylin and eosin staining. The ABC Elite method with hematoxylin (CK5, CK8, PTEN, pAKT, and SYP) or methyl green (Ki67, EZH2, and p63) counterstaining was performed. Scale bar, 60 μm for all images. (B and C) A quantitative analysis of the proliferation rate (B) and frequency of SYP positive cells (C) in distal regions of prostatic ducts. *P<0.05; **P<0.01. Error bars denote SD. (A-C) All results are representative of at least three mice per genotype.

Table 4.1 Prostatic Lesions in *Mme*$^{-/-}$, *Pten*$^{PE-/-}$ and *Mme*$^{-/-}$*Pten*$^{PE-/-}$ Mice

Strain	Prostatic region	Lesion	Age (months)		
			3	7	16
Mme$^{-/-}$	Proximal	None	100 (3/3)*	100 (7/7)	100 (15/15)
		Dysplasia	0 (0/3)	0 (0/7)	0 (0/15)
		Early adenocarcinoma	0 (0/3)	0 (0/7)	0 (0/15)
		Advanced adenocarcinoma[#]	0 (0/3)	0 (0/7)	0 (0/15)
	Distal	None	100 (3/3)	100 (7/7)	100 (15/15)
		Low-grade PIN	0 (0/3)	0 (0/7)	0 (0/15)
		High-grade PIN	0 (0/3)	0 (0/7)	0 (0/15)
		Early adenocarcinoma	0 (0/9)	0 (0/7)	0 (0/15)
		Advanced adenocarcinoma	0 (0/9)	0 (0/7)	0 (0/15)
Pten$^{PE-/-}$	Proximal	None	100 (16/16)	100 (11/11)	100 (0/9)
		Dysplasia	0 (0/16)	0 (0/11)	0 (0/9)
		Early adenocarcinoma	0 (0/16)	0 (0/11)	0 (0/9)
		Advanced adenocarcinoma	0 (0/16)	0 (0/11)	0 (0/9)
	Distal	None	100 (0/16)	0 (0/11)	0 (0/9)
		Low-grade PIN	6 (1/16)	0 (0/11)	0 (0/9)
		High-grade PIN	94 (15/16)	100 (11/11)	67 (6/9)
		Early adenocarcinoma	0 (0/16)	0 (0/11)	33 (3/9)
		Advanced adenocarcinoma	0 (0/16)	0 (0/11)	0 (0/9)
Mme$^{-/-}$ *Pten*$^{PE-/-}$	Proximal	None	83 (5/6)	0 (0/8)	0 (0/12)
		Dysplasia	17 (1/6)	87 (7/8)	50 (6/12)
		Early adenocarcinoma	0 (0/6)	13 (1/8)	42 (5/12)
		Advanced adenocarcinoma	0/(0/6)	0 (0/8)	8 (1/12)
	Distal	None	0 (0/6)	0 (0/8)	0 (0/12)
		Low-grade PIN	0 (0/6)	0 (0/8)	0 (0/12)
		High-grade PIN	100 (6/6)	100 (8/8)	17 (2/12)
		Early adenocarcinoma	0 (0/6)	0 (0/8)	58 (7/12)
		Advanced adenocarcinoma	0 (0/6)	0 (0/8)	25 (3/12)

*% (number of mice with lesion out of total number of mice).
[#]Advanced adenocarcinoma is defined as adenocarcinoma with vascular invasion

4.4.2 MME loss promotes activities of PTEN-deficient mouse prostate stem/progenitor cells

The proximal regions of prostatic ducts are particularly enriched in prostate epithelium stem/progenitor cells (Leong et al., 2008; Salm et al., 2005; Tsujimura et al., 2002; Wang et al., 2007; Zhou et al., 2007). Thus, we evaluated potential effects of MME and PTEN deficiency on prostate stem/progenitor cells, isolated as the $CD49f^{hi}/Sca\text{-}1^{+}$ fraction by fluorescence-activated cell sorting (FACS) (Figure 4.4A). *Mme*$^{-/-}$ mice had the same number of stem/progenitor cells as age-matched WT mice (5.7% vs 5.6%). In contrast, *Pten*$^{PE-/-}$ mice showed a significant increase of the stem cell pool (8.4%), consistent with previous reports, suggesting that PTEN is involvd in regulation of prostate stem/progenitor cells (Abou-Kheir et al., 2010; Dubrovska et al., 2009; Mulholland et al., 2009; Wang et al., 2006). The pool of $CD49f^{hi}/Sca\text{-}1^{+}$ cells deficient for both PTEN and MME constituted 12.1% of the prostate epithelium, representing an additional 44% increase compared to PTEN deficient $CD49f^{hi}/Sca\text{-}1^{+}$ cells (Figure 4.4A, $P<0.0001$).

Prostasphere formation is used as a functional cell culture test for presence, growth, and self-renewal potential of prostate stem/progenitor cells. Consistent with FACS results, $CD49f^{hi}/Sca\text{-}1^{+}$ cells isolated from prostates of *Mme*$^{-/-}$*Pten*$^{PE-/-}$mice showed the highest frequency of prostaspheres in multiple consecutive sphere dissociation and regeneration passages (Figure 4.4B). Furthermore, prostaspheres deficient for both genes were larger in size, compared to WT, MME-deficient or PTEN-deficient stem/progenitor cells (Figure 4.4C). In all groups $CD49f^{lo}/Sca\text{-}1^{-}$ luminal cells

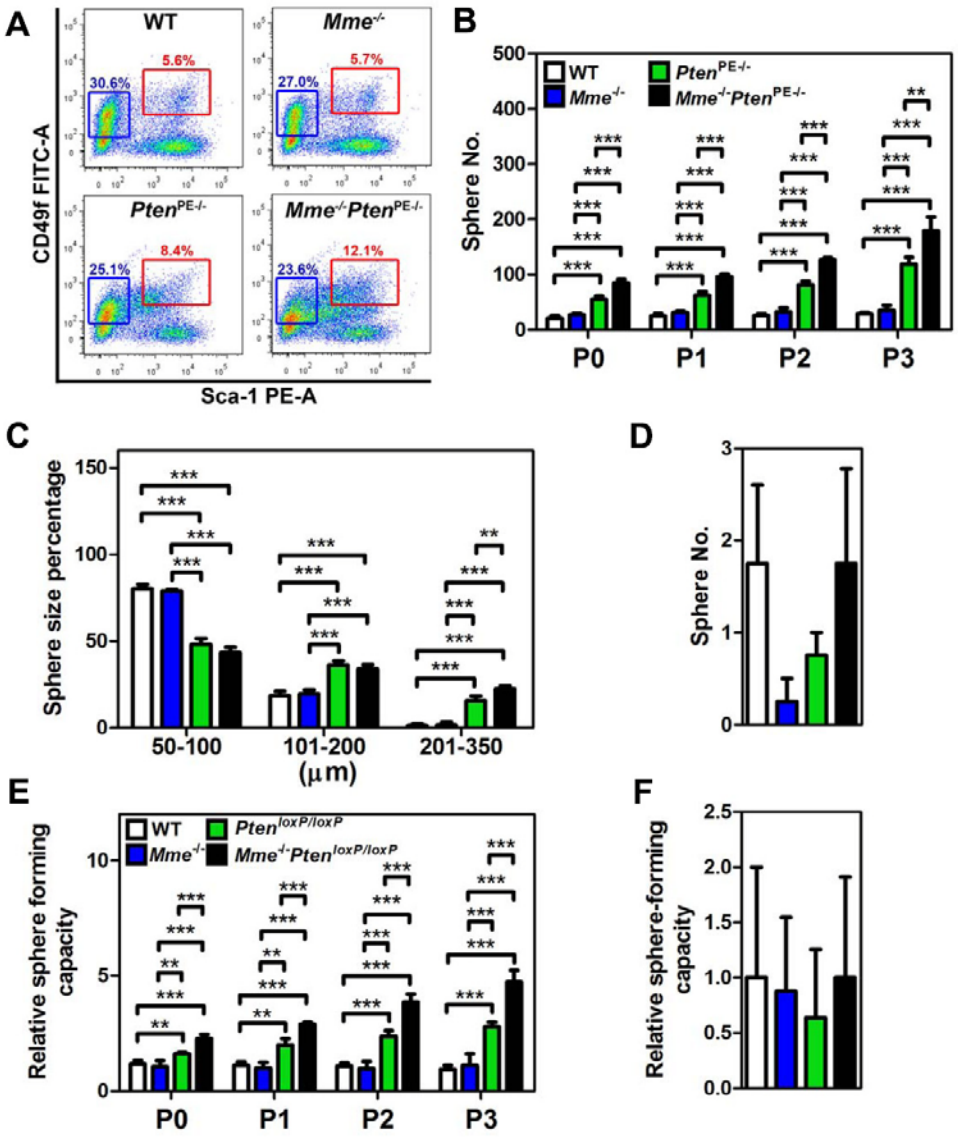

Figure 4.4 Lack of *Mme* promotes *Pten*-deficient prostate stem/progenitor cell expansion and sphere-forming capacity. (A) Quantitative analysis of distribution of CD49f^{hi}/Sca-1^{+} stem/progenitor cells and CD49f^{lo}/Sca-1^{-} luminal cells isolated from 3-month-old WT, *Mme*$^{-/-}$, *Pten*$^{PE-/-}$, and *Mme*$^{-/-}$*Pten*$^{PE-/-}$ mice (n=3 per genotype). Red and blue frames represent stem/progenitor cell and luminal cell populations, respectively. (B-D) Frequency (B, D) and size (C) of spheres formed by CD49f^{hi}/Sca-1^{+} stem/progenitor cells (B, C) and CD49f^{lo}/Sca-1^{-} (D) luminal cells from 3-month-old WT, *Mme*$^{-/-}$, *Pten*$^{PE-/-}$, and *Mme*$^{-/-}$*Pten*$^{PE-/-}$ mice (n=3 per genotype). (E, F) Relative frequency of sphere formation by CD49f^{hi}/Sca-1^{+} stem/progenitor cells (E) and CD49f^{lo}/Sca-1^{-} luminal cells (F) isolated from 3-month-old WT, *Mme*$^{-/-}$, *Pten*$^{loxP/loxP}$, and *Mme*$^{-/-}$ *Pten*$^{loxP/loxP}$ mice followed by Ad-*Cre* infection (n=3 per genotype). Spheres counts were normalized to the Ad-*blank*-infected spheres of each passage. P0-P3, passages 0-3. **P<0.01, ***P<0.001. Error bars denote SD. (A-F) Data represent three independent experiments.

formed very few spheres after the first plating and no spheres were observed after the first passage (Figure 4.4D). Thus, PTEN and/or MME deficiency are unlikely to reprogram differentiated cells towards stem cell state.

To test if the observed properties represent direct effects of MME and/or PTEN on prostate stem/progenitor cells we have isolated CD49f^{hi}/Sca-1^{+} stem/progenitor cells and CD49f^{lo}/Sca-1^{-} luminal cells from prostates of WT, *Mme*$^{-/-}$, *Pten*$^{loxP/loxP}$, and *Mme*$^{-/-}$ *Pten*$^{loxP/loxP}$ mice and infected them with adenovirus expressing Cre recombinase (Ad-*Cre*). Consistent with our previous experiments, lack of both *Pten* and *Mme* had the most pronounced effect on frequency of CD49f^{hi}/Sca-1^{+} stem/progenitor cells in consecutive passages (Figure 4.4E). Luminal cells formed only a few spheres with the same frequency in all groups (Figure 4.4F). Taken together, these results showed that MME cooperates with PTEN in regulation of prostate stem/progenitor cell activity.

4.4.3 GRP promotes activities of PTEN-deficient mouse prostate stem/progenitor cells

To identify mechanisms by which MME may affect regulation of prostate stem/progenitor cells, we have tested expression of its main substrates, GRP, neurotensin (NT), and vasoactive intestinal peptide (VIP) in the prostates of WT, *Mme*$^{-/-}$, *Pten*$^{PE-/-}$, and *Mme*$^{-/-}$*Pten*$^{PE-/-}$ strains. Strong GRP expression was detected only in prostates of *Mme*$^{-/-}$*Pten*$^{PE-/-}$ mice, while NT and VIP were not detected in all cases (Figure 4.5).

To test if GRP recapitulates effects of MME deficiency, we isolated prostate cells

from *Mme*$^{-/-}$*Pten*$^{PE-/-}$ mice, and either performed knockdown of the GRP receptor (GRPR, Figure 4.6A) or administered GRPR antagonist ([Tyr^4, D-Phe^{12}]-Bombesin) (Heinz-Erian et al., 1987). Both approaches reversed effects of MME deficiency on formation frequency and size of prostaspheres (Figures 4.6B and 4.6C).

Consistent with frequent vascular invasion by prostate adenocarcinomas in *Mme*$^{-/-}$*Pten*$^{PE-/-}$ mice, we have observed increased cell motility and invasion of prostate cells isolated from *Mme*$^{-/-}$*Pten*$^{PE-/-}$ mice, compared to those prepared from *Pten*$^{PE-/-}$ mice (Figures 4.6D and 4.6E). Notably, both parameters were normalized by either GRPR knockdown or treatment with [Tyr^4, D-Phe^{12}]-Bombesin.

To test if GRP directly affects function of PTEN-deficient prostate stem/progenitor cells, CD49f^{hi}/Sca-1$^+$ prostate stem cells isolated from *Pten*$^{loxP/loxP}$ were infected with Ad-*Cre* followed by treatment with GRP and/or [Tyr^4, D-Phe^{12}]-Bombesin. GRP addition reproduced the effects of MME deficiency on formation frequency and size of prostasphere, but these effects were abrogated by [Tyr^4, D-Phe^{12}]-Bombesin (Figures 4.6F and 4.6G). In sum, these results showed that GRP may be a key MME target, responsible for its effects on prostate stem/progenitor cells and on progression of cancer associated with PTEN deficiency.

4.4.4 GRP promotes expansion of human prostate cancer propagating cells

To assess the relevance of our observations to human disease, we tested the effects of GRP and [Tyr^4, D-Phe^{12}]-Bombesin on human prostate cancer cells, DU145 and PC3 (Figure 4.7). In both cell lines, GRP promoted cell proliferation, migration, and invasion.

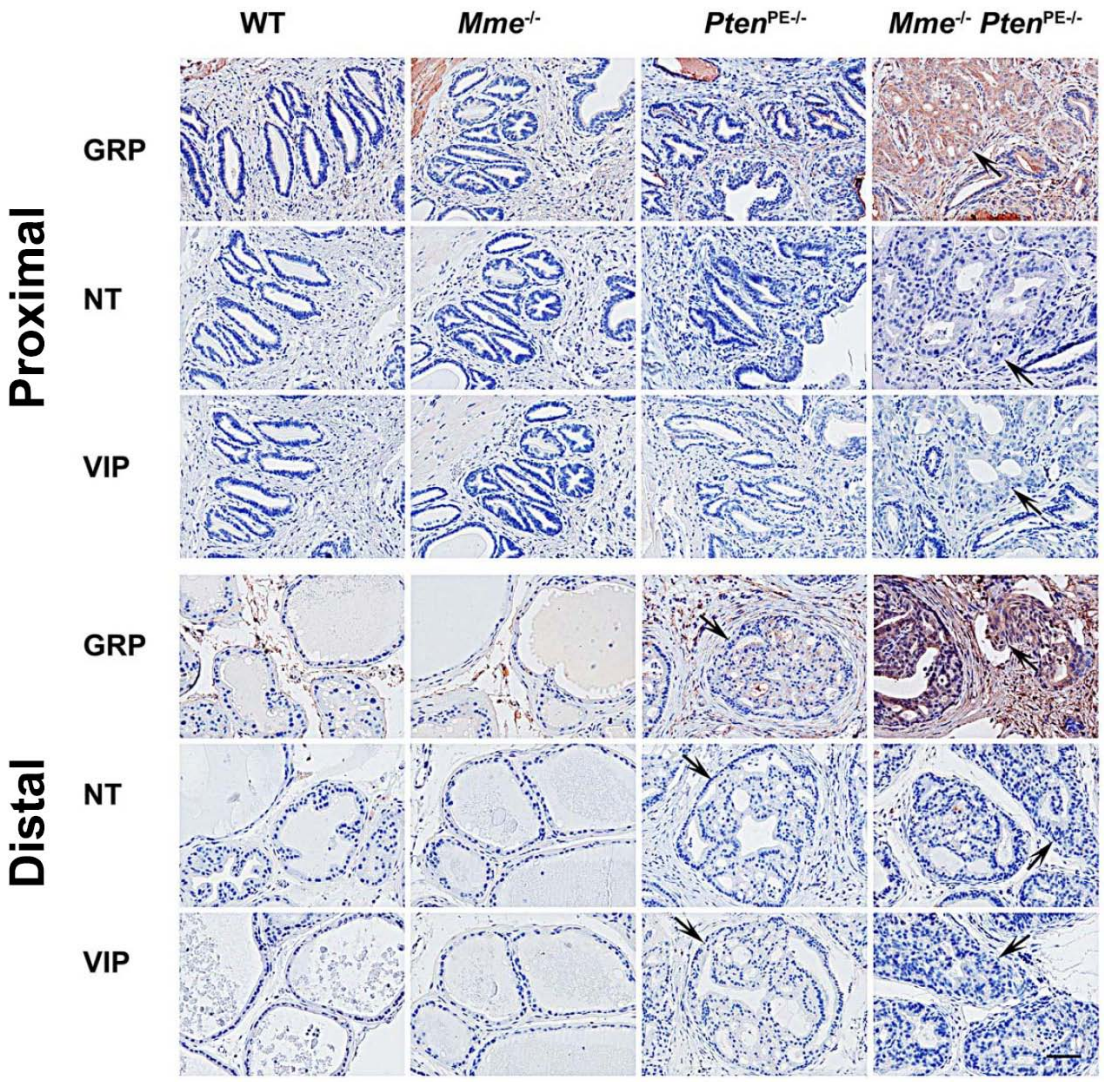

Figure 4.5 GRP accumulation in mouse prostatic lesions deficient for *Mme* and *Pten*. GRP, NT, and VIP expression in the proximal and distal regions of prostatic ducts in 16-month-old WT (n=5), *Mme*$^{-/-}$ (n=15), *Pten*$^{PE-/-}$ (n=9), and *Mme*$^{-/-}$*Pten*$^{PE-/-}$ (n=12) mice are shown. Arrows, prostatic lesions. The ABC Elite method with hematoxylin counterstaining was performed. Scale bar, 60 μm.

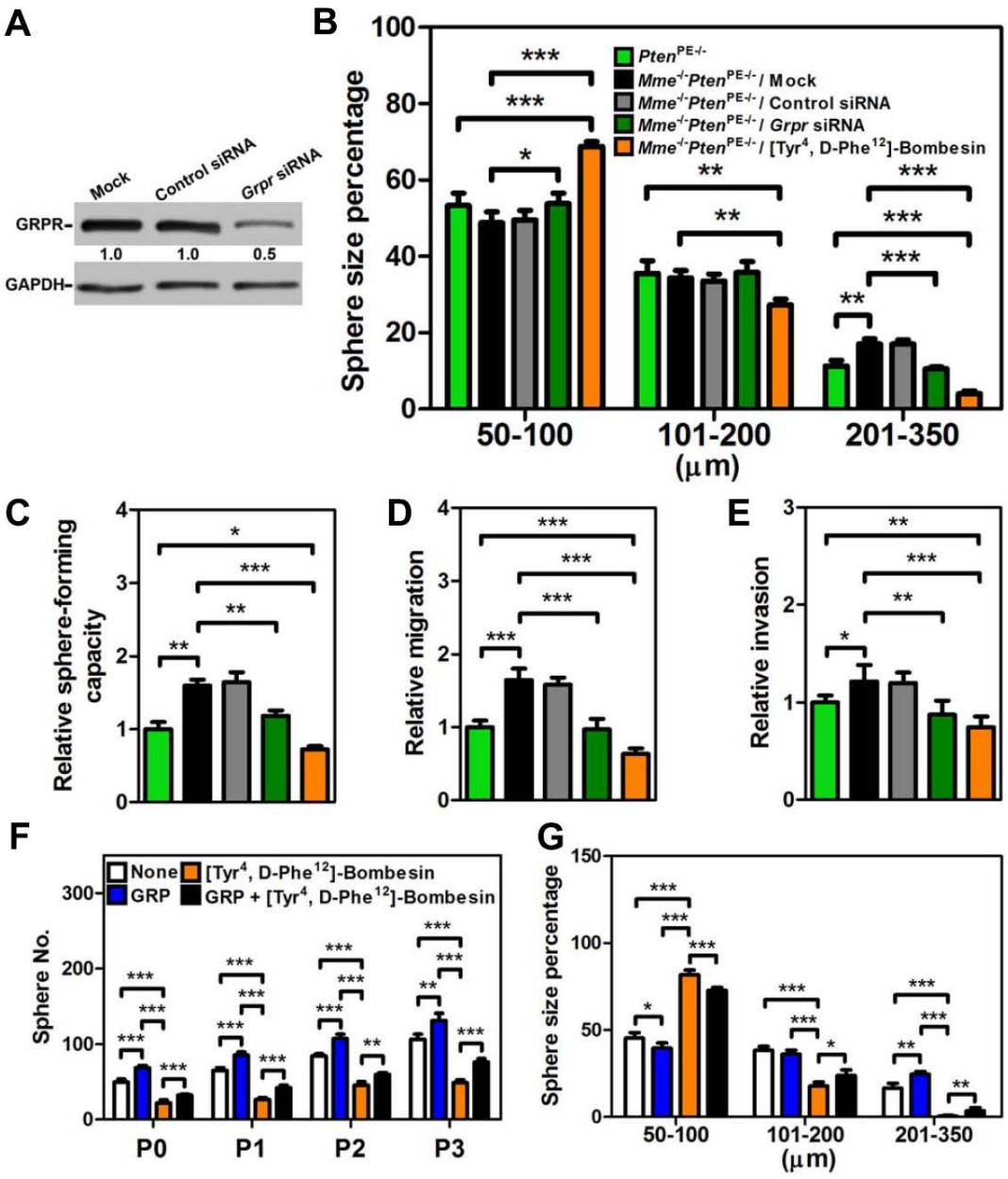

Figure 4.6 GRP promotes *Pten*-deficient mouse prostate stem/progenitor cell expansion and sphere-forming capacity. (A-E) Western blot of GRPR expression (A), prostasphere size (B), sphere-forming capacity (C), migration (D), and invasion (E) of prostate cells isolated from 3-month-old *Pten*$^{PE-/-}$ and *Mme*$^{-/-}$*Pten*$^{PE-/-}$ mice (n=3 per genotype) were performed. (F, G) Frequency (F) and size (G) of prostaspheres formed by Ad-*Cre*-infected CD49f^{hi}/Sca-1^{+} stem/progenitor cells isolated from 3-month-old *Pten*$^{loxP/loxP}$ mice (n=3) with treatments of GRP and/or [Tyr^{4}, D-Phe^{12}]-Bombesin were performed. P0-P3, passages 0-3. *P<0.05, **P<0.01, ***P<0.001. All error bars denote SD. (A-G) Data represent three independent experiments.

All these effects were negated by addition of [Tyr^4, D-Phe^{12}]-Bombesin, consistent with our observations on mouse prostate epithelium cells. Moreover, GRPR knockdown rescued the stimulating effects of GRP and inhibitory effects of [Tyr^4, D-Phe^{12}]-Bombesin, suggesting a crucial role for GRP/GRPR in control of the above parameters.

Prostate cancer propagating cells can be identified by either high enzymatic activity of ALDH (ALDERFLUOR assay) (Burger et al., 2009; Li et al., 2010b) or by detection of CD44 expression (Leong et al., 2008; Patrawala et al., 2007; Patrawala et al., 2006). In both approaches, cancer propagating cells increased in number after GRP treatment (Figures 4.8A-4.8D). Cancer propagating cells treated with GRP also formed spheres in greater number and size. These changes were diminished by [Tyr^4, D-Phe^{12}]-Bombesin and/or *GRPR* siRNA (Figures 4.8A-4.8G).

To study the effect of GRP on human prostate cancer *in vivo*, immunodeficient NSG mice were subcutaneously injected with PC-3 cells and then treated with [Tyr^4, D-Phe^{12}]-Bombesin when the tumor size reached 10 mm^3 (Figures 4.8H-4.8J). Daily intraperitoneal injections of [Tyr^4, D-Phe^{12}]-Bombesin reduced both tumor volume and weight by 70% by the time the animals were euthanized at 26 days after beginning treatment. Importantly, according to the ALDERFLUOR assay, a fraction of prostate cancer propagating cells was significantly reduced in tumors treated with [Tyr^4, D-Phe^{12}]-Bombesin compared to controls treated with vehicle alone. Thus GRPR antagonist inhibits tumorigenicity of prostate cancer cells by diminishing a population of cancer propagating cells.

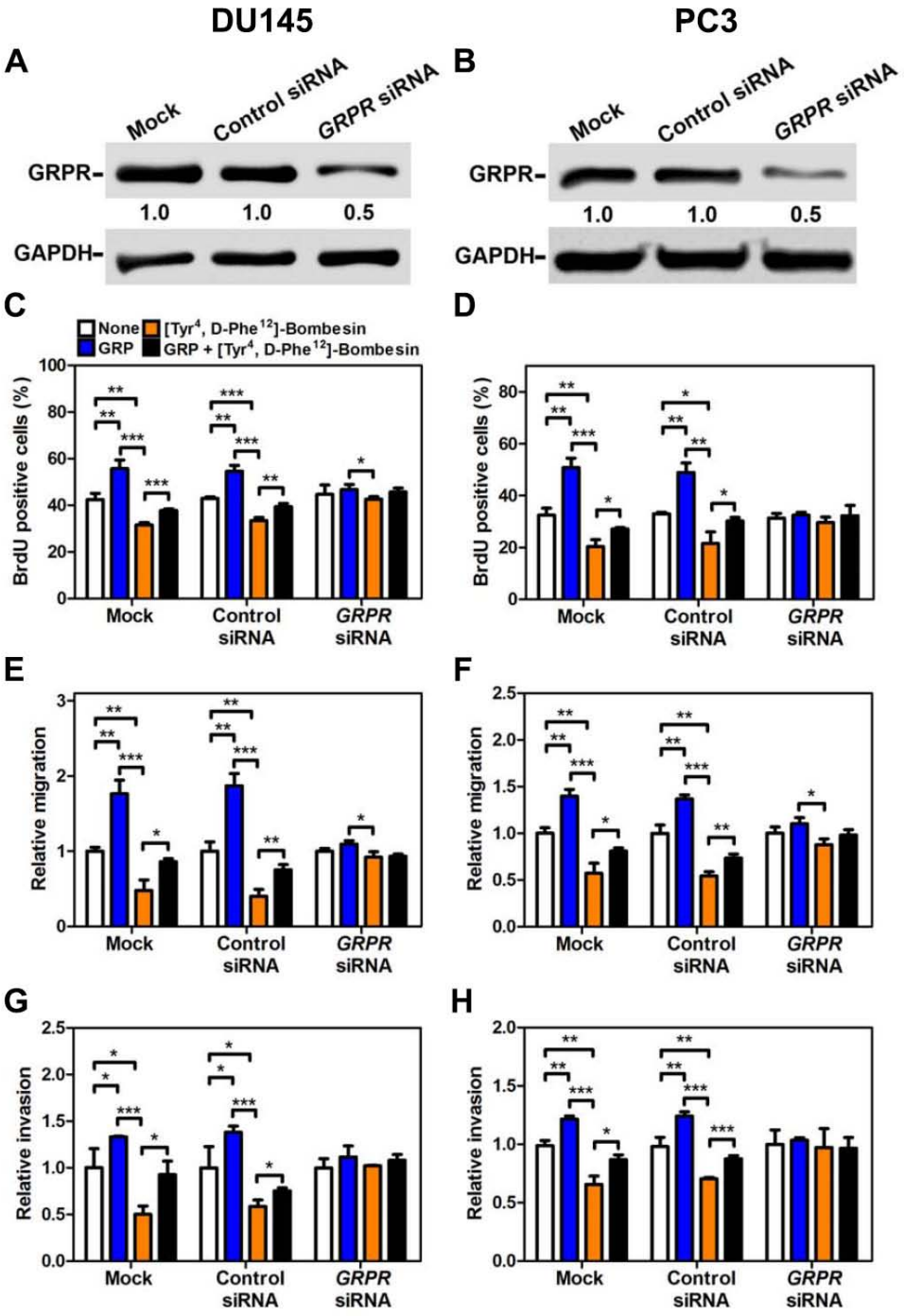

Figure 4.7 GRP promotes activities of human prostate cancer cells. (A-H) Western blot of GRPR expression (A, B) and BrdU positive cells (%) (C, D), migration (E, F), and invasion (G, H) of DU145 (A, C, E, and G) and PC3 (B, D, F, and H) human prostate cancer cells with treatments of GRP and/or [Tyr^4, D-Phe^{12}]-Bombesin are shown. *P<0.05, **P<0.01, ***P<0.001. All error bars denote SD. (A-H) Data represent three independent experiments.

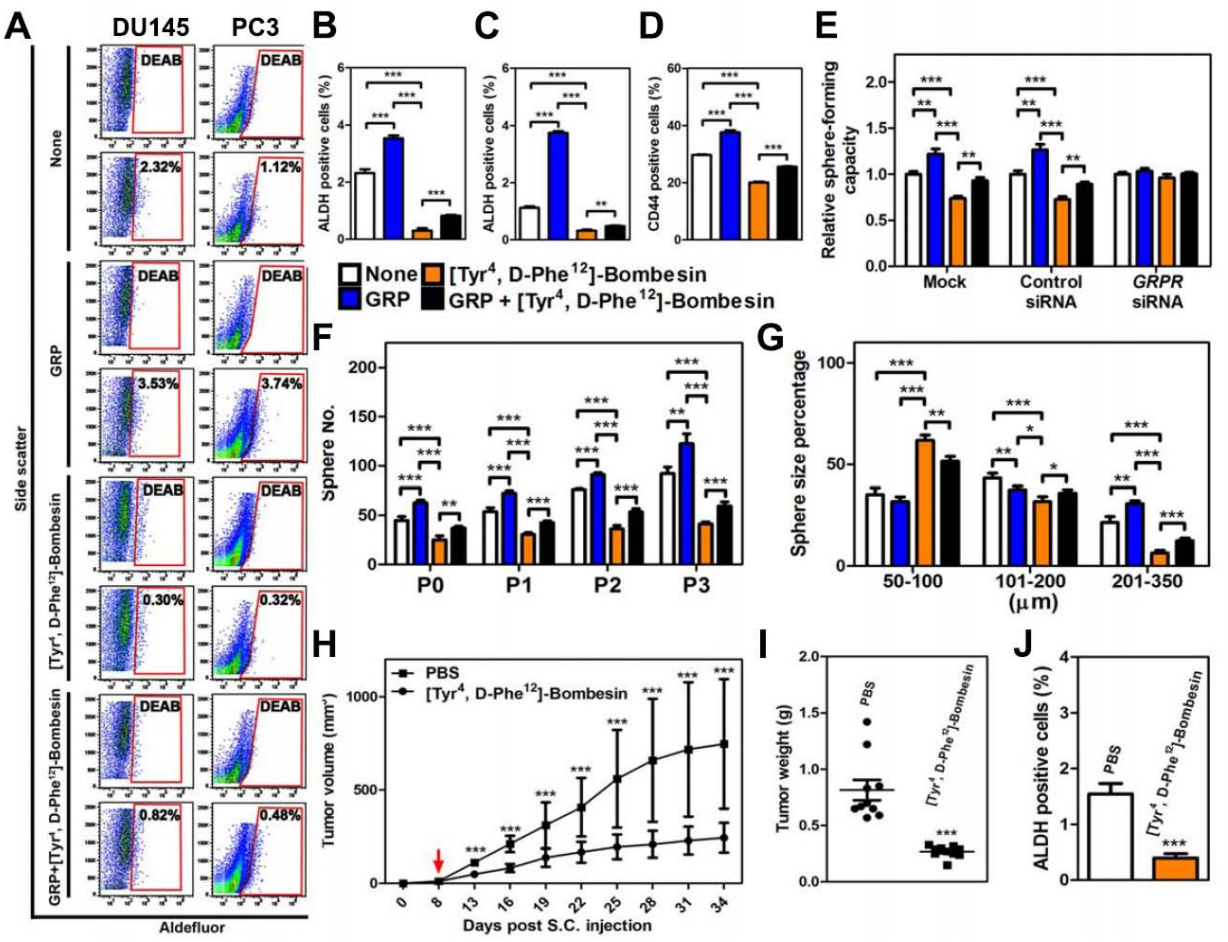

Figure 4.8 GRP promotes activities of human prostate cancer propagating cells. (A-E) ALDEFLUOR assay (A), quantitative analysis of ALDH positive cancer propagating cells (%) of DU145 (B) and PC3 (C), CD44 positive cancer propagating cells (%) of DU145 (D), and sphere-forming capacity of DU145 (E) with treatment of GRP and/or [Tyr^4, D-Phe^{12}]-Bombesin were performed. (A) The number in each red frame represents the percentage of ALDH positive cancer propagating cells. (F, G) Frequency (F) and size (G) of prostaspheres formed by FACS-purified CD44 positive cancer propagating cells of DU45 with treatments of GRP and/or [Tyr^4, D-Phe^{12}]-Bombesin are shown. P0-P3, passages 0-3. (H) Average volume of PC3 tumor xenografts at indicated time points. Red arrow indicates the starting day of i.p. injection of [Tyr^4, D-Phe^{12}]-Bombesin or PBS. (I) Average weight of PC3 tumor xenografts at sacrifice (day 34). (J) ALDH positive cancer propagating cells (%) of PC3 tumor xenografts. *P<0.05, **P<0.01, ***P<0.001. All error bars denote SD. Data represent three independent experiments (A-G), and two groups of five mice with injection of [Tyr^4, D-Phe^{12}]-Bombesin or PBS, respectively (H-J).

4.5 Discussion

It is well established that cancer cells frequently acquire stem cell-like properties. In many cases, such properties are specifically associated with subpopulations of cancer cells known as cancer propagating or cancer stem cells (Greaves and Maley, 2012; Kreso and Dick, 2014; Visvader, 2011). Such cells are characterized by long-term self-renewal, high potential for proliferation, high tumorigenicity, and capacity to generate the whole spectrum of heterogeneity of the original tumors. However, the cell of origin of cancer propagating cells remains far less elucidated and is likely to depend on specific cell lineages affected by carcinogenic events. Some cancer may originate from adult stem/progenitor cells (Cheng et al., 2014; Flesken-Nikitin et al., 2013; Schepers et al., 2012), while others may originate from more differentiated cells (Friedmann-Morvinski et al., 2012; Schwitalla et al., 2013). As our study shows, alterations in specific genes involved in the maintenance of normal adult stem cells may also contribute to defining susceptibility of specific stages of lineage formation to transformation.

Until recently, studies of specific stem/progenitor populations mainly relied on approaches based on isolation of cells according to their display of stem cell-specific markers. However, it has become obvious that many stem cell niches are well defined anatomically (Blanpain et al., 2007; Clevers, 2013; Flesken-Nikitin et al., 2013), thereby allowing histopathological assessment of early neoplastic lesions and laying ground for development of stem cell pathology as a discipline. The mouse prostate represents an attractive subject of such studies. Each mouse prostatic duct consists of a proximal region attached to the urethra, an intermediate region, and a distal tip. Proliferating,

transit-amplifying cells are preferentially located in the distal region of the prostatic ducts, whereas cells with stem cell-like properties, such as low cycling rate, self-renewal, high ex vivo proliferative potential, and androgen withdrawal resistance, mainly reside in the proximal region of the prostatic ducts (Leong et al., 2008; Tsujimura et al., 2002; Wang et al., 2007; Zhou et al., 2007).

Our findings, based on conditional deletion of *Pten* in $CD49f^{hi}/Sca\text{-}1^{+}$ prostate stem/progenitor cells, are consistent with the earlier observations of the role of *Pten* in regulation of the prostate stem/progenitor cell compartment (Dubrovska et al., 2009; Mulholland et al., 2009; Wang et al., 2006). Interestingly, however, PTEN deficiency alone does not lead to pronounced dysplastic lesions in the proximal regions of prostatic ducts. However, combined lack of *Mme* and *Pten* leads to formation of dysplastic lesions and adenocarcinomas in such areas. Furthermore, malignant neoplasms deficient for both genes are more advanced as evidenced by frequent intravascular invasion. Taken together with the effects of *Mme* and *Pten* deficiency on increased number and growth potential of prostate stem/progenitor cells, our observations suggest a critical non-overlapping role of both genes in regulation of prostate stem/progenitor cells and suggests that dysregulation of MME functions may represent a critical step in cancer progression.

In addition to catalytic inactivation of neuropeptides, MME has other, non-catalytic functions affecting cell growth and motility (Sumitomo et al., 2000) (Sumitomo et al., 2004). For example, the cytoplasmic domain of MME interacts with PTEN (Sumitomo et al., 2004). MME recruits endogenous PTEN to the cell membrane, leading to prolonged PTEN protein stability and increased PTEN phosphatase activity, resulting

in downregulation of AKT activity (Sumitomo et al., 2004). At the same time, MME interactions with PTEN may not completely explain MME tumor suppressive functions because levels of MME expression inversely correlate with tumorigenicity of some human prostate cancer cell lines mutant for *PTEN*. For example, low tumorigenic cell line LNCaP has a high level of MME, whereas highly tumorigenic PC3 expresses a low level of MME (Freedland et al., 2003; Witkowski et al., 1993). Furthermore, homozygous deletion of *PTEN* is observed in 33% of MME-deficient cases of human metastatic prostate cancers, according to bioinformatic analysis (Cerami et al., 2012; Gao et al., 2013) of alterations reported in (Taylor et al., 2010). Future studies should determine whether or not non-catalytic functions of MME also play a role in regulation of prostate stem/progenitor cells.

Neuroendocrine cells are important for prostate development (Cheng et al., 2013). However, it remains debatable if an increased number of neuroendocrine cells, as defined by their expression of neuroendocrine markers, such as synaptophysin and calcitonin gene-related peptide, is associated with accelerated progression of prostate adenocarcinoma (Bonkhoff and Berges, 2010; Debes and Tindall, 2004; Hansson and Abrahamsson, 2001, 2003; Sun et al., 2009). Our findings suggest the possibility that MME downregulation mitigates the requirement for neuroendocrine cell expansion in prostate cancers. Indeed, a significantly higher number of neuroendocrine cells was observed in prostate neoplastic lesions of *Pten*$^{PE-/-}$ mice, in agreement with our previous studies (Liao et al., 2007). However, no further increase in the number of such cells was observed in mice also lacking *Mme.* It is possible that accumulation of un-cleaved neuropeptides leads to a feedback inhibition of neuroendocrine cell differentiation.

Further studies should address this possibility, thereby allowing better delineation of the role of neuroendocrine cells in prostate cancer pathogenesis.

Our study provides direct genetic support to previous reports proposing the role of *Mme* as a tumor suppressor gene. Furthermore, it shows that effects of MME on prostate stem/progenitor cells depend on the presence of its downstream effector, GRP. GRP is the mammalian homologue of the amphibian bombesin, which regulates various physiological functions in gastrointestinal and central nervous systems. Its roles relevant to carcinogenesis such as mitosis, morphogenesis, angiogenesis, cell migration, and cell adhesion in different cancers have been reported (Mansi et al., 2013; Patel et al., 2006; Rick et al., 2013). GRP binds with high affinity to GRPR (Jensen et al., 2008), which is one of three mammalian bombesin receptors (Fathi et al., 1993; Gorbulev et al., 1992; Jensen et al., 2008). GRPR is detected in normal, malignant human prostate tissues and prostatic cancer cell lines (LNCaP, DU145, PC-3) and is the only bombesin receptor overexpressed in human prostate cancer (Bartholdi et al., 1998; Fleischmann et al., 2009; Maddalena et al., 2009; Markwalder and Reubi, 1999; Reile et al., 1994; Reubi et al., 2002; Sturzu et al., 2013; Sun et al., 2000; Weber, 2009).

Our study supports earlier observations of general effects of GRP on cell motility and invasion of cancer cells (Hohla and Schally, 2010; Mansi et al., 2013; Stangelberger et al., 2008). However, it also identifies a previously unknown role of GRP in regulation of the prostate stem cell niche and shows that abrogation of GRPR signaling may diminish the pool of cancer propagating cells. These findings offer new insights into the role of neuropeptide-mediated dysregulation in prostate cancer pathogenesis. Furthermore, they provide a rationale for using the MME/GRP pathway

for targeting of cancer propagating cells, perhaps as a part of combinatorial therapy approaches.

REFERENCES

Abou-Kheir, W.G., Hynes, P.G., Martin, P.L., Pierce, R., and Kelly, K. (2010). Characterizing the contribution of stem/progenitor cells to tumorigenesis in the Pten-/- TP53-/- prostate cancer model. Stem cells *28*, 2129-2140.

Adisetiyo, H., Liang, M., Liao, C.P., Aycock-Williams, A., Cohen, M.B., Xu, S., Neamati, N., Conway, E.M., Cheng, C.Y., Nikitin, A.Y.*, et al.* (2013). Loss of survivin in the prostate epithelium impedes carcinogenesis in a mouse model of prostate adenocarcinoma. PloS one *8*, e69484.

Amorino, G.P., and Parsons, S.J. (2004). Neuroendocrine cells in prostate cancer. Crit Rev Eukaryot Gene Expr *14*, 287-300.

Aprikian, A.G., Tremblay, L., Han, K., and Chevalier, S. (1997). Bombesin stimulates the motility of human prostate-carcinoma cells through tyrosine phosphorylation of focal adhesion kinase and of integrin-associated proteins. Int J Cancer *72*, 498-504.

Bartholdi, M.F., Wu, J.M., Pu, H., Troncoso, P., Eden, P.A., and Feldman, R.I. (1998). In situ hybridization for gastrin-releasing peptide receptor (GRP receptor) expression in prostatic carcinoma. Int J Cancer *79*, 82-90.

Blanpain, C., Horsley, V., and Fuchs, E. (2007). Epithelial stem cells: turning over new leaves. Cell *128*, 445-458.

Bonkhoff, H., and Berges, R. (2010). From pathogenesis to prevention of castration resistant prostate cancer. The Prostate *70*, 100-112.

Burger, P.E., Gupta, R., Xiong, X., Ontiveros, C.S., Salm, S.N., Moscatelli, D., and Wilson, E.L. (2009). High aldehyde dehydrogenase activity: a novel functional marker of murine prostate stem/progenitor cells. Stem cells *27*, 2220-2228.

Cairns, P., Okami, K., Halachmi, S., Halachmi, N., Esteller, M., Herman, J.G., Jen, J., Isaacs, W.B., Bova, G.S., and Sidransky, D. (1997). Frequent inactivation of PTEN/MMAC1 in primary prostate cancer. Cancer research *57*, 4997-5000.

Cerami, E., Gao, J., Dogrusoz, U., Gross, B.E., Sumer, S.O., Aksoy, B.A., Jacobsen, A., Byrne, C.J., Heuer, M.L., Larsson, E.*, et al.* (2012). The cBio cancer genomics portal:

an open platform for exploring multidimensional cancer genomics data. Cancer discovery *2*, 401-404.

Chanda, N., Kattumuri, V., Shukla, R., Zambre, A., Katti, K., Upendran, A., Kulkarni, R.R., Kan, P., Fent, G.M., Casteel, S.W.*, et al.* (2010). Bombesin functionalized gold nanoparticles show in vitro and in vivo cancer receptor specificity. Proceedings of the National Academy of Sciences of the United States of America *107*, 8760-8765.

Chen, Z., Trotman, L.C., Shaffer, D., Lin, H.K., Dotan, Z.A., Niki, M., Koutcher, J.A., Scher, H.I., Ludwig, T., Gerald, W.*, et al.* (2005). Crucial role of p53-dependent cellular senescence in suppression of Pten-deficient tumorigenesis. Nature *436*, 725-730.

Cheng, C.Y., Hwang, C.I., Corney, D.C., Flesken-Nikitin, A., Jiang, L., Oner, G.M., Munroe, R.J., Schimenti, J.C., Hermeking, H., and Nikitin, A.Y. (2014). miR-34 Cooperates with p53 in Suppression of Prostate Cancer by Joint Regulation of Stem Cell Compartment. Cell reports *6*, 1000-1007.

Cheng, C.Y., Zhou, Z., and Nikitin, A.Y. (2013). Detection and organ-specific ablation of neuroendocrine cells by synaptophysin locus-based BAC cassette in transgenic mice. PloS one *8*, e60905.

Clevers, H. (2013). The intestinal crypt, a prototype stem cell compartment. Cell *154*, 274-284.

Corney, D.C., Hwang, C.I., Matoso, A., Vogt, M., Flesken-Nikitin, A., Godwin, A.K., Kamat, A.A., Sood, A.K., Ellenson, L.H., Hermeking, H.*, et al.* (2010). Frequent downregulation of miR-34 family in human ovarian cancers. Clin Cancer Res *16*, 1119-1128.

Dai, J., Shen, R., Sumitomo, M., Stahl, R., Navarro, D., Gershengorn, M.C., and Nanus, D.M. (2002). Synergistic activation of the androgen receptor by bombesin and low-dose androgen. Clin Cancer Res *8*, 2399-2405.

Debes, J.D., and Tindall, D.J. (2004). Mechanisms of androgen-refractory prostate cancer. N Engl J Med *351*, 1488-1490.

Dubrovska, A., Kim, S., Salamone, R.J., Walker, J.R., Maira, S.M., Garcia-Echeverria, C., Schultz, P.G., and Reddy, V.A. (2009). The role of PTEN/Akt/PI3K signaling in the maintenance and viability of prostate cancer stem-like cell populations. Proceedings of the National Academy of Sciences of the United States of America *106*, 268-273.

Erdos, E.G., and Skidgel, R.A. (1989). Neutral endopeptidase 24.11 (enkephalinase) and related regulators of peptide hormones. FASEB J *3*, 145-151.

Fathi, Z., Corjay, M.H., Shapira, H., Wada, E., Benya, R., Jensen, R., Viallet, J., Sausville, E.A., and Battey, J.F. (1993). BRS-3: a novel bombesin receptor subtype selectively expressed in testis and lung carcinoma cells. J Biol Chem *268*, 5979-5984.

Fleischmann, A., Waser, B., and Reubi, J.C. (2009). High expression of gastrin-releasing peptide receptors in the vascular bed of urinary tract cancers: promising candidates for vascular targeting applications. Endocr Relat Cancer *16*, 623-633.

Flesken-Nikitin, A., Hwang, C.I., Cheng, C.Y., Michurina, T.V., Enikolopov, G., and Nikitin, A.Y. (2013). Ovarian surface epithelium at the junction area contains a cancer-prone stem cell niche. Nature *495*, 241-245.

Freedland, S.J., Seligson, D.B., Liu, A.Y., Pantuck, A.J., Paik, S.H., Horvath, S., Wieder, J.A., Zisman, A., Nguyen, D., Tso, C.L.*, et al.* (2003). Loss of CD10 (neutral endopeptidase) is a frequent and early event in human prostate cancer. The Prostate *55*, 71-80.

Fridman, R., Benton, G., Aranoutova, I., Kleinman, H.K., and Bonfil, R.D. (2012). Increased initiation and growth of tumor cell lines, cancer stem cells and biopsy material in mice using basement membrane matrix protein (Cultrex or Matrigel) co-injection. Nat Protoc *7*, 1138-1144.

Friedmann-Morvinski, D., Bushong, E.A., Ke, E., Soda, Y., Marumoto, T., Singer, O., Ellisman, M.H., and Verma, I.M. (2012). Dedifferentiation of neurons and astrocytes by oncogenes can induce gliomas in mice. Science *338*, 1080-1084.

Gao, J., Aksoy, B.A., Dogrusoz, U., Dresdner, G., Gross, B., Sumer, S.O., Sun, Y., Jacobsen, A., Sinha, R., Larsson, E.*, et al.* (2013). Integrative analysis of complex cancer genomics and clinical profiles using the cBioPortal. Science signaling *6*, pl1.

Gkonos, P.J., Krongrad, A., and Roos, B.A. (1995). Neuroendocrine peptides in the prostate. Urol Res *23*, 81-87.

Gorbulev, V., Akhundova, A., Buchner, H., and Fahrenholz, F. (1992). Molecular cloning of a new bombesin receptor subtype expressed in uterus during pregnancy. Eur J Biochem *208*, 405-410.

Greaves, M., and Maley, C.C. (2012). Clonal evolution in cancer. Nature *481*, 306-313.

Hansson, J., and Abrahamsson, P.A. (2001). Neuroendocrine pathogenesis in adenocarcinoma of the prostate. Ann Oncol *12 Suppl 2*, S145-152.

Hansson, J., and Abrahamsson, P.A. (2003). Neuroendocrine differentiation in prostatic carcinoma. Scand J Urol Nephrol Suppl, 28-36.

Heinz-Erian, P., Coy, D.H., Tamura, M., Jones, S.W., Gardner, J.D., and Jensen, R.T. (1987). [D-Phe12]bombesin analogues: a new class of bombesin receptor antagonists. Am J Physiol *252*, G439-442.

Hohla, F., and Schally, A.V. (2010). Targeting gastrin releasing peptide receptors: New options for the therapy and diagnosis of cancer. Cell Cycle *9*, 1738-1741.

Hoosein, N.M., Logothetis, C.J., and Chung, L.W. (1993). Differential effects of peptide hormones bombesin, vasoactive intestinal polypeptide and somatostatin analog RC-160 on the invasive capacity of human prostatic carcinoma cells. J Urol *149*, 1209-1213.

Horiguchi, A., Zheng, R., Goodman, O.B., Jr., Shen, R., Guan, H., Hersh, L.B., and Nanus, D.M. (2007). Lentiviral vector neutral endopeptidase gene transfer suppresses prostate cancer tumor growth. Cancer Gene Ther *14*, 583-589.

Iida, K., Zheng, R., Shen, R., and Nanus, D.M. (2012). Adenoviral neutral endopeptidase gene delivery in combination with paclitaxel for the treatment of prostate cancer. Int J Oncol *41*, 1192-1198.

Ittmann, M., Huang, J., Radaelli, E., Martin, P., Signoretti, S., Sullivan, R., Simons, B.W., Ward, J.M., Robinson, B.D., Chu, G.C*., et al.* (2013). Animal models of human prostate cancer: the consensus report of the New York meeting of the Mouse Models of Human Cancers Consortium Prostate Pathology Committee. Cancer research *73*, 2718-2736.

Jensen, R.T., Battey, J.F., Spindel, E.R., and Benya, R.V. (2008). International Union of Pharmacology. LXVIII. Mammalian bombesin receptors: nomenclature, distribution, pharmacology, signaling, and functions in normal and disease states. Pharmacol Rev *60*, 1-42.

Kreso, A., and Dick, J.E. (2014). Evolution of the cancer stem cell model. Cell stem cell *14*, 275-291.

Lawson, D.A., Zong, Y., Memarzadeh, S., Xin, L., Huang, J., and Witte, O.N. (2010). Basal epithelial stem cells are efficient targets for prostate cancer initiation. Proceedings of the National Academy of Sciences of the United States of America *107*, 2610-2615.

Leong, K.G., Wang, B.E., Johnson, L., and Gao, W.Q. (2008). Generation of a prostate from a single adult stem cell. Nature *456*, 804-808.

Lesche, R., Groszer, M., Gao, J., Wang, Y., Messing, A., Sun, H., Liu, X., and Wu, H. (2002). Cre/loxP-mediated inactivation of the murine Pten tumor suppressor gene. Genesis *32*, 148-149.

Li, J., Yen, C., Liaw, D., Podsypanina, K., Bose, S., Wang, S.I., Puc, J., Miliaresis, C., Rodgers, L., McCombie, R.*, et al.* (1997). PTEN, a putative protein tyrosine phosphatase gene mutated in human brain, breast, and prostate cancer. Science *275*, 1943-1947.

Li, T., Su, Y., Mei, Y., Leng, Q., Leng, B., Liu, Z., Stass, S.A., and Jiang, F. (2010). ALDH1A1 is a marker for malignant prostate stem cells and predictor of prostate cancer patients' outcome. Lab Invest *90*, 234-244.

Liao, C.P., Zhong, C., Saribekyan, G., Bading, J., Park, R., Conti, P.S., Moats, R., Berns, A., Shi, W., Zhou, Z.*, et al.* (2007). Mouse models of prostate adenocarcinoma with the capacity to monitor spontaneous carcinogenesis by bioluminescence or fluorescence. Cancer research *67*, 7525-7533.

Lu, B., Gerard, N.P., Kolakowski, L.F., Jr., Bozza, M., Zurakowski, D., Finco, O., Carroll, M.C., and Gerard, C. (1995). Neutral endopeptidase modulation of septic shock. J Exp Med *181*, 2271-2275.

Lukacs, R.U., Goldstein, A.S., Lawson, D.A., Cheng, D., and Witte, O.N. (2010). Isolation, cultivation and characterization of adult murine prostate stem cells. Nat Protoc *5*, 702-713.

Maddalena, M.E., Fox, J., Chen, J., Feng, W., Cagnolini, A., Linder, K.E., Tweedle, M.F., Nunn, A.D., and Lantry, L.E. (2009). 177Lu-AMBA biodistribution, radiotherapeutic efficacy, imaging, and autoradiography in prostate cancer models with low GRP-R expression. J Nucl Med *50*, 2017-2024.

Mansi, R., Fleischmann, A., Macke, H.R., and Reubi, J.C. (2013). Targeting GRPR in urological cancers--from basic research to clinical application. Nat Rev Urol *10*, 235-244.

Markwalder, R., and Reubi, J.C. (1999). Gastrin-releasing peptide receptors in the human prostate: relation to neoplastic transformation. Cancer research *59*, 1152-1159.

Mulholland, D.J., Xin, L., Morim, A., Lawson, D., Witte, O., and Wu, H. (2009). Lin-Sca-1+CD49fhigh stem/progenitors are tumor-initiating cells in the Pten-null prostate cancer model. Cancer research *69*, 8555-8562.

Nagakawa, O., Ogasawara, M., Fujii, H., Murakami, K., Murata, J., Fuse, H., and Saiki, I. (1998). Effect of prostatic neuropeptides on invasion and migration of PC-3 prostate cancer cells. Cancer Lett *133*, 27-33.

Nagakawa, O., Ogasawara, M., Murata, J., Fuse, H., and Saiki, I. (2001). Effect of prostatic neuropeptides on migration of prostate cancer cell lines. Int J Urol *8*, 65-70.

Nikitin, A., and Lee, W.H. (1996). Early loss of the retinoblastoma gene is associated with impaired growth inhibitory innervation during melanotroph carcinogenesis in Rb+/- mice. Genes Dev *10*, 1870-1879.

Osman, I., Yee, H., Taneja, S.S., Levinson, B., Zeleniuch-Jacquotte, A., Chang, C., Nobert, C., and Nanus, D.M. (2004). Neutral endopeptidase protein expression and prognosis in localized prostate cancer. Clin Cancer Res *10*, 4096-4100.

Papandreou, C.N., Usmani, B., Geng, Y., Bogenrieder, T., Freeman, R., Wilk, S., Finstad, C.L., Reuter, V.E., Powell, C.T., Scheinberg, D.*, et al.* (1998). Neutral endopeptidase 24.11 loss in metastatic human prostate cancer contributes to androgen-independent progression. Nat Med *4*, 50-57.

Park, J.H., Walls, J.E., Galvez, J.J., Kim, M., Abate-Shen, C., Shen, M.M., and Cardiff, R.D. (2002). Prostatic intraepithelial neoplasia in genetically engineered mice. The American journal of pathology *161*, 727-735.

Patel, O., Shulkes, A., and Baldwin, G.S. (2006). Gastrin-releasing peptide and cancer. Biochim Biophys Acta *1766*, 23-41.

Patrawala, L., Calhoun-Davis, T., Schneider-Broussard, R., and Tang, D.G. (2007). Hierarchical organization of prostate cancer cells in xenograft tumors: the CD44+alpha2beta1+ cell population is enriched in tumor-initiating cells. Cancer research *67*, 6796-6805.

Patrawala, L., Calhoun, T., Schneider-Broussard, R., Li, H., Bhatia, B., Tang, S., Reilly, J.G., Chandra, D., Zhou, J., Claypool, K.*, et al.* (2006). Highly purified CD44+ prostate cancer cells from xenograft human tumors are enriched in tumorigenic and metastatic progenitor cells. Oncogene *25*, 1696-1708.

Pinski, J., Schally, A.V., Halmos, G., and Szepeshazi, K. (1993). Effect of somatostatin analog RC-160 and bombesin/gastrin releasing peptide antagonist RC-3095 on growth of PC-3 human prostate-cancer xenografts in nude mice. Int J Cancer *55*, 963-967.

Reile, H., Armatis, P.E., and Schally, A.V. (1994). Characterization of high-affinity receptors for bombesin/gastrin releasing peptide on the human prostate cancer cell lines PC-3 and DU-145: internalization of receptor bound 125I-(Tyr4) bombesin by tumor cells. The Prostate *25*, 29-38.

Reubi, J.C., Wenger, S., Schmuckli-Maurer, J., Schaer, J.C., and Gugger, M. (2002). Bombesin receptor subtypes in human cancers: detection with the universal radioligand (125)I-[D-TYR(6), beta-ALA(11), PHE(13), NLE(14)] bombesin(6-14). Clin Cancer Res *8*, 1139-1146.

Rick, F.G., Abi-Chaker, A., Szalontay, L., Perez, R., Jaszberenyi, M., Jayakumar, A.R., Shamaladevi, N., Szepeshazi, K., Vidaurre, I., Halmos, G.*, et al.* (2013). Shrinkage of experimental benign prostatic hyperplasia and reduction of prostatic cell volume by a gastrin-releasing peptide antagonist. Proceedings of the National Academy of Sciences of the United States of America *110*, 2617-2622.

Salm, S.N., Burger, P.E., Coetzee, S., Goto, K., Moscatelli, D., and Wilson, E.L. (2005). TGF-{beta} maintains dormancy of prostatic stem cells in the proximal region of ducts. J Cell Biol *170*, 81-90.

Schepers, A.G., Snippert, H.J., Stange, D.E., van den Born, M., van Es, J.H., van de Wetering, M., and Clevers, H. (2012). Lineage tracing reveals Lgr5+ stem cell activity in mouse intestinal adenomas. Science *337*, 730-735.

Schwitalla, S., Fingerle, A.A., Cammareri, P., Nebelsiek, T., Goktuna, S.I., Ziegler, P.K., Canli, O., Heijmans, J., Huels, D.J., Moreaux, G.*, et al.* (2013). Intestinal tumorigenesis initiated by dedifferentiation and acquisition of stem-cell-like properties. Cell *152*, 25-38.

Shappell, S.B., Thomas, G.V., Roberts, R.L., Herbert, R., Ittmann, M.M., Rubin, M.A., Humphrey, P.A., Sundberg, J.P., Rozengurt, N., Barrios, R.*, et al.* (2004). Prostate pathology of genetically engineered mice: definitions and classification. The consensus

report from the Bar Harbor meeting of the Mouse Models of Human Cancer Consortium Prostate Pathology Committee. Cancer research *64*, 2270-2305.

Shipp, M.A., and Look, A.T. (1993). Hematopoietic differentiation antigens that are membrane-associated enzymes: cutting is the key! Blood *82*, 1052-1070.

Shultz, L.D., Lyons, B.L., Burzenski, L.M., Gott, B., Chen, X., Chaleff, S., Kotb, M., Gillies, S.D., King, M., Mangada, J.*, et al.* (2005). Human lymphoid and myeloid cell development in NOD/LtSz-scid IL2R gamma null mice engrafted with mobilized human hemopoietic stem cells. Journal of immunology *174*, 6477-6489.

Siegel, R., Ma, J., Zou, Z., and Jemal, A. (2014). Cancer statistics, 2014. CA: a cancer journal for clinicians *64*, 9-29.

Stangelberger, A., Schally, A.V., and Djavan, B. (2008). New treatment approaches for prostate cancer based on peptide analogues. Eur Urol *53*, 890-900.

Sturzu, A., Sheikh, S., Echner, H., Nagele, T., Deeg, M., Amin, B., Schwentner, C., Horger, M., Ernemann, U., and Heckl, S. (2013). Rhodamine-marked bombesin: a novel means for prostate cancer fluorescence imaging. Invest New Drugs.

Sumitomo, M., Iwase, A., Zheng, R., Navarro, D., Kaminetzky, D., Shen, R., Georgescu, M.M., and Nanus, D.M. (2004). Synergy in tumor suppression by direct interaction of neutral endopeptidase with PTEN. Cancer Cell *5*, 67-78.

Sumitomo, M., Milowsky, M.I., Shen, R., Navarro, D., Dai, J., Asano, T., Hayakawa, M., and Nanus, D.M. (2001). Neutral endopeptidase inhibits neuropeptide-mediated transactivation of the insulin-like growth factor receptor-Akt cell survival pathway. Cancer research *61*, 3294-3298.

Sumitomo, M., Shen, R., Walburg, M., Dai, J., Geng, Y., Navarro, D., Boileau, G., Papandreou, C.N., Giancotti, F.G., Knudsen, B.*, et al.* (2000). Neutral endopeptidase inhibits prostate cancer cell migration by blocking focal adhesion kinase signaling. The Journal of clinical investigation *106*, 1399-1407.

Sun, B., Halmos, G., Schally, A.V., Wang, X., and Martinez, M. (2000). Presence of receptors for bombesin/gastrin-releasing peptide and mRNA for three receptor subtypes in human prostate cancers. The Prostate *42*, 295-303.

Sun, Y., Niu, J., and Huang, J. (2009). Neuroendocrine differentiation in prostate cancer. Am J Transl Res *1*, 148-162.

Taylor, B.S., Schultz, N., Hieronymus, H., Gopalan, A., Xiao, Y., Carver, B.S., Arora, V.K., Kaushik, P., Cerami, E., Reva, B.*, et al.* (2010). Integrative genomic profiling of human prostate cancer. Cancer Cell *18*, 11-22.

Trotman, L.C., Niki, M., Dotan, Z.A., Koutcher, J.A., Di Cristofano, A., Xiao, A., Khoo, A.S., Roy-Burman, P., Greenberg, N.M., Van Dyke, T.*, et al.* (2003). Pten dose dictates cancer progression in the prostate. PLoS biology *1*, E59.

Tsujimura, A., Koikawa, Y., Salm, S., Takao, T., Coetzee, S., Moscatelli, D., Shapiro, E., Lepor, H., Sun, T.T., and Wilson, E.L. (2002). Proximal location of mouse prostate epithelial stem cells: a model of prostatic homeostasis. J Cell Biol *157*, 1257-1265.

Uchida, K., Masumori, N., Takahashi, A., Itoh, N., Kato, K., Matusik, R.J., and Tsukamoto, T. (2006). Murine androgen-independent neuroendocrine carcinoma promotes metastasis of human prostate cancer cell line LNCaP. The Prostate *66*, 536-545.

Visvader, J.E. (2011). Cells of origin in cancer. Nature *469*, 314-322.

Wang, G.M., Kovalenko, B., Wilson, E.L., and Moscatelli, D. (2007). Vascular density is highest in the proximal region of the mouse prostate. The Prostate *67*, 968-975.

Wang, S., Gao, J., Lei, Q., Rozengurt, N., Pritchard, C., Jiao, J., Thomas, G.V., Li, G., Roy-Burman, P., Nelson, P.S.*, et al.* (2003). Prostate-specific deletion of the murine Pten tumor suppressor gene leads to metastatic prostate cancer. Cancer Cell *4*, 209-221.

Wang, S., Garcia, A.J., Wu, M., Lawson, D.A., Witte, O.N., and Wu, H. (2006). Pten deletion leads to the expansion of a prostatic stem/progenitor cell subpopulation and tumor initiation. Proceedings of the National Academy of Sciences of the United States of America *103*, 1480-1485.

Weber, H.C. (2009). Regulation and signaling of human bombesin receptors and their biological effects. Curr Opin Endocrinol Diabetes Obes *16*, 66-71.

Witkowski, C.M., Rabinovitz, I., Nagle, R.B., Affinito, K.S., and Cress, A.E. (1993). Characterization of integrin subunits, cellular adhesion and tumorgenicity of four human prostate cell lines. J Cancer Res Clin Oncol *119*, 637-644.

Wu, X., Wu, J., Huang, J., Powell, W.C., Zhang, J., Matusik, R.J., Sangiorgi, F.O., Maxson, R.E., Sucov, H.M., and Roy-Burman, P. (2001). Generation of a prostate epithelial cell-specific Cre transgenic mouse model for tissue-specific gene ablation. Mechanisms of development *101*, 61-69.

Zheng, R., Iwase, A., Shen, R., Goodman, O.B., Jr., Sugimoto, N., Takuwa, Y., Lerner, D.J., and Nanus, D.M. (2006). Neuropeptide-stimulated cell migration in prostate cancer cells is mediated by RhoA kinase signaling and inhibited by neutral endopeptidase. Oncogene *25*, 5942-5952.

Zhou, Z., Flesken-Nikitin, A., Corney, D.C., Wang, W., Goodrich, D.W., Roy-Burman, P., and Nikitin, A.Y. (2006). Synergy of p53 and Rb deficiency in a conditional mouse model for metastatic prostate cancer. Cancer research *66*, 7889-7898.

Zhou, Z., Flesken-Nikitin, A., and Nikitin, A.Y. (2007). Prostate cancer associated with p53 and Rb deficiency arises from the stem/progenitor cell-enriched proximal region of prostatic ducts. Cancer research *67*, 5683-5690.

CHAPTER 5

SUMMARY AND FUTURE DIRECTIONS

5.1 Summary

In chapter 2, in order to dissect the precise role of miR-34 in vivo, we generated mice with *mir-34* conventional and conditional targeted mutations. Unexpectedly, mice with conventional and prostate epithelium conditional inactivation of *mir-34* did not give rise to neoplastic lesions up to 18 months old, consistent with the previous study by Ventura group (Concepcion et al., 2012). This observation also has shown that loss of miR-34 is not as critical as loss of p53 (Donehower et al., 1992; Jacks et al., 1994) in the initiation of carcinogenesis (Chapter 1.3.3). Various studies have suggested that miR-34 may be regulated by a p53-independent pathway (Chapter 1.3.4). To test this possibility, we conditionally deleted both *p53* and *mir-34* in the prostate epithelium in mice and found development of early invasive adenocarcinoma and high-grade prostatic intraepithelial neoplasia in the proximal and distal regions of prostatic ducts, respectively, whereas no such lesions were observed after inactivation of *mir-34* or *p53* genes alone. This piece of evidence not only clarified the tumor suppressor role of miR-34 but also p53-indepentdent function of miR-34 in vivo. Consistent with our previous finding of a feedforward loop regulation of MET by a dual miR-34/p53 mechanism (Hwang et al., 2011), combined deficiency of p53 and miR-34 leads to acceleration of MET-dependent growth, self-renewal, and motility of prostate stem/progenitor cells, and thus alterations

in joint regulation of stem cell compartment may lead to cancer. MET inhibitors may be an important component of targeting prostate CPCs, particularly in the context of combined p53 and miR-34 deficiency. Taken together, the miR-34-centered regulatory network independent of p53 emerges. It is of interest to further study the cooperative interaction of p53/miR-34/MET in stem/progenitor cells of other cell lineages. Furthermore, it would also be interesting to verify if any other targets are under p53/miR-34 dual regulation. Gaining insight into the p53-miR-34 circuit may bring value for clinical diagnosis and therapy in cancer prevention and treatment in future.

The precise functions of NE cells in prostate development and carcinogenesis are not well understood. In chapter 3, we have generated the transgenic mice, Tg(*Syp-EGFP^{loxP}-DTA)147^{Ayn}* (*SypELDTA*), in which DTA is driven by the *Syp* promoter, suitable for flexible tissue-specific ablation of NE cells. By crossing the *SypELDTA* mouse line with prostate epithelium-specific expressing Cre mice, *PB-Cre4,* we have shown a substantial decrease in the number of NE cells and associated prostate hypotrophy, suggesting that NE cells play an important role in prostate development. The *Syp*-containing BAC cassette and generated mice should provide useful tools for studies of NE cell biological roles in development and maintenance of various tissues and organs. Furthermore, this transgenic line can be used to study the role of NE cells in carcinogenesis by crossing with other established mouse cancer lines with preferential NE cell differentiation.

To further study the role of NE cells and their secreted neuropeptides in prostate carcinogenesis, the *Mme*-null mouse model was chosen in chapter 4. Deficiency of MME, the enzyme responsible for metabolism of neuropeptides, is associated with poor

prostate cancer prognosis (Freedland et al., 2003; Osman et al., 2004; Papandreou et al., 1998). However, mice deficient for *Mme* did not develop prostate cancer by 18 months of age, and so its role in prostate carcinogenesis remains insufficiently elucidated. Here, we report that in the autochthonous mouse model of prostate cancer associated with *Pten* deficiency, lack of *Mme* leads to expansion of the neoplastic lesions with increased proliferation and accelerated carcinogenesis, especially in the prostate stem cell-enriched niche. The pathological lesions may result from aberrant regulation of prostate stem cell activities, such as stem cell pool expansion, growth, and self-renewal. To understand the mechanisms by which large MME deficiency may affect the regulation of stem cell activities, GRP, one of the main MME substrates, has been tested in mouse prostate stem cells and human prostate CPCs. Consistently, GRP can expand pool, growth, and self-renewal of mouse prostate *Pten*-deficient stem cells and human prostate CPCs and can be successfully blocked by GRP antagonist, [Tyr^4, D-Phe^{12}]-Bombesin. Importantly, [Tyr^4, D-Phe^{12}]-Bombesin can inhibit growth of human xenografts and lead to decreased pool of CPCs in formed tumors. In summary, our results show a GRP-mediated effect of MME deficiency in control of prostate stem and CPCs, and suggest that GRPR antagonists may be an important component of targeting CPCs, particularly in the context of Pten deficiency.

5.2 Future Directions

5.2.1 p53/miR-34/Met pathway in stem cells and early carcinogenesis

MET plays an important role in growth, survival, motility, invasion, and metastasis in cancers (Birchmeier et al., 2003; Trusolino et al., 2010; Trusolino and Comoglio, 2002), and its overexpression is associated with poor prognosis in several different types of cancers, including prostate cancer (Di Renzo et al., 1994; Di Renzo et al., 1995a; Di Renzo et al., 1995b; Ferracini et al., 1995; Humphrey et al., 1995; Morello et al., 2001; Natali et al., 1996; Olivero et al., 1996; Takeo et al., 2001; Taniguchi et al., 1998). Our previous finding indicates that p53 has miR-34-dependent and miR-34-independent mechanisms to control MET expression by feedforward loop regulation (Hwang et al., 2011). In Chapter 2, by using the autochthonous model of cancer, we also found that p53-dependent and p53-independent miR-34 functions may cooperate to inhibit MET expression in the stem cell compartment, jointly suppressing prostate carcinogenesis. Therefore, it would be of interest to further study differential MET expression and prognosis combined with *p53* and *mir-34* status in human prostate cancer specimens. In addition, given our findings and studies by others, it is becoming increasingly obvious that MET is also involved in regulation of stem/progenitor cells and CPCs in different tissues (Boccaccio and Comoglio, 2006; De Bacco et al., 2012; Forte et al., 2006; Joo et al., 2012; Li et al., 2011a; Li et al., 2011b; Nicoleau et al., 2009; Rajasekhar et al., 2011; Son et al., 2006; Suzuki et al., 2004; Tesio et al., 2011; Vermeulen et al., 2010; Yoshioka et al., 2013). Therefore, it would be interesting to test if p53/miR-34 feedforward loop regulation of the MET-dependent stem/progenitor cell pool is also present in other types of normal and neoplastic cells. Such study could be performed by tissue-specific inactivation of *p53* and *mir-34*. It is also worth noting that our histopathological studies of the mouse model with prostate epithelium-specific

inactivation of *p53* and *mir-34* indicate that neoplastic lesions are already present during the early stages of carcinogenesis. Thus therapeutic targeting of MET in both p53 and miR-34 deficient cells might be effective from the earliest stages of prostate cancer.

5.2.2 Generation of the knockin mouse model for NE cell ablation

In Chapter 3, although we used the BAC construct, likely containing all the cis-elements of the *Syp* locus, to make the transgenic mouse model (Yang and Gong, 2005), the stochastic insertion of the transgene, which might affect functions of other genes, may become a concern for our mouse model. To avoid this problem, knockin mice would be a better option to study the exogenous expression of the given protein driven by the endogenous *Syp* promoter. In this way, the genetic environment surrounding the transgene can be controlled completely, and the transgene will not incorporate into random locations. Thus, we would be more certain that any resulting phenotype is due to the exogenous expression of the transgene because a targeted transgene is not interfering with any other critical loci. More importantly, site-specific knockin results in a more consistent level of expression of the transgene from generation to generation because the transgene is under the control of the endogenous *Syp* promoter.

Another potential probelm with our mouse model is presence of DTA in the transgenic construct. It has been shown that one molecule of DTA is sufficient to kill the cell, indicating high toxicity of DTA (Yamaizumi et al., 1978). The advantage of high toxicity is that even low DTA expression can have efficient cell ablation. However, nonspecific leakage of DTA expression, even at a low level, may jeopardize mouse

embryogenesis and phenotype as well as the outcome of following experiments. Although we did not observe significant cell death in luminal and basal cells in any regions of the prostate due to a tight regulation of the *Syp* promoter in prostate non-NE epithelium cells (Figure 3.18), the issue cannot be completely ruled out in the prostate and/or other organs. Use of diphtheria toxin receptor (DTR) has become an alternative method (Buch et al., 2005; Cha et al., 2003; Saito et al., 2001). The advantage of this method is not only that DTR itself is not toxic, but also spatio-temporal cell ablation can be manipulated by injecting DT, leading to the death of the DTR positive cells in the given tissue by crossing with tissue-specific Cre-expressing mice. The DTR approach has been extensively applied to different mouse models (Luquet et al., 2005; Rother et al., 2012; Thorel et al., 2010; Tian et al., 2011; Tittel et al., 2012). However, there have been reports of DT toxicity in long-term mouse experiments (Tian et al., 2011). Thus, DTA and DTR approaches may complement each other.

In our case, we can knockin the *loxP-EGFP-Neo cassette-Stop-loxP-DTR-bpA* before exon 1 of the *Syp* locus by homologous recombination to generate Cre-inducible DTR knockin mice in which Cre-mediated excision of a *Stop* cassette renders SYP-positive cells sensitive to DT (Figure 5.1). Thus, ablating prostate NE cells can be achieved by crossing newly generated knockin mice with *ARR$_2$PB-Cre* mice (Wu et al., 2001) or tamoxifen-inducible *ARR$_2$PB-Cre-ER(T2)* mice (Birbach et al., 2009; Luchman et al., 2008), allowing us to study the role of NE cells in prostate development accurately. Furthermore, crossing these knockin mice with prostate cancer mouse models with preferential NE differentiation, such as *Pten* knockout mice (Chen et al., 2005; Liao et al., 2007; Trotman et al., 2003; Wang et al., 2003), TRAMP mice (Gingrich

et al., 1996; Kaplan-Lefko et al., 2003), or LADY mice (Kasper et al., 1998; Masumori et al., 2001), could also allow us to examine the role of NE cells in prostate carcinogenesis.

5.2.3 Cell origin of NE cell lineage and NE cell differentiated prostate cancer

Lineage tracing is a tool to study stem cell hierarchy. Recent studies of cell fate based on lineage tracing have revealed the existence of multipotent basal stem/progenitor cells, unipotent basal cells, and luminal stem/progenitor cells (Choi et al., 2012; Liu et al., 2011b; Ousset et al., 2012; Wang et al., 2009a; Wang et al., 2013). Although some evidence supports the notion that NE cells originate from basal stem/progenitor cells (Leong et al., 2008; Ousset et al., 2012; Wang et al., 2013) or luminal stem/progenitor cells (Wang et al., 2009a), whether or not there are unipotent or even multipotent NE stem/progenitor cells residing in the prostate stem cell hierarchy is still an open question. Inspired by the studies above, we can generate the NE cell-specific inducible Cre mice (*Syp-CreERT2*) in which CreER is driven by the promoter of *Syp*, a NE cell marker. In addition, the *mTmG* mouse line is a double fluorescent reporter line that replaces the expression of a membrane-targeted Tomato-Red (mT) protein with a membrane-targeted enhanced green fluorescence protein (mG) upon Cre-*loxP*-mediated homologous recombination (Muzumdar et al., 2007). After breeding of the double fluorescent reporter line *mTmG* with *Syp-CreER* mice to generate *Syp-CreER; mTmG* mice, NE cell lineage can be traced by GFP expression after a tamoxifen pulse. Thus, to determine the fate of prostate NE cells, we are able to induce prostate epithelial turnover by the regression-regeneration assay as schematically illustrated in

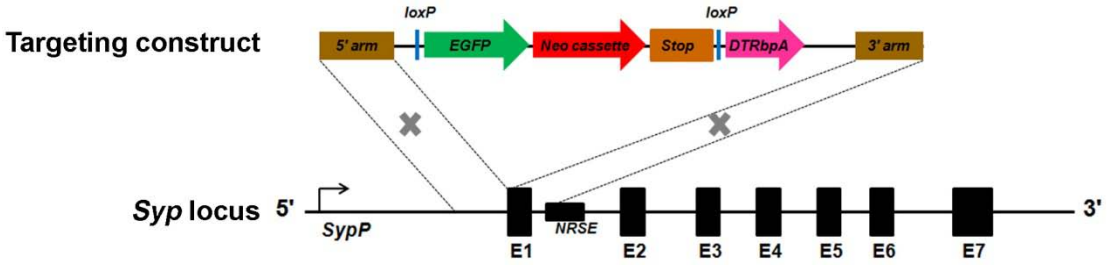

Figure 5.1 Generation of the Cre-inducible DTR knockin mouse model. (A) The targeting strategy was to knockin the *loxP-EGFP-Neo cassette-Stop-loxP-DTR-bpA* before the exon 1 of *Syp* locus by homologous recombination. *SypP*: *synaptophysin* promoter. *NRSE*: neuro-restrictive suppressor element. *DTR*: *diphtheria toxin receptor*.

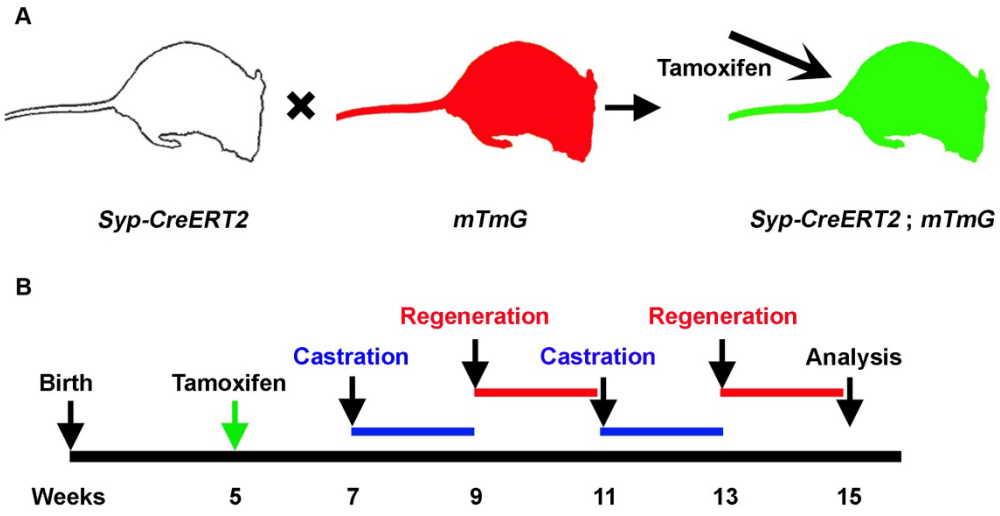

Figure 5.2 Schematic illustration of the lineage-tracing strategy. (A) After crosses of *Syp-CreERT2* mice and *mTmG* reporter mice, NE cell lineage can be traced by GFP expression after tamoxifen administration in *Syp-CreERT2; mTmG* mice. (B) Timeline for androgen deprivation and replacement experiments.

Figure 5.2. In response to fluctuating serum testosterone levels, epithelial cell turnover is induced after cycles of prostate regression-regeneration. Immunofluorescence analyses of luminal (K8), basal (K5), as well as NE (SYP) cells can be applied to examine co-expression of GFP with these three markers, which may illustrate the hierarchy of NE cell lineage.

Likewise, the cell of origin of prostate cancer with NE differentiation remains to be established. Previously, it has been proposed that NE cells are the result of trans-differentiation from predominant luminal cells within prostate adenocarcinoma. For example, clinical genetic analysis showed that prostate cancer cells with NE differentiation have allelic profiles identical to non-NE prostate cancer cells but distinct from those of the normal prostatic epithelium or normal NE cells (Sauer et al., 2006). Two human prostatic small cell carcinoma cell lines, NCI-H660 (Carney et al., 1985) and PSK-1 (Kim et al., 2000), in which NE cells are the predominant cell type, express K8/18 (luminal cell markers) but not K5/14 (basal cell markers) (van Bokhoven et al., 2003). Our lab also detected co-expression of luminal cell marker (K8, AR) and NE cell marker (SYP, CgA) in neoplastic cells of the mouse model with prostate epithelium-specific deletion of *p53* and *Rb* (Zhou et al., 2007) and *Pten* (Liao et al., 2007). Moreover, accumulating cell culture studies showed that luminal cells in prostate cancer cell lines can acquire NE phenotype under certain conditions (Chapter 1.4.2). Collectively, these results suggest that luminal cells could trans-differentiate into NE cells in prostate cancer. However, some studies using cell lineage-specific Cre lines did not show that prostate cancer arising from luminal cells (*Nkx3-1*$^{CreERT2/+}$*; Pten*$^{flox/flox}$, *K8-CreERT2*$^{Tg/wt}$*; Pten*$^{flox/flox}$) or basal cells (*K14-CreER*$^{Tg/Tg}$*; Pten*$^{flox/flox}$) with *Pten* deletion

could trans-differentiate to the NE phenotype (Choi et al., 2012; Wang et al., 2009a; Wang et al., 2013). Since those results are inconsistent with findings of NE cells in prostatic neoplasms in *ARR$_2$PB-Cre; Pten$^{flox/flox}$* mice (Liao et al., 2007), additional lineage tracing studies of prostate stem cell fate with particular attention to the proximal regions of prostatic ducts are well-merited. Another possibility is that NE cells themselves could represent a target of oncogenic transformation in prostate cancer. To investigate these hypotheses, we may generate the mouse model with targeted deletion of the *Pten* in NE cells (*Syp-CreERT2; Pten$^{flox/flox}$*). Tamoxifen would be administered to 8-week-old *Syp-CreERT2; Pten$^{flox/flox}$* mice so that *Pten* is specifically disrupted in prostate NE cells. The *ARR$_2$PB-Cre; Pten$^{flox/flox}$* mouse model for prostate cancer can be used as a positive control, in which *ARR$_2$PB* can drive Cre expression to ablate *Pten* in luminal, basal, and NE cells (Cheng et al., 2013; Lawson et al., 2010; Liao et al., 2007; Wang et al., 2006; Zhang et al., 2010).

5.2.4 The role of neuropeptides in induction of senescence in Pten-deficient neoplasms

Senescence is a hallmark of aging and opposing cancer progression (Campisi, 2013; Collado and Serrano, 2010; Prieur and Peeper, 2008; Rodier and Campisi, 2011). MME activity increases with age in the brain (Miners et al., 2010), and its expression is upregulated during the replicative senescence of human skin fibroblasts (Morisaki et al., 2010) and in human lung fibroblasts (Kletsas et al., 1998), suggesting neuropeptides might play a role in senescence response.

Conditional inactivation of *Pten* in prostate epithelium caused cellular senescence, restricting carcinogenesis but was rescued by concomitant loss of *p53* (Chen et al., 2005). By p53 IHC (Figure 5.3A, E, I, M, Q), p53 expression is low in WT (Figure 5.3A) and *Mme*$^{-/-}$ (Figure 5.3E) prostates. Consistent with previous reports, p53 is upregulated after *Pten* inactivation, which has increased accumulation of p53 in the nuclei of prostate epithelial cells in the *Pten*$^{PE-/-}$ prostate (Figure 5.3I), but p53 is downregulated after MME loss in the *Mme*$^{-/-}$*Pten*$^{PE-/-}$ prostate (Figure 5.3M). Expression status of senescence-associated markers, such as senescence-associated beta-galactosidase (SA-β-Gal) (Figure 5.3B, F, J, N, R), p16^{INK4a} (Figure 5.3C, G, K, O, S), p27^{Kip1} (Figure 5.3D, H, L, P, T), and p21^{Cip1} (Figure 5.4) was studied (Bringold and Serrano, 2000; Kuilman et al., 2010). Similar to p53 expression, expression level of SA-β-Gal (Figure 5.3J, N, R), p16^{INK4a} (Figure 5.3K, O, S), and p27^{Kip1} (Figure 5.3L, P, T) is upregulated in the *Pten*$^{PE-/-}$ (Figure 5.3J, K, L) prostate but downregulated with concomitant MME loss in the *Mme*$^{-/-}$*Pten*$^{PE-/-}$ prostate (Figure 5.3N, O, P). Interestingly, p27^{Kip1} expression of the *Mme*$^{-/-}$ prostate is comparable to that of the *Pten*$^{PE-/-}$ prostate (Figure 5.3H, L, T), suggesting a synergistic effect of PTEN and MME loss on suppressing p27^{Kip1} expression. However, cytoplasmic p21^{Cip1} expression increases in the *Mme*$^{-/-}$*Pten*$^{PE-/-}$ prostate compared to the *Pten*$^{PE-/-}$ prostate (Figure 5.4). Taken together, MME loss can rescue the senescence in *Pten*-deficient tumors, possibly through suppressing the p16^{INK4a}/Rb pathway and the PTEN/p27^{Kip1} pathway, but not the p53/p21^{Cip1} pathway (Bringold and Serrano, 2000), although p53 is downregulated in *Mme*$^{-/-}$*Pten*$^{PE-/-}$ prostate (Figure 5.3M). Overexpression and associated cytoplasmic accumulation of p21^{Cip1} has been found in many human cancers and is correlated with aggressive tumors and poor

prognosis, including in prostate cancer (Abbas and Dutta, 2009). Thus, *Mme*$^{-/-}$*Pten*$^{PE-/-}$ prostates exhibit prominent cytoplasmic expression of p21 in our model, which might be indicative of aggressive carcinogenesis.

So far our preliminary results did not show significant differences in senescence after treatment with GRP and/or its antagonist, [Tyr^4, D-Phe^{12}]-Bombesin, on CD44-positive DU145 human prostate CPCs (Figure 5.5). It may suggest that the senescent mechanism is important only in some types of neoplasms and/or at specific stages of cancer progression. Alternatively, other neuropeptides processed by MME or neuropeptide-catalysis-independent functions of MME play a role in senescence response. Therefore, it will be of interest to further investigate the effects of NE signaling on senescence in human cancers stratified according to their histological and molecular features and stage of progression. Such research may lead to identification of new therapeutic targets responsive to the effects of neuropeptides.

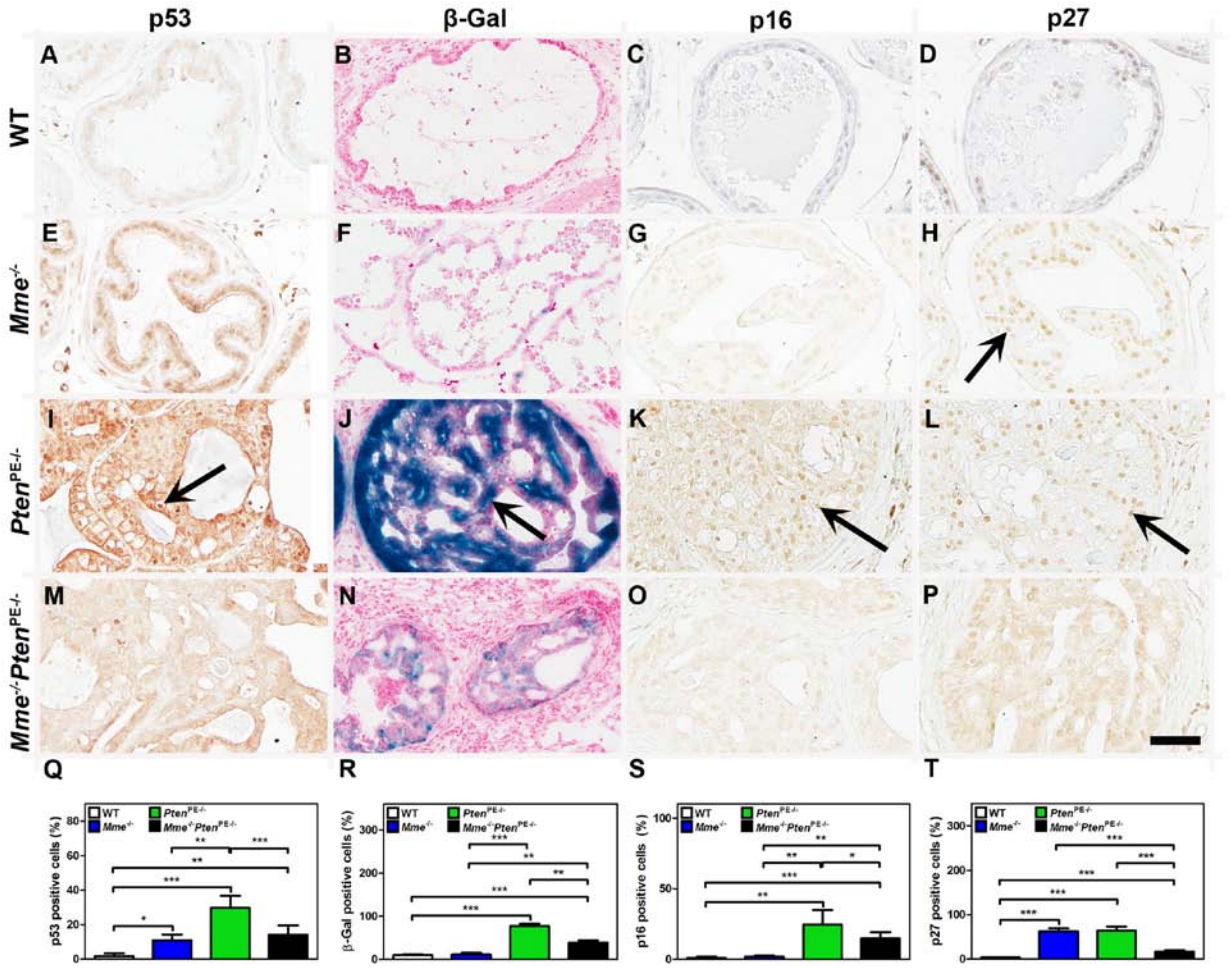

Figure 5.3 MME loss rescues cellular senescence in *Pten*-deficient prostate neoplastic lesions. (A-T) p53 (A, E, I, M), β-Gal (B, F, J, N), p16 (C, G, K, O), p27 (D, H, L, P) immunostaining and quantitative analysis of p53 (Q), β-Gal © p16 (S), p27 (T) positive cells in prostates of aged-matched WT (A-D), *Mme*$^{-/-}$ (E-H), *Pten*$^{PE-/-}$ (I-L) and *Mme*$^{-/-}$*Pten*$^{PE-/-}$ (M-P) mice (n=3). (A, C, D, E, G, H, I, K, L, M, O, P) ABC Elite method, methyl green counterstain. (B, F, J, N) Nuclear fast blue counterstain. Arrows indicate p53 (I), β-Gal (J), p16 (K), and p27 (H, L) positive cells. Scale bar: 50 μm (A, C, D, E, G, H, I, K, L, M, O, P), 100 μm (B, F, J, N). *P<0.05, **P<0.01, ***P<0.001. All error bars denote SD.

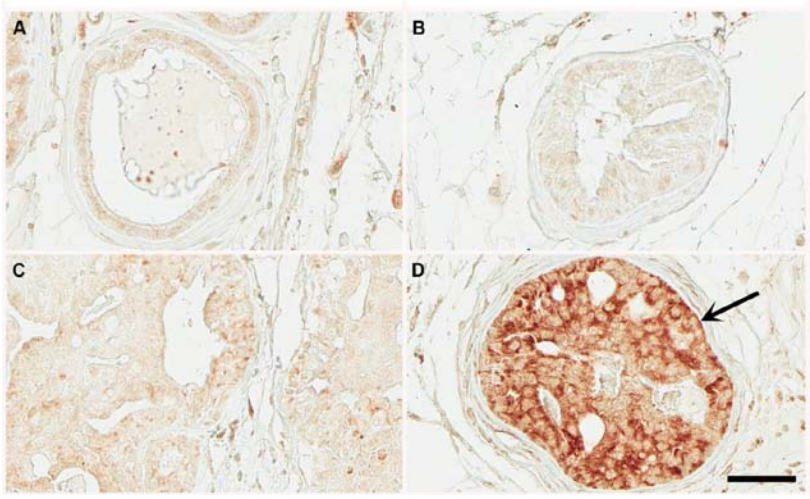

Figure 5.4 *Mme*$^{-/-}$*Pten*$^{PE-/-}$ prostate shows cytoplamic overexpression of p21. (A-D) p21 immunostaining of prostate from WT (A), *Mme*$^{-/-}$ (B), *Pten*$^{PE-/-}$ (C) and *Mme*$^{-/-}$*Pten*$^{PE-/-}$ (D) mice by 18 months of age (n=3). The arrow indicates p21 positive cells (D). (A-D) ABC Elite method, methyl green counterstain. Scale bar: 50 μm (A-D).

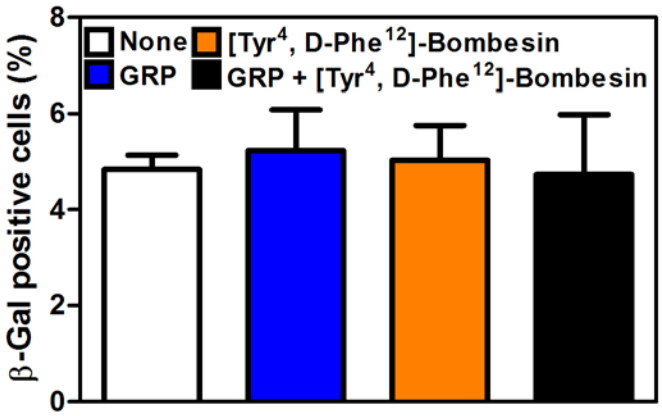

Figure 5.5 GRP has no effect on regulating senescence of CD44-positive DU145 human prostate cancer propagating cells. β-Gal staining of CD44-positive DU145 human prostate cancer propagating cells with GRP and/or GRPR antagonist [Tyr^4, D-Phe^{12}]-Bombesin. All error bars denote SD.

REFERENCES

Abbas, T., and Dutta, A. (2009). p21 in cancer: intricate networks and multiple activities. Nature reviews Cancer *9*, 400-414.

Birbach, A., Casanova, E., and Schmid, J.A. (2009). A Probasin-MerCreMer BAC allows inducible recombination in the mouse prostate. Genesis *47*, 757-764.

Birchmeier, C., Birchmeier, W., Gherardi, E., and Vande Woude, G.F. (2003). Met, metastasis, motility and more. Nature reviews Molecular cell biology *4*, 915-925.

Boccaccio, C., and Comoglio, P.M. (2006). Invasive growth: a MET-driven genetic programme for cancer and stem cells. Nature reviews Cancer *6*, 637-645.

Bringold, F., and Serrano, M. (2000). Tumor suppressors and oncogenes in cellular senescence. Experimental gerontology *35*, 317-329.

Buch, T., Heppner, F.L., Tertilt, C., Heinen, T.J., Kremer, M., Wunderlich, F.T., Jung, S., and Waisman, A. (2005). A Cre-inducible diphtheria toxin receptor mediates cell lineage ablation after toxin administration. Nature methods *2*, 419-426.

Campisi, J. (2013). Aging, cellular senescence, and cancer. Annual review of physiology *75*, 685-705.

Carney, D.N., Gazdar, A.F., Bepler, G., Guccion, J.G., Marangos, P.J., Moody, T.W., Zweig, M.H., and Minna, J.D. (1985). Establishment and identification of small cell lung cancer cell lines having classic and variant features. Cancer research *45*, 2913-2923.

Cha, J.H., Chang, M.Y., Richardson, J.A., and Eidels, L. (2003). Transgenic mice expressing the diphtheria toxin receptor are sensitive to the toxin. Molecular microbiology *49*, 235-240.

Chen, Z., Trotman, L.C., Shaffer, D., Lin, H.K., Dotan, Z.A., Niki, M., Koutcher, J.A., Scher, H.I., Ludwig, T., Gerald, W.*, et al.* (2005). Crucial role of p53-dependent cellular senescence in suppression of Pten-deficient tumorigenesis. Nature *436*, 725-730.

Cheng, C.Y., Zhou, Z., and Nikitin, A.Y. (2013). Detection and organ-specific ablation of neuroendocrine cells by synaptophysin locus-based BAC cassette in transgenic mice. PloS one *8*, e60905.

Choi, N., Zhang, B., Zhang, L., Ittmann, M., and Xin, L. (2012). Adult murine prostate basal and luminal cells are self-sustained lineages that can both serve as targets for prostate cancer initiation. Cancer cell *21*, 253-265.

Collado, M., and Serrano, M. (2010). Senescence in tumours: evidence from mice and humans. Nature reviews Cancer *10*, 51-57.

Concepcion, C.P., Han, Y.C., Mu, P., Bonetti, C., Yao, E., D'Andrea, A., Vidigal, J.A., Maughan, W.P., Ogrodowski, P., and Ventura, A. (2012). Intact p53-dependent responses in miR-34-deficient mice. PLoS genetics *8*, e1002797.

De Bacco, F., Casanova, E., Medico, E., Pellegatta, S., Orzan, F., Albano, R., Luraghi, P., Reato, G., D'Ambrosio, A., Porrati, P.*, et al.* (2012). The MET oncogene is a functional marker of a glioblastoma stem cell subtype. Cancer research *72*, 4537-4550.

Di Renzo, M.F., Olivero, M., Katsaros, D., Crepaldi, T., Gaglia, P., Zola, P., Sismondi, P., and Comoglio, P.M. (1994). Overexpression of the Met/HGF receptor in ovarian cancer. International journal of cancer Journal international du cancer *58*, 658-662.

Di Renzo, M.F., Olivero, M., Serini, G., Orlandi, F., Pilotti, S., Belfiore, A., Costantino, A., Vigneri, R., Angeli, A., Pierotti, M.A.*, et al.* (1995a). Overexpression of the c-MET/HGF receptor in human thyroid carcinomas derived from the follicular epithelium. Journal of endocrinological investigation *18*, 134-139.

Di Renzo, M.F., Poulsom, R., Olivero, M., Comoglio, P.M., and Lemoine, N.R. (1995b). Expression of the Met/hepatocyte growth factor receptor in human pancreatic cancer. Cancer research *55*, 1129-1138.

Donehower, L.A., Harvey, M., Slagle, B.L., McArthur, M.J., Montgomery, C.A., Jr., Butel, J.S., and Bradley, A. (1992). Mice deficient for p53 are developmentally normal but susceptible to spontaneous tumours. Nature *356*, 215-221.

Ferracini, R., Di Renzo, M.F., Scotlandi, K., Baldini, N., Olivero, M., Lollini, P., Cremona, O., Campanacci, M., and Comoglio, P.M. (1995). The Met/HGF receptor is over-expressed in human osteosarcomas and is activated by either a paracrine or an autocrine circuit. Oncogene *10*, 739-749.

Forte, G., Minieri, M., Cossa, P., Antenucci, D., Sala, M., Gnocchi, V., Fiaccavento, R., Carotenuto, F., De Vito, P., Baldini, P.M.*, et al.* (2006). Hepatocyte growth factor effects on mesenchymal stem cells: proliferation, migration, and differentiation. Stem cells *24*, 23-33.

Freedland, S.J., Seligson, D.B., Liu, A.Y., Pantuck, A.J., Paik, S.H., Horvath, S., Wieder, J.A., Zisman, A., Nguyen, D., Tso, C.L.*, et al.* (2003). Loss of CD10 (neutral endopeptidase) is a frequent and early event in human prostate cancer. The Prostate *55*, 71-80.

Gingrich, J.R., Barrios, R.J., Morton, R.A., Boyce, B.F., DeMayo, F.J., Finegold, M.J., Angelopoulou, R., Rosen, J.M., and Greenberg, N.M. (1996). Metastatic prostate cancer in a transgenic mouse. Cancer research *56*, 4096-4102.

Humphrey, P.A., Zhu, X., Zarnegar, R., Swanson, P.E., Ratliff, T.L., Vollmer, R.T., and Day, M.L. (1995). Hepatocyte growth factor and its receptor (c-MET) in prostatic carcinoma. The American journal of pathology *147*, 386-396.

Hwang, C.I., Matoso, A., Corney, D.C., Flesken-Nikitin, A., Korner, S., Wang, W., Boccaccio, C., Thorgeirsson, S.S., Comoglio, P.M., Hermeking, H.*, et al.* (2011). Wild-type p53 controls cell motility and invasion by dual regulation of MET expression. Proceedings of the National Academy of Sciences of the United States of America *108*, 14240-14245.

Jacks, T., Remington, L., Williams, B.O., Schmitt, E.M., Halachmi, S., Bronson, R.T., and Weinberg, R.A. (1994). Tumor spectrum analysis in p53-mutant mice. Current biology : CB *4*, 1-7.

Joo, K.M., Jin, J., Kim, E., Ho Kim, K., Kim, Y., Gu Kang, B., Kang, Y.J., Lathia, J.D., Cheong, K.H., Song, P.H.*, et al.* (2012). MET signaling regulates glioblastoma stem cells. Cancer research *72*, 3828-3838.

Kaplan-Lefko, P.J., Chen, T.M., Ittmann, M.M., Barrios, R.J., Ayala, G.E., Huss, W.J., Maddison, L.A., Foster, B.A., and Greenberg, N.M. (2003). Pathobiology of autochthonous prostate cancer in a pre-clinical transgenic mouse model. The Prostate *55*, 219-237.

Kasper, S., Sheppard, P.C., Yan, Y., Pettigrew, N., Borowsky, A.D., Prins, G.S., Dodd, J.G., Duckworth, M.L., and Matusik, R.J. (1998). Development, progression, and androgen-dependence of prostate tumors in probasin-large T antigen transgenic mice: a

model for prostate cancer. Laboratory investigation; a journal of technical methods and pathology *78*, i-xv.

Kim, C.J., Kushima, R., Okada, Y., and Seto, A. (2000). Establishment and characterization of a prostatic small-cell carcinoma cell line (PSK-1) derived from a patient with Klinefelter syndrome. The Prostate *42*, 287-294.

Kletsas, D., Caselgrandi, E., Barbieri, D., Stathakos, D., Franceschi, C., and Ottaviani, E. (1998). Neutral endopeptidase-24.11 (NEP) activity in human fibroblasts during development and ageing. Mechanisms of ageing and development *102*, 15-23.

Kuilman, T., Michaloglou, C., Mooi, W.J., and Peeper, D.S. (2010). The essence of senescence. Genes & development *24*, 2463-2479.

Lawson, D.A., Zong, Y., Memarzadeh, S., Xin, L., Huang, J., and Witte, O.N. (2010). Basal epithelial stem cells are efficient targets for prostate cancer initiation. Proceedings of the National Academy of Sciences of the United States of America *107*, 2610-2615.

Leong, K.G., Wang, B.E., Johnson, L., and Gao, W.Q. (2008). Generation of a prostate from a single adult stem cell. Nature *456*, 804-808.

Li, C., Wu, J.J., Hynes, M., Dosch, J., Sarkar, B., Welling, T.H., Pasca di Magliano, M., and Simeone, D.M. (2011a). c-Met is a marker of pancreatic cancer stem cells and therapeutic target. Gastroenterology *141*, 2218-2227 e2215.

Li, Y., Li, A., Glas, M., Lal, B., Ying, M., Sang, Y., Xia, S., Trageser, D., Guerrero-Cazares, H., Eberhart, C.G.*, et al.* (2011b). c-Met signaling induces a reprogramming network and supports the glioblastoma stem-like phenotype. Proceedings of the National Academy of Sciences of the United States of America *108*, 9951-9956.

Liao, C.P., Zhong, C., Saribekyan, G., Bading, J., Park, R., Conti, P.S., Moats, R., Berns, A., Shi, W., Zhou, Z.*, et al.* (2007). Mouse models of prostate adenocarcinoma with the capacity to monitor spontaneous carcinogenesis by bioluminescence or fluorescence. Cancer research *67*, 7525-7533.

Liu, J., Pascal, L.E., Isharwal, S., Metzger, D., Ramos Garcia, R., Pilch, J., Kasper, S., Williams, K., Basse, P.H., Nelson, J.B.*, et al.* (2011). Regenerated luminal epithelial cells are derived from preexisting luminal epithelial cells in adult mouse prostate. Molecular endocrinology *25*, 1849-1857.

Luchman, H.A., Friedman, H.C., Villemaire, M.L., Peterson, A.C., and Jirik, F.R. (2008). Temporally controlled prostate epithelium-specific gene alterations. Genesis *46*, 229-234.

Luquet, S., Perez, F.A., Hnasko, T.S., and Palmiter, R.D. (2005). NPY/AgRP neurons are essential for feeding in adult mice but can be ablated in neonates. Science *310*, 683-685.

Masumori, N., Thomas, T.Z., Chaurand, P., Case, T., Paul, M., Kasper, S., Caprioli, R.M., Tsukamoto, T., Shappell, S.B., and Matusik, R.J. (2001). A probasin-large T antigen transgenic mouse line develops prostate adenocarcinoma and neuroendocrine carcinoma with metastatic potential. Cancer research *61*, 2239-2249.

Miners, J.S., van Helmond, Z., Kehoe, P.G., and Love, S. (2010). Changes with age in the activities of beta-secretase and the Abeta-degrading enzymes neprilysin, insulin-degrading enzyme and angiotensin-converting enzyme. Brain pathology *20*, 794-802.

Morello, S., Olivero, M., Aimetti, M., Bernardi, M., Berrone, S., Di Renzo, M.F., and Giordano, S. (2001). MET receptor is overexpressed but not mutated in oral squamous cell carcinomas. Journal of cellular physiology *189*, 285-290.

Morisaki, N., Moriwaki, S., Sugiyama-Nakagiri, Y., Haketa, K., Takema, Y., and Imokawa, G. (2010). Neprilysin is identical to skin fibroblast elastase: its role in skin aging and UV responses. The Journal of biological chemistry *285*, 39819-39827.

Muzumdar, M.D., Tasic, B., Miyamichi, K., Li, L., and Luo, L. (2007). A global double-fluorescent Cre reporter mouse. Genesis *45*, 593-605.

Natali, P.G., Prat, M., Nicotra, M.R., Bigotti, A., Olivero, M., Comoglio, P.M., and Di Renzo, M.F. (1996). Overexpression of the met/HGF receptor in renal cell carcinomas. International journal of cancer Journal international du cancer *69*, 212-217.

Nicoleau, C., Benzakour, O., Agasse, F., Thiriet, N., Petit, J., Prestoz, L., Roger, M., Jaber, M., and Coronas, V. (2009). Endogenous hepatocyte growth factor is a niche signal for subventricular zone neural stem cell amplification and self-renewal. Stem cells *27*, 408-419.

Olivero, M., Rizzo, M., Madeddu, R., Casadio, C., Pennacchietti, S., Nicotra, M.R., Prat, M., Maggi, G., Arena, N., Natali, P.G.*, et al.* (1996). Overexpression and activation of

hepatocyte growth factor/scatter factor in human non-small-cell lung carcinomas. British journal of cancer *74*, 1862-1868.

Osman, I., Yee, H., Taneja, S.S., Levinson, B., Zeleniuch-Jacquotte, A., Chang, C., Nobert, C., and Nanus, D.M. (2004). Neutral endopeptidase protein expression and prognosis in localized prostate cancer. Clinical cancer research : an official journal of the American Association for Cancer Research *10*, 4096-4100.

Ousset, M., Van Keymeulen, A., Bouvencourt, G., Sharma, N., Achouri, Y., Simons, B.D., and Blanpain, C. (2012). Multipotent and unipotent progenitors contribute to prostate postnatal development. Nature cell biology *14*, 1131-1138.

Papandreou, C.N., Usmani, B., Geng, Y., Bogenrieder, T., Freeman, R., Wilk, S., Finstad, C.L., Reuter, V.E., Powell, C.T., Scheinberg, D.*, et al.* (1998). Neutral endopeptidase 24.11 loss in metastatic human prostate cancer contributes to androgen-independent progression. Nature medicine *4*, 50-57.

Prieur, A., and Peeper, D.S. (2008). Cellular senescence in vivo: a barrier to tumorigenesis. Current opinion in cell biology *20*, 150-155.

Rajasekhar, V.K., Studer, L., Gerald, W., Socci, N.D., and Scher, H.I. (2011). Tumour-initiating stem-like cells in human prostate cancer exhibit increased NF-kappaB signalling. Nature communications *2*, 162.

Rodier, F., and Campisi, J. (2011). Four faces of cellular senescence. The Journal of cell biology *192*, 547-556.

Rother, E., Belgardt, B.F., Tsaousidou, E., Hampel, B., Waisman, A., Myers, M.G., Jr., and Bruning, J.C. (2012). Acute selective ablation of rat insulin promoter-expressing (RIPHER) neurons defines their orexigenic nature. Proceedings of the National Academy of Sciences of the United States of America *109*, 18132-18137.

Saito, M., Iwawaki, T., Taya, C., Yonekawa, H., Noda, M., Inui, Y., Mekada, E., Kimata, Y., Tsuru, A., and Kohno, K. (2001). Diphtheria toxin receptor-mediated conditional and targeted cell ablation in transgenic mice. Nature biotechnology *19*, 746-750.

Sauer, C.G., Roemer, A., and Grobholz, R. (2006). Genetic analysis of neuroendocrine tumor cells in prostatic carcinoma. The Prostate *66*, 227-234.

Son, B.R., Marquez-Curtis, L.A., Kucia, M., Wysoczynski, M., Turner, A.R., Ratajczak, J., Ratajczak, M.Z., and Janowska-Wieczorek, A. (2006). Migration of bone marrow and cord blood mesenchymal stem cells in vitro is regulated by stromal-derived factor-1-CXCR4 and hepatocyte growth factor-c-met axes and involves matrix metalloproteinases. Stem cells *24*, 1254-1264.

Suzuki, A., Zheng, Y.W., Fukao, K., Nakauchi, H., and Taniguchi, H. (2004). Liver repopulation by c-Met-positive stem/progenitor cells isolated from the developing rat liver. Hepato-gastroenterology *51*, 423-426.

Takeo, S., Arai, H., Kusano, N., Harada, T., Furuya, T., Kawauchi, S., Oga, A., Hirano, T., Yoshida, T., Okita, K.*, et al.* (2001). Examination of oncogene amplification by genomic DNA microarray in hepatocellular carcinomas: comparison with comparative genomic hybridization analysis. Cancer genetics and cytogenetics *130*, 127-132.

Taniguchi, K., Yonemura, Y., Nojima, N., Hirono, Y., Fushida, S., Fujimura, T., Miwa, K., Endo, Y., Yamamoto, H., and Watanabe, H. (1998). The relation between the growth patterns of gastric carcinoma and the expression of hepatocyte growth factor receptor (c-met), autocrine motility factor receptor, and urokinase-type plasminogen activator receptor. Cancer *82*, 2112-2122.

Tesio, M., Golan, K., Corso, S., Giordano, S., Schajnovitz, A., Vagima, Y., Shivtiel, S., Kalinkovich, A., Caione, L., Gammaitoni, L.*, et al.* (2011). Enhanced c-Met activity promotes G-CSF-induced mobilization of hematopoietic progenitor cells via ROS signaling. Blood *117*, 419-428.

Thorel, F., Nepote, V., Avril, I., Kohno, K., Desgraz, R., Chera, S., and Herrera, P.L. (2010). Conversion of adult pancreatic alpha-cells to beta-cells after extreme beta-cell loss. Nature *464*, 1149-1154.

Tian, H., Biehs, B., Warming, S., Leong, K.G., Rangell, L., Klein, O.D., and de Sauvage, F.J. (2011). A reserve stem cell population in small intestine renders Lgr5-positive cells dispensable. Nature *478*, 255-259.

Tittel, A.P., Heuser, C., Ohliger, C., Llanto, C., Yona, S., Hammerling, G.J., Engel, D.R., Garbi, N., and Kurts, C. (2012). Functionally relevant neutrophilia in CD11c diphtheria toxin receptor transgenic mice. Nature methods *9*, 385-390.

Trotman, L.C., Niki, M., Dotan, Z.A., Koutcher, J.A., Di Cristofano, A., Xiao, A., Khoo, A.S., Roy-Burman, P., Greenberg, N.M., Van Dyke, T.*, et al.* (2003). Pten dose dictates cancer progression in the prostate. PLoS biology *1*, E59.

Trusolino, L., Bertotti, A., and Comoglio, P.M. (2010). MET signalling: principles and functions in development, organ regeneration and cancer. Nature reviews Molecular cell biology *11*, 834-848.

Trusolino, L., and Comoglio, P.M. (2002). Scatter-factor and semaphorin receptors: cell signalling for invasive growth. Nature reviews Cancer *2*, 289-300.

van Bokhoven, A., Varella-Garcia, M., Korch, C., Johannes, W.U., Smith, E.E., Miller, H.L., Nordeen, S.K., Miller, G.J., and Lucia, M.S. (2003). Molecular characterization of human prostate carcinoma cell lines. The Prostate *57*, 205-225.

Vermeulen, L., De Sousa, E.M.F., van der Heijden, M., Cameron, K., de Jong, J.H., Borovski, T., Tuynman, J.B., Todaro, M., Merz, C., Rodermond, H.*, et al.* (2010). Wnt activity defines colon cancer stem cells and is regulated by the microenvironment. Nature cell biology *12*, 468-476.

Wang, S., Gao, J., Lei, Q., Rozengurt, N., Pritchard, C., Jiao, J., Thomas, G.V., Li, G., Roy-Burman, P., Nelson, P.S.*, et al.* (2003). Prostate-specific deletion of the murine Pten tumor suppressor gene leads to metastatic prostate cancer. Cancer cell *4*, 209-221.

Wang, S., Garcia, A.J., Wu, M., Lawson, D.A., Witte, O.N., and Wu, H. (2006). Pten deletion leads to the expansion of a prostatic stem/progenitor cell subpopulation and tumor initiation. Proceedings of the National Academy of Sciences of the United States of America *103*, 1480-1485.

Wang, X., Kruithof-de Julio, M., Economides, K.D., Walker, D., Yu, H., Halili, M.V., Hu, Y.P., Price, S.M., Abate-Shen, C., and Shen, M.M. (2009). A luminal epithelial stem cell that is a cell of origin for prostate cancer. Nature *461*, 495-500.

Wang, Z.A., Mitrofanova, A., Bergren, S.K., Abate-Shen, C., Cardiff, R.D., Califano, A., and Shen, M.M. (2013). Lineage analysis of basal epithelial cells reveals their unexpected plasticity and supports a cell-of-origin model for prostate cancer heterogeneity. Nature cell biology *15*, 274-283.

Wu, X., Wu, J., Huang, J., Powell, W.C., Zhang, J., Matusik, R.J., Sangiorgi, F.O., Maxson, R.E., Sucov, H.M., and Roy-Burman, P. (2001). Generation of a prostate epithelial cell-specific Cre transgenic mouse model for tissue-specific gene ablation. Mechanisms of development *101*, 61-69.

Yamaizumi, M., Mekada, E., Uchida, T., and Okada, Y. (1978). One molecule of diphtheria toxin fragment A introduced into a cell can kill the cell. Cell *15*, 245-250.

Yang, X.W., and Gong, S. (2005). An overview on the generation of BAC transgenic mice for neuroscience research. Current protocols in neuroscience / editorial board, Jacqueline N Crawley [et al] *Chapter 5*, Unit 5 20.

Yoshioka, T., Otero, J., Chen, Y., Kim, Y.M., Koutcher, J.A., Satagopan, J., Reuter, V., Carver, B., de Stanchina, E., Enomoto, K.*, et al.* (2013). beta4 Integrin signaling induces expansion of prostate tumor progenitors. The Journal of clinical investigation *123*, 682-699.

Zhang, L., Zhang, B., Valdez, J.M., Wang, F., Ittmann, M., and Xin, L. (2010). Dicer ablation impairs prostate stem cell activity and causes prostate atrophy. Stem cells *28*, 1260-1269.

Zhou, Z., Flesken-Nikitin, A., and Nikitin, A.Y. (2007). Prostate cancer associated with p53 and Rb deficiency arises from the stem/progenitor cell-enriched proximal region of prostatic ducts. Cancer research *67*, 5683-5690.

APPENDIX

SUMMARY OF ADDITIONAL RELEVANT PUBLICATIONS WITH CONTRIBUTIONS BY THE AUTHOR

NEUROENDOCRINE CELLS: POTENTIAL CELLS OF ORIGIN FOR SMALL CELL LUNG CARCINOMA.

Chieh-Yang Cheng, and Alexander Yu. Nikitin, (2011). Cell Cycle. 10: 3629-3630. PMID: 22024916.

Comment on: Park KS, et al. Cell Cycle 2011; 10:2806-2815.

OVARIAN SURFACE EPITHELIUM AT THE JUNCTION AREA CONTAINS A CANCER-PRONE STEM CELL NICHE

Andrea Flesken-Nikitin, Chang-Il Hwang, Chieh-Yang Cheng, Tatyana V. Michurina, Grigori Enikolopov, and Alexander Yu. Nikitin, (2013). Nature. 495 (7440): 241-245. PMID: 23467088.

Abstract

Epithelial ovarian cancer (EOC) is the fifth leading cause of cancer deaths among women in the United States, but its pathogenesis is poorly understood. Some epithelial cancers are known to occur in transitional zones between two types of epithelium, whereas others have been shown to originate in epithelial tissue stem cells. The stem cell niche of the ovarian surface epithelium (OSE), which is ruptured and regenerates during ovulation, has not yet been defined unequivocally. Here we identify the hilum region of the mouse ovary, the transitional (or junction) area between the OSE, mesothelium and tubal (oviductal) epithelium, as a previously unrecognized stem cell niche of the OSE. We find that cells of the hilum OSE are cycling slowly and express stem and/or progenitor cell markers ALDH1, LGR5, LEF1, CD133 and CK6B. These cells display long-term stem cell properties ex vivo and in vivo, as shown by our serial sphere generation and long-term lineage-tracing assays. Importantly, the hilum cells show increased transformation potential after inactivation of tumour suppressor genes *Trp53* and *Rb1*, whose pathways are altered frequently in the most aggressive and common type of human EOC, high-grade serous adenocarcinoma. Our study supports experimentally the idea that susceptibility of transitional zones to malignant transformation may be explained by the presence of stem cell niches in those areas. Identification of a stem cell niche for the OSE may have important implications for understanding EOC pathogenesis.

LOSS OF SURVIVIN IN THE PROSTATE EPITHELIUM IMPEDES CARCINOGENESIS IN A MOUSE MODEL OF PROSTATE ADENOCARCINOMA

Helty Adisetiyo, Mengmeng Liang, Chun-Peng Liao, Ari Aycock-Williams, Michael B. Cohen, Shili Xu, Nouri Neamati, Edward M. Conway, Chieh-Yang Cheng, Alexander Yu. Nikitin, Pradip Roy-Burman, (2013). PLoS One. 8 (7): e69484. PMID: 23936028.

Abstract

The inhibitor of apoptosis protein survivin is expressed in most cancers. Using the conditional *PTEN* deletion mouse model, we previously reported that survivin levels increase with prostate tumor growth. Here we evaluated the functional role of survivin in prostate tumor growth. First, we demonstrated that mice lacking the *survivin* gene in prostate epithelium were fertile and had normal prostate growth and development. We then serially, from about 10–56 weeks of age, evaluated histopathologic changes in the prostate of mice with *PTEN* deletion combined with *survivin* mono- or bi-allelic gene deletion. While within this time period most of the animals with wild-type or monoallelic survivin deletion developed adenocarcinomas, the most severe lesions in the biallelic survivin deleted mice were high-grade prostatic intra-epithelial neoplasia with distinct histopathology. Many atypical cells contained large hypertrophic cytoplasm and desmoplastic reaction in the prostatic intra-epithelial neoplasia lesions of this group was minimal until the late ages. A reduced proliferation index as well as apoptotic and senescent cells were detected in the lesions of mice with compound *PTEN/survivin* deficiency throughout the time points examined. *Survivin* deletion was also associated with reduced tumor expression of another inhibitor of apoptosis member, the X-linked inhibitor of apoptosis. Our findings suggest that survivin participates in the progression of prostatic intraepithelial neoplasia to adenocarcinoma, and that survivin interference at the prostatic intraepithelial neoplasia stages may be a potential therapeutic strategy to halt or delay further progression.